ANALYSIS AND DESIGN OF DEEP LEARNING BASED APPROACH FOR REDUCING DIABETIC RETINOPATHY

Thesis Submitted for the Award of the Degree of

DOCTOR OF PHILOSOPHY

in

Computer Science and Engineering

By

A Aruna Kumari

Registration Number: 41900485

Supervised By

Dr.Avinash Bhagat (11002)

School Of Computer Application

(Associate Professor)

Lovely Professional University, Punjab

Co-Supervised by

Dr.Santosh Kumar Henge

Department Of Computer Science & Engineering

(Associate Professor)

Koneru Lakshmaiah University, A.P

LOVELY PROFESSIONAL UNIVERSITY, PUNJAB

2024

DECLARATION

I, hereby declared that the presented work in the thesis entitled **" ANALYSIS AND DESIGN OF DEEP LEARNING BASED APPROACH FOR REDUCING DIABETIC RETINOPATHY "** in fulfillment of degree of **Doctor of Philosophy (Ph. D.)** is outcome of research work carried out by me under the supervision of Dr. Avinash Bhagat, working as Associate Professor, in the School of Computer Application of Lovely Professional University, Punjab, India. In keeping with general practice of reporting scientific observations, due acknowledgement have been made whenever work described here has been based on findings of other investigator. This work has not been submitted in part or full to any other University or Institute for the award of any degree.

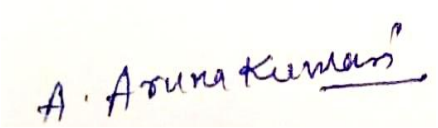

A Aruna Kumari

41900485

School of Computer Science and Engineering

Lovely Professional University,

Punjab, India

CERTIFICATE

This is to certify that the work reported in the Ph. D. thesis entitled **" ANALYSIS AND DESIGN OF DEEP LEARNING BASED APPROACH FOR REDUCING DIABETIC RETINOPATHY "** submitted in fulfillment of the requirement for the award of degree of **Doctor of Philosophy (Ph.D.)** in the School of Computer Science and Engineering, is a research work carried out by **A Aruna Kumari** , 41900485, is bonafide record of his/her original work carried out under my supervision and that no part of thesis has been submitted for any other degree, diploma or equivalent course.

Supervised by

(Dr. Avinash Bhagat)

Associate Professor

Lovely Professional University

Phagwara, Punjab

India

Co-Supervised by

(Dr.Santosh Kumar Henge)

Associate Professor

Koneru lakshmaiah University

Vaddeswaram, Andhrapradesh

India

ABSTRACT

One of the leading causes of blindness worldwide, Diabetic Retinopathy (DR) is a progressive microvascular complication that affects a large number of diabetics. The condition affects the retina and causes blood vessels to grow abnormally and fluid to leak, which can damage the optic nerve and eventually cause vision loss.

Early identification and treatment of DR are fundamental in forestalling vision misfortune, yet the conventional manual screening process is tedious, costly, and inclined to blunders. When it comes to the analysis and design of an automated DR screening and diagnosis system, approaches based on deep learning have the potential to significantly enhance the accuracy and efficacy of DR detection, thereby preventing patients from losing their vision.

Due to their capacity to automatically learn and extract features from large datasets, deep learning algorithms are being utilized in medical imaging in an increasing number of applications. They can precisely order and portion clinical pictures, lessening the requirement for manual intercession and empowering opportune conclusion and treatment.

The proposed exploration will zero in on the improvement of a profound learning-based approach for lessening DR. A convolutional neural network (CNN) will be used in this strategy to automatically detect and classify DR from images of the retinal fundus. The CNN will be prepared on a huge dataset of retinal fundus pictures of diabetic patients with fluctuating levels of DR. Expert ophthalmologists will annotate the images to provide the deep learning model with ground truth labels for training.

The proposed CNN design will be streamlined utilizing different hyperparameters tuning strategies, and the exhibition of the model will be assessed utilizing a few presentation measurements like responsiveness, explicitness, precision, and AUC-ROC. The accuracy, effectiveness, and cost-effectiveness of the proposed deep learning approach will be evaluated by comparing them to the conventional manual screening procedure.

This research has the potential to have a significant impact because its goal is to develop an automated and effective tool for DR screening and diagnosis. Ophthalmologists may see a significant reduction in workload as a result of the proposed strategy, which will result in faster and more accurate diagnosis and treatment, which will ultimately improve patient outcomes and lessen the burden of DR on healthcare systems.

Scope of the Research

A deep learning-based strategy for using retinal fundus images to reduce diabetic retinopathy (DR) is the goal of this study. A convolutional neural network (CNN) for automatically detecting and classifying DR from retinal fundus images will be analyzed and designed as part of the research.

A substantial collection and pre-processing of retinal fundus images from diabetic patients with varying degrees of DR will be part of the research. The images will be annotated by experienced ophthalmologists to provide the deep learning model with real-world labels for training. The proposed CNN design will be enhanced utilizing different hyperparameters tuning methods, and the model's exhibition will be assessed utilizing a few presentation measurements like responsiveness, particularity, precision, and region under the recipient working trademark bend (AUC-ROC).

The proposed method will be compared to the conventional manual screening procedure in order to evaluate its accuracy, effectiveness, and cost-effectiveness.
The use of retinal fundus images for DR detection and classification is the sole focus of this study. Other types of medical imaging or clinical data will not be used in the study. The development of a deep learning-based strategy will be the primary focus of the research; clinical validation of the proposed strategy will not be included.

Research Limitations

- Only the analysis and design of a CNN for the automatic detection and classification of DR using retinal fundus images will be included in the deep learning-based approach that is being proposed. Other types of medical imaging or clinical data will not be taken into account in the study.
- The proposed approach will not be clinically validated as part of the study. As a result, this study's findings will be limited to the proposed method's accuracy, efficiency, and cost-effectiveness in detecting and classifying DR using retinal fundus images.
- The quality and size of the dataset used to train the deep learning model may affect how well the proposed method works. As a result, if the dataset is biased or insufficient, it may limit the proposed method's generalizability.
- The proposed approach's performance will only be evaluated on a specific population in the study, so it may not apply to other populations or ethnic groups.
- The proposed approach might require specific equipment or programming, which may not be generally accessible in some medical care settings. In some clinical settings, this limitation may limit the proposed strategy's viability and acceptance.

Future Scope

The future scope of this research involves several possibilities for further improvement and expansion of the proposed deep learning-based approach. These include:

1. Extension to include other medical imaging modalities such as OCT or FFA to improve DR diagnosis and classification accuracy.
2. Expansion to include other ocular diseases such as glaucoma or AMD to develop an integrated diagnostic system for multiple ocular diseases.

3. Integration with telemedicine systems to enable remote screening and diagnosis of DR in underserved or rural areas.
4. Optimization to reduce the number of false positives and false negatives, thus improving the accuracy and reliability of DR diagnosis.
5. Integration with EMRs to enable real-time monitoring of DR progression and treatment outcomes, thus improving the overall management and care of diabetic patients with DR.

The successful implementation of these future possibilities can contribute to improving patient outcomes, reducing healthcare costs, and advancing the field of medical imaging and deep learning in ophthalmology.

Letter of Candidacy

LOVELY PROFESSIONAL UNIVERSITY

Centre for
Research Degree Programmes

LPU/CRDP/PHD/EC/20210602/001648

Dated: 03 Mar 2021

A Aruna Kumari
Registration Number: 41900485
Programme Name: Doctor of Philosophy (Computer Science and Engineering)

Subject: Letter of Candidacy for Ph.D.

Dear Candidate,

We are very pleased to inform you that the Department Doctoral Board has approved your candidacy for the Ph.D. Programme on 03 Mar 2021 by accepting your research proposal entitled: "Analysis and Design of Deep Learning based Approach for Reducing Diabetic Retinopathy"

As a Ph.D. candidate you are required to abide by the conditions, rules and regulations laid down for Ph.D. Programme of the University, and amendments, if any, made from time to time.

We wish you the very best!!

In case you have any query related to your programme, please contact Centre of Research Degree Programmes.

Head

Centre for Research Degree Programmes

Note:-This is a computer generated certificate and no signature is required. Please use the reference number generated on this certificate for future conversations.

Jalandhar-Delhi G.T.Road, Phagwara, Punjab (India) - 144411
Ph : +91-1824-444594 E-mail : drp@lpu.co.in website : www.lpu.in

Acknowledgment

I express my sincere thanks and deep gratitude to my guides, Dr.Avinash Bhagat and Dr.Santosh Kumar Henge, for their unwavering support, suggestions, encouragement, guidance, and patience in accomplishing this work. With great respect, I express my gratitude to them for their valuable contribution during the progress and development of my research. I have been benefitted a lot because of their help and guidance that inspired me greatly. They possess knowledge of immense breadth and depth coupled with great talent and enthusiasm for research. They have led me into the area of wireless sensor networks and simulated my research interest. They have taught me how to undertake research work and communicate effectively in the form of a research paper. I am fortunate to be associated with them. Their active participation, untiring efforts, affection, guidance, and approach have brought this work to the present stage.

During my thesis writing, I had a lot of support and advice from many different people. Still, as a researcher, Mr.Deb advice is unrivalled. From framing research problems to conducting analyses, from simulation to paper writing, and from the finer points of grammar to the finer points of teaching classes, he has spent countless hours assisting me in completing this work. He has been of great assistance to me, and I am pretty thankful. Even though I was tired and dissatisfied at times throughout this time, I always trusted and believed that Dr. Kalpana was there to support and advise me and answer all my questions and provide me strength and direction. She always found time whenever I needed for intelligent fruitful discussions. She always encouraged me whenever I became frustrated.

I give my deepest and sincere thanks to my beloved parents Akula Nageswar Rao and Akula Bhagyamma, my brothers Akula Achutha Rao, Akula Satyanarayana ,Akula Srinivas ,my husband Narendra Krishna Kumar Vemula, and my kid Chandra Prateek Vemula for their infinite love, encouragement, and enthusiastic support.

Last but not least, I would like to take the opportunity to thank my colleagues for their constant encouragement, hours of sitting together, and frequent, lively discussions, which helped me and encouraged me to complete the work.

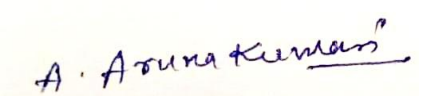

A. Aruna Kumari

Table of Contents

List of Figures

List of Tables

CHAPTER 1
INTRODUCTION

1.1 Human Health and Eye Diseases

The term "human health" refers to a person's complete state of health, which includes their physical, mental, and social well-being. Genetics, way of life, environmental variables, and availability of healthcare are only a few of the many complicated interactions that influence it. Properly operating the body's systems and organs, including the immunological, digestive, respiratory, and cardiovascular systems, is necessary for physical health. Maintaining physical health requires a healthy diet, consistent exercise, adequate sleep, and refraining from risky habits like smoking and binge drinking [1].

A person's emotional and psychological well-being is called mental health. It involves the capacity to manage stress, uphold wholesome relationships, and partake in satisfying pursuits. Genetic characteristics, life experiences, and environmental factors, including social support, resource accessibility, and exposure to trauma or violence, can all impact mental health.

The ability to participate in social interactions and connections with others is referred to as social health. It entails having dependable connections, a sense of belonging, and a community. Cultural norms, economic situations, and resource accessibility are only a few variables that might impact social health. Access to healthcare is another important factor in determining one's health [2]. It entails prompt access to healthcare services and therapies to treat, diagnose, and prevent disease. The idea of human health is intricate and varied, involving numerous variables. People can enhance their general health and well-being by leading a healthy lifestyle, getting the proper medical care, and cultivating a happy social life.

Diseases

Disorders or abnormal situations that interfere with the body's ability to operate normally are diseases. Genetic abnormalities, infections, lifestyle choices, environmental variables, or a mix of these factors are a few causes of disease. Infectious, chronic, autoimmune, and hereditary conditions are only a few of the various forms of diseases. Infectious and contagious illnesses are caused by pathogens such as “bacteria, fungus, viruses, or parasites”. On the other hand, chronic diseases, like diabetes, heart disease, or cancer, are long-lasting ailments that advance gradually and may not have a solution. Genetic illnesses are inherited ailments brought on by gene mutations, while “autoimmune diseases” are conditions where the “body's immune system” targets its healthy tissues. Depending on the type of disease and the body areas affected, the symptoms and effects of diseases can vary considerably [3]. While some diseases may only have minor or no symptoms, others may be serious and life-threatening. Pain, exhaustion, fever, coughing, and difficulty breathing are common symptoms of illnesses. The diagnosis and treatment of disorders is a key aspect of healthcare. By adopting preventive measures like vaccination, leading a healthy lifestyle, and shunning risky habits like smoking or binge drinking, many diseases can be prevented. Depending on the nature and severity of the disease, many treatments may be used to treat it, such as drugs, surgery, lifestyle changes, or a combination of these.

1.2 Eyes and Eye Diseases

The eyes are one of the most important and intricate organs in the human body. They help us see and understand the world around us. The primary function of the eyes is to provide vision, which is one of the most important senses for humans. Our eyes allow us to see objects, shapes, colors, and movements and safely navigate our environment. Our eyes play a crucial role in nonverbal communication, allowing us to convey emotions, thoughts, and intentions to others through facial expressions and eye contact [4]. Vision is essential for learning and development, particularly in children. Good vision is necessary for reading, writing, and other academic activities, as well as for participating in sports and other physical activities. Clear vision is essential for driving,

operating machinery, and performing other tasks that require good visual acuity. Poor vision can increase the risk of accidents and injuries.

Due to the potential correlation between some eye disorders and other illnesses like diabetes or high blood pressure, the eyes can offer crucial insights into general health. Regular eye exams can help detect and prevent these conditions.

The eyes are essential for our quality of life, and it is vital to take care of them by practicing good eye hygiene, wearing protective eyewear when necessary, and getting regular eye exams.

Eye Diseases:

Eye diseases refer to a wide range of conditions affecting the eyes and vision. Some common eye diseases include:

- Cataracts: a clouding of the natural lens of the eye that impairs vision and makes it challenging to see in strong light.
- Glaucoma: a group of disorders of the eyes that damage the “optic nerve” and can cause “blindness or vision loss.”
- AMD: a condition that progressively damages the “macula”, the center of the retina, and impairs central vision.
- Diabetic retinopathy: Diabetes often damages the blood vessels of the eye and causes visual impairment
- Inflammation and visual issues are brought on by “dry eye syndrome”, a condition in which the “eyes do not produce enough tears or they evaporate too quickly”.
- Conjunctivitis: an inflammation of the transparent membrane covering the white area of the eye, the conjunctiva, which results in redness, irritation, and discharge.

Treatment for eye diseases varies depending on the condition and may include medication, surgery, or lifestyle changes. It is essential to seek medical attention if you experience any changes in your vision or eye health.

1.3 Diabetes

Elevated blood sugar levels as a result of inadequate insulin synthesis or decreased insulin function define diabetes, a chronic metabolic condition. Type 1 diabetes, Type 2 diabetes, and gestational diabetes are the three primary kinds of the disease [5].

Insulin-producing pancreatic beta cells are damaged, which results in "**type 1** diabetes, an autoimmune disease."

"Type 2 diabetes" arises when the pancreas is unable to "generate enough insulin to regulate blood sugar levels, or when the body becomes resistant to insulin". Estimates place the global prevalence of diabetes at 463 million people, making it a serious public health concern. Many consequences, including cardiovascular disease, kidney damage, nerve damage, and blindness, might result from it [6].

Diabetes is often treated with medicine, such as insulin or oral hypoglycemic medications, as well as dietary and exercise modifications. Furthermore, crucial are regular medical examinations and blood sugar level monitoring [7].

1.4 Medical Field and Medical Imaging

The medical field is essential for maintaining and improving human health, advancing knowledge, supporting public health, and providing employment. It plays a critical role in ensuring the wellbeing of individuals and society as a whole. The prevention, diagnosis, and treatment of illnesses and injuries fall under the umbrella of the medical discipline, which includes a diverse variety of professions and practices.

The medical field is responsible for developing and implementing treatments, medications, and procedures that improve and maintain the health of individuals and populations. This includes preventative care, such as vaccinations and treatment for illnesses and injuries. Medical professionals save lives daily through emergency care, surgery, and other life- saving interventions. Their expertise and quick action can mean the difference between life and death for many patients. Medical research helps advance our understanding of diseases, how they develop, and how they can be treated or prevented. This knowledge can lead to new treatments and cures for illnesses that

were once thought to be incurable. The medical field also plays a crucial role in promoting public health through initiatives such as disease surveillance, health education, and policy development. This helps ensure that the public has access to the resources and information needed to stay healthy and prevent the spread of disease.

Medical Imaging

A crucial component of clinical practice is medical imaging, or the utilization of technology to observe inside body parts. When it comes to diagnosing and treating a variety of disorders, these images can be an extremely useful resource for medical professionals. To produce images of the body's structures, such as bones, organs, and tissues, medical imaging techniques make use of a variety of energy sources, such as X- rays, magnetic fields, or sound waves. Common forms of medical imaging include “CT, MRI ultrasound, and nuclear medicine imaging” [8]. In contrast to CT scans, which use “X-rays to produce precise “cross-sectional images” of the body, “X-rays are used in X-rays to produce images of dense structures like bones”. An MRI uses radio waves and magnetic fields to produce extremely detailed images of soft tissues like the brain, muscles, and organs. Nuclear medicine imaging uses tiny amounts of radioactive material to make images of the body's processes and activities, whereas ultrasound uses high-frequency sound waves to make images of inside structures. Medical imaging is an important tool for diagnosing and treating a wide range of conditions, from cancer to broken bones. It can assist with the ID and localization of oddities or wounds, the observing of the adequacy of medicines, and the preparation of surgeries. However, medical imaging also makes use of energy sources like radiation or other forms of radiation that, if not used appropriately, could be harmful. The clinical business incorporates a great many callings and fortes and manages the counteraction, conclusion, and treatment of illnesses and wounds. Clinical imaging is a fundamental piece of clinical practice that utilization innovation to make pictures of the inside organs and substantial designs, giving supportive data to clinical experts. Medical imaging is quite effective in diagnosis and suggesting proper measures to treat a known diseas.

1.5 Technologies: Artificial Intelligence, Machine Learning, and Deep Learning

The development of computers capable of doing tasks that have historically required human intellect, such understanding spoken language, identifying patterns in pictures, and making data-driven judgments, is known as artificial intelligence (AI), and it is a subfield of computer science [9]. AI comes in a variety of forms, each having advantages and disadvantages, such as “rule-based systems, decision trees, artificial neural networks, and DL.”

AI has several uses in a variety of fields, including healthcare, finance, and transportation. It keeps progressing in new domains, such program synthesis. Personalized suggestions on streaming services, self-driving cars, and facial recognition software, for instance, are all applications of AI. Many fields of computer science, including computer vision, natural language processing (NLP), robotics, and computational biology, have seen significant transformation as a result of machine learning. A number of commercial applications, including security, recommendation systems, search, translation, and medical data analysis, are currently powered by deep learning (DL), which has expedited research in these areas.

Artificial intelligence (AI) includes machine learning as a subfield (ML). This approach trains computers to handle data more effectively. To investigate the patterns and extract relevant information from the data, we employ machine learning.

Modifications to systems that perform tasks related to artificial intelligence are most frequently referred to as "machine learning" (AI). They include forecasting, organizing, controlling robots, diagnosing, and recognizing. The "changes" could involve making adjustments to systems that are currently operational or starting from scratch to develop new ones. The Figure below provides a high-level breakdown of an ML workflow's steps.

We may divide the processing in a typical machine-learning application into two stages:

Learning Phase: This stage starts as the application is being developed or built. It entails the following actions:

- Data collection: where the data scientist collects as much information as possible.
- The obtained data are appropriately cleaned and structured for the learning algorithm. This is known as feature engineering or data preparation.
- Pick a model: Because different algorithms are good for various jobs, the developer should select the most effective method.
- Train the model: To decrease an error function, the algorithm's parameters are changed. How frequently the algorithm predicts incorrectly is shown by the error function.
- Weigh the model: New data is used to test the model and verify its accuracy. If the model performs well, it might be applied. If not, the programmer must create better data preparation techniques or learning hyperparameters.
- Deployment: The model is set up on a platform so users can use it.

Inference Phase: In this step, predictions are made about fresh data provided by the user using the model created in the phase before.

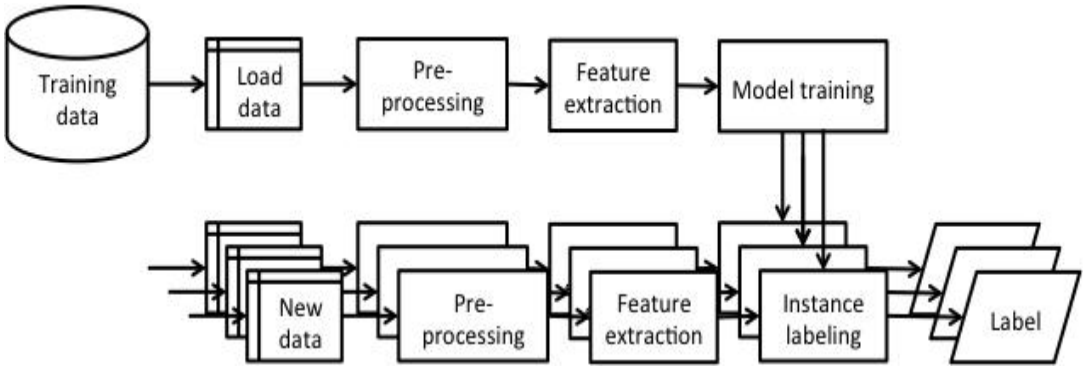

Figure 1.1: machine learning application workflow [1]

Machine learning algorithms and models have progressed from being just statistical to using models like neural networks that are bio-inspired. They are now separated into two groups:

- Deep learning
- Traditional or Classical Machine Learning models

Customary AI techniques are just fit for dealing with natural normal information.

Planning the fitting component extractor, which would change over crude information into the legitimate configuration (for the most part an element vector), from which a classifier could track down designs or characterize the info, requires significant space skill. Deep learning can solve this problem.

A normal AI strategy, for example, would either use every pixel's worth as a component or utilize a client characterized capability to remove the edges, structures, and varieties, which the classifier would then use as highlights. The convolutional neural network, on the other hand, will automatically extract the features and determine which ones are useful for categorization when using deep learning.

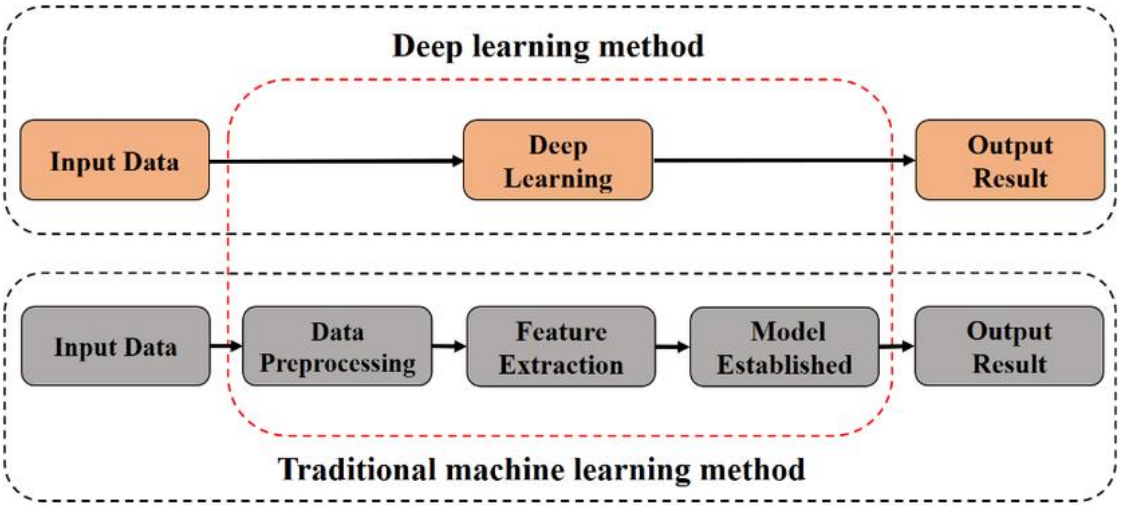

Figure 1.2: "Comparison of machine learning and deep learning" [2]

As its name suggests, deep learning is a method for training computers to learn like young children. Deep Neural Networks, a design influenced by biology, are used in Deep Learning. With this engineering, the machine may naturally separate the portrayal it needs for the expected assignment subsequent to being taken care of crude information (Grouping, Discovery, and so on) [10].

Driver-less cars, language translation, and even predictive software used by some hospitals to manage patients in emergency waiting rooms are just a few of the amazing applications powered by this technology. DL is a method of ML that has significantly incorporated our knowledge of the human brain, applied mathematics, and statistics over the past few decades.

Deep Neural Networks

To comprehend deep learning, it is necessary to explain how its fundamental components work: The Deep Neural Networks.

A deep neural network is an algorithm with a bio-inspired design. visual representation is a hierarchy of levels, where each level represents a vertical cluster of nodes. Every node is a processing unit that first applies a linear function to raw input data before applying a nonlinear activation function. Each layer of the data representation will be changed with the aid of this program, creating a statistical model that will aid us in the task of categorization and detection. The end result is a set of probabilistic nodes, each of which represents the likelihood that an input will fall into a particular class.

The universal approximation theorem states that by combining numerous layers of representations, we may learn extremely complicated functions (Activation functions), provided that the suitable non-linear functions are used. Due to the amount of processing stages that data was passed through and changes were made, the word "deep" was created.

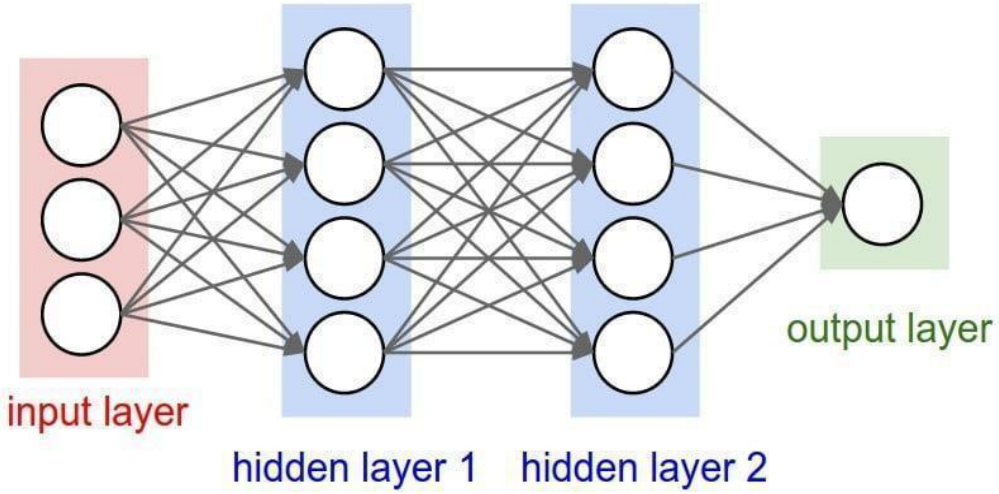

Figure 1.3: Deep Neural Networks [3]

Given enough data and computation time, neural networks may be trained to approximate any function. The network is initially naive since it is unaware of the

function that maps inputs to outputs. We train the network by changing the network's parameters in response to each step's loss.

For example, the mean squared loss (MSL) is often used in binary classification problems and regression problems. To determine these parameters, we need to know how badly the network predicts the actual outputs. As a result, we determine a loss function, also known as a cost, which represents the prediction error.

$$MSL = \frac{1}{n}\sum_{i=1}^{n}(Y_i - \hat{Y}_i)^2 \qquad \text{— (1.1)}$$

In this case, Yi stands for the actual labels, n for the number of "training samples, and $\hat{Y}$i for the expected labels."

We can identify settings where the network can accurately anticipate the right labels by minimizing this "loss in relation to the network's parameters. "To find this minimum, we use the gradient descent method. The gradient, which indicates the direction of the quickest change, is the slope of the loss function. Then, we want to follow the gradient to reach the minimum in the shortest period (downwards).

Two principal passes in the training process need to be explained:

Feed Forward:

In neural networks, feedforward [187] describes how input is converted into output. It is the outcome of data processing by the neural network. We close in on one processing unit in the image below to observe what happens: Each unit receives some data, multiplies each input by the appropriate weights, and then adds all of these results together before applying an activation function.

We apply the "linear transformation L1 with weights W1 and biases b1 to the input x in the feedforward pass." Next, the result is placed through a linear transformation (L2) and sigmoid operation (S). Next, we calculate the loss l. We use the loss to determine the precision of the network's prediction

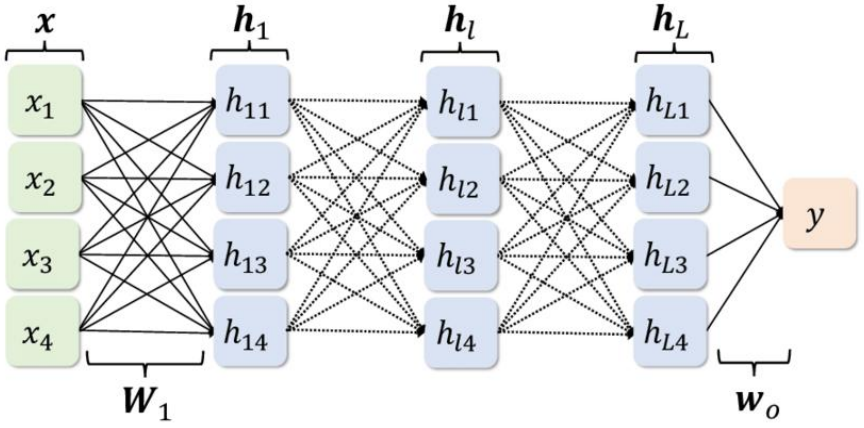

Figure 1.4: L1 Transformation Feed-Forward Networks [4]

Backpropagation: The chain rule, which is used to train multilayer networks, has a calculus application. The gradient of the loss was dispersed backward over the network. Every activity has a gradient between its inputs and outcomes. We multiply the incoming gradient by the gradient for the operation as we transmit the gradients backward. The chain rule can be used to quickly and quantitatively compute the gradient of the loss with respect to the weights.

$$\frac{\partial l}{\partial W_1} = \frac{\partial L_1}{\partial W_1}\frac{\partial S}{\partial L_1}\frac{\partial L_2}{\partial S}\frac{\partial l}{\partial L_2} \qquad \text{—(1.2)}$$

Utilizing this gradient and a certain learning rate α, we update the weights.

$$W'_1 = W_1 - \alpha\frac{\partial l}{\partial W_1} \qquad \text{—(1.3)}$$

Effectively set is the learning rate. Both large enough to cause the iterative technique to miss the minimum and small enough to prevent convergence to the minimum. These two fundamental algorithms—Feedforward and Backpropagation—that form the basis of all deep learning models teach deep neural networks new information by repeating them.

Acceleration Factors for Deep Learning

Three significant technological breakthroughs have led to a growth in deep learning in recent years:

Online, a Lot of Data Is Available By 2025, the Global Datasphere will have increased from 33 Zettabytes in 2018 to 100 Zettabytes, according to IDC.

A variety of readily available GPUs for parallel computation. On this kind of technology, matrix multiplications—which are widely utilized in deep learning computations—can be easily parallelized. In 2017, Tensor Processing Units (TPU) were also unveiled as an application-specific integrated circuit designed to accelerate workloads related to machine learning. They were expanding the selection of Deep Learning software, both for purchase and as open source. The time and complexity involved in creating neural networks from scratch using matrices is avoided by academics and developers thanks to these tools, which offer a clear abstraction of deep learning models.

1.6 The Deep Learning Models

Two categories of machine learning models, i.e., supervised and unsupervised [188], can be found in the earlier literature. The primary distinction between the two is seen in their training methods.

Unsupervised models are given input data without labels from which they can learn, in contrast to supervised models, which are trained using projected results (the input data are labelled).

In deep learning, a model's type can be inferred from the problem it helps to solve:

Deep learning with supervision (supervised models): Face recognition, object identification, image classification, etc.

Unsupervised deep learning: Image encoding and word embedding.

Applications for deep learning are being developed for various use cases, and the area is expanding. A different paradigm predominates and provides the optimum efficiency in each use scenario. The key models are described below.

Fully Connected Neural Networks

Multiple layers of perceptron's are stacked together to form dense neural networks (also known as multi-layer perceptron (MLP) or fully linked neural networks).

In order to create an output from many inputs, a perceptron or neuron uses a linear model, which typically multiplies an input by a vector of weights and adds bias.

$$Z = \vec{w}.X + b \qquad \text{—(1.4)}$$

A non-linear activation function is then used. Which results in a neuron's actual operation:

$$Z = \sigma(\vec{w}.\text{X+b}) \qquad \text{—(1.5)}$$

A layer is made up of several perceptron's when they are stacked. When all the layers are connected ("every neuron in the input and output layers is connected to every other neuron."), we refer to this network as a dense neural network.

Activation functions

A biological neuron fires only when it reaches a predetermined threshold while simulating the behavior of the neurons in the human brain. The first linear equation above produces values without upper or lower bounds. When deciding whether to terminate someone or not, this kind of value is useless. We include activation functions as a result.

Step function: Setting a threshold for this linear operation, the first intuitive function activates when Z is bigger.

$$Z = 1, if\ \vec{w}.X + b >= threshold \qquad \text{—(1.6)}$$

0, otherwise

Determining the threshold, which relies on the issue and the facts at hand, is the function's toughest obstacle.

The sigmoid function: One of the most often used functions is this one. It is non-linear, offers a gradual gradient, and restricts the result to the interval [0, 1].

$$Z = \frac{1}{1+e^{-\vec{w}.X+b}} \qquad \text{—(1.7)}$$

However, the "Vanishing Gradient" problem is brought on by this function since there are some places where the model will not change significantly (refuses to learn more). This issue arises when we reach either end of the sigmoid, as shown in the graph below.

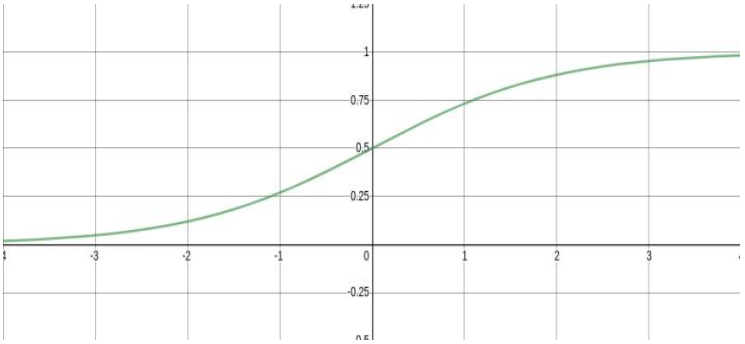

Figure 1.5: Sigmoid Graph [5]

Tanh Function: Simply put, this is a scaled sigmoid. As a result, it exhibits the same traits and causes the vanishing gradient problem.

$$Z = \frac{2}{1+e^{-2(\vec{w}.X+b)}} - 1 \qquad \text{—(1.8)}$$

ReLu Function: This is to make neuron activity sparse, in contrast to Sigmoid and Tanh. This indicates that the neuron does not fire continuously and that its value occasionally reaches zero. Due to this characteristic, this activation function is among the best at categorization.

$$Z = max(0, \vec{w}.X + b) \qquad \text{—(1.9)}$$

Note: All subsequent models, as well as the fully connected model, employ these activation functions.

1.7 Convolution Neural Networks

Convolutional neural networks (CNN) acquired prominence around 2010 when they outscored all other network architectures on visual input, despite the fact that the concept behind them is considerably older [189]. It is heavily influenced by the human visual system.

Large amounts of "labeled data and neural network topologies that automatically extract characteristics from the data are used to train deep learning models." This specific feature extraction property is advantageous for photographs. Before convolution neural networks, a collection of kernels that would help in extracting the desired feature were defined. For instance, Figure 3.6 demonstrates how to locate the edges in a picture (filters) using the Sobel-Feldman or Laplacian operators.

When attempting to detect objects or identify faces, this manual definition of filters is not entirely applicable. With the aid of convolution neural networks, we can automatically discover the correct filters for a given set of issues.

CNN works by removing all of the filters from the images. As a result, rather than being pre-trained, the network learns the relevant attributes as it trains on a set of images DL models are "incredibly accurate for computer vision applications like object categorization because of this automatic feature extraction."

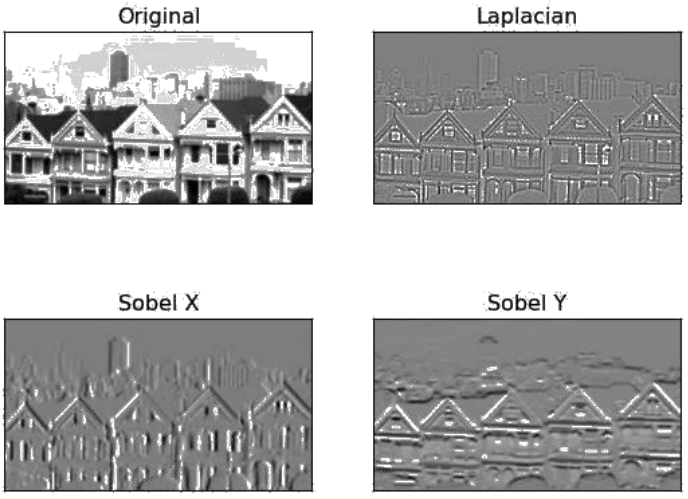

Figure 1.6: Edge detection in image using different filters [6]

Layers in Convolutional neural network

The input images undergo many different procedures before being sent to a CNN model (layers). In this section, we define each operation and discuss its use:

Convolution Layer: An n-d array is subjected to a mathematical procedure called convolution that involves applying a filter (image). A number array known as a weights or parameters array also makes up the filter.

As it slides, the filter multiplies its values by the input image's initial pixel values, or convolves, around the image. In other words, it computes the multiplication of elements. All of these multiplications are added together. As a result, we obtain a filtered image by sliding the filter along the entire image (called an activation map).

It's important to note that in this layer, the initial image is subjected to various filters, each consisting of a set of weights we acquire during the training process.

An activation function layer could come after a convolution layer.

Pooling Layer

Reducing the spatial size of the Convolved Feature is the responsibility of the Pooling layer. The processing power needed to process the data will go down with dimensionality reduction. It also helps in identifying the most significant and prominent features. Among the several pooling operations are:

- The greatest value from the image area that the “Kernel has covered is returned by Max Pooling.”
- The Average Pooling method returns the average value for the area of the picture that the Kernel has covered.
- Sum Pooling: This technique gives the sum of the values it has covered.

Fully Connected layer: After the final attributes have been collected, a dense neural network is utilized to categorize the photos into the proper groups and provide output probabilities based on the training process. (This neural network and the dense neural network detailed in the section devoted to it both have the same basic structure.)

1.7.1 Conventional CNNs

Here, we list the key CNN architectures that served as the cornerstone for contemporary advances in computer vision.

AlexNet: The Alexnet design was greatly influenced by the LeNet architecture, which is commonly recognized as the first attempt at a convolution neural network. The architecture consists of 3 fully connected layers, 5 convolutional layers, and 8 total layers. This model gained a competitive edge in 2012 when it combined these eight layers with two innovative concepts: MaxPooling and ReLU activation.
Many strategies, “including Dropout, Augmentation, and Stochastic Gradient Descent with momentum, were employed to attain this efficiency.”

VGG: VGGNet is the 2014 ImageNet Challenge's runner-up. VGGNet offers two easy guidelines that should be followed:
The only thing separating the two convolution layers is their number of kernels. We halve the picture size at each pooling layer.
ResNet: The ResNet (Residual Network) was first proposed in the 2015 Imagenet competition. The network debuted a novel tactic called "skip connections." The top-5 mistake rate dropped to 3.57%, which is lower than the top-5 rate of human error.

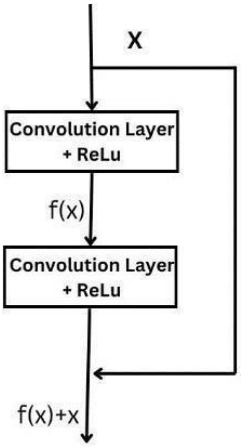

Figure 1.7: Building Blocks of Resnet Architecture [7]

Direct interconnections between two non-consecutive layers are known as skip connections. Including the input x into the output after a few convolutional layers avoids the vanishing gradient issue. In these kinds of blocks, our goal is to identify the residual (difference) between a layer's output and input. We get the same outcome as before when adding the actual input.

MobileNet and SqueezeNet: SqueezeNet and MobileNet are two network topologies that excel at mobile devices and outperform AlexNet in terms of accuracy.
They both attempt to keep the models small and useful without compromising too much accuracy (Re- snet18 - Resnet200; 18 and 200 refer to the number of layers in each design). This is in contrast to the current tendency of constructing more profound networks to enhance accuracy.

1.8 Recurrent neural network

The RNN [190] networks give us the means to add memory to neural networks, and they are essential for processing sequential input. One example of sequential data is a network that predicts what to cook today based on the weather and the dishes from yesterday. Text creation, stock forecasting, voice recognition, and basic networks are a few examples.
Due to how sentences are composed as a series of words, RNNs are most frequently related to text processing and production.
The CONTEXT UNIT at the top of the picture symbolizes the output from the previous instant, and the BTSXPE at the bottom of the drawing denotes the input example at the present time in this illustration of an early primary recurrent network (or Elman RNNs).

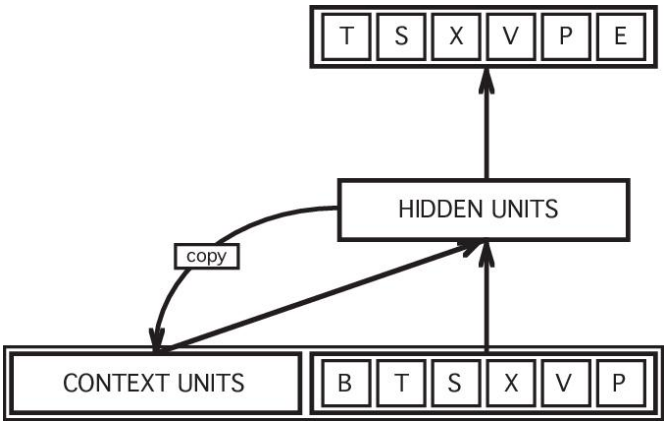

Figure 1.8: Simple Recurrent Network Diagram [8]

1.8.1 RNN Variants

Over time, many RNN variants have been developed, mainly to address the vanishing problem.

Elman RNNs or simple RNNs: This configuration is comparable to a fully connected neural network with a few context neurons. The hidden layer neurons feed information to context neurons. The statuses of the hidden units might then be given back to them during the following input step in this fashion.

By using feed-forward, the input and context units activate the hidden units, which in turn activate the output units. The context units are likewise triggered by feedback from the hidden units. This is what the forward activation entails. There may or may not be a learning period in this time cycle, depending on the work. If this is the case, connection strengths are gradually modified through backpropagation of error after comparing the output with teacher input. The default value for recurrent connections is 1.0 and cannot be altered. The same process is repeated at time step t+1. This time, the hidden units' values at time t exactly match the context units' values. As a result, these context units provide memory to the network.

Each cell in a basic RNN represents the singular operator tanh. A sentence's words are first encoded to a vector known as the embeddings. The cell is then given this vector, and in addition to the final result yet, an intermediate value ht is also computed.

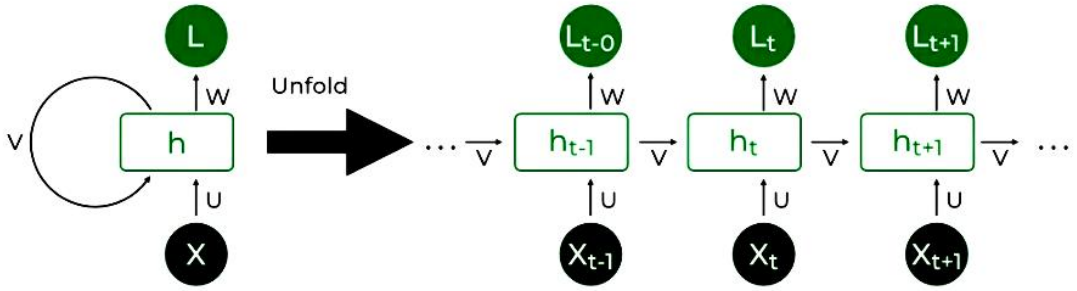

Figure 1.9: Simple Recurrent Neural Networks [9]

Long Short-Term Memory Cells (LSTM) : A gradient is utilized to modify the weight matrices during the backpropagation process. Gradients are computed during the procedure by repeatedly multiplying derivatives. The gradient may practically "vanish" due to these continuous multiplications since the value of these derivatives may be so minimal. In other words, because too tiny gradients predict too few changes to these weights later on, the starting weights of the neural network may never be learned.

LSTM is one remedy for the Vanishing Gradient problem in RNNs [191].

All RNN structures resemble a series of sequential repeating neural network modules. There is only one repeating layer at every step in the straightforward RNN. Instead, there are four in LSTM, and they interact uniquely. The interior of one chain cell can be examined in the figure below.

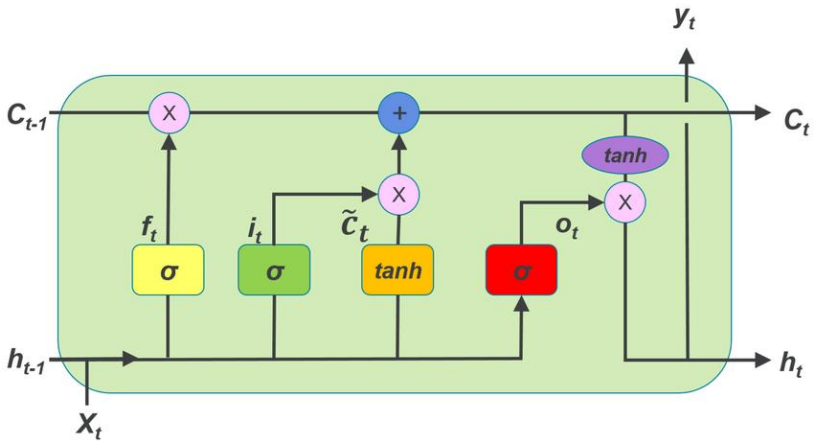

Figure 1.10: Long-Short Memory Neural Network [10]

By examining the image above, we can see that a gating mechanism is employed to prevent large-scale information additions and deletions (An activation function, such as a sigmoid or a tanh, is used to convey additional information).

Gated Recurrent Unit (GRU): In contrast to LSTM, the recurrent gated unit (GRU) [192] only has three gates and lacks an internal cell state. The hidden state of the gated recurrent unit contains the data stored in the internal cell state of the LSTM recurrent unit. This data batch is being moved to the next Gated Recurrent Unit. Each GRU gate is described as follows:

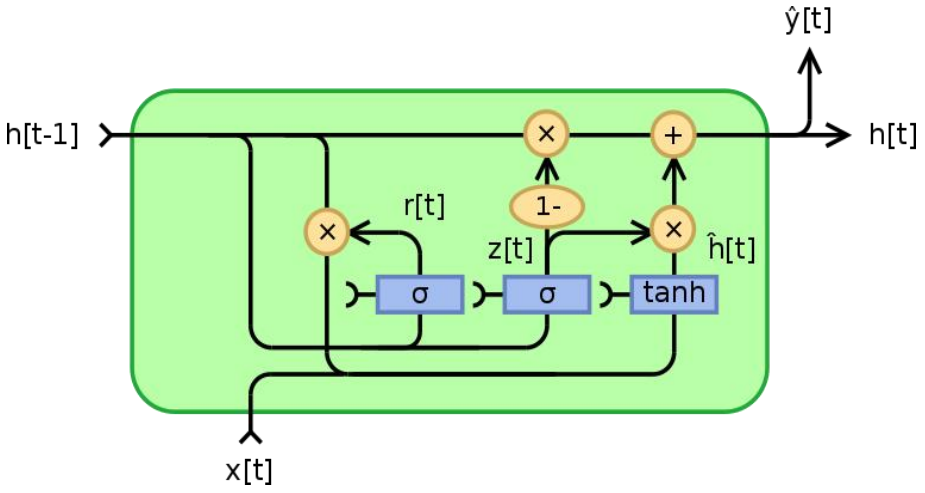

Figure 1.11: Gated Recurrent Unit [11]

The Update Gate(z): determines the amount of prior information that needs to be imparted to future generations. It is similar to the Output Gate of the LSTM recurrent unit.

Reset Gate(r): It determines how much historical data may be eliminated. It functions similarly to the input gate and forget gate of an LSTM recurrent unit.

Current Memory Gate: A common explanation of a gated recurrent unit network typically ignores the current memory gate. It is utilized to give the input some nonlinearity and make the input Zero-mean and is incorporated into the Reset Gate similarly to how the Input Modulation Gate is a part of the Input Gate. By include it in the Reset gate, it also lessens the impact that data received in the past has on data sent in the future.

Bidirectional Recurrent Neural Network: Two RNNs make up a bidirectional recurrent neural network (BRNN). The first is fed an input sequence in reversed order, while the second is fed an input sequence in regular time order throughout training. For every time step, the output from both RNNs is merged via concatenation or summation.

1.9 The Problem: Diabetic Retinopathy

Retina

What the eyes do is enable visual perception. They take in light from the surroundings and provide visual information to your brain. Many different animals have various types of light- sensitive organs. Simple eyes can only tell whether their environment is light or dark, enough to synchronize circadian rhythms, but scarcely qualifies as vison. Complex eyes can discriminate between forms and colors. Some of these complex eyes, like those of humans, have their visual fields significantly overlapped to improve binocular vision, and other complex eyes, like those of rabbits and chameleons, have their visual fields situated with the least amount of overlap possible [11].

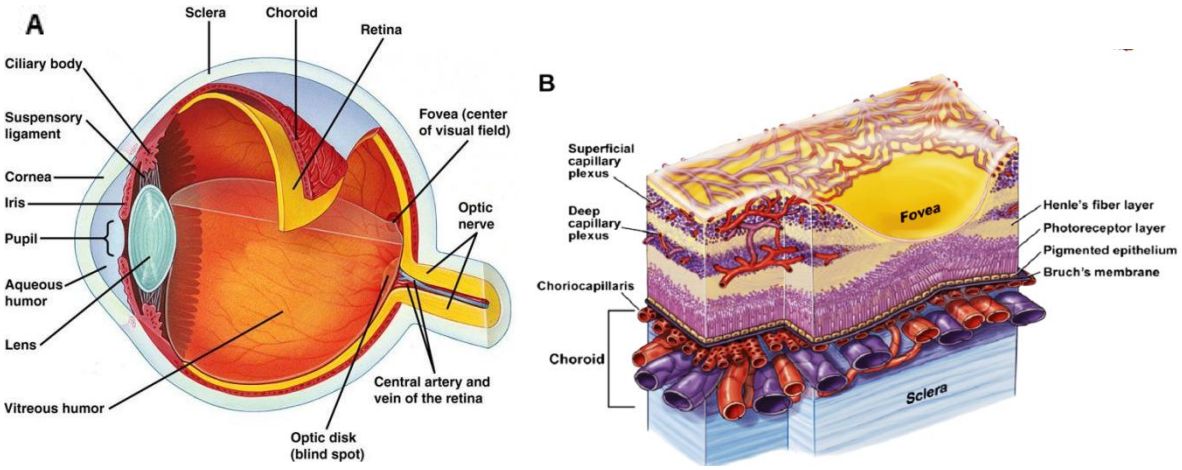

Figure 1.12: Schematic diagram of the retinal vasculature [12]

The retina is the term used to describe the cells that line the interior of the back of your eye. The central and choroidal circulatory systems supply nutrients to the retina, which is a highly vascular structure. The retinas detect light and convert it into electrical or neurological impulses. Cones, which sense color, and rods, which aid in low-light vision, are two types of cells found in the retina that enable vision in low light. Figure 1.1 displays a schematic illustration of the retinal vasculature.

The central blood artery supplies 30% of the retina's blood supply to the inner retina. After passing through the optic disc, the central retinal artery (CRA), which is followed by superior and inferior arteries with 150 m diameters, enters the inner layer of the retina. Eventually, a 5 m-diameter network of capillaries is formed. Nevertheless, the central retinal vein (CRV) receives blood from the retina. The choroidal blood artery, which also serves the photoreceptor-retinal pigment epithelium (RPE) complex near Bruch's membrane, provides about 70% of the blood supply to the retina.

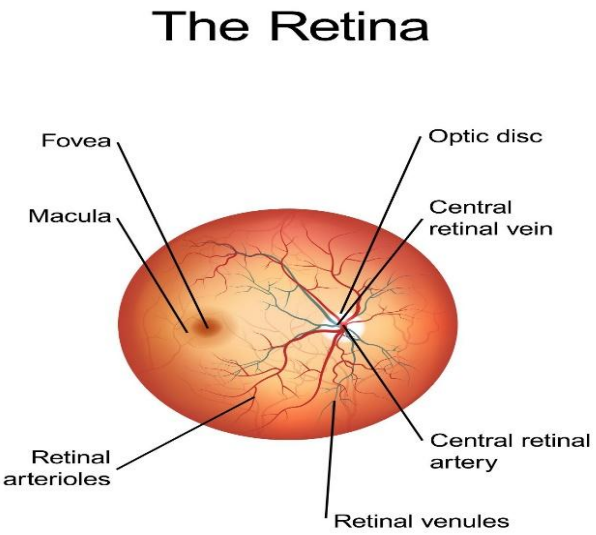

Figure 1.13: Structural elemental features of the retina [13]

The retinal vasculature is made up of arterioles and veins, and the focal retinal conduit is divided into four portions that supply the internal retinal layers in each of the four quadrants at or close to the optic disc. The arteries have a lesser reflectivity than other layers of the retina. They appear darker than the background due to this phenomena.

From the retina, “the optic nerve” sends data to the brain. The optic disc is the portion of the optic nerve head that is most visible inside the retina. Even more brilliant than the surroundings are how spherical it is. Because the pigmentation of average eyes varies, the disc has a contrasted look. [13]

The retina is a well-known source of biomarkers that allow for the early detection of a number of human diseases, including diabetic retinopathy (DR), hypertension, and cardiac conditions [14]. Many eye conditions target the retinal blood vessels specifically. Atherosclerosis, high blood pressure, and other pre-existing vascular diseases, as well as the aging-related natural hardening of artery walls, can all contribute to retinal vascular abnormalities. Retinal vein occlusion (RVO), hypertensive retinopathy, diabetic retinopathy, and central retinal artery occlusion (CRAO) are the most prevalent retinal vascular diseases.

Diabetic Retinopathy

Diabetic retinopathy (DR)would affect one-third of those with diabetes . This ailment is listed as the fifth most frequent reason for blindness worldwide. Diabetic retinopathy is the term used to describe the disease's early stages. The retina's circulatory system is impacted by diabetes. During this stage, the retina's arteries weaken and bleed, creating tiny, dot-like hemorrhages [15]. These leaky veins frequently cause the retina to bulge or edema, impairing vision. The following stage is called proliferative diabetic retinopathy, and it is characterized by parts of the retina that are oxygen-deprived or ischemic due to circulation issues.

Depending on the disease's stage, diabetic retinopathy has a wide range of effects on eyesight. The following list includes some typical signs of diabetic retinopathies; however, diabetes can also result in additional eye ailments [16] like Vision fuzziness, Flashes and floaters, Sudden vision loss.

Patients with diabetes need regular eye exams so that associated eye issues can be found and treated as soon as feasible. Most diabetic patients undergo routine examinations from an internist or endocrinologist who collaborates closely with the ophthalmologist [17]. Vital signs of diabetic retinopathy include changes to the retinal vasculature, such as hemorrhages, neovascularization, cotton-wool patches, and blockages.

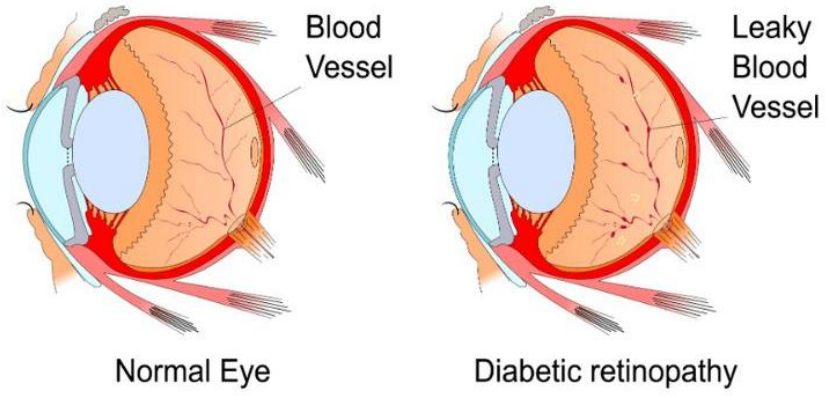

Figure 1.14: The effect of diabetic retinopathy [14]

1.9.1 Hard Exudates

Hard exudates were seen in the outer layer of diabetic patients' retinal vasculature as yellow or white flecks. Hard exudates, often referred to as microaneurysms, are distinguished by their white patches and the absence of blood in the lumen. On rare occasions, these exudates may be deposited right next to the retinal vein. Hard exudates are thought to be the best inter-retinal protein build-up for identifying diabetes mellitus.

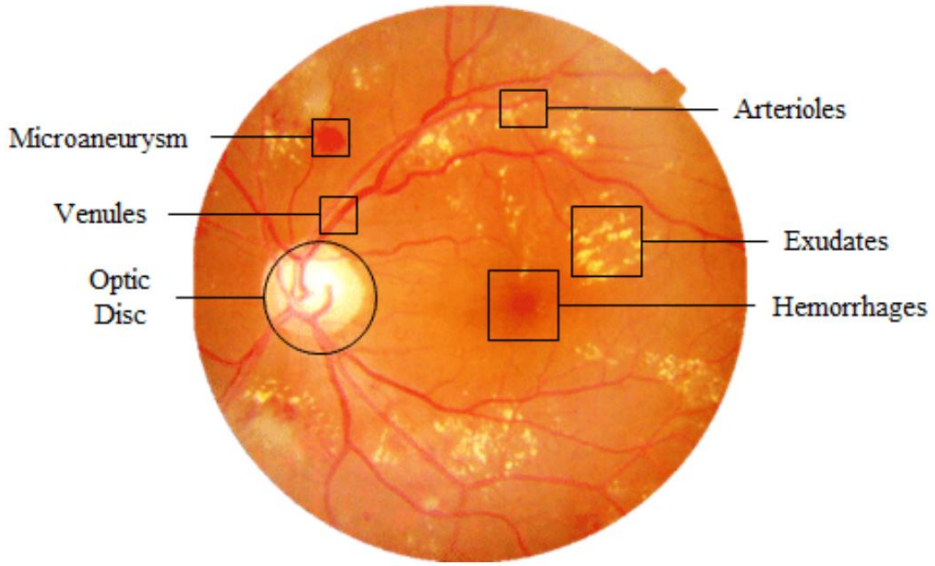

Figure 1.15: Hard exudates in fundus retinal image [15]

1.9.2 Cotton Wool Spots

Cotton Wool Spots (CWS), an anomaly that resembles a fluffy white patch, are discovered in the fundoscopic examination of the retina of human eyes. These are also referred to as retinal infarcts, which refer to tissue damage caused by a lack of oxygen due to a blockage in the blood flow to the tissues. This most commonly occurs in the retina of diabetic patients, placing them at risk for having an immediate stroke.

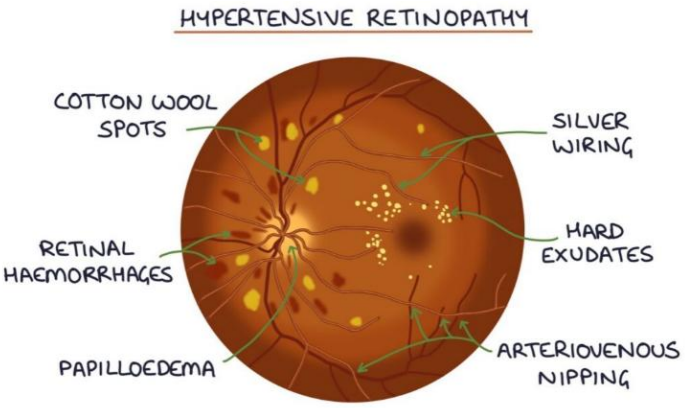

Figure 1.16: Cotton wool spots [16]

1.9.3 Microaneurysm

Typically, a microaneurysm is a tiny region seen in the fundus picture's microvasculature and seems inflated. After examining the eye images, it has been determined that microaneurysm is a biomarker of diabetic neuropathy and an indication of ischemic stroke or an acute stroke typically seen in the fundus retinal imaging.

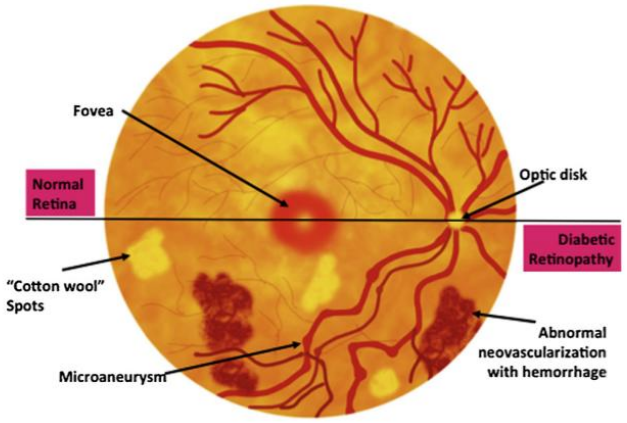

Figure 1.17: Microaneurysm [17]

1.10 Stages of Diabetic Retinopathy

The classification of diabetic retinopathy (DR) into different kinds is based on severity. Proliferative diabetic retinopathy (PDR) and non - proliferative diabetic retinopathy are the two distinct stages of diabetic retinopathy (NPDR). Patients with DR are

asymptomatic in the early stages, but as the condition progresses, floaters, distortions, blurred sight , and a gradual loss of visual acuity develop.[18]

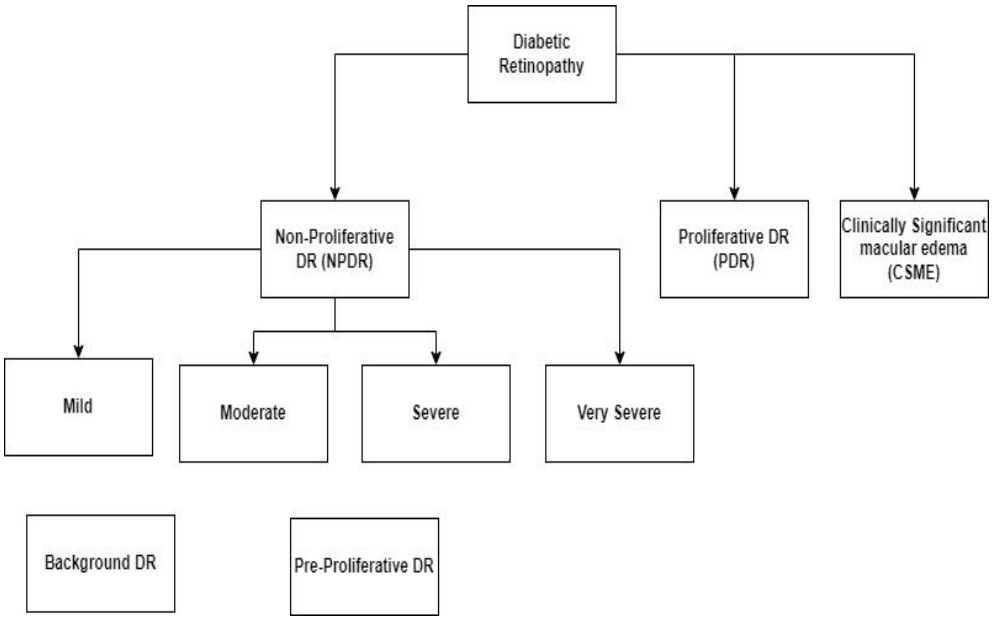

Figure 1.18: Stages of DR [18]

Mild Non-proliferative DR begins with a condition called diabetic retinopathy. It can be recognized by the retina of the eye's existence of spots, red markings, microaneurysms, and hemorrhage. Hemorrhage occur in the focal layer of the retina of the eye. Hemorrhage indicate irregular blood flow from the blood vessels in the retina. Patches of inflated, tiny blood vessels in the retina of the eye are known as micro aneurysms, and they are caused by a change in their makeup.

“Moderate non-proliferative diabetic retinopathy” is the second stage of the disease. Several microscopic blood vessels in the retina of the eye may get blocked at this time due to a reduction in the supply of oxygen and nutrients to those areas.

With severe non-proliferative diabetic retinopathy, a sizable portion of the retina's tiny retinal blood capillaries become clogged, affecting additional areas of the retina. When the blood vessels in the retina do not receive enough oxygen an d nutrients, it is known as retinal ischemia.

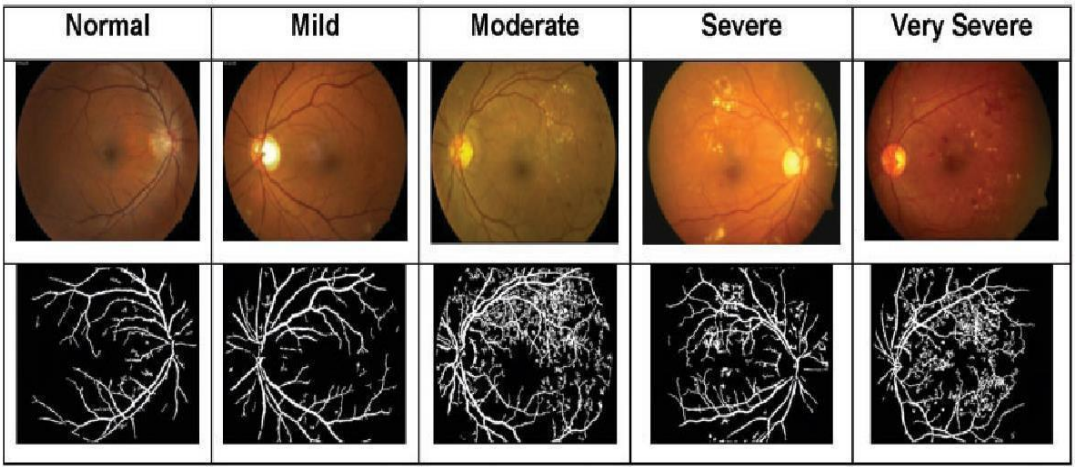

Figure 1.19: Fundal images of stages of DR [19]

Proliferative retinopathy, the final stage of DR, is characterized by the development of abnormally new blood vessels, which raises the possibility of visual loss. These aberrant blood vessels grow quite quickly. The retina of the eye tries to compensate for the restricted flow caused by the formation of aberrant retinal blood vessels in response to a lack of oxygen. The aberrant blood arteries are fragile and paper-thin, and they are prone to breaking. As a result, the retina may separate or crumple. The PDR displays a more severe visual impairment than the NPDR because it affects both central and peripheral vision [19].

1.11 Research Gaps in Diabetic Retinopathy

Despite significant advancements in the detection and management of diabetic retinopathy (DR), several research gaps still need to be addressed. Some of the significant research gaps in diabetic retinopathy are:

Early Detection: Early detection of DR remains a significant research gap. More research is needed to develop better screening tools for early detection, including non-invasive imaging modalities and biomarkers.

Risk Prediction: There is a need to develop better risk prediction models to identify individuals at high risk for DR. Such models can help tailor screening intervals and treatment strategies.

Understanding Progression: The mechanisms underlying DR progression remain poorly understood. More research is needed to understand better the biological pathways and factors involved in DR progression.

Personalized Treatment: There is a lack of personalized treatment options for DR. Future research should focus on developing personalized treatment strategies based on individual patient characteristics.

Telemedicine: The use of telemedicine for DR screening and management is a promising area, but more research is needed to validate its effectiveness and identify best practices.

Patient Education: Patient education is an essential component of DR management, yet there is a lack of research on effective educational interventions.

Cost-Effectiveness: There is a need for more research on the cost-effectiveness of DR screening and management strategies to inform policy decisions and resource allocation.

Addressing these research gaps can help to improve the prevention, detection, and management of diabetic retinopathy and ultimately improve patient outcomes.

1.12 Research Objectives

- To analyze the existing approaches and supporting datasets for distinguishing between “Proliferating and non-proliferating diabetic retinopathy”
- To design and implementation of the DL system for the detection of DR stages
- To implement the proposed approach with various risk control factors to reduce vision loss in Diabetic Retinopathy
- Evaluation of the proposed approach with existing models

1.13 Research Questions

The thesis aims to research the most efficient methods for early detection of DR. It analyses the impact of DR on pregnant women and children. It also aims to present the modern techniques used to detect DR.

The following are the research questions which is answered in this thesis

1. What are the traditional methods used to detect DR?
2. What are various methods proposed by the researchers in the literature?
3. What is the effect of DR on pregnant women and children?
4. What is the role of Computer Vision in the detection of DR?
5. What is the effect of Diabetic Retinopathy on Pregnant women?
6. What is the best approach to recognizing DR stages?

1.14 Problem Formulation

The leading cause of blindness worldwide, DR is a progressive microvascular complication that affects a considerable number of diabetic patients. Early identification and treatment of DR are crucial in preventing vision loss and improving patient outcomes. However, the conventional manual screening process for DR is time-consuming, expensive, and prone to errors. A deep learning-based method using convolutional neural networks (CNNs) is suggested to overcome these drawbacks and improve the precision and effectiveness of DR detection.

Creating and evaluating a CNN model that can automatically identify and categorize DR from retinal fundus pictures is the main objective of this study. The research will entail gathering and pre-processing a large number of retinal fundus pictures from diabetic individuals with different degrees of diabetic retinopathy. Expert ophthalmologists will annotate the images to provide ground truth labels for training the deep learning model.

The problem can be defined as follows:

Given a large dataset of retinal fundus images from diabetic patients, the objective is to design and optimize a convolutional neural network (CNN) model for automated DR detection and classification. The CNN should accurately classify retinal fundus images into different DR categories based on disease severity, ranging from mild to severe stages. The performance of the proposed CNN model will be evaluated using various

performance metrics, including “Accuracy, Precision, Recall and area under the receiver operating characteristic curve (AUC-ROC).”

The research will assess the performance of the proposed DL approach with the conventional manual screening procedure to assess its accuracy, effectiveness, and cost-effectiveness in DR detection. The study will also acknowledge potential limitations, such as the quality and size of the training dataset, the model's generalizability to diverse populations, and the availability of specific equipment or software in clinical settings.

Overall, the successful development and implementation of the deep learning-based approach could lead to a significant reduction in the workload of ophthalmologists, faster and more accurate DR diagnosis and treatment, improved patient outcomes, and decreased burden on healthcare systems due to DR-related complications. Furthermore, the future scope of the research includes potential extensions to incorporate other medical imaging modalities, the integration of telemedicine systems, and the optimization of the proposed approach to further enhance its diagnostic capabilities in ophthalmology.

1.15 How the research can contribute to reducing diabetic retinopathy:

1. **Early Detection and Diagnosis:**
    - The use of machine learning and deep learning algorithms allows for the development of automated systems that can accurately and efficiently analyze retinal images for signs of diabetic retinopathy.
    - Early detection is crucial in preventing the progression of diabetic retinopathy to more severe stages, as timely interventions can be initiated to address the condition.
2. **Improved Screening Procedures:**
    - The research proposes the use of advanced technologies to enhance screening procedures, replacing or supplementing traditional methods that may be time-consuming and prone to human error.

- Automated screening systems based on deep learning models can process large datasets, improving the effectiveness and scalability of screening programs.

3. **Customized Treatment Plans:**
    - By identifying individuals at high risk through improved risk prediction models, the research contributes to the development of personalized and customized treatment plans.
    - This allows healthcare professionals to tailor interventions based on the severity and progression of diabetic retinopathy in individual patients.
4. **Efficient Telemedicine:**
    - The study suggests that telemedicine shows promise for diabetic retinopathy screening and management. Implementing efficient telemedicine practices can enhance accessibility to healthcare services, particularly in remote or underserved areas.
    - Patients can benefit from remote screening, reducing the need for physical visits to healthcare facilities.
5. **Reduction in False Positives:**
    - Machine learning models, when properly trained and validated, can reduce false-positive diagnoses. This means that fewer patients are unnecessarily referred for further evaluation, leading to more targeted and efficient use of healthcare resources.
6. **Speed and Accessibility:**
    - The use of machine learning and deep learning algorithms can significantly speed up the diagnosis process. Automated systems can quickly analyze retinal images, providing timely results to both patients and healthcare providers.
    - The increased efficiency contributes to better accessibility to screening, especially in regions with limited access to specialized healthcare services.
7. **Integration into Clinical Workflows:**
    - The successful integration of machine learning-based diabetic retinopathy screening systems into clinical workflows and electronic health records enhances practical applicability in real-world healthcare settings.

- Seamless integration facilitates the incorporation of these technologies into routine healthcare practices, ensuring widespread adoption.

1.16 Chapter Summary

Chapter 1 provides an overview of various aspects of medical imaging, with a specific focus on diabetic retinopathy (DR) and the application of deep learning (DL) in its detection and classification. The chapter covers fundamental concepts in medical imaging technologies, introduces artificial intelligence (AI), machine learning, and deep learning, and elucidates the stages of DR. The research objectives outlined in this chapter include analyzing existing approaches, designing a DL system, and addressing research gaps in DR. It concludes by formulating research questions and problem statements, emphasizing the imperative for early detection and improved management of DR through the implementation of convolutional neural networks (CNNs).

1.17 Thesis Organization

The next chapters of the Thesis are organized as below

Chapter 2: Literature Survey
Following the introduction, Chapter 2 delves into a thorough Literature Survey. This chapter critically reviews existing research and studies related to diabetic retinopathy detection, emphasizing various methodologies and techniques employed by researchers globally. It highlights the evolution of techniques over time and identifies gaps or areas requiring further exploration.

Chapter 3: Image Processing Techniques and Evaluation Metrics
Chapter 3 is dedicated to Image Processing Techniques and Evaluation Metrics. It elucidates the various image processing methodologies applied in diabetic retinopathy detection. The chapter outlines the rationale behind the chosen techniques and details the evaluation metrics used to assess the performance of these methodologies.

Chapter 4: Design and Implementation Using Machine Learning Based Methodology

Building upon the literature review and image processing techniques, Chapter 4 transitions into the Design and Implementation phase. This section outlines the methodology chosen for diabetic retinopathy detection, with a primary focus on machine learning. It discusses the design considerations and the intricacies of implementing a machine learning-based model for this specific medical application.

Chapter 5: Results and Analysis

The core findings of the research are presented in Chapter 5. This chapter provides a detailed analysis of the results obtained from the implemented machine learning model. It discusses the model's efficacy in detecting diabetic retinopathy, supported by quantitative and qualitative analyses. The chapter also addresses any challenges faced during the implementation and their implications on the results.

Chapter 6: Conclusion and future work

The thesis culminates in Chapter 6, where the researcher draws conclusions based on the findings. This section synthesizes the entire research journey, highlighting key takeaways, contributions to existing knowledge, and implications for future research. Additionally, the chapter may discuss the real-world applicability of the developed model and propose recommendations for further refinement or application in clinical settings.

This structured approach ensures a logical flow of information, guiding the reader through the research process from the introductory concepts to the final insights and conclusions.

CHAPTER 2
LITERATURE SURVEY

A microvascular condition of diabetes called (DR) is a main global purpose of vision loss and blindness. It affects roughly one-third of diabetics, and as the prevalence of diabetes rises, so does its occurrence. To prevent or delay vision loss, early detection and prompt management are essential. The best method for detecting and keeping track of DR is diabetic retinopathy (DRG), which includes using a fundus camera to take photographs of the retina. Unfortunately, manual DRG picture interpretation is laborious, subjective, and sensitive to both inter- and intra-observer variation. Hence, reliable and effective DR detection requires the use of automated algorithms to analyze DRG pictures. In recent years, research on DR detection has increased dramatically using ML and DL techniques. This review of the literature attempts to highlight the existing issues and research gaps while also reviewing and summarizing recent developments in automated DR detection. With this research, the intricacy of diabetic retinopathy is identified, and a greater understanding of it is gained.

2.1 Diabetic Retinopathy Literature Survey

The various earlier research on Diabetic Retinopathy is categorized and presented below:

1. Diabetic Retinopathy Detection and Classification using Deep Learning:

A deep learning ensemble strategy is presented in the research article [20] by Qummar et al. (2019) to increase the precision of diabetic retinopathy detection. “CNNs and LSTMs” are two examples of the DL models that the authors suggest merging to improve the effectiveness of detection algorithms. The predictions from each model are pooled using a weighted averaging method after each model has been trained on a distinct subset of data. The findings highlight the promise of the ensemble technique for the early identification and management of diabetic retinopathy by showing that it outperforms individual models and conventional machine learning algorithms.

A data mining framework for classifying retinal pictures based on a new multistage prediction algorithm is presented in the research article [21] by AL-Saedi and Jelinek (2018). The authors suggest a unique method that integrates several data mining approaches to raise the classification accuracy of retinopathy. The framework uses numerous prediction phases, each of which improves on the findings of the preceding step. The experimental outcomes reveal the proposed algorithm's effectiveness in correctly identifying retinopathy photos, highlighting its potential to help with the diagnosis and treatment of retinal illnesses.

The clinical study [22] by Yabe et al. (2019) explores the effects of dietary instructions on prediabetes subjects. The study focuses on dietary balance and meal sequencing as management strategies for prediabetes. The experiment evaluated many aspects of glucose metabolism and cardiovascular risk variables using an exploratory, cluster-randomized methodology. The results highlight the importance of dietary tactics in the prevention and treatment of diabetes by indicating that dietary interventions emphasizing meal sequencing and nutritional balance might have a favorable influence on prediabetes outcomes.

A system for identifying DR using DL algorithms is described in the research article [23] by Qiao et al. (2020). The authors suggest a two-stage strategy that combines an early detection technique for non-proliferative diabetic retinopathy with the prognosis of microaneurysms. The system's deep learning algorithms are quite accurate in identifying and categorizing retinal defects linked to diabetic retinopathy. The suggested technique could help in diabetic retinopathy early identification and treatment.

The study article presents a U-net based approach for automatically segmenting hard exudates in fundus pictures [24] by Zong et al. (2020). To increase the segmentation accuracy, the suggested technique makes use of a residual connections and an Inception module.

The outcomes show how well the method works at precisely segmenting hard exudates, which are crucial signs of diabetic retinopathy development. The technique has the potential to improve the efficacy and precision of methods for screening for and monitoring diabetic retinopathy.

A deep image mining strategy is presented in the publication [25] by Quellec et al. (2017). The authors suggest a method for classifying retinal pictures for the presence of diabetic retinopathy by extracting pertinent characteristics using deep learning techniques and image mining algorithms. The strategy employs a hierarchical feature extraction procedure to record both global and local picture properties. The findings show the method's ability to screen for diabetic retinopathy with high accuracy and efficiency, advancing the design of automated screening devices.

A thorough analysis of the use of CNNs in medical image interpretation is provided in the publication [26] by Sarvamangala and Kulkarni (2021). The authors discuss several CNN designs and their uses for disease detection, segmentation, and classification in medical imaging tasks. The survey highlights the promise of these models in enhancing diagnosis, treatment planning, and patient care while discussing the difficulties and developments in CNN-based medical image interpretation.

The paper [27] by Khojasteh, Aliahmad, and Kumar (2018) focuses on the examination of fundus images for the identification of exudates, hemorrhages, and microaneurysms, which are significant indicators of diabetic retinopathy. The authors suggest a technique to recognize these retinal lesions using deep learning characteristics obtained from fundus pictures. The study shows how well the method works for precisely locating and identifying anomalies, which helps with the early diagnosis and treatment of diabetic retinopathy.

A two-step CNN technique is suggested in the study [28] by Eftekhari et al. (2019). Microaneurysms are significant indicators of diabetic retinopathy. The authors create a network architecture that first pinpoints potential areas with microaneurysms before identifying whether they are genuine positives or false positives. The technique shows

great promise for early identification and follow-up of diabetic retinopathy by detecting microaneurysms with excellent precision.

CNN technique for the diagnosis of DR using retinal fundus pictures is presented in the publication [29] by Garca et al. (2017). The authors create a CNN model that learns to categorize the illness severity levels based on visual attributes. The efficiency of CNNs in automated disease screening and diagnosis is demonstrated by the suggested method's excellent accuracy in detecting diabetic retinopathy.

A two-stage deep convolutional neural network (CNN) architecture is suggested in the study [30] by Yang et al. (2017) for the identification and classification of diabetic retinopathy lesions. The authors create a CNN model that identifies lesions initially and then categorizes them according to their severity. The method is a helpful tool for the early detection and monitoring of diabetic retinopathy because of its high lesion identification and grading accuracy.

Chudzik et al. (2018) published an article titled [31] that describes a fully convolutional neural network (CNN) method for detecting microaneurysms in retinal fundus pictures. The authors create a CNN architecture that allows for pixel-level categorization of microaneurysms by processing the entire picture at once. The suggested technique successfully detects microaneurysms with accuracy, aiding in the early identification and treatment of diabetic retinopathy.

Williams et al. (2004) published a study titled [32] that offers a comprehensive assessment of the subject's epidemiology. The frequency and incidence rates of these disorders are examined through an analysis of the body of research by the writers, who also go through the risk factors that contribute to their emergence. Understanding the impact of these illnesses is made easier by the review's insightful observations on the epidemiological features of diabetic retinopathy and macular edema.

The paper [33] by Wang et al. (2020) describes a system for “Automated DR grading and lesion detection that is based on the modified R-FCN (Region-based Fully

Convolutional Networks) object-detection algorithm". The R-FCN algorithm is modified by the authors to recognize and categorize lesions connected to diabetic retinopathy. The technology shows potential for automated diabetic retinopathy evaluation by achieving encouraging results in terms of accuracy and efficiency.

Casanova et al. (2014) published a study [34] that uses random forest techniques to categorize diabetic retinopathy. The use of random forests, a machine learning approach, is investigated by the authors for the analysis and classification of retinal pictures associated with diabetic retinopathy. The study demonstrates the possibility of the random forest technique for classifying diabetic retinopathy and assesses its effectiveness.

Using image analysis, [35] by Pires et al. (2017) describes a direct method for referring patients with diabetic retinopathy. The authors provide a strategy for determining the necessity for referral that goes beyond particular lesions and takes into account the general features of the retinal picture. The study offers an alternate viewpoint for assessing diabetic retinopathy, emphasizing the early detection of situations that need for specialist care.

A thorough overview of automatic diabetic retinopathy detection is provided in the publication [36] by Mateen et al. (2020). The authors go over several datasets, techniques, and assessment criteria that are applied in the field. The paper provides insights into the cutting-edge methodologies and performance evaluation of deep learning approaches, machine learning algorithms, and image processing techniques for diabetic retinopathy identification.

In the paper [37] by delaPava et al. (2021), a DL model for the categorization of DR in eye fundus photographs is presented. The authors suggest a two-stage method that involves first identifying retinal lesions and then categorizing diabetic retinopathy in accordance with the existence and kind of these lesions. The study emphasizes the value of DL methods for categorizing DR.

“The feasibility of detecting the Gravity and particular features of DR in fundus photography” is examined in [38] by Wang et al. (2019). The authors suggest a method for properly determining the severity of and identifying distinctive characteristics of diabetic retinopathy that blends deep learning methods with image analysis. The study highlights fundus imaging's potential for precise diabetic retinopathy identification.

The paper [39] by Wei et al. (2019) presents a “DL-based smartphone application for the real-time diagnosis of retinal abnormalities, including DR, in fundus pictures.” The authors suggest a smartphone- deployable deep learning model for processing on-device and quick detection of retinal problems. The work emphasizes the possibility for effective and convenient diabetic retinopathy screening using smartphone-based deep learning apps.

Gondal et al. (2018) published a work titled [40] that focuses on this subject. The authors suggest a technique for automatically locating and categorizing lesions connected to diabetic retinopathy using weakly-supervised learning. The work shows the possibility for accurate lesion diagnosis in diabetic retinopathy screening using weakly-supervised learning approaches.

Gayathri et al. (2020) published a study titled [41] that focuses on the automated classification of diabetic retinopathy utilizing these characteristics. The authors provide a strategy for categorizing diabetic retinopathy into binary and multiclass categories that combines texture analysis with Haralick characteristics and multiresolution analysis. The work shows the potential for feature- based methods for precisely classifying diabetic retinopathy.

The study [42] by Richey et al. (2020) describes the real-time detection of maize crop disease utilizing a deep learning-based smartphone application. This article investigates the application of deep learning and smartphone technologies for crop disease diagnosis, albeit it is not directly connected to diabetic retinopathy. The work emphasizes the applicability of comparable strategies for further image-based classification challenges.

Majumder and Kehtarnavaz (2021) place focus on [43], which highlights the use of inertial sensing in conjunction with vision to identify human activity. Although not explicitly related to diabetic retinopathy, the work investigates the integration of sensory modalities for human action detection, which may have consequences in several domains of computer vision and pattern recognition.

The 2016 study [44] by Chandrakumar and Kathirvel focuses on the classification of DR using DL. The authors suggest using deep learning to categorize the various phases of diabetic retinopathy. The study shows how deep learning algorithms may be used to accurately classify diabetic retinopathy.

According to Wang et al. (2019), [45] presents a deep learning-based approach for finding lesions connected to the disease. In order to concentrate on possible lesion sites and enhance detection performance, the authors offer an architecture that conducts zoom-in operations. The work demonstrates the promise of deep learning algorithms for precise diabetic retinopathy lesion diagnosis.

The paper [46] by Pour et al. (2020) suggests an automated system for detecting and monitoring diabetic retinopathy that makes use of contrast limited adaptive histogram equalization (CLAHE) and efficient convolutional neural networks (CNNs). Based on retinal fundus pictures, the authors show the efficacy of their method for precisely identifying and tracking diabetic retinopathy.

The publication [47] by Majumder et al. (2020) describes a smartphone application for the five stages of DR that is based on DL. The authors develop a deep learning model that can be used on a smartphone to identify and classify the various phases of diabetic retinopathy in real-time. The work shows the possibility for effective and convenient diabetic retinopathy screening using deep learning models on mobile devices.

Deep neural networks (DNNs) are the main subject of the study [48] by Gao et al. (2019). Based on retinal fundus pictures, the scientists suggest a DNN-based method for precisely identifying diabetic retinopathy.

The study shows how well the suggested DNN model performs in categorizing the various degrees of diabetic retinopathy severity.

The recognition of retinal abnormalities using regional multitask learning is covered in the work [49] by Wang et al. (2019). The authors suggest a DL-based method for precise retinal abnormality diagnosis that makes use of regional information in fundus pictures. The study shows that the suggested regional multitask learning model is capable of correctly identifying a number of retinal defects.

According to Marn et al. (2011), [50] is a supervised technique for segmenting blood vessels in retinal images. For precise segmentation of blood vessels, the authors suggest an approach that combines characteristics based on moment invariants and grey levels. The study shows how well the suggested strategy works for precisely segmenting blood arteries in retinal pictures.

Goatman et al. (2011) published an article titled [51] with the main goal of identifying new vessels on the optic disc. The authors offer a strategy that makes use of image processing tools to find new blood vessels and test its effectiveness using retinal images. The study shows how the suggested strategy works well for precisely identifying new vessels on the optic disc.

Li et al. (2014) published a study titled [52] that examines the use of CNNs for this purpose. The authors offer a CNN-based method for categorizing medical pictures, which has uses across several medical specialties. According to the study, CNNs are good at correctly identifying medical pictures and have the potential to help doctors make diagnoses.

In their study [53] published in 2021, Mushtaq and Farheen Siddiqui describe the use of deep learning to identify diabetic retinopathy. The authors suggest using deep learning to automatically identify diabetic retinopathy in retinal pictures. The paper demonstrates the potential of DL in the identification of DR and assesses the effectiveness of the suggested technique.

[54] by S. K. Pandey and V. Sharma: This study examines the rising prevalence of diabetic retinopathy in recognition of World Diabetes Day 2018. It emphasizes how crucial it is to control diabetic retinopathy, a serious consequence of diabetes, via early identification and treatment. The essay focuses on the importance of education and preventative actions in the fight against DR.

Zago et al. offer a approach for identifying DR in their 2020 publication [55] that combines convolutional neural networks (CNNs) with red lesion location.. The authors create a system for detecting diabetic retinopathy from retinal images that comprises picture pre-processing, red lesion localization, and a CNN-based classification algorithm. The study shows how well the suggested method works for precisely identifying diabetic retinopathy.

A suggested worldwide clinical severity scale for diabetic retinopathy and diabetic macular edema is presented in the publication [56] by Wilkinson et al. (2003). Based on clinical symptoms seen in retinal scans, the authors offer recommendations for assessing the severity of various disorders. Through the use of severity measures, various clinical settings can assess diabetic retinopathy and diabetic macular edema consistently.

The paper [57] by Dai et al. (2021) presents a DL method for the diagnosis of DR throughout the disease spectrum. The authors develop a convolutional neural network (CNN) model and train it on a large dataset of retinal images. The deep learning algorithm has great accuracy in identifying diabetic retinopathy and may help medical practitioners make an early diagnosis and start treating the condition.

This article by Sadda et al. (2020) is titled [58]and it focuses on the quantitative evaluation of the condition's severity. The authors go over numerous imaging techniques and quantitative data that may be used to gauge the severity of diabetic retinopathy, including fundus autofluorescence, retinal vascular analysis, and optical coherence tomography. The need of objective and quantitative assessment for the management of diabetic retinopathy is emphasized in the study.

He et al. (2016) published a study titled [59]that presents the idea of residual learning as a solution to the degradation issue in deep neural networks. Instead of explicitly learning the required underlying mappings, the authors suggest a deep residual network design that enables the learning of residual mappings. This method makes it possible to build very deep neural networks, which enhances performance on image recognition tasks.

Feature pyramid networks (FPN), a network architecture created for object detection tasks, are presented in the paper [60] by Lin et al. (2017). By building a pyramid of multi-scale feature maps, FPN overcomes the difficulty of identifying things at various sizes. In order to create feature pyramids that can efficiently collect features at various sizes and enhance object identification performance, the authors suggest a top-down approach with lateral linkages.

The publication [61] by Kumaran and Patil (2018) explains how to segment data and pre-process it for the purpose of detecting diabetic retinopathy in human eyes. The authors go through a number of feature extraction, segmentation, and image enhancement algorithms that are used in the identification of diabetic retinopathy. The review emphasizes how crucial these methods are for increasing the precision of diabetic retinopathy identification.

Knowledge matters: The value of previous information for optimization is covered in the 2016 study [62] by Gülçehre and Bengio. The authors emphasize the significance of past knowledge in directing learning, regularization, and enhancing model generalization abilities. The importance of include past information in the design and training of machine learning algorithms is emphasized in the study.

An overview of current advancements in the diagnosis of diabetic retinopathy is given in [63] by Amin et al. (2016). The authors describe numerous methods for the automatic identification of diabetic retinopathy using retinal pictures, such as image processing methods, machine learning algorithms, and deep learning models. The review emphasizes the developments and difficulties in this area.

It is suggested to use piecewise threshold probing and a matching filter response to identify blood vessels in retinal images in the publication [64] by Hoover et al. The authors outline a technique that improves blood vessel visibility and makes it possible to segment them in retinal pictures. The research advances automated methods for the examination of retinal vasculature.

The University of Auckland's [65] by Abdulla and Chalakkal (2018) is a database that includes retinal pictures for diabetic retinopathy research. It is a useful resource for developing and testing algorithms for the study and identification of diabetic retinopathy. In the study [66] by Li et al. (2019), the effectiveness of deep learning systems for diabetic retinopathy screening is evaluated. With the use of a sizable dataset of retinal pictures, the authors evaluate the diagnostic efficacy of several models. The study emphasizes the potential of deep learning methods for detecting diabetic retinopathy. Alyoubi et al.'s review article [67] offers an overview of deep learning methods for detecting diabetic retinopathy. The authors go over several methods and architectures that deep learning models utilize to reliably identify diabetic retinopathy in retinal pictures.

In their article [68] published in 2020, Mishra et al. investigate the application of DL for the diagnosis of DR. The scientists' suggested deep learning-based technique for the automated detection of DR employs (CNNs). The work offers proof that DL can improve the precision of detection.

The focus of [69] by Ayala et al. (2021) is on the advancement of diabetic retinopathy detection via the application of DL methods. For precise identification of diabetic retinopathy characteristics in retinal pictures, the authors suggest a deep learning model that combines a CNN with attention processes.

A multi-channel convolutional neural network (CNN) is presented in the paper [70] by Butt et al. (2019) to identify diabetic retinopathy from fundus pictures. The authors suggest a deep learning architecture with several input channels to increase the detection precision of diabetic retinopathy. A compute supported diagnostic system for

different degrees of diabetic retinopathy is presented in the research [71] by Abdel Maksoud et al. (2022). To reliably categorize various phases of DR, the authors suggest a hybrid deep learning approach that integrates many neural network topologies.

An overview of deep learning methods for categorization and diagnosis of diabetic retinopathy using fundus pictures is given in the review paper [72] by Tsiknakis et al. (2021). The authors go over several DL techniques and how they might be used to diagnose DR.

The 2020 study [73] verifies a method based on DCNN for detecting DR. By comparing the algorithm's effectiveness for detecting diabetic retinopathy with that of human practitioners, the authors show the potential of artificial intelligence in this area.

The study [74] by Sebti et al. (2022) presents a DL method for the detection of DR. The efficacy of a deep learning model, specifically created by the authors for the diagnosis of diabetic retinopathy, is assessed. The study helps to create diabetic retinopathy detection techniques that are more precise and effective. Shi et al.'s paper, [75] is concerned with evaluating image quality in color fundus retinal images. For an appropriate study and diagnosis of diabetic retinopathy, the authors suggest a method to assess the quality of retinal pictures.

The paper [76] by Henge and Rama (2016) describes how to classify and recognize mixed connective consonants and symbols using a closed-loop neural fuzzy hybrid system. It illustrates how neural fuzzy networks can be utilized for pattern identification applications, while not having anything to do with diabetic retinopathy.This study proposes a neural fuzzy hybrid rule-based inference system for the estimation of the likelihood of a heart attack, titled [77]. Although unrelated to diabetic retinopathy, it illustrates how neural fuzzy networks might be used to make predictions in the field of medicine.

Henge and Rama (2016) published [78] in which they compare and analyze optical character recognition (OCR) algorithms. The article discusses character recognition techniques, which may be useful for processing text in medical pictures even if it has nothing to do with diabetic retinopathy specifically. Henge and Rama (2018) published a study titled [79] that explores the implications and results of a proposed methodology for optical character recognition (OCR). It offers insights into the creation and assessment of OCR systems by presenting a graphical representation and algorithmic flow for OCR.

In their work titled [80] published in 2022, Gundluru et al. discuss how to improve the diagnosis of diabetic retinopathy by combining a deep learning model and the Harris Hawks Optimization technique. To increase the precision of diabetic retinopathy diagnosis in retinal fundus pictures, the authors suggest a hybrid technique.

The prevalence and features of diabetic retinopathy in the Asia-Pacific are covered in [81] by Chua et al. (2017). The epidemiology, risk factors, screening, and therapy of diabetic retinopathy in this group are briefly discussed by the authors.
From Harvard Health Publishing, [82] This website offers details about retinopathy, including as its description, causes, symptoms, diagnosis, and therapy. It provides a thorough analysis of retinopathy and its effects on eye health.

According to Naz et al. (2022), [83] describes an automated unsupervised deep learning-based method for detecting diabetic retinopathy. The authors suggest a technique for analyzing retinal pictures and determining the existence of diabetic retinopathy using a deep learning model.

A pneumonia diagnosis scheme is presented in [84] by Masud et al. (2021). This method takes use of an ensemble learning algorithm and hybrid features that are taken from chest radiographs. The authors propose a strategy that integrates a number of parameters and makes use of ensemble learning techniques to improve the accuracy of pneumonia detection.

By applying texture-based techniques, [85] by Choras (2013) examines the study of firearm striations for forensics image retrieval. For photos of firearm striations, the author suggests a texture analysis method that, by matching and obtaining pertinent photographs from a database, can help with forensic investigations.

In their paper titled [86] published in 2018, Yang and Jiang introduce an adaptive bi-weighting approach for automatic initialization and model selection in Hidden Markov Model (HMM)-based hybrid meta-clustering ensembles. To increase the effectiveness and resilience of meta-clustering ensembles, the authors provide an approach that adaptively weights various clustering outcomes.

2. Retinal Image Analysis and Segmentation:

A technique for identifying melanoma from dermoscopy photos using an artificial neural network (ANN) is presented in the publication [87] by Majumder et al. (2019). To categorize melanoma, the authors suggest an ANN design and train it using attributes collected from dermoscopy pictures. The work illustrates the possibility for accurate and automated melanoma detection using ANN-based techniques.

The work [88] by Wisaeng and Sa-Ngiamvibool (2019) describes a technique for identifying exudates, one of the symptoms of diabetic retinopathy, using the morphology mean shift algorithm. The authors create an automated detection method using the exudates' morphological traits. The study shows that the suggested method is capable of correctly recognizing exudates in retinal pictures.

The 2013 work [89] by Ranamuka and Meegama focuses on the use of fuzzy logic to identify hard exudates, a typical sign of diabetic retinopathy. For the purpose of identifying hard exudates in retinal pictures, the authors suggest a fuzzy logic-based method that takes into account a variety of characteristics. The work emphasizes the potential of fuzzy logic methods for the automated identification of lesions associated with diabetic retinopathy.

By Jaafar et al. (2011)[90] This study proposes an automated approach for identifying and grading hard exudates, a defining hallmark of diabetic retinopathy, using retinal fundus images. To reliably identify and rank the severity of hard exudates, the authors suggest combining image processing methods with machine learning algorithms. The study shows the possibility for effective diabetic retinopathy screening with automated technologies.

In their study [91] published in 2018, Kar and Maity discuss the progression of diabetic retinopathy on reconstructed pictures. The authors suggest an approach for reconstructing retinal pictures and grading the severity of diabetic retinopathy that blends compressed sensing with image processing methods. The work emphasizes the possibility of compressed sensing for effective and precise evaluation of diabetic retinopathy.

The article [92] by Zeng et al. (2019) describes an automated approach for detecting diabetic retinopathy that is based on a CNN. The authors suggest a network design that uses siamese-like network branches to conduct classification while also extracting information from retinal pictures. The study's use of the suggested method to identify diabetic retinopathy yielded encouraging findings.

A two-stage deep convolutional neural network (CNN) technique is suggested in the publication [93] by Yang et al. (2017). The authors create a network that initially looks for lesions before evaluating them according to their severity. The study shows how well the suggested strategy works for precisely identifying and classifying diabetic retinopathy lesions.

Convolutional neural networks (CNNs) are investigated for diabetic retinopathy in the publication [94] by Pratt et al. (2016). The authors examine several CNN designs and assess how well they perform in categorizing the severity levels of diabetic retinopathy. The study demonstrates CNNs' potential for precisely identifying and categorizing diabetic retinopathy.

The categorization of DR photos using DL models is covered in the work [95] by Dutta et al. (2018). The authors suggest a DL-based method for correctly categorizing the degrees of DR severity using retinal pictures. The study shows how the suggested method is successful in correctly classifying diabetic retinopathy.

The segmentation of retinal lesions on fundus pictures is addressed in the study [96] by Playout et al. (2019). The authors create a deep learning network that uses little supervision to separate both brilliant and red lesions simultaneously. The study shows how the suggested multitask architecture performs well at precisely segmenting retinal lesions.

Playout et al. (2018) published a study titled [97] that outlines a multitask learning architecture for segmenting both types of lesions simultaneously in fundus images. The authors suggest a deep learning model that uses shared and task- specific layers to perform multitask learning to segment various types of lesions. The study's precise segmentation of both bright and red lesions in fundus pictures demonstrates encouraging findings.

An automated approach for detecting microaneurysms in retinal images is presented in the publication [98] by Fleming et al. (2006). The authors suggest a method for detecting microaneurysms, which are early indicators of diabetic retinopathy, that combines local contrast normalization with local vessel identification. The study shows how the suggested strategy works well for precisely identifying microaneurysms.

Principal component analysis (PCA) and machine learning techniques are the main topics of the study [99] by Cao et al. (2018). The authors suggest a technique that uses machine learning techniques to detect microaneurysms and applies PCA to extract useful characteristics from retinal pictures. Using the suggested method, the study demonstrates encouraging results in reliably identifying microaneurysms.

The study [100] by Anumol Sajan, Anamika K, and Simy Mary Kurian (2022) focuses on the application of DL techniques to identify diabetic retinopathy. The automatic identification of DR from retinal pictures is performed by the authors using deep learning approaches, such as CNN. The research shows how deep learning can effectively identify DR.

Publication [101] was made in 1987 by the Early Treatment Diabetic Retinopathy Study Research Group. This study provides clinical advice for photocoagulation of diabetic macular edema as well as therapy options. Based on certain criteria, it suggests photocoagulation as a therapy option for diabetic macular edema and reports outcomes from the Early therapy Diabetic Retinopathy Study (ETDRS).

The Fundus Disease Group in the Chinese Medical Association's Ophthalmology Branch published [102] in 2017 as a guide for retinal image acquisition and reading. It offers advice on how to get retinal pictures technically as well as standardized techniques for interpreting and evaluating diabetic retinopathy based on these images.

The difficulty of fundus image quality evaluation for diabetic retinopathy screening is discussed in the publication [103] by Shen et al. (2020). For precise diagnosis and evaluation of diabetic retinopathy, the authors suggest a domain-invariant interpretable approach for assessing the quality of fundus pictures. The paper offers a methodology for evaluating the quality of fundus pictures that combines deep learning and interpretable models.

[104] by Preetha et al. (2020): This study investigates how machine learning techniques may be used to forecast the development of diabetes illness. The authors test the accuracy of these models in foretelling the development of diabetes by applying several machine learning algorithms to a dataset of patient information. Through machine learning-based methods, the study seeks to aid in the early detection and prevention of diabetes.

The article [105] by Kaur et al. (2019) focuses on the application of neural network techniques to identify diabetic retinopathy. The authors suggest using neural networks to diagnose diabetic retinopathy automatically from retinal scans. They examine the possibilities of utilizing neural networks in the diagnosis of diabetic retinopathy and assess the effectiveness of their model.

Ying et al. (2016) published a paper [106] that investigates the link between age-related macular degeneration (AMD) and the usage of antiplatelet or anticoagulant medications and the occurrence of retinal or subretinal hemorrhage. The study examines data from clinical trials and offers insights into how these drugs may affect people with AMD's risk of retinal hemorrhage.

A ridge-based technique for segmenting blood vessels in colored retinal pictures is presented in the publication [107] by Staal et al. (2004). The authors provide an algorithm that examines the local structure of the picture to find vessel ridges. The work demonstrates the effectiveness of the ridge-based technique in vascular segmentation, a critical step in the automated processing of retinal images for the detection of DR.

Abramoff et al. (2013) published a paper [108] that focuses on automated analysis of retinal images for the identification of referable DR. The authors suggest a method for analyzing retinal pictures in order to find traits that are typical of diabetic retinopathy. The study shows the possibility of automated analysis for quick identification of diabetic retinopathy.

In their article [109] Decencière et al. (2014), they explain the Messidor database, which is a Publicly Distributed Database of Retinal Images for Diabetic Retinopathy Screening. The database's importance to the creation and assessment of algorithms for the identification of diabetic retinopathy is highlighted by the authors in their review of the database and its application in research.

Lay et al. (1983) published a study [110] that focuses on the automated recognition of microaneurysms in retinopathy fluoro-angiogram pictures. The authors suggest an approach for identifying microaneurysms, a crucial aspect of DR, using image processing techniques.

In their publication [111] (Chetoui and Akhloufi, 2020), the researchers recommend a clear end-to-end DL strategy for diagnosing DR. The authors highlight how challenging it is to recognize diabetic retinopathy across different datasets and present a deep learning model that provides predictability.

Scikit-learn is a well-known machine learning package for Python that is introduced in the publication [112] by Pedregosa et al. (2011). The authors outline the functions and features of scikit-learn, which offers a variety of machine learning tools and techniques for modelling and data analysis.

Using machine learning classifiers, Jha et al.'s work [113] (2020) focuses on the prediction of heart disease. The authors highlight the best classifiers for this job by comparing and evaluating several machine learning methods for the prediction of heart disease.

Heart disease prediction using a hybrid strategy comprising a genetic algorithm and neural networks is the subject of the publication [114] by Jha et al. (2022). Although it doesn't specifically address diabetic retinopathy, it does cover the use of hybrid systems for medical prediction problems.

The research [115] by Tripathi et al. (2022) investigates people with diabetes mellitus' knowledge of this condition. The authors look at patient knowledge and comprehension of diabetic retinopathy and talk about the value of awareness in early management and diagnosis. Jahan et al.'s study, [116] (2022), looks into the prevalence and related risk indicators of retinopathy in a rural Bangladeshi population with and without diabetes. In this particular cohort, the authors look at the prevalence of retinopathy and pinpoint possible risk factors.

This work [117] by Mahmoud (2022), focuses on utilizing DL to predict the advancement of DR. The author creates a deep learning algorithm that can evaluate retinal pictures and forecast how diabetic retinopathy will develop.

The book [118] by Jain (1989) provides an overview of the basic ideas and procedures of digital image processing. It provides a strong foundation in the area of digital image processing by covering subjects including picture enhancement, restoration, segmentation, and compression.

The relative effectiveness of ensemble techniques and deep convolutional neural networks (CNNs) for image classification tasks is compared in [119] by Ju et al. (2017). The authors assess several ensemble techniques and examine how well they enhance deep CNN models' classification accuracy.

Roth and Pernkopf's study from 2018 titled [120] describes Bayesian neural networks with weight sharing. In order to increase the effectiveness and adaptability of the model, the authors suggest a technique that makes use of Dirichlet processes to automatically identify the number of shared weights in Bayesian neural networks.

3. Computer-Aided Diagnosis and Detection of Diabetic Retinopathy:

A unique method for identifying the optic disc in RGB retinal fundus pictures is presented in the study [121] by Kamil et al. (2017). The authors suggest a system to precisely identify the optic disc, a crucial landmark in retinal image analysis, by combining image processing methods and machine learning algorithms. The suggested method successfully locates the optic disc with high precision, laying the groundwork for later study and diagnosis of retinal disorders.

The article [112] by Hop, Allgood, and Yu (2018) examines the use of geometric deep learning in the field of chemical feature engineering. The authors show that deep learning models may learn chemical properties on their own from molecular structures without depending on manually created features created by subject-matter experts. The

work emphasizes the promise of geometric deep learning in drug development, where precise and automated feature extraction can increase screening effectiveness and result in the identification of novel therapeutic candidates.

The difficulty of feature extraction from dermoscopy pictures to enable efficient detection of melanoma skin cancer is discussed in the study [123] by Majumder and Ullah (2018). The authors suggest a technique for classifying melanoma that combines texture and color information with machine learning methods. The study stresses the value of feature extraction in creating precise and effective melanoma diagnosis systems.

Antal and Hajdu (2012) provide [124] which outlines an “ensemble-based system for microaneurysm detection and diabetic retinopathy grading”. The authors suggest an approach to increase the precision of microaneurysm identification and diabetic retinopathy grading by combining different classifiers. The work illustrates the utility of ensemble-based methods for diabetic retinopathy-related retinal image analysis.

According to Pires et al. (2013), their article [125] focuses on determining the necessity of referral in automatic diabetic retinopathy diagnosis. The authors suggest a way for deciding whether to refer a patient for additional testing based on the severity of the lesions that have been found. The study emphasizes how critical it is to accurately estimate the need for referrals in order to maximize healthcare resources for diabetic retinopathy screening.

A method for automatically detecting exudates, a common sign of diabetic retinopathy, using non-dilated retinal pictures is described in the paper [126] by Sopharak et al. (2008). The authors segment and identify exudates using mathematical morphological techniques. The work shows the potential of mathematical morphology methods for automatically identifying traits associated with diabetic retinopathy.

Majumder and Kehtarnavaz's review article, [127] (published in 2021), gives an overview of real-time human action recognition methods utilizing vision sensing. The

study discusses several strategies and algorithms used for real-time human action identification, which is not directly relevant to diabetic retinopathy but may have wider ramifications in the field of computer vision.

Abràmoff et al. (2016) published a study titled [128] that focuses on enhancing automated detection of DR using DL methods. The authors incorporate deep learning algorithms into an already-existing detection system and assess its effectiveness using a dataset that is openly available. The study demonstrates advances in the identification of diabetic retinopathy using deep learning techniques.

Gandhi and Dhanasekaran (2013) published a paper titled [129] that focuses on morphological methods and an SVM classifier for the diagnosis of diabetic retinopathy. The authors suggest a technique that employs morphological procedures to improve retinal pictures before classifying the data with an SVM classifier. The study emphasizes the value of integrating morphological techniques with machine learning for the diagnosis of diabetic retinopathy.

Singh and Henge's paper, [130] (2020), describes a hybrid neural-fuzzy inference system with SVM for identifying misleading signals in stock market forecasts. Despite not having anything to do with diabetic retinopathy, it demonstrates how hybrid systems can be used to predict financial consequences.

4. Machine Learning Techniques for Diabetic Retinopathy Detection:

The study article presents a U-net based method for automatically segmenting hard exudates in fundus pictures [131] by Zong et al. (2020). To increase the segmentation accuracy, the suggested technique makes use of a residual connections and an Inception module. The outcomes show how well the method works at precisely segmenting hard exudates, which are crucial signs of diabetic retinopathy development. The technique has the potential to improve the efficacy and precision of methods for screening for and monitoring diabetic retinopathy.

Orlando et al. (2018) provides [132] as a method for identifying red lesions in fundus images, which are a sign of diabetic retinopathy. To increase the precision of red lesion identification, the scientists create a system that integrates various DL models, such as CNN. The variety of the various models is taken advantage of in the ensemble technique to improve performance as a whole. The outcomes show how well the suggested approach works for precisely detecting red lesions, enabling early identification and intervention in diabetic retinopathy.

The topic of the 2017 study [133] by Gargeya and Leng is the automated identification of diabetic retinopathy. For the purpose of classifying retinal pictures as either having diabetic retinopathy or being healthy, the authors create a DL model based on convolutional neural networks. The model shows the potential for automated screening and identification of diabetic retinopathy and achieves good accuracy. The study emphasizes how deep learning might help diagnose diabetic retinopathy more quickly and easily, especially in environments with limited resources.

The article [134] by Patel et al. (2020) gives a summary of machine learning techniques and how they may be used in drug development. The authors talk about several machine learning techniques, such as deep learning, and how they may be applied to predict drug molecule attributes, enhance drug design, and increase the effectiveness of the drug development process. The paper emphasizes the advantages and disadvantages of machine learning's incorporation into the pharmaceutical sector, as well as its potential to speed up drug discovery.

A silicon circuit that combines digital selection and analog amplification and is inspired by the cortex is discussed in [135] by Hahnloser et al. (2000). It is a noteworthy piece of work in the realm of brain circuitry and computing, despite not having a direct connection to diabetic retinopathy.

Henge and Rama's (2017) [136] for the characterization of mixed connective conjunct consonants and numerals, the author suggests a “five-layered neural fuzzy closed-loop hybrid control system”. It demonstrates how neural fuzzy networks may be utilized for

pattern identification applications, while having nothing to do with diabetic retinopathy.

5. Detection of Microaneurysms and Bright Lesions:

In this article by Gambhir (2020) [137], advanced techniques images of the fundus are used for diabetic retinopathy classification and identification. Deep learning and image processing approaches are only two of the many techniques and algorithms the author provides an overview of. The research emphasizes the need of precise diabetic retinopathy detection and categorization for early diagnosis and efficient therapy. It offers details on the most cutting-edge methods now available and how they could be used in clinical settings.

An accurate method for evaluating diabetic retinopathy using a support vector machine (SVM) classifier is shown in the research [138] by Kamil et al. (2018). In order to correctly categorize the severity of diabetic retinopathy, the authors first suggest a feature extraction approach that extracts pertinent information from retinal pictures. This method is followed by the use of an “SVM classifier”. The outcomes show how well the suggested approach performs in precisely assessing and categorizing diabetic retinopathy, offering doctors an important tool for controlling and treating this illness.

A system for detecting DR using DL algorithms is described in the research article [139] by Qiao et al. (2020). The authors suggest a two-stage strategy that combines an early detection technique for non-proliferative diabetic retinopathy with the prognosis of microaneurysms. The system's deep learning algorithms are quite accurate in identifying and categorizing retinal defects linked to diabetic retinopathy. The suggested technique could help in diabetic retinopathy early identification and treatment.

An automated approach for detecting microaneurysms in retinal images is presented in the publication [140] by Fleming et al. (2006). The authors suggest a method for detecting microaneurysms, which are early indicators of diabetic retinopathy, that

combines local contrast normalization with local vessel identification. The study shows how the suggested strategy works well for precisely identifying microaneurysms.

Principal component analysis (PCA) and machine learning techniques are the main topics of the [141] by Cao et al. (2018). The authors suggest a technique that uses machine learning techniques to detect microaneurysms and applies PCA to extract useful characteristics from retinal pictures. Using the suggested method, the study demonstrates encouraging results in reliably identifying microaneurysms.

Fatima et al.'s paper, [142] (2022), is concerned with entropy enhancement-based diabetic retinopathy detection. For the precise diagnosis of diabetic retinopathy, the authors suggest a unified method that combines entropy-based picture enhancement with a neural network.

The topic of [143] by Mayya et al. (2021) is on automated microaneurysm detection for diabetic retinopathy early diagnosis. The authors go over numerous strategies for automating the identification of microaneurysms, significant indicators of diabetic retinopathy.

6. Diabetic retinopathy identification through image processing – Retinal Fundus Images:

Patil et al. (2016) published a work titled [144] in which the authors suggest a technique for segmenting blood vessels in color retinal images using unsupervised texture classification. The method makes use of texture analysis methods to recognize and categorize blood vessels in retinal pictures. The technique provides precise segmentation of blood arteries by collecting pertinent data and using unsupervised classification techniques. This segmentation, which enables efficient analysis and treatment planning, is essential for identifying and tracking retinal disorders.

In the article by Gambhir (2020) [145], advanced methods for recognizing and classifying diabetic retinopathy from fundus images are addressed. Just two of the various methods and algorithms the author gives an outline of are deep learning and image processing approaches. The study accentuates the necessity of accurate diabetic retinopathy identification and categorization for early diagnosis and effective management. It provides information on the newest techniques that are currently accessible and how they might be applied in clinical situations.

A unique method for identifying the optic disc in RGB retinal fundus pictures is presented in the study [146] by Kamil et al. (2017). The authors suggest a system to precisely identify the optic disc, a crucial landmark in retinal image analysis, by combining image processing methods and machine learning algorithms. The suggested method successfully locates the optic disc with high precision, laying the groundwork for later study and diagnosis of retinal disorders.

Porwal et al. (2018)[147], describes the Indian Diabetic Retinopathy Image Dataset (IDRiD), a vast collection that has been carefully curated for research on diabetic retinopathy screening. The dataset, which contains fundus photos from patients with and without diabetes, is collected and annotated in detail by the authors. Researchers may progress the field and enhance the diagnosis and treatment of this ailment with the help of IDRiD, which offers a significant resource for creating and assessing algorithms and models for diabetic retinopathy detection.

[148].”The development and validation of a deep learning algorithm for the detection of diabetic retinopathy in retinal fundus photographs” are presented in by Gulshan et al. (2016), a seminal paper. The authors show how well a CNN in identifying diabetic retinopathy and its severity using a huge dataset of retinal pictures. A potential method for universal screening of diabetic retinopathy and enhancing access to prompt diagnosis and treatment, the deep learning algorithm yields excellent sensitivity and specificity, equivalent to that of human ophthalmologists.

[149]. “Using retinal images from multi-ethnic populations with diabetes”, article by Ting et al. (2017) focuses on the creation and validation of a DL system for the identification of DR and eye diseases. The authors demonstrate the excellent accuracy of a deep learning model they trained to identify various retinal abnormalities using retinal pictures from a broad group of diabetics. The work emphasizes the potential of deep learning for population-based diabetic retinopathy detection and treatment.

[150]. The segmentation of retinal lesions on fundus pictures is addressed in the study by Playout et al. (2019). The authors create a deep learning network that uses little supervision to separate both brilliant and red lesions simultaneously. The study shows how the suggested multitask architecture performs well at precisely segmenting retinal lesions.

[151]. The research by Acharya et al. presents a computer-based method for identifying different phases of DR using digital fundus images. The authors offer a method for feature extraction, categorization, and picture pre-processing that makes use of machine learning techniques. The study shows that automated computer-based approaches for detecting the stage of diabetic retinopathy are feasible.

[152]. The article by Budai et al. (2013) describes a reliable technique for segmenting vessels in fundus images. For precise vessel segmentation, the authors suggest an approach that makes use of several picture characteristics and a random forest classifier. The work focuses on vascular segmentation, a significant job that is essential for detecting diabetic retinopathy.

[153]. In the paper by Acharya et al., a computer-based method for identifying the phases of diabetic retinopathy using digital fundus images is given. The authors propose an automated technique that makes use of image processing techniques and classification algorithms to identify the stages of retinopathy from fundus images.

[154]. The automated identification of DR using SVM is covered in the work by Carrera et al. (2017). The authors suggest an SVM-based method for classifying retinal

pictures as either normal or suggestive of diabetic retinopathy based on analysis of the images.

[155]. CNN and hybrid deep convolutional neural networks are used in the paper by R. Yasashvini et al. (2022). For reliable categorization of diabetic retinopathy, the authors suggest a CNN-based strategy as well as a hybrid approach that integrates CNN with other deep learning methods.

7. Data Sets and Databases for Diabetic Retinopathy:

[156]. An accurate method for evaluating diabetic retinopathy using a support vector machine (SVM) classifier is shown in the research by Kamil et al. (2018). In order to correctly categorize the severity of diabetic retinopathy, the authors first suggest a feature extraction approach that extracts pertinent information from retinal pictures. This method is followed by the use of an SVM classifier. The outcomes show how well the suggested approach performs in precisely assessing and categorizing diabetic retinopathy, offering doctors an important tool for controlling and treating this illness.

[157]. The 2019 study by Leeza and Farooq focuses on the BoF model's usage to determine the severity level of diabetic retinopathy. The authors suggest a technique that uses a BoF model to classify severity levels and extracts visual information from retinal pictures. The study reveals the BoF model's potential for precise diagnosis and grading of the severity of DR.

[158]. The frequency of DR in individuals with a HbA1C level higher than 6.5% is discussed in the publication by Raja Memon et al. (2017). The research gives details on the prevalence of diabetic retinopathy in individuals with increased HbA1C levels, albeit it is not directly connected to algorithms or approaches for diagnosis or categorization.

[159]. Wan et al. (2018) published a study that describes a deep convolutional neural network (CNN) method for detecting diabetic retinopathy through image classification.

The authors suggest a CNN architecture that successfully classifies the severity levels of diabetic retinopathy by learning discriminative characteristics from retinal pictures. The study shows how well the suggested method works for correctly categorizing diabetic retinopathy using image classification.

[160]. The article by Hardik Deshmukh explains how to build a convolutional neural network (CNN) model for the classification of medical X-ray images, specifically for the detection of pneumonia. To categorize a dataset of X-ray pictures into pneumonia and non-pneumonia cases, the author creates a CNN architecture from scratch and trains it on the dataset.

[161]. Studies the significance of many stages of development in diabetic retinopathy, according to Klein et al. (2001). The number of stages that the disease needs progress through in order to significantly impact visual outcomes is ascertained by the authors using data analysis from the Wisconsin Epidemiologic Study of Diabetic Retinopathy. The research clarifies the differences in diabetic retinopathy stages' clinical relevance.

[162]. The use of Local Binary Patterns (LBP) and ML approaches for the identification of diabetic retinopathy is explored in the study by De Calleja et al. (2014). The authors suggest a technique that uses machine learning techniques to classify retinal pictures by extracting LBP characteristics. The work shows the possibility for detecting diabetic retinopathy by integrating LBP with machine learning.

[163]. A dataset and challenge for the intelligent detection of ocular disorders, such as diabetic retinopathy, is called Ocular Disease Intelligent detection (ODIR-2019). It gives scientists a platform to create and test algorithms for the automatic identification and categorization of eye disorders.

[164]. A dataset devoted solely to diabetic retinopathy is called DeepDR Diabetic Retinopathy Image Dataset (DeepDRiD). It includes retinal photos that have been annotated for different stages of diabetic retinopathy. The dataset is a useful tool for developing and testing machine learning models for the identification of diabetic retinopathy.

[165]. The performance of DL algorithms for DR screening is assessed in the research by Li et al. (2019). With the use of a sizable dataset of retinal pictures, the authors evaluate the diagnostic efficacy of several models. The study emphasizes the potential of deep learning methods for detecting diabetic retinopathy.

[166]. Alyoubi et al.'s review article (2020) offers an overview of deep learning methods for detecting diabetic retinopathy. The authors go over several methods and architectures that deep learning models utilize to reliably identify diabetic retinopathy in retinal pictures.

[167]. Mishra et al. examine the use of DL in the detection of DRin their 2020 paper. CNN are used in the scientists' proposed deep learning-based method for the automated identification of DR. This paper provides evidence that deep learning can enhance detection precision.

8. Additional Studies and Related Topics

[168]. Majumder and Ullah's study, (2019), focuses on feature extraction from dermoscopy images for the diagnosis of melanoma, a form of skin cancer. In order to classify melanoma, the scientists suggest using machine learning algorithms to extract pertinent information from dermoscopy pictures. The research aids in the creation of efficient non-invasive imaging approaches for melanoma diagnosis.

[169]. Majumder and Ullah's research from 2019 titled describes a computational method for extracting relevant characteristics for the detection of melanoma skin lesions. The authors suggest a strategy for classifying melanoma that combines texture and color data from dermoscopy pictures with machine learning methods. The study emphasizes how crucial feature extraction is to enhancing the precision and dependability of melanoma detection.

[170]. Majumder and Kehtarnavaz's review article, (published in 2021), gives an overview of real-time human action recognition methods utilizing vision sensing. The

study discusses several strategies and algorithms used for real-time human action identification, which is not directly relevant to diabetic retinopathy but may have wider ramifications in the field of computer vision.

[171]. The frequency of diabetic retinopathy in individuals with a HbA1C level higher than 6.5% is discussed in the publication by Raja Memon et al. (2017). The research gives details on the prevalence of diabetic retinopathy in individuals with increased HbA1C levels, albeit it is not directly connected to algorithms or approaches for diagnosis or categorization.

[172]. Wan et al. (2018) published a study titled that describes a DCNN method for detecting DR through image classification. The authors suggest a CNN architecture that successfully classifies the severity levels of diabetic retinopathy by learning discriminative characteristics from retinal pictures. The study shows how well the suggested method works for correctly categorizing diabetic retinopathy using image classification.

[173]. The article by Hardik Deshmukh explains how to build a convolutional neural network (CNN) model for the classification of medical X-ray images, specifically for the detection of pneumonia. To categorize a dataset of X-ray pictures into pneumonia and non-pneumonia cases, the author creates a CNN architecture from scratch and trains it on the dataset.

[174]. According to Klein et al. (2001), examines the importance of several phases of advancement in diabetic retinopathy. The number of stages that must occur for the illness to advance in order to have a significant effect on visual outcomes is determined by the authors through analysis of data from the “Wisconsin Epidemiologic Study of Diabetic Retinopathy”. The study sheds light on the clinical significance of various diabetic retinopathy phases.

[175]. The use of Local Binary Patterns (LBP) and ML approaches for the identification of DR is explored in the study by De Calleja et al. (2014). The authors

suggest a technique that uses machine learning techniques to classify retinal pictures by extracting LBP characteristics. The work shows the possibility for detecting diabetic retinopathy by integrating LBP with machine learning.

[176]. The paper by Henge and Rama (2016) explains a closed-loop neural fuzzy hybrid system for the classification and recognition of mixed connective consonants and symbols. It illustrates how neural fuzzy networks can be utilized for pattern identification applications, while not having anything to do with diabetic retinopathy.

[177]. The automated identification of diabetic retinopathy using Support Vector Machines (SVM) is covered in the work by Carrera et al. (2017). The authors suggest an SVM-based method for classifying retinal pictures as either normal or suggestive of diabetic retinopathy based on analysis of the images.

[178]. CNN and hybrid deep convolutional neural networks are used in the paper by R. Yasashvini et al. (2022). For reliable categorization of diabetic retinopathy, the authors suggest a CNN-based strategy as well as a hybrid approach that integrates CNN with other deep learning methods.

[179]. High dynamic range (HDR) imaging is a method used to record and show a broader range of luminance values than conventional imaging methods, and it is the subject of by Banterle et al. (2017). The authors provide a thorough review of the discipline while discussing the fundamentals, techniques, and applications of HDR photography.

[180]. By applying texture-based techniques, by Choras (2013) examines the study of firearm striations for forensics image retrieval. For photos of firearm striations, the author suggests a texture analysis method that, by matching and obtaining pertinent photographs from a database, can help with forensic investigations.

[181]. The research by Choi et al. (2021) describes a method for detecting automobile crashes that makes use of both these two types of data. The authors suggest a technique

for reliably detecting automobile collisions that incorporates deep learning models with multimodal data (such as video and audio).

[182]. In their paper titled published in 2018, Yang and Jiang introduce an adaptive bi-weighting approach for automatic initialization and model selection in Hidden Markov Model (HMM)-based hybrid meta-clustering ensembles. To increase the effectiveness and resilience of meta-clustering ensembles, the authors provide an approach that adaptively weights various clustering outcomes.

[183]. The relative effectiveness of ensemble techniques and deep CNNs for image classification tasks is compared in by Ju et al. (2017). The authors assess several ensemble techniques and examine how well they enhance deep CNN models' classification accuracy.

[184]. Roth and Pernkopf's study from 2018 titled describes Bayesian neural networks with weight sharing. In order to increase the effectiveness and adaptability of the model, the authors suggest a technique that makes use of Dirichlet processes to automatically identify the number of shared weights in Bayesian neural networks.

[185]. The impact of body mass index (BMI) on virtual coronary artery calcium scoring is examined in the paper by Perez-Cervera et al. (2022). In order to shed light on the possible influence of BMI on this diagnostic technique, the authors examine the association between BMI and the precision of virtual calcium scoring in the evaluation of coronary artery disease.

Table 2.1 Literature Review

S No.	Reference number	Year of Publication	Index of Journal (Scopus/SCI Index etc)	Main Findings or conclusion relevant to proposed research work	Remarks
1	56	2022	Scopus	Preprocessing of the retinal image and analysis using a convolutional neural network classifier, which categorizes the condition into several stages based on a threshold, were required for the diagnosis of all phases of diabetic retinopathy.	The authors combine deep learning methods with image cropping to improve the accuracy of detecting diabetic retinopathy. The study's usage of the proposed hybrid model yields favourable findings for the identification of diabetic retinopathy.
2	57	2022	Scopus	Through the analysis of fundus images taken under various lighting situations and with different fields of view to develop an automated classification system utilising cutting-edge machine learning technique to reliably assess and classify the severity of diabetic retinopathy (DR).	This cutting-edge system successfully classifies fundus images into 5 categories (ranging from 0 to 4) that represent the severity of diabetic retinopathy (DR), enabling effective identification and management of proliferative DR, the most severe stage of the disease, with an 80% sensitivity, 82% accuracy, 82% specificity, and 0.904 AUC.

S No.	Reference number	Year of Publication	Index of Journal (Scopus/SCI Index etc)	Main Findings or conclusion relevant to proposed research work	Remarks
3	146	2022	Scopus	An excellent method for identifying photos of diabetic retinopathy is a computationally efficient hybrid neural network. An entropy enhancement technique uses discrete wavelet modifications to make subtle characteristics more prominent, hence increasing the visibility of the medical images.	The entropy enhancement strategy successfully improves diabetic retinopathy (DR) images. The obtained findings further suggest the successful classification of these enhanced pictures using a computationally efficient hybrid neural network.
4	73	2022	SCI	Building the new hybrid deep learning technique, E-DenseNet. by using transfer learning to combine the EyeNet and DenseNet models, adding dense blocks to the original EyeNet model to make it unique, and fine-tuning the hyperparameters of the resultant hybrid E-DensNet model.	The suggested system obtained average values of 91.2%, 91.2%, 96%, 96.0%, 69%, 69.0%, 92.45%, 92.45%, and 0.883 for accuracy (ACC), sensitivity (SEN), specificity (SPE), Dice similarity coefficient (DSC), quadratic Kappa score (QKS), and calculation time (T) in minutes (m), respectively.

S No.	Reference number	Year of Publication	Index of Journal(Scopus/ SCI Index etc)	Main Findings or conclusion relevant to proposed research work	Remarks
5	138	2022		A deep learning approach using a convolutional neural network (CNN) algorithm to develop an automated system for classifying diabetic retinopathy in a set of retina images and successfully recognises and categorises the levels of the disease, offering an automated diagnosis for diabetic retinopathy.	The effectiveness of a deep learning model the authors created specifically for detecting diabetic retinopathy is assessed. The study contributes to the development of more accurate and efficient diabetic retinopathy detection methods.
6	116	2022		A technique for automatic retinal image analysis (ARIA) that separates poor image quality caused by artefacts from poor image quality caused by eye abnormalities on color fundus retinal images. This technique uses a transfer net ResNet50 deep network.	For comparing high quality against bad quality, the corresponding values for sensitivity, specificity, and accuracy were 98.0%, 99.1%, and 98.6%; correspondingly, for distinguishing between ocular abnormality-associated poor quality and artefact-associated poor quality, the corresponding values were 92.2%, 93.8%, and 93.0%.
7	80	2022		Determining the likelihood of a heart attack so that individuals can take precautions. It suggests using the n-dimensional function-based neural fuzzy inference system (NFIS) to represent training data. When the mistakes have been measured, the NFIS includes an error calculating module to improve the learning instructi	This study included more than 13000 fuzzification rules to provide the best decision-making, a normalisation process, and planting strategies to make it possible to calculate the probability of having a heart attack, and it obtained a 94 percent accuracy rate. This study can be expanded to create auto-altering and advisory systems with hardware peripheral circuit device integration.

S No.	Reference number	Year of Publication	Index of Journal(Scopus/ SCI Index etc)	Main Findings or conclusion relevant to proposed research work	Remarks
8	114	2022		Analysis of the hybrid system's implementation for predicting heart disease, which combines genetic algorithms and neural networks. Describe this in further detail	This paper is able to cover the use of hybrid systems for medical prediction problems.
9	119	2022		A deep learning model that improves diabetic retinopathy identification with the use of the Harris Hawks Optimization technique. To increase the precision of diabetic retinopathy identification in retinal fundus pictures, the authors suggest a hybrid strategy.	The recommended system used principal component analysis to Select the best features. The results of the proposed architecture were compared with the most popular machine learning methods.
10	83	2022		Proposes an approach that uses preprocessing, regularisation, and augmentation stages to expand and prepare the picture dataset of XHO for training and enhance performance, which addresses the issue of the existing dataset. Then, in order to detect DR, it combines the advantages of CNN with three distinct residual neural network (ResNet) structures: ResNet-101, ResNet-50, and VggNet-16.	Doctors can diagnose DR more quickly and accurately with the help of the automatic classification of DR fundus images. It has demonstrated that the CNN method can be used to approach the two-class problem for nationwide screening of DR.

S No.	Reference number	Year of Publication	Index of Journal(Scopus/ SCI Index etc)	Main Findings or conclusion relevant to proposed research work	Remarks
11	156	2022		A technique that makes use of hybrid deep learning capabilities to recognize diabetic retinopathy from photographs of the fundus. “To improve the accuracy of diagnosing DR, the authors provide a system that integrates various deep learning techniques.	The best multiclass classification accuracy was achieved by the suggested revised technique, with scores of 89.29% and 97.8%. It provides a hybrid method for the early diagnosis of DR by using transfer learning to extract fundus image features from ResNet-18 and GoogleNet models.
12	157	2022		To determine how many patients with diabetes mellitus who attend a hospital in North India are aware of diabetic retinopathy. The authors discuss the importance of awareness in early management and diagnosis while taking a look at patient understanding and comprehension of diabetic retinopathy.	A total of 272 people with diabetes mellitus participated in the study (55.5% of them were men and 44.4% were women). The average age of the research participants was 53.4 ñ 10^9 years. Of the 272 patients, 79% knew that diabetes can affect the eyes and that DR can result in blindness.
13	205	2022		Identify the associated risk factors for developing retinopathy in this population as well as the prevalence of retinopathy among those with normal and impaired glucose metabolism in a remote rural community in Bangladesh.	This rural Bangladeshi population showed a significant frequency of retinopathy. In rural Bangladeshi communities, screening for hypertension, obesity, hyperlipidemia, and proteinuria as well as proper treatment of these risk markers may prevent retinopathy in addition to blood glucose control for diabetes.

S No.	Reference number	Year of Publication	Index of Journal(Scopus/ SCI Index etc)	Main Findings or conclusion relevant to proposed research work	Remarks
14	84	2022		The modified fuzzy clustering technique (MdFCM) is obtained by changing the target function and discussing k-means and the fuzzy clustering method. To integrate the MdFCM with features and get better results, a modified convolutional neural network is recommended.	With the suggested system, the accuracy rate was improved to 98.6%. The outcomes demonstrate that our suggested approach outperforms the most recent algorithm. We want to create a tool for early identification of diabetic retinopathy utilising the suggested system.
15	121	2022		Introduce a "recurrent CNN (R-CNN)" model to identify impending visual field examinations and forecast the progression of diabetic retinopathy. This study uses "a benchmark dataset of 7000 eyes from both healthy and diabetic retinopathy progress patients throughout time".	R-CNN outperformed regression in terms of classification accuracy across the board in the visual field. Furthermore, the R-CNN network provides better accuracy in the central regions when compared to alternative methods. These discoveries have clinical importance since they protect the center visual region.
16	85	2022		The suggested method makes use of principal component analysis (PCA) and deep networks to learn inter-class and intra-class differences from the raw image characteristics. Then, using the acquired deep features, ensemble machine learning classifiers are used to achieve high classification accuracy and resilient performance.	The proposed method has been compared with various conventional CNN-based algorithms on the Messidor-2 (two categories) and EyePACS (two, five categories) datasets. The results of the trial show that our proposed method outperforms others (up to 95.58% accuracy), which makes it a potentially valuable technique.

S No.	Reference number	Year of Publication	Index of Journal(Scopus/ SCI Index etc)	Main Findings or conclusion relevant to proposed research work	Remarks
17	86	2022		Employs Deep Learning (DL) and transfer learning algorithms to facilitate the study of different phases of diabetic retinopathy and the diagnosis of the condition. "CNN, hybrid CNN with ResNet, and hybrid CNN with DenseNet are applied on a large dataset of around 3662 training photos to automatically determine the stage of DR that has progressed."	Employs transfer learning and deep learning (DL) methods to investigate different phases of diabetic retinopathy and to diagnose the condition. "CNN, hybrid CNN with ResNet, and hybrid CNN with DenseNet are used on a large dataset of around 3662 train pictures to automatically determine the advanced stage of DR."
18	185	2022		Traditional non-contrast coronary artery calcium scoring (TNC) may not be necessary in some cases thanks to virtual non-contrast (VNC) CAC. There is no information on how the body mass index (BMI) affects the dependability of VNC. Our goal was to assess how BMI affected the CAC agreement between VNC and TNC.	BMI significantly affects how accurate VNC CAC is. VNC CAC works poorly when BMI is greater than 40 kg/m2, although it exhibits significant agreement in non-obese patients.
19	204	2023		Uses retinal fundus pictures to provide a unique IoT and DL enabled diabetic retinopathy diagnosis model (IoTDL-DRD). The Internet of Things Deep Learning - Diabetic Retinopathy Diagnosis (IoTDL-DRD) technology that is being shown uses IoT devices to collect data, which is then delivered to a cloud server for processing.	The IoTDL-DRD approach that has been presented enables IoT devices to collect data for processing on a cloud server. The retinal fundus images are then pre-processed to reduce noise and boost contrast.

2.2 Research Gaps Identified from above Literature

1. **Inadequate Exploration of Comprehensive Analysis on Proliferative and Non-Proliferative Diabetic Retinopathy Classification**

The Literature Survey provides an overview of various methods and datasets for diabetic retinopathy but lacks a comprehensive analysis of approaches specifically focused on distinguishing between proliferative and non-proliferative stages. The research gap is the absence of a detailed examination of existing techniques for the classification of these distinct diabetic retinopathy stages.

2. **Limited Scrutiny of Deep Learning-Based Approaches for Diabetic Retinopathy Detection**

Although the Literature Survey touches upon deep learning methods, it falls short in providing an in-depth exploration of the current advancements and gaps in deep learning-based approaches for detecting diabetic retinopathy stages. The research gap lies in the need for a more detailed understanding of the state-of-the-art deep learning techniques and their limitations in diabetic retinopathy detection.

3. **Insufficient Integration of Risk Control Factors in Diabetic Retinopathy Detection**

The Literature Survey lacks a thorough investigation into the integration of various risk control factors within diabetic retinopathy detection models. The research gap is evident in the absence of a comprehensive analysis of how incorporating factors such as patient history, lifestyle, or other health indicators could enhance the accuracy and reliability of diabetic retinopathy detection.

4. **Inadequate Exploration of Vision Loss Reduction Strategies**

The Literature Survey does not extensively address strategies aimed at reducing vision loss in diabetic retinopathy patients. The research gap lies in the limited exploration of proposed approaches that actively consider risk control factors and implement preventive measures to mitigate the impact of diabetic retinopathy on vision loss.

5. **Limited Comparative Evaluation of Proposed Approach with Existing Models**

While the Literature Survey mentions the evaluation of the proposed approach, it lacks a comprehensive comparative analysis with existing models. The research gap is evident in the need for a detailed assessment of the proposed method against

established models, providing insights into its effectiveness and potential improvements over current approaches.

2.3 Chapter Summary

The chapter, divided into nine parts, centers around the literature survey on diabetic retinopathy (DR), a microvascular condition causing vision issues in diabetics. The primary focus is on automated DR detection using machine learning (ML) and deep learning (DL) techniques. Various studies within the chapter introduce methods such as deep learning ensembles, data mining frameworks, dietary interventions, and DL algorithms for the early identification and management of DR. Furthermore, the chapter sheds light on the prevalence and incidence rates of DR, offering insights into risk factors and the epidemiological features of the condition.

The chapter emphasizes the growing significance of ML and DL techniques in DR detection, highlighting their potential to enhance diagnosis, treatment planning, and patient care. It also points out research gaps, including the need for a comprehensive analysis of proliferative and non-proliferative stages, in-depth exploration of DL approaches, integration of risk control factors, exploration of vision loss reduction strategies, and a comparative evaluation of proposed methods against existing models.

CHAPTER -3

Image Processing Techniques and Evaluation Metrics

An eye disorder brought on by diabetes is called diabetic retinopathy. It is brought on by damage to the retina's blood vessels. Retinal blood vessels may deteriorate, leak, or constrict as a result of complications from diabetic mellitus, impairing the delivery of nutrients and oxygen to various regions of the retina over time and impairing vision. Blockages can result in the development of abnormal blood vessels on the retina's surface, thereby increasing the risk of hemorrhage and fluid leakage. Vision blurriness and even retinal detachment and glaucoma may develop as a result of such structural abnormalities in their early stages.

3.1 Retina health evaluation

A doctor may do the following tests to assess the health of the retina in the eyes:

An ophthalmoscope is a specialized microscope that permits examination of the retina, vitreous, and other internal eye tissues. The different parts of the eye can be mirrored using this device.

A visual field or perimetry examination evaluates both the central and peripheral vision of the examined eye. This examination finds any blind spots that have developed in the peripheral vision.

One of the most important procedures for identifying and treating retinal diseases is fluorescein angiography. The retina's blood vessels can be seen by the doctor using fluorescein angiography. The patient receives an injection of a vegetable-based dye. Rapid, successive eye photos are obtained as the retina's blood flow occurs. These images reveal important details regarding its state.

B-scan ultrasonography [193] uses high-frequency sound pulses to image the rear of the eye. This technology provides a detailed image of the eye's surface that can also be used to evaluate the health of the retina.

Using specialized cameras, fundus photography documents and monitors the progression of specific retinal diseases, such as diabetic retinopathy, as well as their treatment. This thesis uses this kind of image to build an automatic diagnosis system.

3.2 Diabetic Retinopathy Fundal Images

All of the processing steps often used in DR screening systems are covered in this section. While there are top-down and bottom-up ways for DR screening systems, most published methodology are based on bottom-up approaches. A system is built from the bottom up utilizing subsystems, each of which has a specific function, such as segmenting HE to identify DR. Although though not all of these blocks are used in contemporary systems, they must be taken into account to carry out a more realistic assessment of DR.

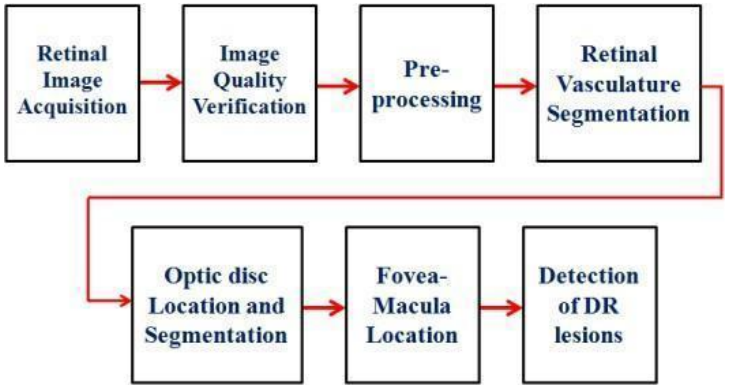

Figure 3.1 Processing steps involved in DR screening systems[20]

3.3 Retinal Image Acquisition

Originally, fundus images were captured on film. To assess DR in 35mm film, two pictures with a field of view (FOV) of 30 degrees were required to catch lesions of the retinal capillaries, such as microaneurysms and IRMA. Digital retinal images are being taken at the moment. For the purpose of DR detection, they are typically taken over a broad FOV of 45, 50, or 60 degrees. The rectangular-shaped images range in size from a few hundred to several thousand pixels. There are typically two methods for taking retinal photos: mydriatic (pupil dilation) or non-mydriatic.

Fluorescein angiography and optical coherence tomography are two additional image capture techniques utilized in addition to retinal fundus pictures to study the retina (OCT). Fluorescein angiography is a procedure that uses a dye tracing approach to look at the flow of blood in retinal arteries. After administering sodium fluorescein to the patient, a picture is obtained by detecting the fluorescence the retina emits when exposed to blue light with a wavelength of 490 nanometers. Hyperfluorescent microaneurysms can be easily recognized from dot-blot hemorrhage with this technique. Although this review focuses on fundus pictures, the first methods for detecting microaneurysms are based on angiography data.

3.4 Image Quality Verification

Images must be of a high caliber to provide a trustworthy diagnosis. According to research, 10 to 20 percent of the photographs in a typical screening scenario were insufficient for a trustworthy diagnosis. According to research by Scanlon et al. (2003), 20.8% of the unreadable photographs from a collection of images gathered from 1542 patients when the images were not captured mydriatically were unreadable, compared to 5.6% of the illegible images taken from 1549 patients when the acquisition was mydriatic. A 2005 research by Philip et al. found that in a DR screening setting, 11.9% of the photos from 5575 individuals were incomprehensible. Eleven percent of the photos in a multi-study analysis comprising 2771 patients were not intelligible. The main reasons of the unintelligible images were found to be poor client fixation, bad focus, media opacity, and a tiny pupil size. External factors and biological

characteristics of the human retina frequently interact to affect retinal image quality. External factors could include camera artifacts, low resolution, image compression, out-of-focus images, and low contrast. The following is a list of the biological and environmental components.

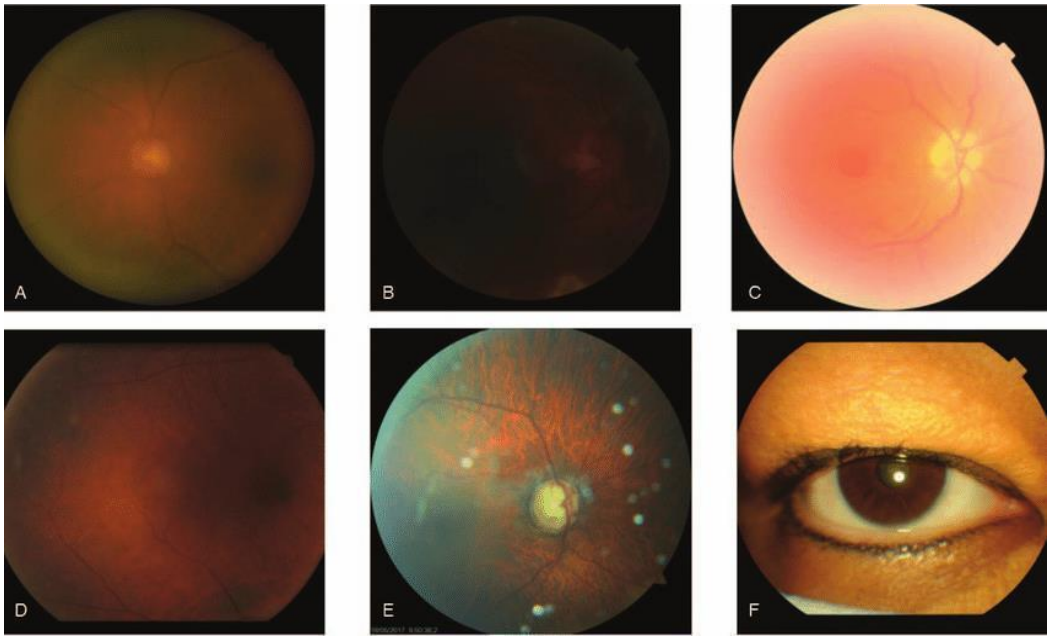

Figure 3.2 Examples of images with poor quality. [21]

An extremely blurry image is shown in the left figure. Because the macula on the right side is so dark, it is challenging to see if there is pathology there.

Biological Elements

The variability in retinal pictures [194] can be partially explained by the biological variables discussed in the literature. Lens coloration: The lens turns yellow as a person matures. Structures in the retina's appearance are altered by this color.

Lesion composition: Lesions that develop in the retina might differ in their chemical composition, which affects how sensitive they are to light. The density of the lesions determines how much light is transmitted or reflected.

Lesion position: Due to the multiple layers of the retina, lesions can manifest in a variety of locations. Location is another factor that affects how they appear in the fundus photographs.

Pigmentation and iris color: Those with poor pigmentation have reddish-colored retinal pictures. The choroidal arteries, which are located in a layer beneath the retina, are typically more well-known in these people because reduced pigmentation entails less reflection.

Illumination: Because of the retina's spherical shape, it is challenging for all of the different regions to receive the same quantity of light, leading to artifacts. Moreover, 3D- shaped structures like vessels produce specular reflection highlights.

Non-mydriatic images: Especially in senior patients, dilating eye drops may be required for retinal imaging. This dilatation differs in intensity for every patient. The retinal image will be of poor quality if the pupil is not sufficiently dilated because the border of the image will have a luminous artifact representing the iris of the eye.

Additional factors including race, eye color, and age: The patient's age has an impact on the retina's appearance and coloring. Due to specular reflection 27 (retinal shimmer) in the retina, children and adolescents may develop artefactual characteristics and coloration. On the other hand, age-related reductions in macular and visual pigment are possible.

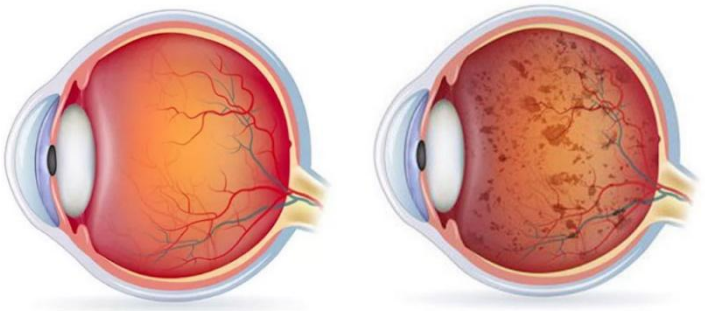

Figure 3.3: Retinas with different types of pigmentation: lower (left side), higher (right side). [22]

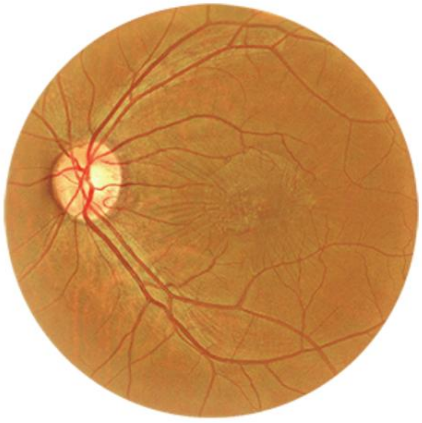

Figure 3.4 Retinal images with bright artifacts. [23]

b) External Factors

Camera: Variations in lighting and the human visual system are not automatically compensated for by the camera's sensors. Regulating the exposure is crucial for creating high-quality images. For instance, adjusting the camera's flash setting is necessary to capture decent photos.

Loss of contrast: unexpected eye movements by the patient may result in low contrast and fuzzy vision.

Eye conditions: In a healthy cornea, light reflected from the retina travels through it without being distorted. In people with cataracts, the cornea becomes opaque and distorts light as it passes through. Overall, the image will look murky.

Images that are hazy are caused by camera focus issues or patient movement.

Acquisition angle: The FOV's angle may also have an impact on the image. It is difficult to capture images in a field other than the macula's center because the patient must retain their attention steady while focusing at an awkward angle. As a result, a field other than field 2 has more inferior photos.

Compression: Blocking artifacts are introduced when photos are compressed into other formats, including "JPEG."

Conrath et al.'s research showed how compression ratios have an impact on how anomalies like IRMA and microaneurysms are classified. They also showed how the JPEG and JPEG2000 JPEG compression codecs affect pathology diagnosis. 29 All of the aforementioned factors have an impact on image quality, which could lead to screening mistakes because an artifact could be misinterpreted for a lesion or conceal a condition that could damage one's vision. A number of scholars have created techniques for assessing an image's quality by looking at its content.

3.5 Color Transformation

This method entails cleaning up the components of a color image. The majority of common color spaces are shown in the table below. Transformations can be produced by weighing each channel and combining them with different mathematical processes. Alternative color spaces than RGB are preferred by some automatic filtering systems.

Figure 3.5: Most Common color space used in eye screening algorithms. [24]

3.6 Diabetic retinopathy grading and classification

An untrained person could have trouble appropriately grading diabetic retinopathy. Classifications for retinopathy include “class 0, no retinopathy, class 1, mild NPDR, class 2, moderate NPDR, class 3, severe NPDR, and class 4, proliferative DR.” The severity of the lesions (micro-aneurysms, hemorrhages, and exudates) present in the retina is determined by these four severity stages.

Few or no symptoms may be present at any stage. In addition, damaged and permeable blood vessels can cause diabetic macular edema, which impairs the patient's eyesight at any stage. Therefore, regular dilated eye exams are crucial for identifying the problem and monitoring its development.

Diabetic retinopathy disease levels are discussed in the sections below:

No apparent diabetic retinopathy (class 0)

The fundus photographs from this class were examined, but no micro-aneurysms or any more complicated abnormalities were found. There is a 1% chance that PDR will manifest in a diabetic patient with no retinopathy within the next four years.

Mild non-proliferative diabetic retinopathy (class 1)

Here, the illness is still in its early stages. Micro-aneurysms are the sole aberration found so far in examinations. A PDR has a 5% risk [195] of appearing in those with type 1 diabetes within the next four years.

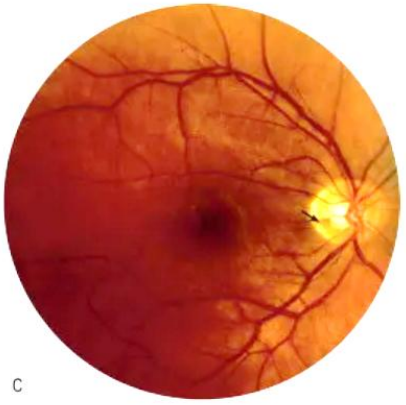

Figure 3.6: Sample image of a Mild NPDR (class 1) [25]

Image of “EyePACS 11736_left”, labelled as one and classified as such by our most accurate predictive model.

Moderate non-proliferative diabetic retinopathy (class 2)

According to the 4:2:1 criterion, moderate NPDR is less severe than severe NPDR and is defined as dot blot hemorrhage or microaneurysms in at least one quadrant, with or without cotton-wool patches, venous beading, or intraretinal microvascular abnormalities (IrMA).

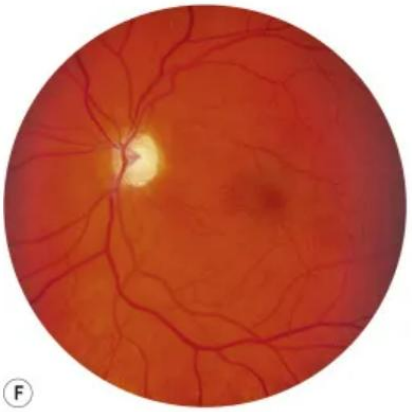

Figure 3.7: Sample image of a Moderate NPDR (class 2) [26]

Figure depicts the EyePACS 681_right image, which was labelled two and classified as two by our most accurate predictive model.

Severe non-proliferative diabetic retinopathy (class 3)

Exam findings of severe NPDR are exemplified by any of the cases listed below: Minimum of twenty dot-blot hemorrhage (intraretinal hemorrhaging) per quadrant. Multiple quadrants Exhibit distinct venous marbling.
Severe intraretinal microvascular abnormality (IRMA) in a quadrant or more

The 4:2:1 rule is named after these three prerequisites, which state that abnormalities must appear in at least quadrants 4, 2, and 1 of the retinas, respectively. Patients with acute NPDR had a 17% one-year risk and a 40% three-year likelihood of developing high-risk PDR.

Figure 3.8: Sample image of a Severe NPDR (class 3) [27]

Figure displays EyePACS 1561_left, which has been labelled as three and classified as three by our most accurate predictive model.

Proliferative diabetic retinopathy (class 4)

The sickness is currently at its most advanced stage. On the retina or optic nerve, small, aberrant new blood vessels are beginning to form at this stage of PDR [196]. There's a chance that these blood vessels will leak, affecting vision. Examinations reveal either pre-retinal or vitreous hemorrhage or a clear neo-vascularization.

Figure below displays EyePACS 11854 left, which according to our best predictive model is tagged as four and categorized as four.

3.7 Evaluation measures for disease grading

An objective evaluation of a human or machine system's categorization skills requires the development of index measurements that enable a precise assessment of performance [197]. Even for the most straightforward classification procedure, binary classification, finding a performance estimate for categorizing needs the usage of several different indices. Binary classification is used to categorize instances of a collection as either belonging to or not belonging to a class. The four possible outcomes are correctly identifying a positive class (true positive; TP), wrongly identifying a positive class (false positive; FP), correctly identifying a negative class (true negative; TN), and incorrectly identifying a negative class (false negative; FN). Additionally, the prediction set may be unbalanced (i.e., include an equal number of positive and negative real items) or balanced (i.e., have more examples of one class

than the other), which would result in a discrepancy between the absolute and relative conclusions. It is difficult to use a single criterion for judging predictive ability due to the abundance of factors. As a result, many indices are accessible, even for binary categorization. The most common binary classification indices are briefly explained below.

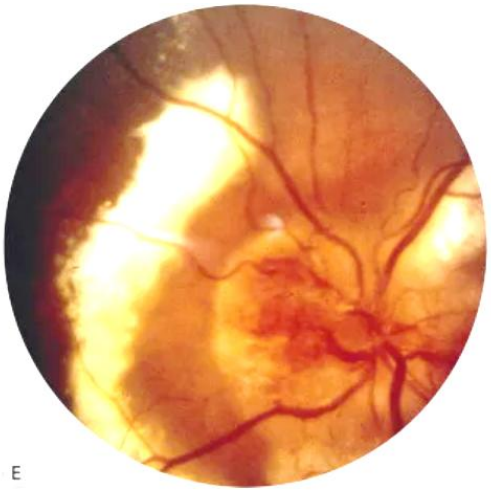

Figure 3.9: Sample image of a PDR (class 4) [28]

3.8 ML Algorithms

ML is a subset of AI. Rather than explicitly programming computers to perform certain tasks, machine learning focuses on instructing them to learn from data and progress over time. In machine learning, algorithms are taught to filter through vast quantities of data in search of patterns and correlations before deciding what to do with the data and making predictions. As more data is accessed, machine learning applications improve and become more precise over time.

The concept of classification and the major lines of investigation in this field are introduced in this chapter. It describes various machine learning techniques and compares them to the proposed methods.

3.8.1 Selected Machine Learning models

Here, we discuss about the many models that were used for the predictive analysis. We select eight of the most admired predictive models based on the characteristics of the classification challenge. Gaussian Naive Bayes, Random Forest, ADA Boost, Decision trees, K-Nearest Neighbors, Linear Discriminant Analysis, and Logistic Regression are their names.

3.8.1.1 Logistic Regression

Machine learning algorithms such as logistic regression [198] are utilized to solve categorization problems. The technique is based on probability and makes use of predictive analysis. Unlike linear regression, logistic regression produces a probability value that may be transferred to two or more discrete classes by modifying its output using the logistic sigmoid function. Linear regression, on the other hand, produces continuous numerical results.

Similar to linear regression, logistic regression uses an equation to represent data.

In a linear regression model, the values (represented by the capital Greek letter Beta) are blended linearly with input values (x) to predict an output value (y). Binary regression differs greatly from linear regression in that the output value being modelled is a binary value (0 or 1) rather than a numerical number. The following is the equation for logistic regression:

$$y=b0 + b1 * x \qquad \text{----(3.1)}$$

When b0 is the bias or intercept term, b1 is the coefficient for a single input value, and b0 is the bias or intercept term, then y is the predicted output (x).
For every input data column, you have to learn the corresponding b coefficients (constant real values) during training.
The real representation of the model can be found in memory or in a file as the coefficients in the equation (the beta value or b's).
Logical regression's algorithm also predicts a value using a linear equation and

independent predictors. It is possible for the expected value to range from negative infinity to positive infinity. The output of the algorithm must be a class variable, i.e., 0 for no and 1 for yes. As a consequence, we condense the output of the linear equation to the interval [0,1]. To reduce the anticipated value to a range between 0 and 1, the sigmoid function or logistic function is utilized.

$$S(z) = \frac{1}{1+e^{-z}} \qquad \text{—(3.2)}$$

To comprehend how the sigmoid function compresses values within the range, consider the sigmoid function's graph.

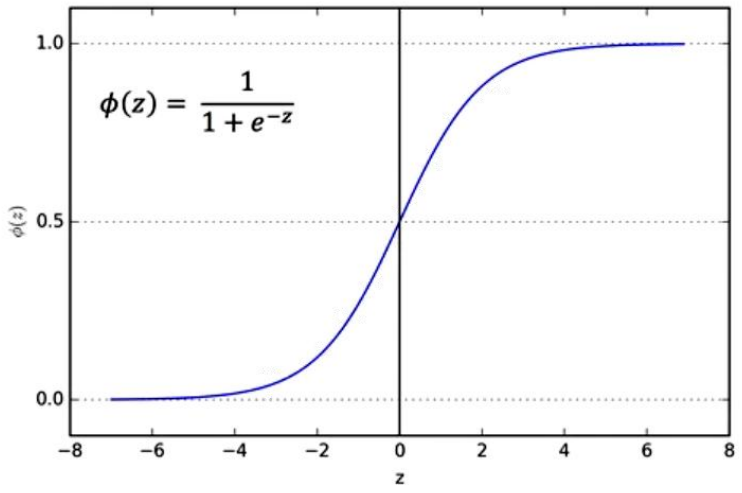

Figure 3.10: Sigmoid Function graph -Logistic Regression[29]

Making Predictions

In a classification problem with one independent variable ('x') and one dependent variable ('y'), logistic regression is represented by the equation:

$$P(y = 1) = sigm(b0 + b1 * x) \qquad \text{—(3.3)}$$

Any probability less than 0.5 is categorized as class 0, and any probability greater than 0.5 is categorized as class 1. This is the default threshold value for logistic regression, which is set to 0.5. This threshold can be altered to meet specific needs.

Consequently, with a threshold of 0.5, the predicted output is as follows:

$$y = 1 \; if \; P(y = 1) >= 0.5 \qquad \text{—(3.4)}$$

$$y = 0 \; if \; P(y = 1) < 0.5 \qquad \text{—(3.5)}$$

3.8.1.2 Linear Discriminant Analysis

Linear discriminant analysis (LDA) [199] is a technique for dimension reduction. It is frequently employed in projects involving pattern categorization and machine learning during the pre-processing phase. A high-dimensional data set can be lowered onto a lower- dimensional space with the use of Linear Discriminant Analysis Python.

Linear Discriminant Analysis, often known as Fisher's Discriminant Analysis, was the first method to be created. This method used two classes. Multiple Discriminant Analysis was the name given to the multi-class version by C.R. Rao. These days, they are referred to collectively as linear discriminant analysis.

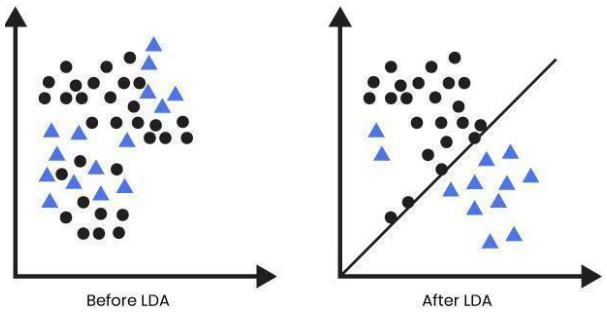

Figure 3.11: Linear Discriminant Analysis Before & After [30]

The statistical characteristics of the dataset serve as the basis for the representation of linear discriminant analysis models. These values are calculated separately for each subject. The mean and variance of the variable are given for each class for a single input variable (x) as an example. The same statistical properties are determined over the multivariate Gaussian, which includes the means and the covariance matrix, when there are several variables. All of these characteristics are explicitly computed from the data and accepted as inputs by the linear discriminant analysis equation.

Making Predictions

Using linear discriminant analysis, one can determine the likelihood that a new set of inputs belongs to each class. Output class is the class with the greatest probability. This is how the LDA makes its forecasts.

The Bayes Theorem is used by LDA to determine the probability. The process by which the Bayes theorem determines the likelihood that each class the data belongs to when the input class is (x) and the output class is (k), assuming that (k) is the output class, is explained below.

$$P(Y = x|X = x) = (PIk * fx(x))/sum(PI| * fl(x)) \quad —(3.6)$$

PIk is the base probability of each class (k) as indicated by the training data (e.g., 0.5 for a 50-50 divide in a two-class problem). In Bayes' Theorem, this is referred to as the prior probability.
The estimated likelihood that x belongs to the class is represented by the following formula, f(x). For f, the Gaussian distribution function is employed (x).

3.8.1.3 K – Nearest Neighbors

The supervised machine learning method known as k-nearest neighbors, or CNN, may be applied to resolve regression and classification problems. It is easy to understand and put into practice.

The kNN model is constructed using the entire training dataset. To determine a value for an unidentified data instance, the kNN method will search the training dataset for the k- most comparable case. The prediction for the unknown instance is delivered back after compiling the prediction attributes from the most comparable examples.

The type of data has an impact on the similarity metric. The Euclidean distance can be applied to data with real values. Hamming distance can be applied to category or binary data, among other forms of data.

The projected attribute's average may be given back when there are issues with regression. In cases of classification, the most prevalent class may be returned.

The instance-based, competitive learning, and slow learning algorithm families all include the kNN algorithm. Algorithms that use data instances (or rows) to model the problem and make predictions are known as instance-based algorithms. Because every

training observation is kept in the model, kNN algorithms are an extreme version of instance-based techniques.

It is a competitive learning method since it relies on competition between model components (data examples) to get a prediction result. Due to the objective similarity measure across data instances, each data instance tries to "win" or be the most similar to a certain unknown data instance and help make a forecast.

The term "lazy learning" [200] describes an algorithm that waits to create a model until a prediction is needed. It only completes its work at the last minute, which makes it lethargic. The advantage of this, known as a localized model, is that it only includes information pertinent to the unseen data. The computational cost of performing the same or comparable searches repeatedly over bigger training datasets is a drawback. Example of KNN Classification:

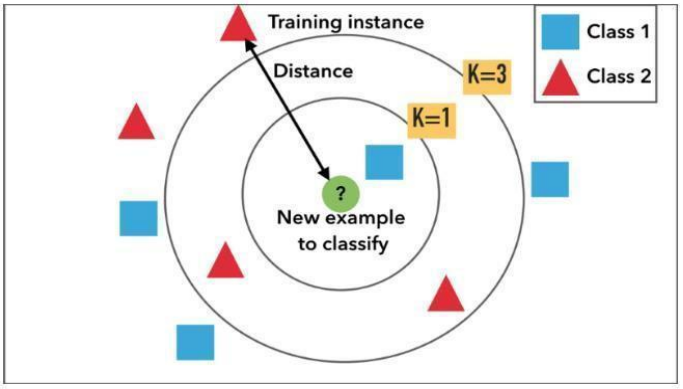

Figure 3.12: An example of KNN classification [31]

The test sample (within a circle) should be designated either the first class of blue squares or the second class of red triangles. Due to the presence of two triangles and one square within the inner circle, if k = 3 (outer circle) it is classified as belonging to the second class. For example, if k = 5, the first class (3 squares versus 2 triangles outside the outer circle) receives k.

The facts determine k's optimal value [201]. In binary (two-class) classification problems, it is possible to calculate an unambiguous majority when there are only two

possible categories by keeping k odd. In general, as k increases, the boundaries between various classes become smoother and clearer. A good k can be chosen using a variety of heuristic methods. The term "nearest neighbor algorithm" refers to the exceptional circumstance in which the class is predicted to be the class of the nearest training sample (i.e., when k = 1).

3.8.1.4 Decision Tree

One example of a supervised learning method that may be used for regression and classification issues is the decision tree. By learning decision rules from previous data, decision trees allow us to build a training model that can be used to predict the class or value of target variables (training data).

The decision tree model is portrayed using a binary tree [202]. In the event that the variable is numerical, a node represents a single input variable (x) and a division point on that variable. A prediction is formed using the output variable (y), which is present in the leaf nodes (sometimes referred to as terminal nodes) of the tree.
Once a tree has been constructed, it can be investigated by adding a new data row to each branch whenever a divide occurs until a conclusion is reached.

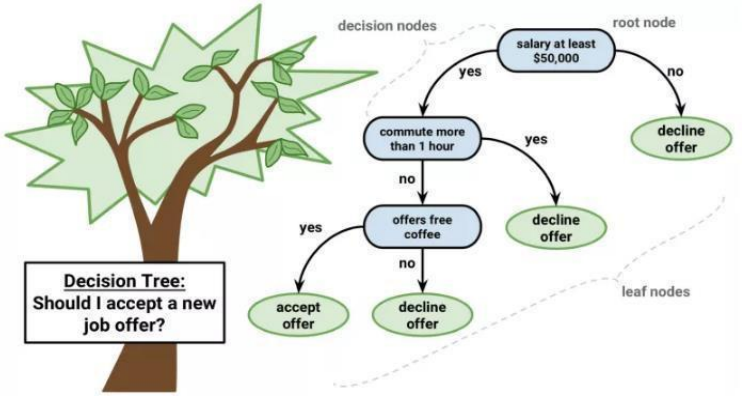

Figure 3.13: Decision Tree Classifier [32]

The decision tree in the aforementioned graphic attempts to decide whether to accept a fresh employment offer or not. The pay component is where it all begins. The pay will be verified to be at least $50,000. If it's untrue, we choose to reject the job offer. If the response is accurate, we will also determine whether our commute will take longer

than an hour. If it's accurate, we turn down the employment offer. If it's untrue, we check to see if we'll get a free coffee. The job offer is rejected if it is untrue. If that is accurate, we will take the job offer though.

Consequently, this example demonstrates unequivocally that a decision tree consists of a number of if-then criteria that are used to make a decision.

Implementing the Decision tree model:

1. Make a split

A division in the dataset consists of a single input attribute and its corresponding value. Training patterns can be split into two groups of rows using this technique. Three steps are required to create a split:

- determining the Gini index.
- Splitting up a dataset.
- Analyzing Every Split

Gini index

A Gini score indicates the quality of a division based on how evenly the classes are distributed between the two resulting categories. A perfect separation results in a Gini value of 0, while the worst-case scenario, in which each group contains 50/50 classes, results in a score of 0. (For a 2-class problem).

Splitting Dataset

A dataset that has been split is split into two lists of rows, each of which is based on the split value and the index of an attribute. Each row is repeatedly traversed to ascertain if the attribute value is above or below the divide value. If so, each row is subsequently assigned to the corresponding left or right group.

Once we have the two categories, we can use our previous Gini score to calculate the cost of the divide.

Analyzing each split

We must examine each value for each attribute in a dataset as a possible split candidate, calculate the split cost, and choose the best split we can get. We may add the ideal division as a node to our decision tree when it has been determined. This algorithm is self-serving and exhaustive.

2. Constructing a Tree

There are three essential components to building a tree:

- Terminal Nodes
- Recursive Splitting
- Building a Tree.

It is crucial to halt a tree's growth at the optimal time. We can accomplish this using the depth and number of rows that each node in the training dataset is responsible for.
The Maximum profundity of a tree. This is the utmost number of nodes that can exist after the tree's root node. The splitting and insertion of new nodes must cease when the tree reaches its utmost depth. Deeper trees are more complex and prone to overfit the training set.
Minimal Documents Needed for Each Node. This is all that a node has to do when it comes to training patterns. Node growth and division must stop when we hit or fall below this level. It is thought that nodes that account for an excessively small number of training patterns are overspecialized and are prone to overfit the training set.

Terminal Node : A terminal node is the point at which growth ceases, and it is used to generate the final forecast. To accomplish this, the most prevalent class value from the collection of data passed to that node is selected.

Recursive splitting:

Child nodes are nodes that are added to an existing parent node. A node may have zero, one, or more offspring. The left and right progeny nodes of a node are referred to as such

in the dictionary representation of that node. By using the same procedure again after a node has been established, we can recursively build child nodes for each chunk of data from the split.

Building a tree

The split() function is called to create the root node, which is then called recursively to construct the entire tree.

Making Predictions

Utilizing the precise row of data presented, a decision tree must be navigated in order to produce predictions. A recursive function can be used to implement this again, invoking the prediction procedure with either the left or right offspring nodes, depending on how the divide affects the input data.

We must determine if a child node contains a dictionary node containing another level of the tree to be considered or a terminal value to be returned as the forecast.

3.8.1.5 Support Vector machines

Support Vector Machine (SVM) is a supervised machine learning technique that may be used for regression and classification issues. Its most common use, nevertheless, is in categorization problems. This method plots each data point as a point in n-dimensional space, where n is the number of characteristics. The value of each characteristic is represented by the value of a particular coordinate.

The objective of a support vector machine is to locate a hyperplane in an n-dimensional space that classifies the data elements with precision[203].
The data columns (columns)' numerical input variables (x) produce an n-dimensional space. For instance, a two-dimensional space would be produced by two input variables.

A hyperplane is a line that divides the space of the input variable. To categorize input variable space points into classes 0 and 1, SVM selects the optimum hyperplane. Assume that a two- dimensional line may entirely divide each of our input nodes.

For illustration:

$$B0 + (B1 * x1) + (B2 * x2) = 0 \qquad \text{—(3.7)}$$

where the learning process determines the coefficients (B1 and B2) that define the slope and intercept (B0) of the line, and x1 and x2 are the two input variables.

By inputting input values into the equation for the line, you can determine whether a new point is above or below the line.

If the equation above the line returns a value greater than 0, the point belongs to the first class (class 0).

If the equation below the line returns a value less than 0, the point belongs to the second class (class 1).

A value along the line produces a result that is close to zero, and the point may be difficult to classify.

If the magnitude of the value is large, the model may be more confident in its prediction.

The margin is the distance between the line and the data points closest to it. The line with the largest margin is the optimal or optimum line for separating the two classes. The Maximal-Margin hyperplane can be seen here.

Only the nearest nodes are used to determine the margin by measuring the angle between them. For drawing the line and creating the classifier, only these details are necessary. The support vectors are these points. They either define or support the hyperplane. The margin is optimized using a method for learning the hyperplane from training data.

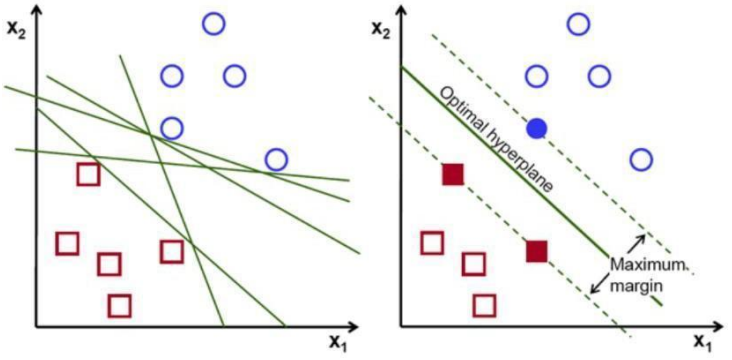

Figure 3.14: Hyperplane – SVM [33]

3.8.1.6 Random Forest

Random forest is an ensemble learning technique that builds a powerful model by combining several weak models. It may be used for regression and classification problems. It also does rather well when managing missing values, outlier values, and other critical data exploration phases using dimensional reduction approaches. The bootstrapping algorithm and decision tree (CART) paradigm are used in random forest. Random forest makes an effort to build and include numerous decision trees in order to enhance the overall effectiveness of the model. The process of selecting replacement data at random from the training data is known as bootstrapping. Each decision tree in Random Forest is trained using different subsamples of data as a result of bootstrapping.

Random feature subsets are used in Random Forest [204] .For instance, if the input contains 50 features, random forest will train only 10 of them on each tree. Thus, each tree will include 17 features for figuring out the best split for each tree node in addition to 10 random training features. Each decision tree's output will be gathered, and then we will combine them to produce the result (vote). The generalization of the model learned in this way is ensured by the use of multiple decision trees and the training of each tree using unique subsets of input. The production of the random forest from the provided input data in detail.

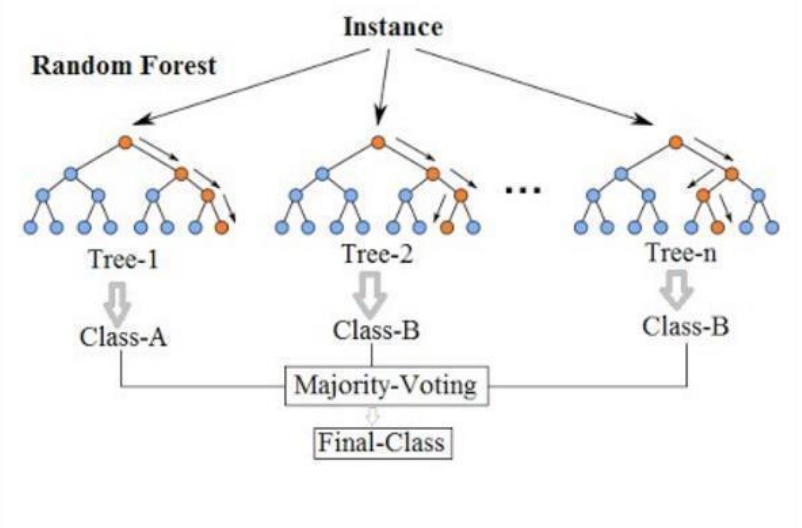

Figure 3.15: Random Forest Classifier [34]

3.8.1.7 Gaussian Naive Bayes

A classification approach known as the Gaussian Nave Bayes method is based on the predictor independence notion and the Bayes Theorem. In essence, a Naive Bayes classifier operates on the assumption that the existence of one feature inside a class does not influence the existence of subsequent characteristics.

We may calculate the probability of a hypothesis given our prior knowledge using Bayes' Theorem.

The formulation of Bayes' Theorem is as follows:

$$P(h|d) = (P(d|h) * P(h)) / P(d) \text{ ---(3.8)}$$

Where,

Prior probability: P(h|d) is the probability that hypothesis h will be true given the value d. The probability that data d would exist if hypothesis h were true is represented by P(d|h)

Prior likelihood of h: The likelihood that a particular hypothesis is correct is denoted by the letter P(h). P(d) is the probability of the data, which is unrelated to the hypothesis.

The probabilities for each hypothesis are condensed in the Nave Bayes model to facilitate their calculation. Assumed to be conditionally independent given the goal value, they are computed as P(d1|h) * P(d2|H) and so on rather than the values of each attribute being calculated as P(d1, d2, d3|h).

For instance, if the class attribute had the class values "go-out" and "stay-home" and the "weather" property had the values "sunny" and "rainy," the conditional probabilities of each weather value for each class value might be determined as follows.:

P(weather=sunny|class=go-out) = count (instances with weather=sunny and class=go-out) / count (instances with class=go-out)
P(weather=sunny|class=stay-home) = count (instances with weather=sunny and class=stay-home) / count (instances with class=stay-home)
P(weather=rainy|class=go-out) = count (instances with weather=rainy and class=go-out) / count (instances with class=go-out)
P(weather=rainy|class=stay-home) = count (instances with weather=rainy and class=stay- home) / count (instances with class=stay-home)

A Gaussian distribution is generally assumed to add real-valued features to Naive Bayes. We can use real-valued inputs to calculate the mean and standard deviation of input values (x) for each class in order to summarize the distribution.
We must record the mean and standard deviation for each input variable for each class in addition to the probabilities for each class.

Calculating the mean and standard deviation of each input variable (x) for each class value is all that is required.

$$mean(x) = 1/n * sum(x) \qquad \text{—(3.9)}$$

Where n represents the number of instances and x represents the input variable values from the training data.

The standard deviation can be calculated using the following formula:

$$standard\ deviation(x) = sqrt(1/n * sum(xi - mean(x)\text{^}2) \quad \text{—(3.10)}$$

Here, n is the number of instances, sqrt () is the square root function, sum () is the sum function, xi is a specific value of the x variable for the i'th instance, mean(x) is defined above, and 2 is the square. This is the square root of the average squared difference between each value of x and the mean value of x.

Making Predictions

To compute the probabilities of new x values, the Gaussian Probability Density Function (PDF) is utilized. When constructing predictions, these parameters and new values for the variable can be inputted into the Gaussian PDF, which will then provide an estimate of the likelihood of the new input value for that class.

$$pdf(x, mean, sd) = (1/sqrt(2 * PI) * sd)) * exp(-((x - mean^2)/(2 * sd^2))) \text{—(3.11)}$$

Where mean and sd are the previously calculated mean and standard deviation, exp() is the numerical constant e, or Euler's number raised to the power, pdf(x) is the Gaussian PDF, and x is the input value for the input variable. The aforementioned equation may then be used to forecast using real-valued inputs by plugging the probabilities in.

Adapting, for instance, one of the preceding calculations with numerical values for weather and automobile:

$$go - out = P(pdf(weather)|class = go - out) * P(pdf(car) |class = go - out) * P(class = go - out) \quad \text{—(3.12)}$$

3.8.1.8 Adaptive Boosting (ADA Boost)

AdaBoost is the acronym for Adaptive Boosting. Ada Boosting was essentially the first boosting algorithm developed for binary classification that was genuinely effective. It is also the ideal starting point for enhancing comprehension. In addition, modern boosting techniques, including stochastic gradient boosting machines, are based on AdaBoost.

Typically, AdaBoost is applied to tiny decision trees. After the initial tree has been created, its performance on each training instance is utilized. In addition, we use it to

determine the significance of the subsequent tree. Therefore, it should monitor each training instance as it is created. As a result, training data with low predictability is given more weight. However, cases that are straightforward to foresee are given less weight.

1. AdaBoost Model - Learning:

Ada Boosting, which is based on binary classification problems, is utilized most effectively to enhance the performance of decision trees.

AdaBoost can be used to increase the effectiveness of any machine learning technique because it is used for classification rather than regression. It works well when teaching underprivileged pupils.

The training dataset's instances are all weighted. The initial weight has been established at:

$$weight(xi) = 1/n \qquad —(3.13)$$

where n is the total number of training examples and xi is the i'th training instance.

2. Training the ADA Boost:

With the aid of weighted samples and training data, a weak classifier is created. Problems of binary classification are supported only. Consequently, just one input variable is chosen by each decision stem. Additionally, the first- or second-class value of the outcome is either +1.0 or -1.0.

The trained model's misclassification rate is calculated. This is often calculated as follows:

$$error = (correct - N)/N \qquad —(3.14)$$

where the incidence of misclassification is referred to as error. While accurate, the model's projected number of training instances. N represents how many training instances there are in total.

Example: In case the errors, the algorithm correctly predicted is 78 out of 100 training occurrences

This is changed to use the training instance weighting:

$$error = sum(w(i) * terror(i))/sum(w) \quad —(3.15)$$

This is the misclassification rate's weighted average.

where w is the training instance weight I

The training instance i's prediction error is terror. What is also 0 if correctly classified and 1 if incorrectly classified.

3. Ensemble Model for AdaBoost:

After being trained using weighted training data, weak models are typically added incrementally.

Typically, the procedure is repeated until a predetermined number of feeble students are created.

After everything has been completed, you are left with a group of students with low stage values.

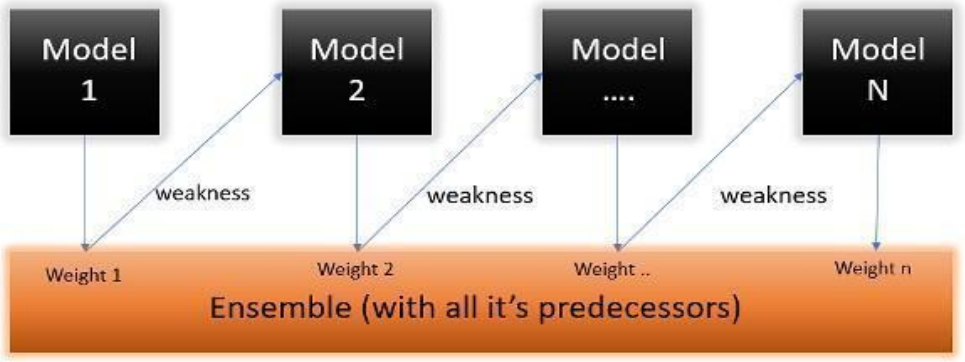

Figure 3.16: Ensemble model of ADABoost [35]

4. Making predictions with AdaBoost:

Calculating the weighted average of the weak classifiers yields predictions.

Each weak learner determines a predicted value for a new input instance as either +1.0 or -1.0. The stage value of each vulnerable learner is used to weight the anticipated values. The weighted mean of each forecast in the ensemble model serves as the prognosis. Predictions for the first class are made if the sum is positive, and predictions for the second class are made if the sum is negative.

For instance, five ineffective classifiers might correctly predict the digits 1, 0, 1, and -1. When there is a majority, the model will forecast a value of 1.0 or the first class. Stage values of 0.2, 0.5, 0.8, 0.2, and 0.9, respectively, may be assigned to these same five subpar classifiers.

Calculating the weighted total of these projections yields -0.8. And whether would be a 1.0-ensemble forecast or a subpar forecast.

5. Data preparation for AdaBoost:

The best heuristics for preparing your data for AdaBoost are listed in this section.

1. **Reliable Data:** The ensemble technique makes an effort to rectify incorrect classifications in the training data. Additionally, you must take care that the training data is of excellent caliber.
2. **Outliers:** In general, outliers will push the ensemble further into the work's rabbit hole. It is quite challenging to adjust for irrational circumstances. The training dataset might be amended to exclude these.
3. **Noisy Data**: In general, disturbance in the output variable can present a problem. However, if practicable, make an effort to separate and clear these from your training dataset.

3.9 Evaluation Metrics

In machine learning, testing the generalizability of the model comes after training it with training data. Simply put, we look at the model's performance in data-driven tests. So how do we assess the model's effectiveness? We use assessment tools (such as regression or classification, for example) to gauge the effectiveness of the model based on the type of issue. Only the evaluation metrics for the classification problem will be covered in this section.

3.9.1 Confusion Matrix

Characterizing the performance of a classification model, often called a "classifier," using a set of test data for which the real values were known is often done using a

confusion matrix. It makes the effectiveness of an algorithm easier to visualize.
A N X N matrix describes the overall efficacy of a model when applied to a dataset, where N is the total number of class labels in the classification task. As shown in the figure, we have a 2 x 2 confusion matrix for binary classification.

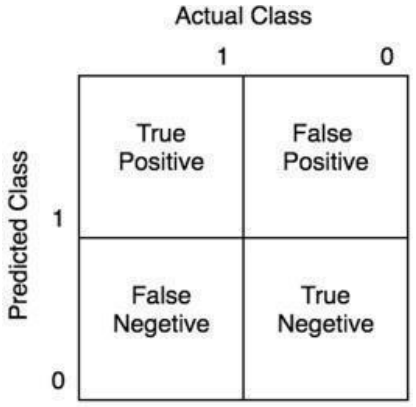

Figure 3.17: Confusion Matrix [36]

A Confusion matrix consists of statistics such as "(TP), (TN), (FP), (FN)" that are calculated using actual and predicted values.

True Positive (TP) is a circumstance in which both the actual and predicted values are positive (e.g., fraud).

False Positive (FP) refers to a situation in which the actual value is negative (normal, for example) but the predicted value is positive.

True Negative (TN) describes a circumstance in which both the actual and predicted values are negative.

False Negative (FN) is a situation in which the actual value is positive (for example, fraud) but the predicted value is negative.

3.9.2 Classification rate or Accuracy

Classification Rate or Accuracy is given by the relation:

$$Accuracy = \frac{(TP+TN)}{(TP+TN+FP+FN} \quad (3.16)$$

However, there are problems with accuracy. It assumes equal costs for both kinds of errors. A 99% accuracy can be excellent, good, mediocre, poor or terrible depending upon the problem.

3.9.3 Recall

Recall is defined as the ratio of all positively classified instances that were correctly classified to all positively classified examples. High Recall indicates precise class recognition (few FNs).

$$Recall = \frac{TP}{TP+FN} \quad \text{—(3.17)}$$

3.9.4 Precision

To get the value of precision we divide the total number of correctly classified positive examples by the total number of predicted positive examples. High Precision indicates an example of labelled as positive is indeed positive (a small number of FP).

$$Precision\ is\ given\ by\ the\ relation: Precision = \frac{TP}{TP+FP} \quad \text{—(3.18)}$$

3.9.5 F1 – Score

It is helpful to have a measurement that reflects both of our measurements, recall and precision. Since the harmonic mean penalizes extreme values more than the arithmetic mean, we utilize it to generate an F-measure.

The F-Measure is always more in line with the lower Precision or Recall number.

$$F - measure = \frac{2*Recall*Precision}{Recall+Precision} \quad \text{—(3.19)}$$

3.9.6 Receiver Operating Characteristic Curve (ROC Curve)

Receiver Conduct In predictive analysis, one of the most regularly used assessment metrics is the characteristic curve. It shows how well a model functions when applied to various probability criteria. For the classification problem, a probability threshold of 0.5 is typically employed.

This graph compares the False Positive Rate (FPR) and True Positive Rate (TPR), commonly referred to as sensitivity. FPR is calculated using (1-Specificity). Formulas 2.7 and 2.8 provide the sensitivity and specificity equations, respectively.

$$Sensitivity = \frac{TP}{TP+FN} \quad \text{—(3.20)}$$

$$Specificity = \frac{TN}{TN+FP} \quad \text{—(3.21)}$$

Sensitivity and specificity are negatively associated when we change the probability threshold (that is, when we lower the threshold, sensitivity rises while specificity falls, and when we raise the threshold, sensitivity falls while specificity rises).

The ROC curve [Bra97] can be used to determine the probability that a model would rank a randomly picked positive instance higher than a randomly selected negative one. The model's ROC is shown by the blue curve in the following image, and its AUC value is 0.966. On the other hand, the random model's ROC with an AUC of 0.5 is represented by the red dotted line.

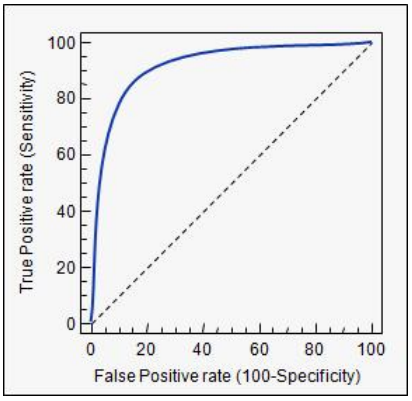

Figure 3.18: An example of ROC curve [37]

3.9.7 Precision-Recall Curve

The precision-recall curve is a crucial evaluation indicator to assess a predictive model's efficacy, particularly when there is an unbalanced distribution of classes. The graphic shows the accuracy and recall values at various probability thresholds. It is based on the precision and recall assessment measures. The area under the PR curve can be used to assess the model's performance.

The figure below illustrates an example of the PR curve.

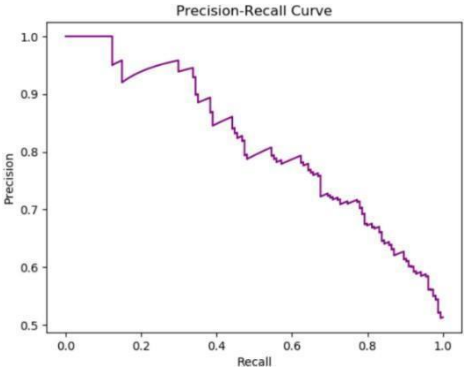

Figure 3.19: An example of PR curve [38]

3.10 Pattern recognition

3.10.1 Traditional models of pattern recognition

he conventional approach to pattern recognition relied on a predefined design made up of a fixed kernel and a fixed set of fundamental features that had to be manually constructed. With the aid of such kernels, texture, statistic, location, and geometry information might be extracted and later integrated with a straightforward classifier. There are many different techniques for extracting features, including Gabor filters, the local binary pattern, histograms of directed gradients, and grey level co-occurrence matrices. It was usual practice to use decision tree-derived techniques such a random forest or gradient boosting during the classification phase, as well as linear discriminant analysis, support vector machines, and k-nearest neighbors. The development of the proper filters for each application in such a pattern recognition pipeline is time-consuming.

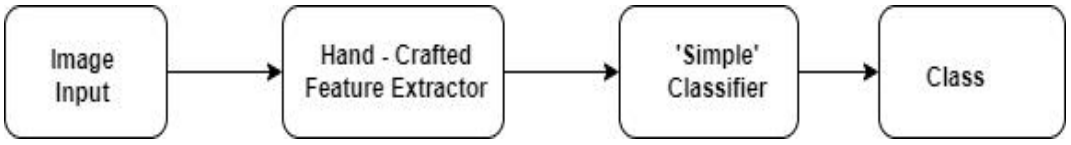

Figure 3.20: Traditional Pattern Recognition Scheme [39]

3.10.2 Deep Learning for pattern recognition

Deep learning for pattern detection represents a change in the design paradigm. Instead of manually building features, an end-to-end automatic learner is constructed by combining a trainable feature extractor with a trainable classifier in a fully trainable model.

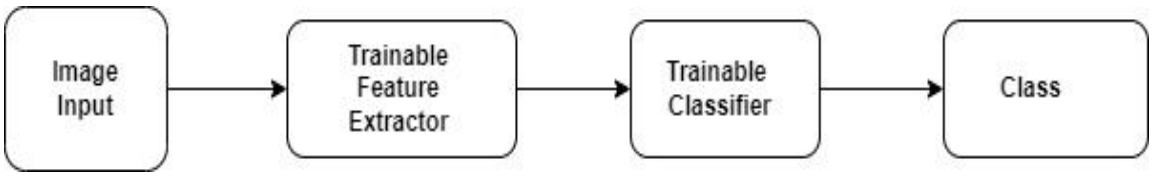

Figure 3.21: Deep Learning Pattern Recognition Scheme (end to-end learning) [40]

3.10.3 Types of DL architectures

A subset of deep learning architectures are neural networks. They were built as directed graphical representations with a preset architecture by the neuron, which is its primary component. Recurrent neural networks, fully connected neural networks, and convolutional neural networks are three examples of common base designs. Each of these architectures, or a combination of them, can be applied to any created network. Each one is appropriate for a specific class of challenges. Recurrent neural networks perform best in situations with serially ordered input, such as those involving text or music. Local correlations, like those found in photographs, are advantageous to convolutional neural networks because of their design. Fully connected layers are designed for usage in circumstances where all the information is equally important, such as in classification layers. The models created for this thesis mostly use convolutional neural networks.

Convolutional Neural Networks

CNNs are neural networks that take advantage of the local correlations that naturally occur in images. In order to disentangle the information in the image and produce features that can be used to solve a specific classification or regression issue, they can

produce local ab- distractions that are joined layer by layer to generate more complicated meta- abstractions.

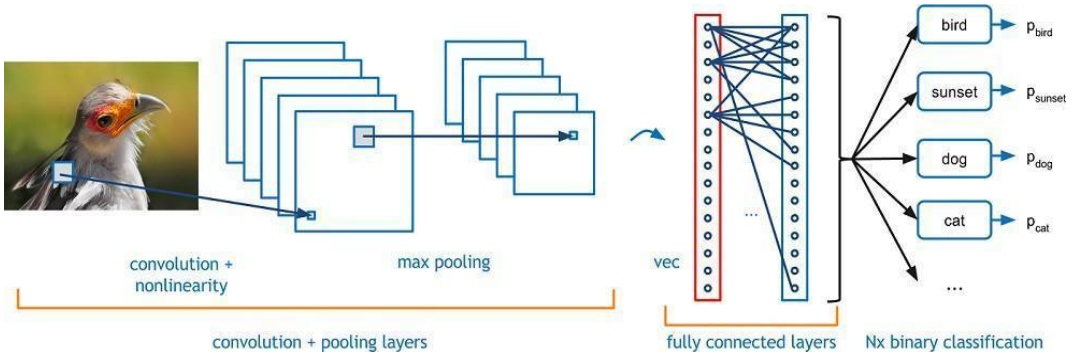

Figure 3.22: An example of a convolutional neural network at a high level [41]

Similar to traditional neural networks, they are made up of a collection of stacked layers. A convolutional operator is present in each layer and allows the conversion of one input tensor into another. The output tensor can undergo additional transformations inside the same layer, such as batch normalization, activation, or functions that reduce the size of the output tensor, such as average or max-pooling blocks. All of these functions are parametric, which means that their learnable parameters can be adjusted using a loss function optimization technique to improve the network's classification and regression abilities. The convolution operator serves as the network's distinctive building block.

The convolution operator is applied repeatedly to a number of localizations of the input. The operator's application is sent to any input location where the starting places of the horizontal and vertical strides are dispersed. A tensor containing the number of feature inputs, convolution width, convolution height, and number of outputs, as well as horizontal and vertical padding and horizontal and vertical stride, are the parameters that define such an operator. In other words, if the input's starting dimensions are width and height, then the input is expanded for applying the operator to (width+ 2 x padding width) x (height + 2 x padding height). The term "padding" refers to the number of pixels that must be added to the input's width and height before it can be applied. The output value is created by linearly combining the convolution parameters and input values.

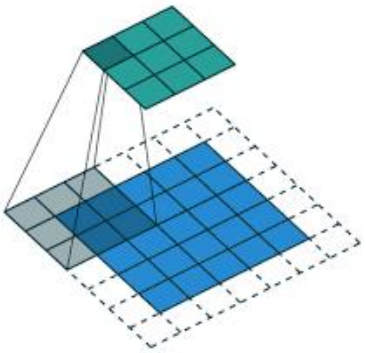

Figure 3.23: A 6x6 input is subjected to a 3x3 convolution operator with stride two and padding 1 in both directions. There is just one input and output feature displayed. [42]

Pooling operators are additional CNN-standard components. They are employed to make feature maps smaller. Max-pooling operators choose the maximum value from a predefined window and ignore the other values. The average is chosen via average pooling. Both are the most typical methods for condensing feature maps.

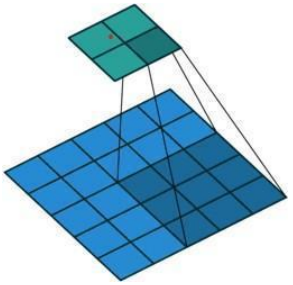

Figure 3.24: Applying a 2x2 max-pooling operator with stride one and padding 0 in both directions to a 5x5 input. [43]

Only one input and output feature are shown

Batch normalization is another common component seen in CNN layers. It normalizes the inputs to improve stability and serves as a regularizer by lowering covariate shifts.

The activation function is important for neural networks. The most adaptable, reliable, and widely used one is ReLU. Due to issues with gradient descent disappearing, the sigmoid function that was most popular in the 1980s is currently only utilized for

certain output layers. Deep learning models would perform exactly as linear functions without them. In the 1980s, the Sigmoid, a supple nonlinear function that is continuously differentiable, was the most popular activation function. It has a crucial issue known as the gradient vanishing problem, despite its intriguing characteristics. Due to gradients that are close to zero, the sigmoid first derivative becomes flat near the origin, which has an impact on network loss optimization. Using ReLUs to approximate stepped sigmoid units, Restricted Boltzmann Machines (RBMs) were improved. ReLU networks are advantageous for sparse representations since the data is represented more reliably and significantly more efficiently as a result.

When working with large networks, the function's and its derivative's quick computing time is also essential. Gradient vanishing is prevented and deeper networks can be built thanks to the gradient's constant value. ReLU has since evolved into the typical activation function for deep learning. LeakyReLU is only one of several different activation functions that have been published; yet, its performance has not been noticeably enhanced.

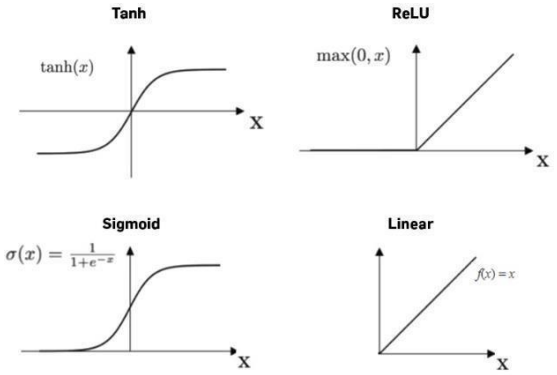

Figure 3.25: Typical activation functions used in Deep Learning [44]

Typical CNN architectures

Complex classification, detection, and segmentation issues can be successfully solved with CNNs. The most effective image net standardized prediction architectures are included in the table in order of how well they performed in the challenging Imagenet classification task. With almost 55 million parameters, InceptionResNetV2 is the more effective network seen in the table. With less than half the parameters, Xception achieves an accuracy comparable to that. The accuracy of MobileNetV2, a mobile

device architecture with only 3.4 million parameters, is comparable to that of previous systems like VGG16 and VGG19, which employed more than 0.1 billion parameters.

3.11 Prediction error: bias vs. variance

Bias and variation are the two main sources of mistake in predictions. The bias is the deviation from the average prediction's expected value. The variance of a model quantifies how well it predicts model variability for a specific data point. Examples of various bias and variance combination scenarios are shown visually in the figure.

A low bias, high variance model makes predictions that are broadly spread around the actual value, but their predicted average is fairly near to that value. Predictions from a model with a high bias and low variance are far from the true value yet show little variation between them. A model with high bias and high variance makes predictions that are distant from the true value and have a wide range. The optimal model is one that predicts values that are close to the actual values and has little variation across individual predictions.

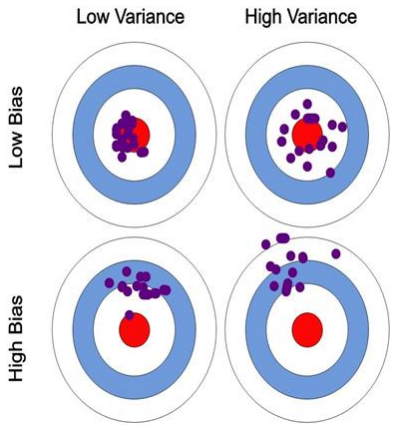

Figure 3.26 : Bias vs. Variance extreme possible scenarios [45]

3.12 Chapter Summary

The chapter delves into a comprehensive exploration of various machine learning algorithms, providing insights into their mathematical foundations, training methodologies, and practical applications. Linear Discriminant Analysis (LDA) is elucidated for predictive modeling, emphasizing the Bayes Theorem and probability estimation. The discussion extends to the k-Nearest Neighbors (kNN) algorithm, elucidating its simplicity and adaptability, particularly in classification tasks.

Decision Trees are introduced as versatile models for both regression and classification, with a focus on constructing, analyzing, and implementing these tree-based structures. Support Vector Machines (SVM) are presented as effective tools for regression and classification, highlighting their utilization in categorization problems and the determination of hyperplanes in multidimensional spaces.

Random Forest, an ensemble learning technique, is detailed for its proficiency in combining weak models to build robust predictions. Gaussian Naive Bayes is explored for classification, leveraging predictor independence assumptions and Bayes' Theorem. Adaptive Boosting (AdaBoost) is introduced as a boosting algorithm, enhancing the performance of decision trees in binary classification problems.

The chapter also covers Convolutional Neural Networks (CNN) in depth, elucidating their architecture, components like convolutional and pooling operators, and their application in solving complex image-related tasks. The chapter concludes with a discussion on prediction error analysis, emphasizing the critical balance between bias and variance for optimal model outcomes.

CHAPTER 4

Design and Implementation Using Machine Learning Based Methodology

1. Label class distribution:

The APTOS dataset, comprising 3662 color fundus images, stands as a cornerstone in our research implementation. This major dataset serves as the primary source for both training and testing deep learning models focused on predicting diabetic retinopathy. The gradation of the Threshold values from 0 to 4 corresponds to different severity levels of diabetic retinopathy, ranging from no indication (0) to proliferative diabetic retinopathy (4). However, a challenge in the dataset lies in its class distribution, as illustrated in Figure 4.1. The uneven distribution across classes reflects the real-world scenario where certain retinopathy grades might be more prevalent than others.

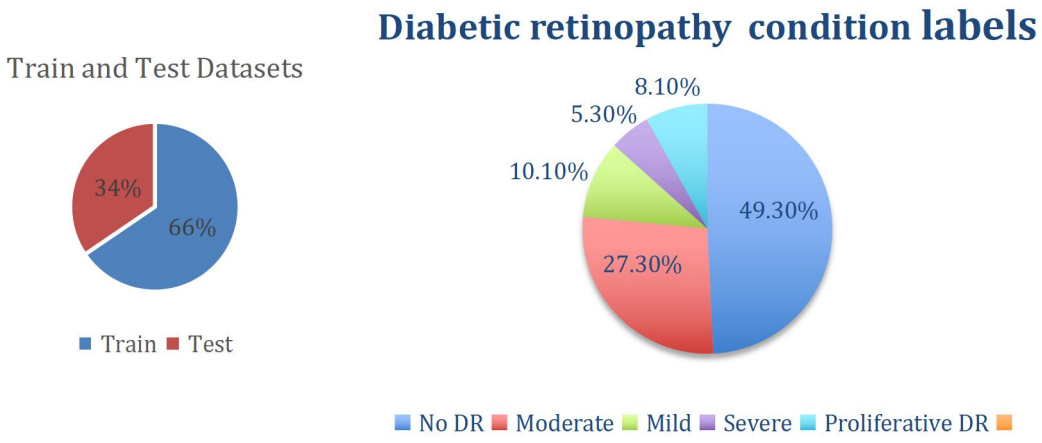

Figure 4.1: Class Label distribution [46]

In the pursuit of effective binary classification, instances of True Positive (TP), True Negative (TN), False Positive (FP), and False Negative (FN) outcomes are paramount. TP represents correctly identified positive cases, while TN signifies accurate negative predictions. On the other hand, FP occurs when a positive prediction is incorrect, and FN is associated with falsely predicting a negative outcome. These outcomes play a pivotal role in

evaluating the robustness and reliability of the trained models.

The classification performance is often measured through accuracy (ACC), a fundamental metric computed by dividing the total number of correct predictions by the overall dataset size. The accuracy score ranges from 0.0 to 1.0, where 1.0 denotes perfect predictions and 0.0 indicates complete mis-classification. While accuracy provides a holistic view of model performance, it may not be sufficient in scenarios with imbalanced class distributions. Hence, complementary metrics like precision, recall, and F1-score are frequently employed to gain a more nuanced understanding of the model's strengths and weaknesses.

This dataset, with its nuanced class distribution and emphasis on binary classification outcomes, not only forms the backbone of our research but also presents an opportunity to delve deeper into the intricacies of diabetic retinopathy prediction. It underscores the need for comprehensive evaluation metrics beyond accuracy alone, ensuring a thorough and insightful analysis of the implemented models.

$$\text{A}ccuracy = (TN + TP)/(TP + FP + TN + FN) \quad \text{—(4.1)}$$

$$Precision = TP/(TP + FP) \quad \text{—(4.2)}$$

$$Recall = TP/(TP + FN) \quad \text{—(4.3)}$$

4.1 A Hybrid Model on Deep Learning for the Diagnosis of Diabetic Retinopathy Using Image Cropping

The efficacy of diabetic retinopathy prediction models hinges significantly on the meticulous pre-processing of fundus images, a critical stage that sets the tone for subsequent analysis and classification. In this endeavor, Ben Graham's method takes center stage, offering a sophisticated approach to enhance the input data. The initial step involves a circle cropping algorithm, carefully chosen for its ability to capture all corners and edges of the fundus image, thereby optimizing image quality. Subsequent processes, including resizing, grayscale conversion, and the application of Gaussian Blur, further refine the images, preparing them for the nuanced analysis of severity

levels. This first part of our research lays the groundwork for a comprehensive exploration of the pre-processing pipeline, illustrating its pivotal role in enhancing the quality and standardization of fundus images for accurate diabetic retinopathy prediction.

The first step is the Ben Graham's method which starts by adopting the input fundus as pre-processing. A circle cropping algorithm is advised because it can recognize all of the image's corners, including the left, right, top, and bottom corners and edges, and it offers better quality. After analyzing the image, Ben can determine the scaling and add the circular crop to the input fundus image. Resize the pictures. Images that are rescaled have the same radius, either 500 or 700 pixels. The local average is mapped to over half of the grey. When your 90 percent crop an image to remove boundary effects, the average of local color is eliminated.

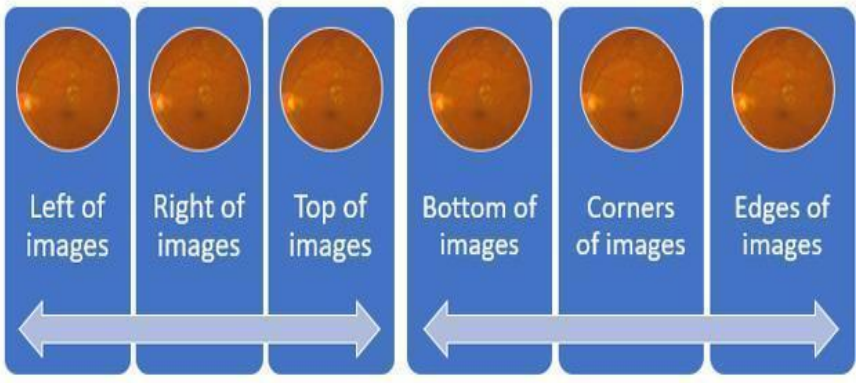

Figure 4.2: Circle cropping algorithm architecture [47]

Image cropping: The black portion has an effect on the method's output since the actual eye image in the data set includes a black area surrounding it. The image was then cropped to remove the black portion, leaving only empty space.

Resizing: Because the dataset image may come in a variety of sizes, we can utilize a radius of the image of 500 pixels to produce images of the desired dimensions.

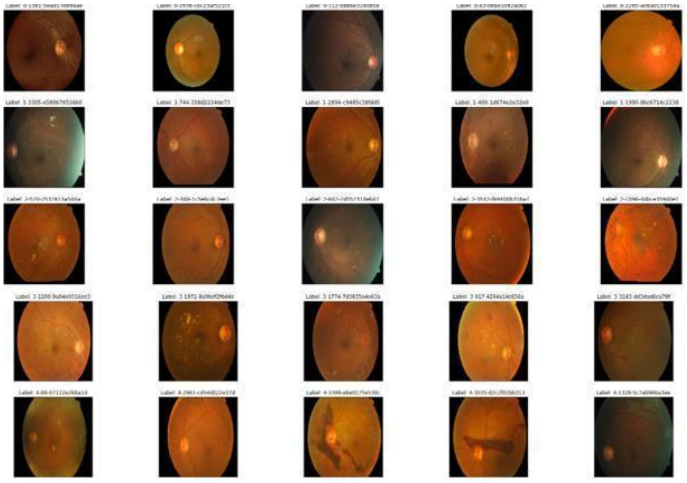

Figure 4.3: Actual dataset images [48]

Let's start by taking a look at the inputs themselves. Every row in Figure above has the ability to show the severity level. It is difficult to recognize these two problems because of how serious they are. First of all, some of the images are very dark. Fig. 0th row 2nd image and Fig. 4th row 4th image both contain examples. Different colors can occasionally be deceptive.

Second, as seen in the first and third images in the fig. 0th row, some images may contain unhelpful dark areas. As informative portions are too small, the picture's size must be reduced. To clip the case's ineffective portions second.

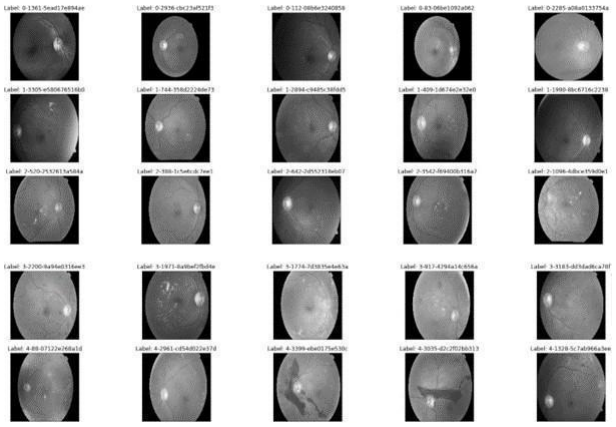

Figure 4.4: The original images convert into grayscale images[49]

Step 1*:* To better understand some photographs, try using a grayscale filter as there won't be any color distractions. At the upper portion of Figure 4.3's and 4.4's fourth-row fourth image, there is additional blood to be seen. The image has a severity rating of 4, and the first and fourth rows of the image both contain instances that are challenging to find. After you've seen the actual image size, can we try increasing it? The following are some unusual conditions: Cotton wool patches and hard exudates in the eyes are especially evident in the lower right corner of the eye. The magnitude of the value and the visual dimension are significant.

Ben Graham's Algorithm:

By auto-cropping, The Ben's make much more progress. The cropping process has been significantly improved by the colorized version (1). Grayscale was our first option before Ben's algorithm, but Ben's color version cropping produces better image quality.

Ben Graham's Algorithm

To generate image aspect ration (path,old_res,new_res = None):
Pass
(old_x -X) / (old_y -Y) = new_x / new_y
Old_x * old_y = resolution of the actual image
New_x * new_y = complete resolution
X = the group of pixels or points that should be cropped off
The y axis to achieve the complete resolution
Y = the group of pixels or points that should be cropped off
The y axis to achieve the complete resolution

Figure 4.5. The Ben Graham's pre-processing Algorithm [50]

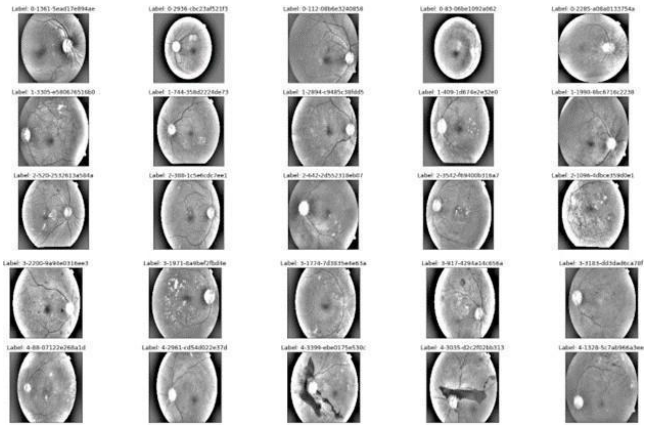

Figure 4.6. The images as Ben Graham's images [51]

The quality of the two methods is contrasted in the following two images. The cropping of Ben's color version is appropriate because it results in a high-quality image.

Gaussian Blur Algorithm:

Step 2: The Gaussian Blur Algorithm is the second stage in computing each point that can multiply by its weight value. Find the center of the point's Gaussian Blur value by putting the nine values together. For each of the image points, repeat this method. Following the Gaussian blur, we will then get the graph. Figure demonstrates that when Ben employs sigmax=20, which may have better performance, the image is clipped from the version of color applying the argument of sigmax=50 of GaussianBlur. The sigmax=20 or sigmax=50 photographs of the golden moon can be both attractive and graphic.

Gaussian Blur Algorithm

Step 1 : The blur can be understood as taking a pixel as the average value of its surrounding pixels
Step 2 : Weight of normal distribution
Step 3 : To calculate the Gaussian function
Step 4 : To evaluate weight matrix
Step 5 : To calculate Gaussian Blur, grayscale value(0-255)
Step 6 : The process for the points at borders

Figure 4.7. The Gaussian Blur Algorithm [52]

Circle Cropping Algorithm:

Step 3:

Circle Cropping Algorithm: The image has some resolution, and an algorithm can convert it: An image's previous resolution is

$$L * M \text{—(4.4)}$$

Let the picture resolution primarily be used for image cropping or resizing. This motion is out of date. Applying the new image resolution is now

$$P * R \qquad \text{—(4.5)}$$

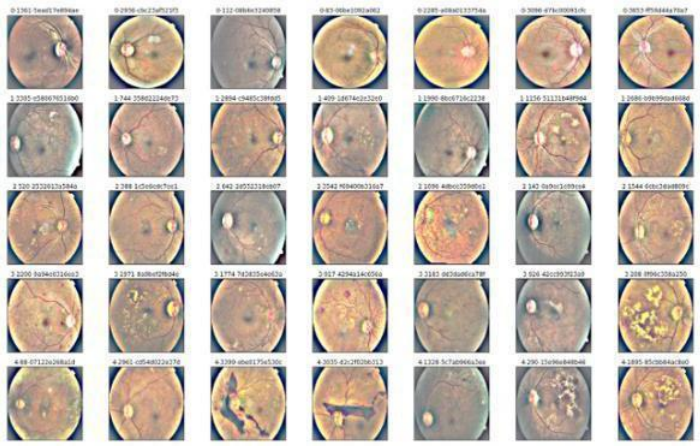

Figure 4.8. Actual images with Gaussian Noise, the Gaussian blur images [53]

Circle Cropping Algorithm

```
When apply the image auto crop <- image , threshold=0:
“””Crops any edges below or equal to threshold
Crops blank image to 1*1.
Returns cropped image.
“””
if len <- image.shape == 3:
flatImage = np.max <- image , 2
else:
flatImage = image
assert len <- flatImage.shape == 2
rows = np.where <- np.max(flatImage ,0) <- threshold)[0]
 if rows.size:
```

```
cols = np.where <- np.max(flatImage,1) <- threshold)[0]
image = image[cols[0]: cols[-1] +1 , row[0]:rows[-1]+1]
else :
image = image[:1, :1]
end if
end if
return image
```

Figure 4.9. The Circle Cropping Algorithm [54]

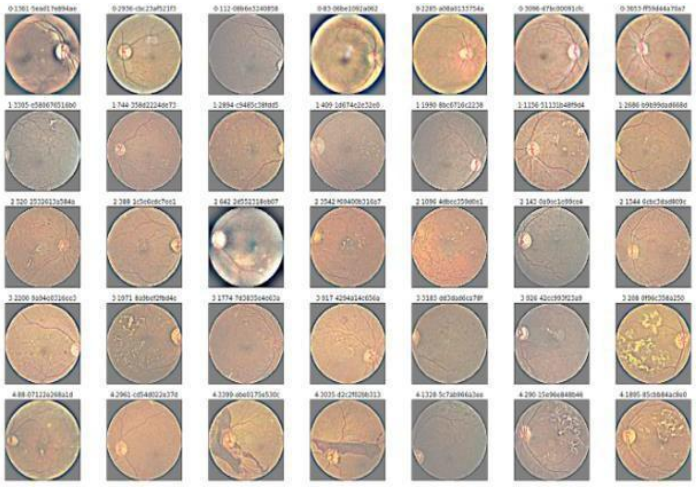

Figure 4.10. The Padding images, Circle Cropping images [55]

In step 3, The new image resolution covers all of the corners of the original image by using the maximum number of points or pixels from the original image. Image resolution or optimization is the process of reducing or rescaling the size of the original image for applications like Facebook profile pictures. Any image on the website could be affected in a general way by it. The cropped image's increased resolution is displayed in Figure (12). The largest image size is used to capture the actual image, and then the image is cropped in accordance with the original image's pixel ratio. To obtain the complete ratio, first apply the resolution to the image. This scenario closely resembles the new resolution's actual appearance.

4.2 Scrutiny of Diabetic Retinopathy Severity Levels using Deep Learning Mapping Sequences

It is not a novel computing strategy to use a deep learning neural network. It has been around for 20 years and is frequently used in speech synthesis, machine translation, cancer prediction, self-driving cars, image segmentation analysis on various diseases, and image analysis. CNN, a deep learning method, aims to specify data structures and broadly construct spatial orientation and interpretations to carry out models. CNN has also been extensively utilized in the search for the ideal compounds to manufacture pharmaceuticals that demand painstaking work, such as determining the molecular characteristics, physical, aqueous solubility, and chemical composition while working with professional biochemists and molecular biologists. In order to interpret and analyze medical images, the convolutional neural network (CNN) model automatically learns the useful feature matrices.

Convolution layers, which accept input, alter the data from the preprocessed image, and then pass it as input values to the next processed layer, are what the CNN is founded on. It is assumed that every conversion is a convolution- based process. The convolutional filter that frames the CNN architecture represents the critical role of a self-learning mechanism for extracting the required features for effective medical image processing and analysis. In order to detect patterns like shapes, edges, curves, objects, colors, textures, and small colored patches, each convolution layer is framed with a number of filters. The small-large matrix functional to an image is preserved by the image kernels filtering in 2x2, 3x3, 4x4, or txt vector ratios.

The convolution layers combined to create a sample input that represented the input image, reducing rationality by conserving the activated features that were crucial to the binding mechanism between the sub-regions. If the stride value is 1, the stride functionality, which describes the movement of the surrounding number of image-pixels of the input, automatically senses the surrounding pixels to move from one to another by turning the filter to 1 pixel at a time; if the stride value is 2, the filter is turned to 2 pixels at a time; If the stride values are 3, shifting the filter to 3 pixels at a

time, and continuing in this manner for successive sliding values and so forth, which extends mode up to changing the filter to 't' pixels at a time if the stride values are 't. With the help of associated filters and the effects of stride values, a huge image will be shrunk to an appropriate size.

Model Framework

This paper has proposed a dual-image multi-layer mapping method based on deep learning. Its main focus was on identifying and diagnosing the milder, moderate, severe, and proliferating forms of DR, such as Non-DR, MiDR, MoDR, and PrDR. All reliable DR stages are found and analyzed based on sequential and non-sequential photos using automatic image-mapping techniques.

Stage 1 → Sequential image eye-retinal color images + Sequential image eye-retinal black-white images

Stage 2 → non-Sequential image eye-retinal color images + non-Sequential image eye retinal black- white images

Stage 3 → Pre-processing of Sequential and Non-sequential image eye-retinal color images and black- white images through augmentation and normalization → Musterfrau A., Mustermann M.: J.UCS Sample Paper... Created the clusters CLUseq = clseq {combination of clu1seq-coli+clu1seq-bwi, clu2seq-coli+clu2seq-bwi ,……, clunseq-coli+clunseq-bwi } Created the clusters CLUnon-seq = clunon-seq {combination of clu1non-seqcoli+clu1non-seq-bwi, clu2non-seq-coli+clu2non-seq-bwi,,……, clunnon-seqcoli+clunnon-seq-bwi}

Stage 4 → Classification of five DR stages-based vectors which frame from Sequential and Non- sequential image eye-retinal color images and black-white images

CLFseq = clfseq {combination of clf1seq-coli+clf1seq-bwi, clf2seq-coli+clf2seq-bwi ……, clfnseq-coli+clfnseq-bwi }

Non-DR ← clf1seq-coli+cl1seq-bwi, MiDR ←clf2seq-coli+cl2seq-bw, MoDR ← clf2seq-coli+cl2seq-bwi SeDR←clf2seq-coli+cl2seq-bwi PrDR ← clf2seq-coli+cl2seq-bwi

CLnon-seq = clnon-seq {combination of cl1non-seq-coli+cl1non-seq-bwi, cl2non-seq-coli+cl2non-seq-bwi,……, clnnon-seq-coli+clnnon-seq-bwi}

Non-DR ← clf1non-seq-coli+cl1 non-seq-bwi,
MiDR ← clf2 non-seq-coli+cl2 non-seq-bw,
MoDR ← clf2 non-seq-coli+cl2seq-bwi
SeDR ← clf2 non-seq-coli+cl2 non-seq-bwi
PrDR ← clf2 non-seq-coli+cl2 non-seq-bwi

Stage 5 → The fifth stage involves recognizing the five stages of DR and determining its phases, such as Non-DR, MiDR, MoDR, SeDR, and PrDR. By identifying many lesions found on the retina, such as "microaneurysms, hard exudates, and hemorrhages", the concerns of these lesions are filtered out. The classification and regression techniques are used using a hybrid InceptionResNet multi-layer mapping approach based on the dual-images. In addition, smart self-tuning pre-processing methods are incorporated in all five stages of DR. The classification, segmentation, and regression techniques are framed based on dual image color fundus input images and black-white images. The proposed approach has introduced an efficient automated tuning system with classification, segmentation, and regression implications by using a hybrid Inception-ResNet multi-layer mapping approach to detect all five DR stages early.

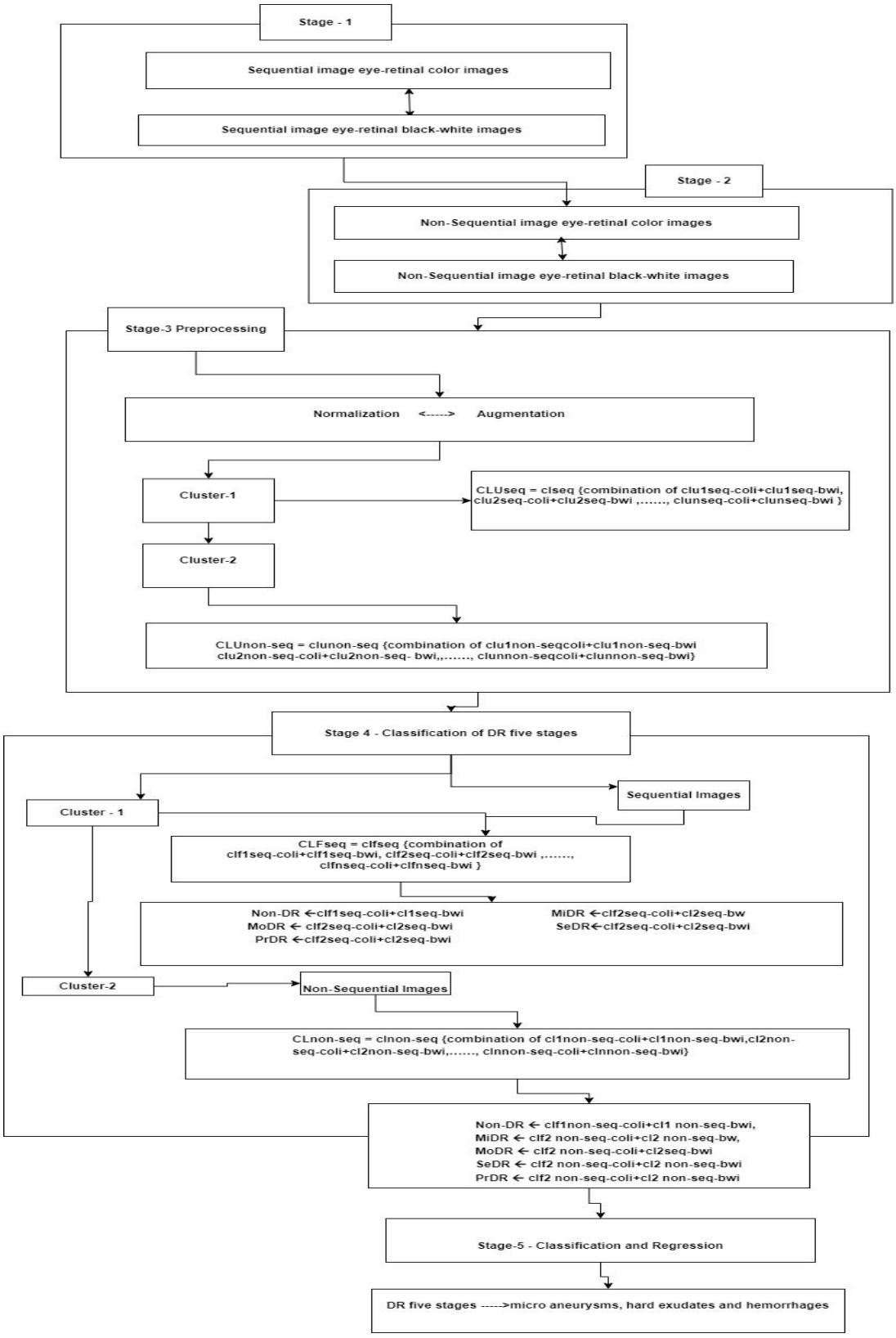

Figure 4. 11. Deep learning-based dual-image multi-layer mapping methodology-based Stage wise development which mainly focused on detecting and identifying the early stage of DR.

4.3 Methodology and model specifications for Classification of Diabetic Retinopathy Severity using Deep learning techniques on Retinal Images

Figure 4.11 is a flowchart depicting the workflow of the suggested DR classification methodology. The entire procedure is divided into four separate parts, which are completed in the sequence listed above.

i. Dataset Description:

We used a new dataset on Kaggle named "APTOS 2019 Blindness Detection" [186] to diagnose and prevent diabetic retinopathy in persons living in remote places where medical screening is difficult to do. Aravind Eye Hospital donated this dataset. Within the dataset, there are 5590 high-quality photos of the fundus. Because this is a competition dataset, all 3662 images have been labelled with their corresponding ground truth. The degree of diabetes retinopathy in each photograph was graded on a scale of 0 to 4, with the normal level being 0, the mild level being 1, the moderate level being 2, the severe level being 3, and the proliferative disease level being 4. Examples of each class in the APTOS 2019 BD dataset[186] are shown in Figure 4.1, along with their labels for future reference.

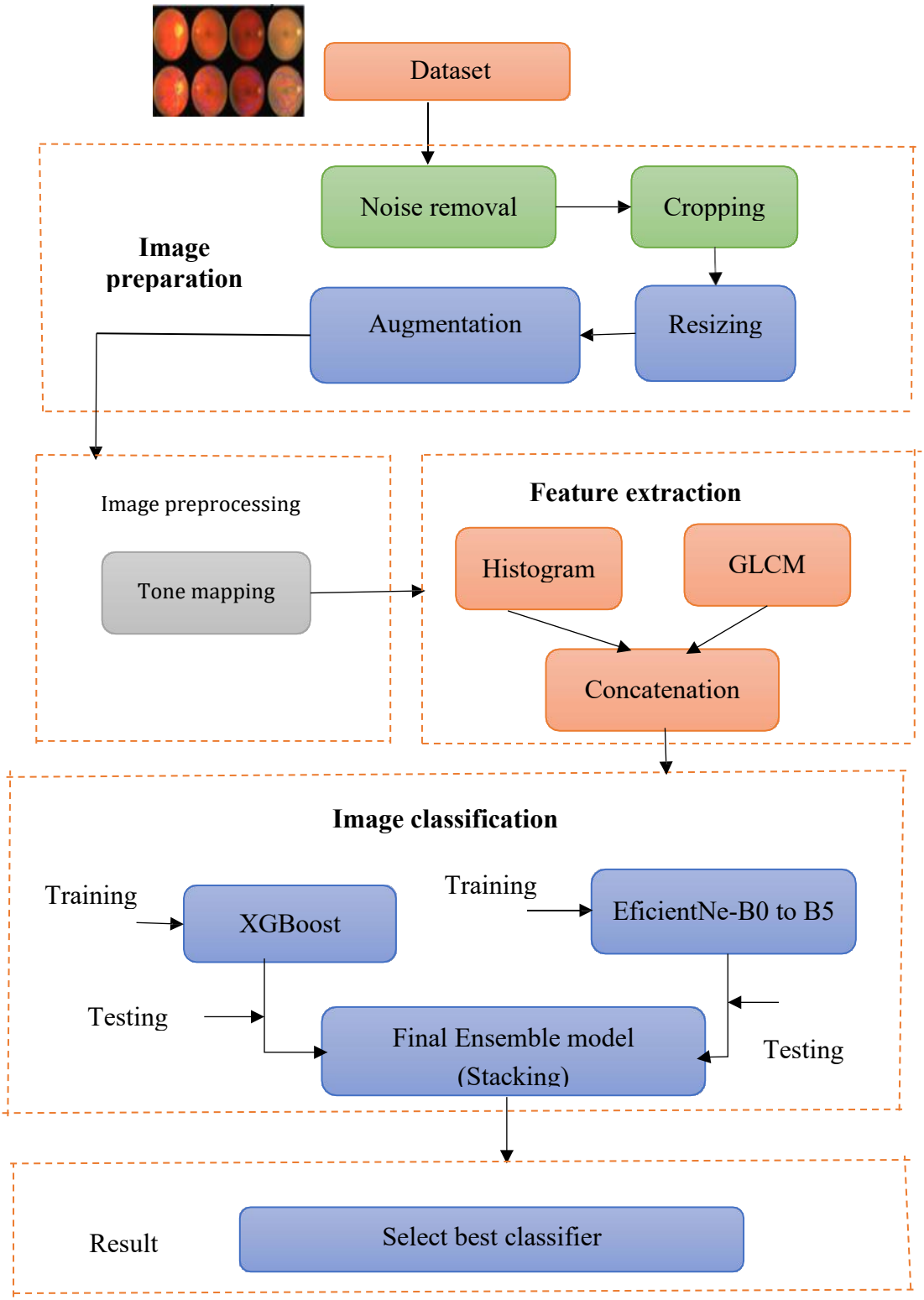

Figure 4.12: Architecture of the Proposed Work

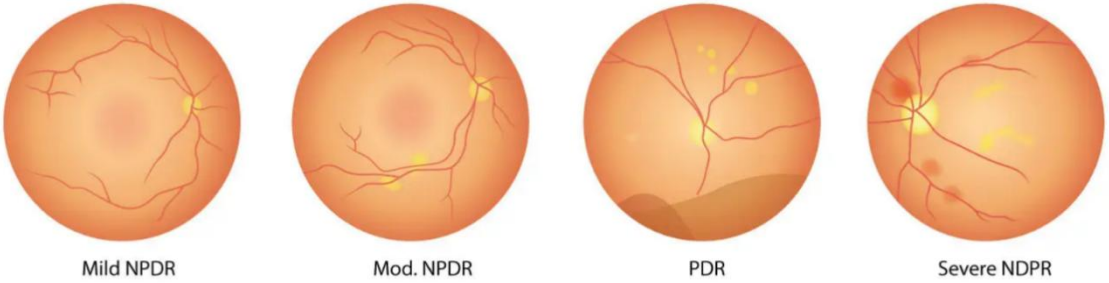

Figure 4.13: Sample images of various DR classes

ii. Image preparation:

Noise removal: Noise can be attributed to a multitude of sources (in this case, the measurement instrument), similar to how images can take on a variety of forms. Following that, the photos are purposefully blurred to emphasize the details. Image blurring techniques can be used to reduce noise. To finish the process of smoothing out the image, one might use one of several methods. A Gaussian filter was used to assist smooth out the image's look. The smooth image was then separated from the original image, and the resulting distinction is known as a mask. This means that the final image, also known as the mask, has a higher concentration of high-frequency components than the original, which were removed using smoothing filters. This mask was placed on top of the primary input images to allow the high-frequency components to be boosted.

Cropping Images: The APTOS 2019 BD collection[186] includes images from several locations and equipment. Because of this, the final images include many retinal component patterns. Instead of the black border, the reddish retina must be examined to diagnose blindness.

Algorithm 1: An algorithm for the cropping of images

Input: A retinal image, *IA*

Output: A cropped image without black borders, *IA0*

Step-1: Determine IA/IB resolution.

$(h, w) \leftarrow$ height & width of IA (in pixel).

Step-2: Find the image's center pixel:

$C_h \leftarrow floor(h/2)$;

$C_w \leftarrow floor(w/2)$

Step-3: Find the first non-black pixel above the center:

for $i = 1$ to h

if $(i, Cw) > 10$ in all three channels

C_1 i ; **break**

directly left to the center pixel:

for $i = 1$ to w

if $(C_h, i) > 10$ in all three channels

$C3$ i ; **break**

Step-4 : Crop the image: for $i = 1$ to 3

$\boldsymbol{I}_A(:, : i)$ $I_A(C_1 : C_2, C_3 : C_{4,} i)$

Step-5 : return IA

Dealing with Uneven Image Resolution (Resizing): Images included in the "APTOS 2019 BD dataset have resolutions that vary from 474 by 358 pixels to 3388 by 2588 pixels in width and height, respectively". These numbers refer to the width and height of the picture. This was discussed previously in the conversation. This dissimilarity could provide a problem for the processing that comes after it. As a result, during this stage, we performed a resizing operation that modified the dimensions of the photographs to 256 pixels by 256 pixels. This step was necessary to maintain the shape of the photographs constant and square, and we didn't want to lose any further information in the process.

Image Augmentation: The table shows that the related classes' instances are unbalanced. Data shows this. The problem persists after removing noisy and duplicate photos. The NO class, which represents the bulk of the population, has roughly eight times the sample size of the "Severe DR (SE) class", which represents the minority.

The NO class may better represent the community. Compared to NO, MI, PR, and NO samples were much smaller. Working with an unevenly dispersed dataset is difficult, but it must be overcome. The most obvious bias in new samples is favoring the class with the majority of members. We created new examples using data from the MI, SE, and PR classes to solve this problem. To obtain four times larger sample sizes, each photo from the aforementioned classes was rotated 90 degrees, 180 degrees, and 270 degrees.

iii. Image pre-processing:

Retinal images were pre-processed using a separate way before extracting features from the harder types. Before examining the clearer images, this was done. Tone mapping, a digital camera technique, was applied at this stage. Tone mapping may reduce the dynamic range of a shot. Digital cameras employ this technology to improve image quality and suit digital screens. However, we used this method to limit retinal images' dynamic range while preserving their most important elements, such as "local contrast, global contrast, details, etc". We maintained image fidelity despite lowering dynamic range. Mapping each tone in the source image creates a viewing tone. The following operator may tone map a three- channel image (IA):

where $R_i \subseteq R$, $Do \subset R_i$, and $Do = [0, 255]$. Tone mapping changes the picture's brightness but not its color. Example of simplifying equation (4):

$$LJ(I_A) = \{ \quad \begin{matrix} L_d = t(H_d); R_i^{hxw} \\ \begin{bmatrix} R_L \\ G_L \\ B_L \end{bmatrix} = L_d \left(\frac{1}{R_d} \begin{bmatrix} R_H \\ G_H \\ B_H \end{bmatrix} \right) \end{matrix} \qquad \text{----- (4.6)}$$

where L_d and H_d a pixel's low and high dynamic range brightness values. The saturation factor symbol is S (0, 1), meaning "zero one." The red, green, and blue channels' low dynamic ranges are RL, GL, and BL, while their high dynamic ranges are RH, GH, and BH. This experiment used the global tone mapping system. This approach assigns every pixel the same t value.

Local tone mapping maps each pixel based on its neighbors. Each retinal pixel may be

scaled linearly, exponentially, or logarithmically. In this *t* may be applied to each pixel in three ways. A factor multiplies the primary image during linear scaling:

$$L_d(p_i)linear = H_d(p_i) \qquad \text{----- (4.7)}$$

where p_i is an illustration of a pixel. The variables in logarithmic mapping and exponential mapping are linked as follows L_d and H_d (7) and (8), respectively, define them in their respective equations.

$$L_d(p_i)_{logarithmic} = \frac{log_{10}(1+k_1 H_d(p_i))}{log_{10}(1+k_1 H_d(p_i)_{max})} \qquad \text{----(4.8)}$$

$$L_d(p_i)_{exponential} = 1 - exp(-\frac{k_1 H_d(p_1))}{1+k_1 H_d(p_1)_{max}} \qquad \text{----(4.9)}$$

where $k_1 \epsilon$ (1, ∝]and $k_2 \epsilon$ (∝ ,1] both remain unaltered. Despite the fact that the end results are aesthetically equivalent, In this study, we attempted to mimic the appearance of retinal images using the exponential mapping method.

iv.Feature Set Creation

After pre-processing retinal pictures, we may extract characteristics. This phase takes the longest. The learning method has little information since most blue channel pixels are dim or virtually black. Eliminating the blue channel from color photographs reduces characteristics. We extracted the histogram and GLCM from each retinal image. Two common imaging methods are discussed below.

Histogram Features: An image's histogram displays the grey levels' relative frequency in decreasing order. The discrete function in the following line describes the range of a typical grey label picture, which is 0 to l minus 1.

$$\sqrt{g_k} = \frac{n_k}{h\,X\,w} \qquad \text{—(4.10)}$$

where "g_k is *k*-th grey label, n_k is the number of pixels with that label, and $h \times w$ is the total image pixels" . Grey labels vary from 0 to 255 in 8-bit color images.

Gray-Level Co-Occurrence Information Extraction: GLCM emphasizes image texture information. A matrix that depends on pixel distance and angle may express it. Retinal images have 256 by 256 pixels with pixel values from 0 to 255. To calculate the GLCM of such a picture, each pixel must be translated into one of eight levels. Scaling values to many levels may be necessary. This experiment employed stages 1-8.

This new matrix is called a "scaled image (*S*)". GLCM shows the frequency of one pixel value (*k*) compared to another (*l*) diagonally, horizontally, or vertically. As shown in Figure 6, the image's co-occurrence matrix (C_m) is generated by a displacement vector with the equation $d = f(\text{row, column})g$. The number of times a k is geographically distant from *l* is shown by the value given by the function $C_m(k, l)$. As a result, the formula for computing $C_m(k, l)$ is as follows:

$$C_m(k,l) = \sum_{k=1}^{8} \sum_{l=1}^{8} \begin{cases} 1, if\ S(i,j) = k\ and \\ S(i \pm d, j \pm d) = 1 \\ 0, otherwise \end{cases} \text{— (4.11)}$$

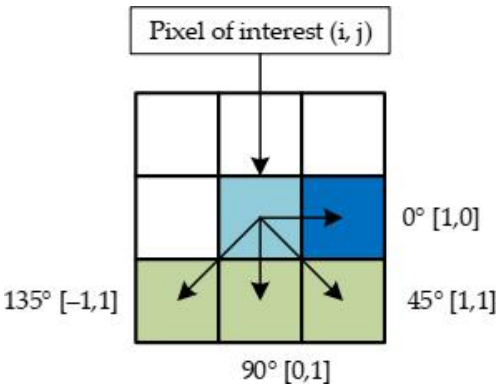

Figure 4.14: The Grey Level Co-occurrence Matrix (GLCM) displacement vector

Feature Concatenation: Each retinal image channel was treated using feature extraction methods. After concatenating the three channel histogram features, 768 features were created. After flattening each channel's GLCM features, we could visualize them as a 64- feature row vector. Three GLCMs and three channels provide 192 characteristics. We generated a database of 960 retinal traits from one shot by integrating these two groupings of attributes. To collect all essential characteristics, all 5285 samples were processed several times.

v. Image Classification:

An “ensemble learning algorithm for classification and regression called XGBoost” is based on DT. These issues are resolved by this remedy. By transforming a group of weak learners into strong learners, it increases prediction power. This algorithm is XGBoost. XGBoost was designed to increase speed and performance using gradient-boosted decision trees. This droves its construction. The phrase "it is a method of boosting machines" is another way of saying that it boosts machines. Extreme Gradient Boosting (XGBoost) helps tree- boosting algorithms utilize memory and hardware efficiently. It may improve algorithms and models and be employed in other computer systems. This makes it competitive. XGBoost can implement gradient, regularized, and stochastic gradient boosting algorithms, making it flexible. It adds and changes regularization parameters, unlike other libraries. It reduces computation time and maximizes memory resources. It is "Sparse Aware," allowing parallel tree construction, missing values, and boosting on fresh data already on the trained model. It may also increase newly learned model data. Training loss and regularization make up the goal function. These two sections comprise the function.

$$obj(\varphi) = TL(\varphi) + R(\varphi) \qquad \text{— (4.12)}$$

XGBoost works by first combining all of the trees constructed from the dataset's predictions and then optimizing the final output. XGBoost adds a new tree at each step of training to maximize the effectiveness of the previously learnt tree. In general, the new objective function, which takes the form of an expansion given by Taylor's theorem, includes up to the second order. At step t, a new objective function is introduced.

$$bj^{(t)} = \sum_{i=1}^{n} [m_i f_t(p_i) + \frac{1}{2} c_i f^2{}_i(p_i)] + R(f_t) \qquad \text{— (4.13)}$$

where *mi* and *ci* are taken as inputs.

$$f_t(p) = wq(p), w \epsilon R^L, q: R^d \rightarrow \{1,2,3,4,\ldots,L\} \qquad (4.14)$$

In the equation above, the symbol w denotes a vector of leaf scores (each data point

using the same leaf receives the same score), and the function q assigns leaves to the correct data points. L indicates leaf count. XGBoost is sophisticated.

$$R(f) = \alpha L + \frac{1}{2}\beta \sum_{j=1}^{L} w^2 j \qquad \text{— (4.15)}$$

The regularization equation may be replaced into equation (8) to get the optimal objective function at step *t*. The *t*th tree is the outcome. These changes resulted in a model that represents the reformed tree model and evaluates its quality $q(p)$. Because it is difficult to compute all tree configurations at once, the tree structure is determined by calculating the regularization, leaf scores, and goal function for each level. This stage builds the tree. Gain is determined at each level as a leaf is separated into a left leaf and a right leaf. Regularization is completed at any further leaves. Each level computes a gain when a leaf splits into left and right leaves. Splitting a leaf into its left and right halves calculates gain level-by-level. The branch is pruned if the benefit is less than the additional regularization value. XGBoost uses trees to classify data, so accuracy and other criteria may be checked.

EfficientNet-based weighted ensemble model

An ensemble model may enhance model prediction by mixing several less effective learning classifiers. For this study, the ensemble classifier is considering hard and soft voting models. Each classifier is equally weighted in all voting models. It suggests that the varied expected performances of the insufficient classifiers cannot be leveraged across the various machine faults.

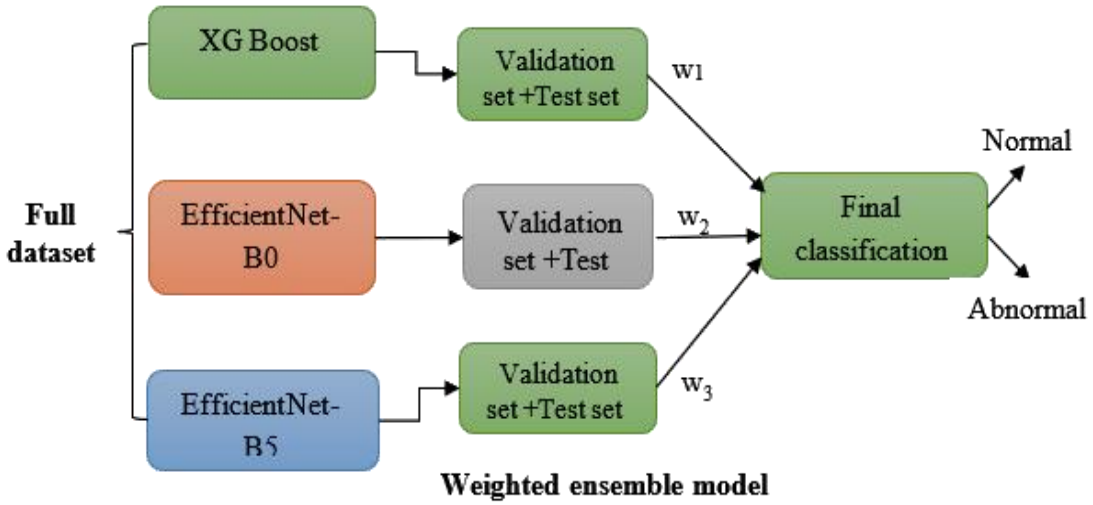

Figure 4.15: A comprehensive outline for the EfficientNet-based weighted ensemble model that was presented before.

The difficulty and distinctions between EfficientNet-B0 and B5 are shown in the figure above. The EfficientNet family's EfficientNet-B0 has the least number of moving parts. Progressive increases in depth, width, and resolution are seen as one advances from EfficientNet-B0 to EfficientNet-B7; however, model size increases as accuracy rises.

(a)

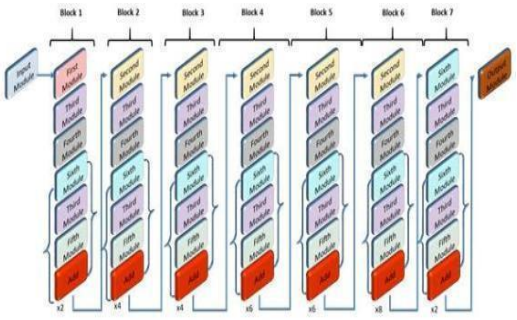

(b)

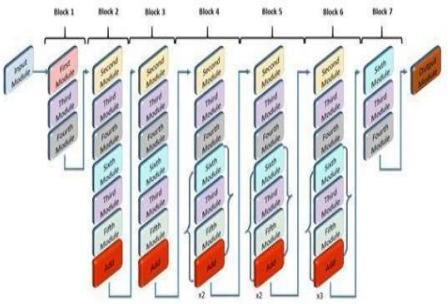

Figure 4.16: EfficientNet architecture comparison (a) EfficientNet-B0 (b) EfficientNet-B5

Weighted voting strategy

Recently, interest in mixed ensemble learning methods has grown. To mitigate the negative effects of overfitting and initialization sensitivity on the system's learning capabilities, these strategies either employ heterogeneous or homogeneous model-generated learners. These challenges might be lessened by learning in mixed ensembles. Each ensemble member receives a grade based on how much weight they carry in one of four categories. Model weights are generated using the Dirichlet distribution approach rather than performing an exhaustive grid search. This is used instead of a comprehensive grid search. Two crucial proportional data models are the Dirichlet distribution and the Dirichlet-multinomial. Both theories are grounded in the Dirichlet equation. The Dirichlet distribution theoretically backs up these claims. When m models are trained on a dataset containing n samples, their outputs are aggregated to classify (predict) each instance *x*:

$$y(x) = \sum_{j=1}^{m} \beta_j(x) h_j(x) \qquad \text{— (4.16)}$$

Here weights *βj* correspond to probabilities V

$$\sum_{j=1}^{m} \beta_j(x) = 1 \; and \; 0 < \beta_j(x) <= 1 \qquad \text{— (4.17)}$$

The fit() method greedily randomly optimizes weights using a validation dataset and the Dirichlet distribution.

Dirichlet distributions model proportions. A probability distribution on the vector (β1 *β2*,....,*βm*) is examined for an experiment with outcomes 0, 1 and probabilities of *β1* *β2*,. ,*βm*. ∑_(j=1)^m⟦β_j (x)⟧=1 is assumed which cannot be defined a density on *β1* *β2*,....,*βm*, but it may be defined on β1 β2,…,βm-1 and then take β_m=1-(j=1)^(*m*-1) (*x*). Thus, pm is the model m percentage since β is a random vector whose members total to 1. The Dirichlet model with parameter vector α has V probability density at *β*.

$$p(\beta) \sim Dir_{(\alpha_1,\ldots,\alpha_m)} = \frac{\Gamma(\Sigma_m \alpha_m)}{\Pi_k \Gamma(\alpha_m)} \Pi_k P_m^{\alpha_{m-1}} \qquad \text{— (4.18)}$$

where

$$\sum_k P_m = 1 \; and \; P_m > 0 \qquad \text{— (4.19)}$$

A validation dataset *D* = (*β1* *β2*,...,*βn*) can estimate α. The maximum-likelihood estimate of α maximizes *p*(*D*|α)=*p*(*β*_i|α).

4.4 Comparative Analysis of Machine Learning Approaches of Prediction of Diabetes Consequences in Pregnancy with Implications of data Matrices

Diabetes belongs to a class of metabolic diseases marked by persistently increased blood sugar levels. Give examples of symptoms like the desire to have high blood sugar, increased thirst, and frequent urination. If diabetes is not addressed, it can cause a variety of problems. Acute difficulties can include one or more integrated hyperosmolar hyperglycemic states, diabetic ketoacidosis, or even death. Among the long-term consequences that can be detrimental are stroke, foot ulcers, chronic renal disease, heart disease, and sensory impairment. Details on the attributes are provided in Table 5.1.

Insulin: Figure 4.17 illustrates insulin for diabetic women (102.5), and healthy women (102.5). (169.5)

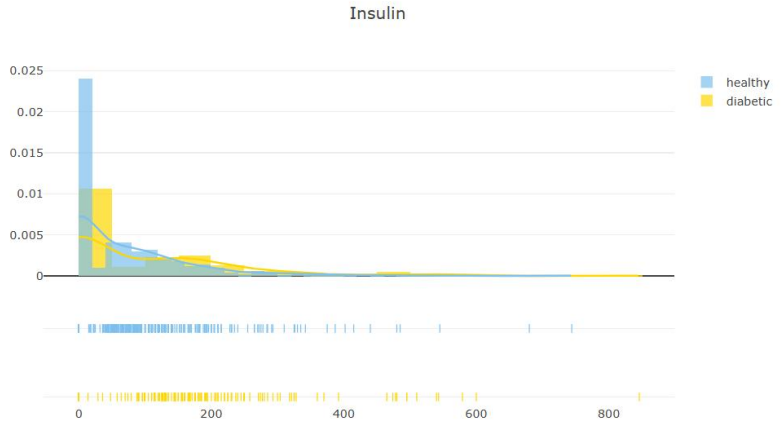

Figure 4.17. Shows the Insulin

Glucose: Figure 4.18 shows that the glucose for Diabetic Women (107.0) and Healthy Women (107.0) must be taken into account (140.0).

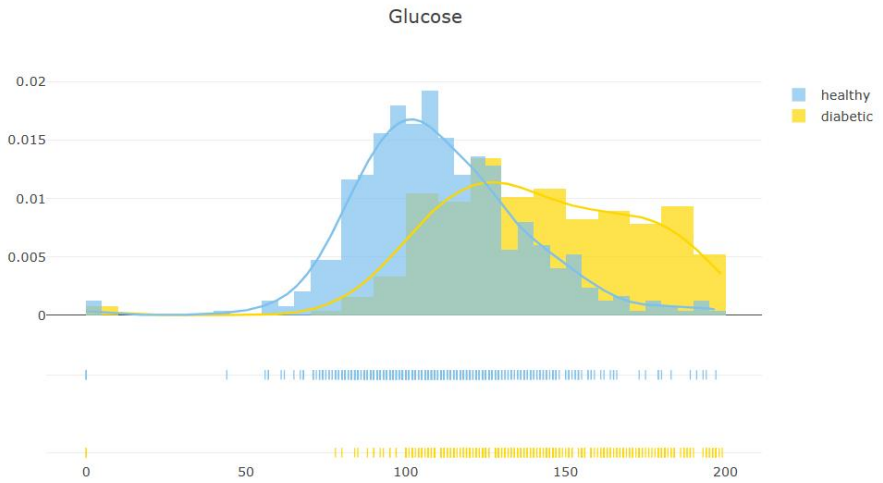

Figure 4. 18. Shows the Glucose

Skin Thickness: Figure 4.19 displays triceps skin fold thickness for diabetic women (32.0) and for women in good health (27.0).

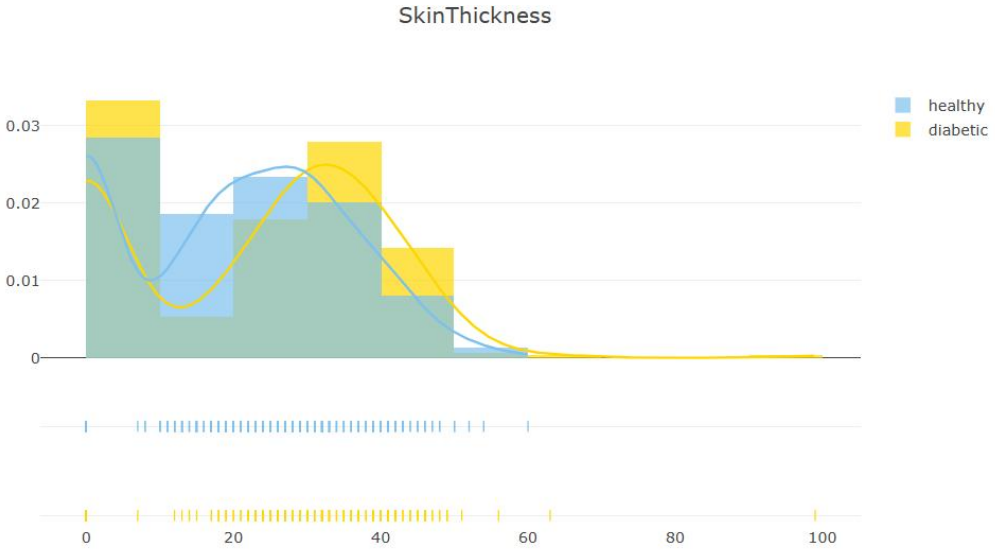

Figure 4.19. Shows the Skin Thickness

Blood Pressure: Figure 4.20 illustrates the results of calculating the blood pressure levels for healthy and diabetic women (74.5).

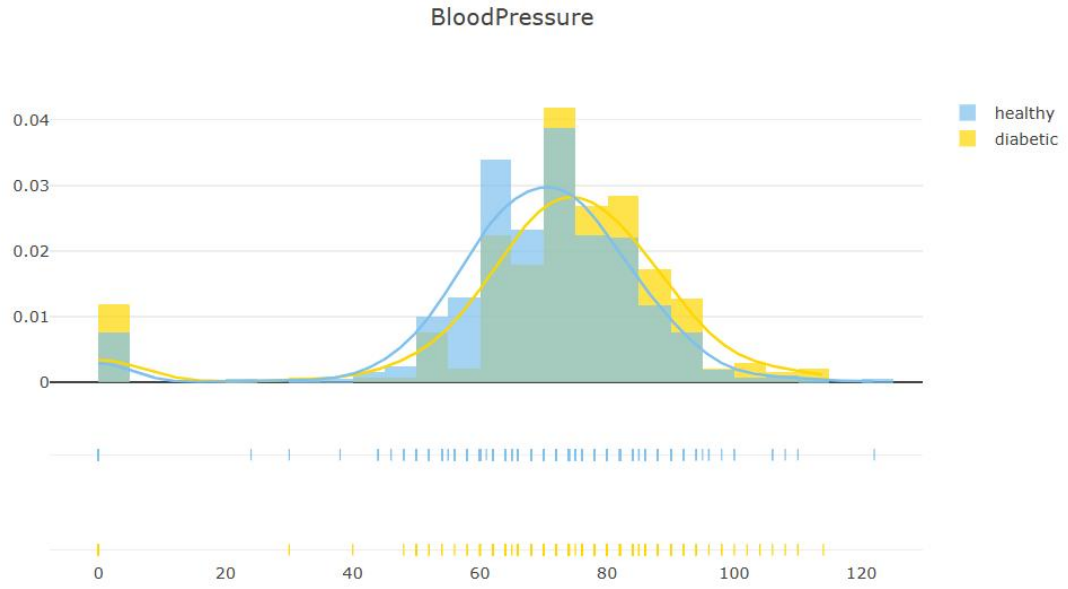

Figure 4.20. Shows the Blood Pressure

BMI: Figure 4.21 illustrates the results of calculating body mass index, which show women in good health (30.1) and women with diabetes (33.8).

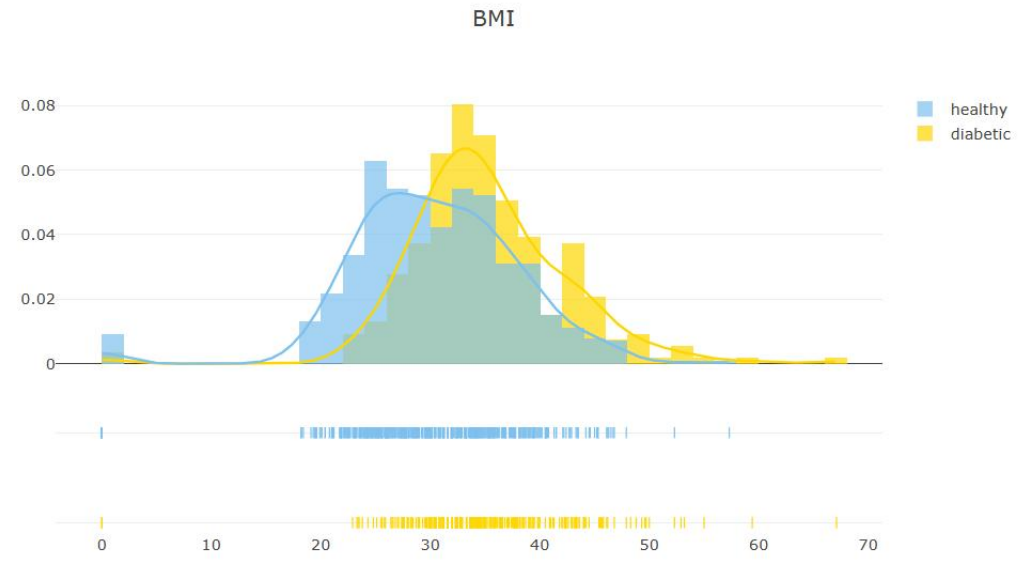

Figure 4.21. Shows the Body mass index

Age Figure 4.22 Healthy women's ages (21–60) and diabetic women's ages (21–60) are shown.

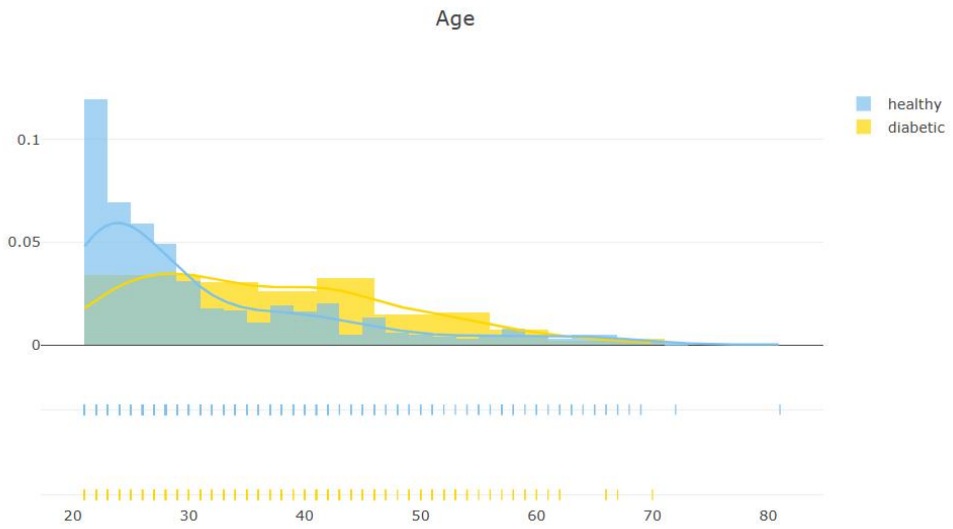

Figure 4.22. Shows the Age

Pregnancies: Figure 4.23 displays the number of pregnancies for Women with diabetes (1–8) and in good health (1–8)

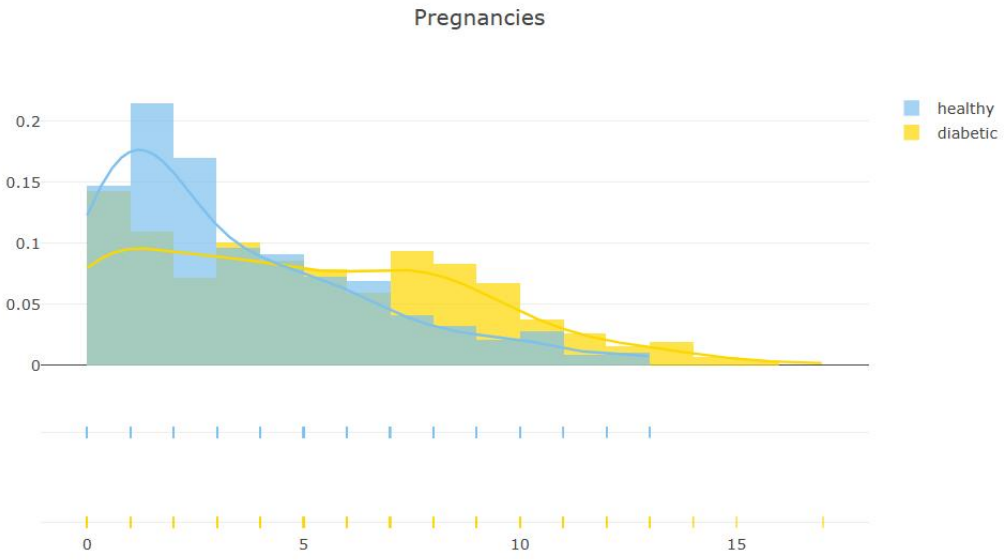

Figure 4.23. Displays Pregnancies

Diabetes Pedigree Function: There are various types of diabetes pedigree. The Healthy Women and Diabetic Women are depicted in Figure 4.24 of the Diabetes Pedigree Function.

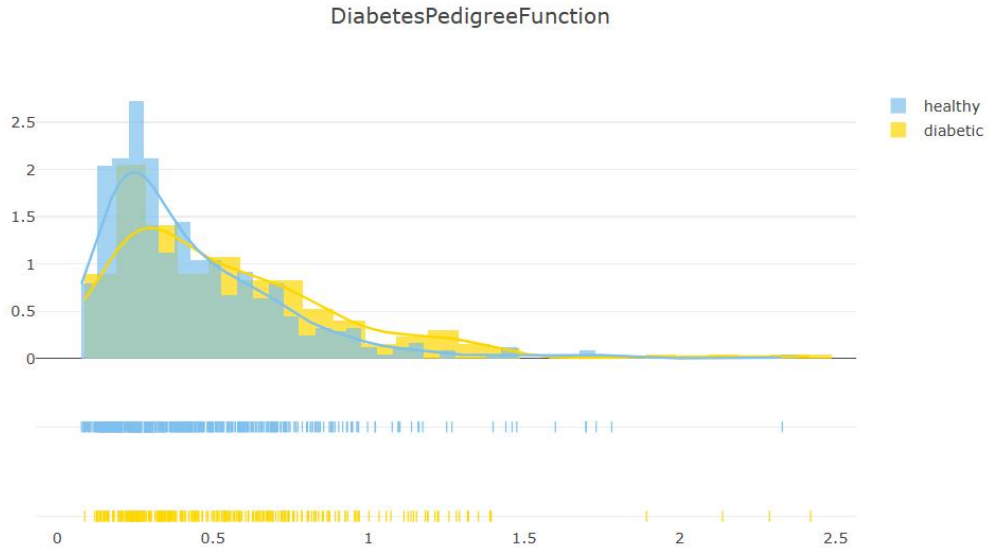

Figure 4.24. Shows the Diabetes Pedigree Function

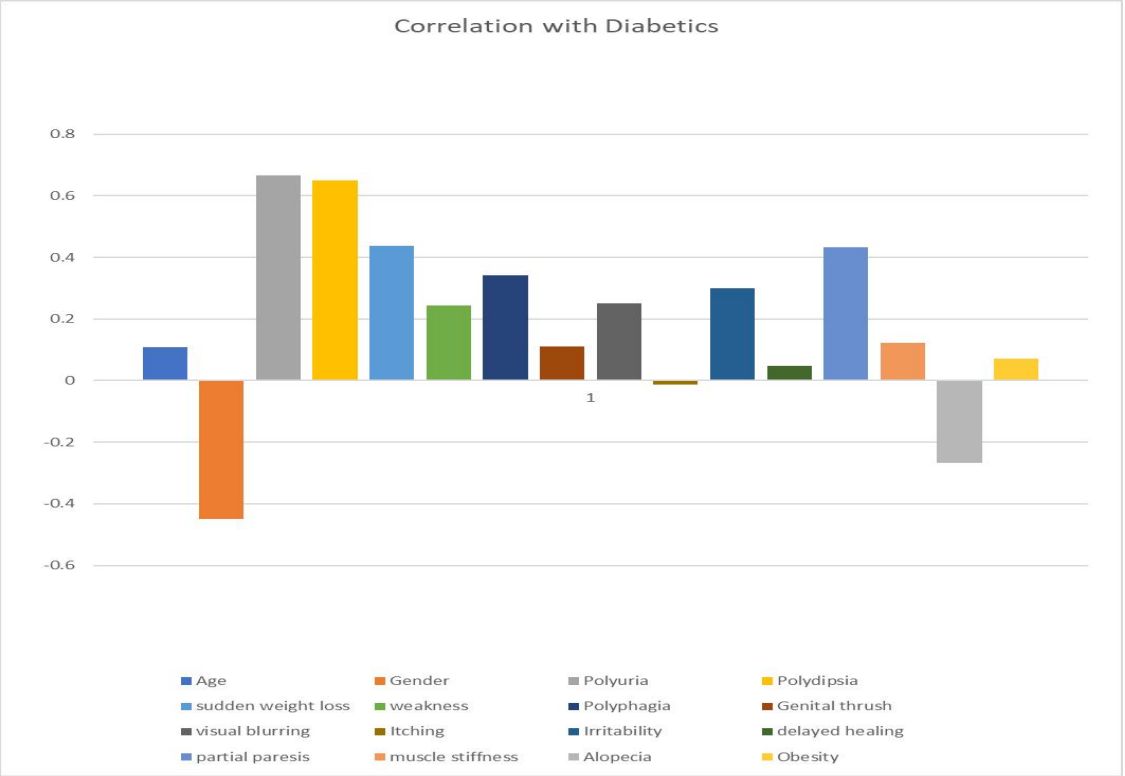

Figure 4.25. Shows the model of roc-score is 0.99 in both train and test set and polydipsia is the major variable to build the model & feature engineering values. [53]

4.5 Methodology and model specifications for Detection of early-stage symptoms of diabetic retinopathy prediction performance in machine learning algorithms

Convolution neural networks fall under the machine learning category. The purpose of using filters in convolution neural network, filters can exist of some dissimilar kinds conferring to persistence. Filters can support to utilize the dimensional located of specific image by implementing a local connection pattern among neurons. the convolution principally a point-by-point reproduction of binary functions to generate tierce function, unity function is image pixels matrix and other one is filters. Figure 2 shows the model of roc-score.

Description of Model Framework

Dataset and Processing stages

Dataset:https://archive.ics.uci.edu/ml/datasets/Early+stage+diabetes+risk+predictio n+dataset

Stage1: Diabetic person

Stage 2: Non-Diabetic person

Stage 3: Class represents the positive, negative values of diabetic symptoms

Stage 4: Classification of diabetic symptoms ->polyuria, polyphagia, genital thrush, sudden weight loss, irritability, delayed healing, partial paresis, muscle stiffness, alopecia, visual blurring, itching age, sex, weakness, class.

Stage 5: Hyperparameters and their min and max values.

Stage 6: n_estimators can be shows the number of boosting stages and default value=100

Stage7: Step size compress the subscription of every tree by their value & default value=0.1. The trade-off among step size and n_estimators.

Stage 8: Max_depth can be shows the extreme depth of discrete regression evaluate and default value = 3. The max depth restrictions in quantity of nodes in the tree.

Stage 9: Under sampling can define the segment of trials used for correct the separate base learners and default value=1.0

Stage 10: Max_features can indicate the number of landscapes to be reflect for best split, possible values are auto, sqrt, log2 and default value = None.

Transformed into numerical. All missing values are removed and the data cleaning number is 480. Data transformation for the dataset is applied.

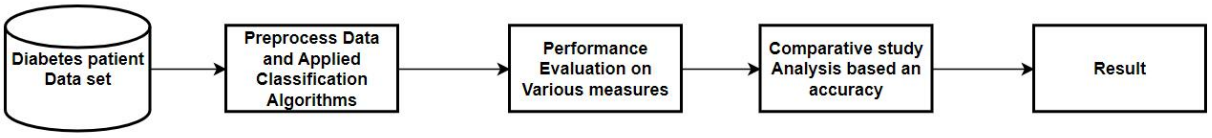

Figure 4.26. Shows the process flow of data and measures

4.6 Automated Decision Making ResNet Feed-Forward Neural Network based Methodology for Diabetic Retinopathy Detection

Methodology

Multi-labelling mapping and classification using D-CNN designs improve DR assessment. There are several types of DR, including those that are proliferative and those that are not. Color retinal FunImgs show DR lesions proportionate to disease severity. Since they share so many features, traditional approaches may be challenging to separate and identify lesions. Hence, a robust CNN model that uses the Dual Image ResNet Mapping Technique will produce the best results. Retinal DR diagnosis allows early detection and faster treatment. This study provides a dual image ResNet mapping auto fine-tuning strategy to accelerate screening by detecting early-to-late DR. Once collected, CNN's high-level properties were mainly used to identify and classify retinal lesions. This research sought the most precise RI interpretation possible to improve DR detection simulations. For the most accurate interpretation, features from a number of pre-trained ConvNet simulations were combined with a multi-modal blended module. The final description step trains a D-CNN to recognize and predict DR severity. Each ConvNet collects its own set of features aggregated via 1D and cross-pooling to give a more accurate interpretation than a single ConvNet could provide

alone. In order to further understand AD, an exploratory research study will first need to be conducted. This research will use Convolutional Neural Networks that are trained using deep learning to accomplish many different goals. The second aim, which is the most crucial for my research, is to provide a new framework and then use it to analyse a dataset that is open to the public. Because deep learning can accommodate both supervised and unsupervised segmentation, the suggested technique module for training the deep comprehension of the image with labels may be able to satisfy the needs of unlabeled data. In conclusion, the empirical evaluation will be carried out to determine whether or not the proposed framework is feasible.

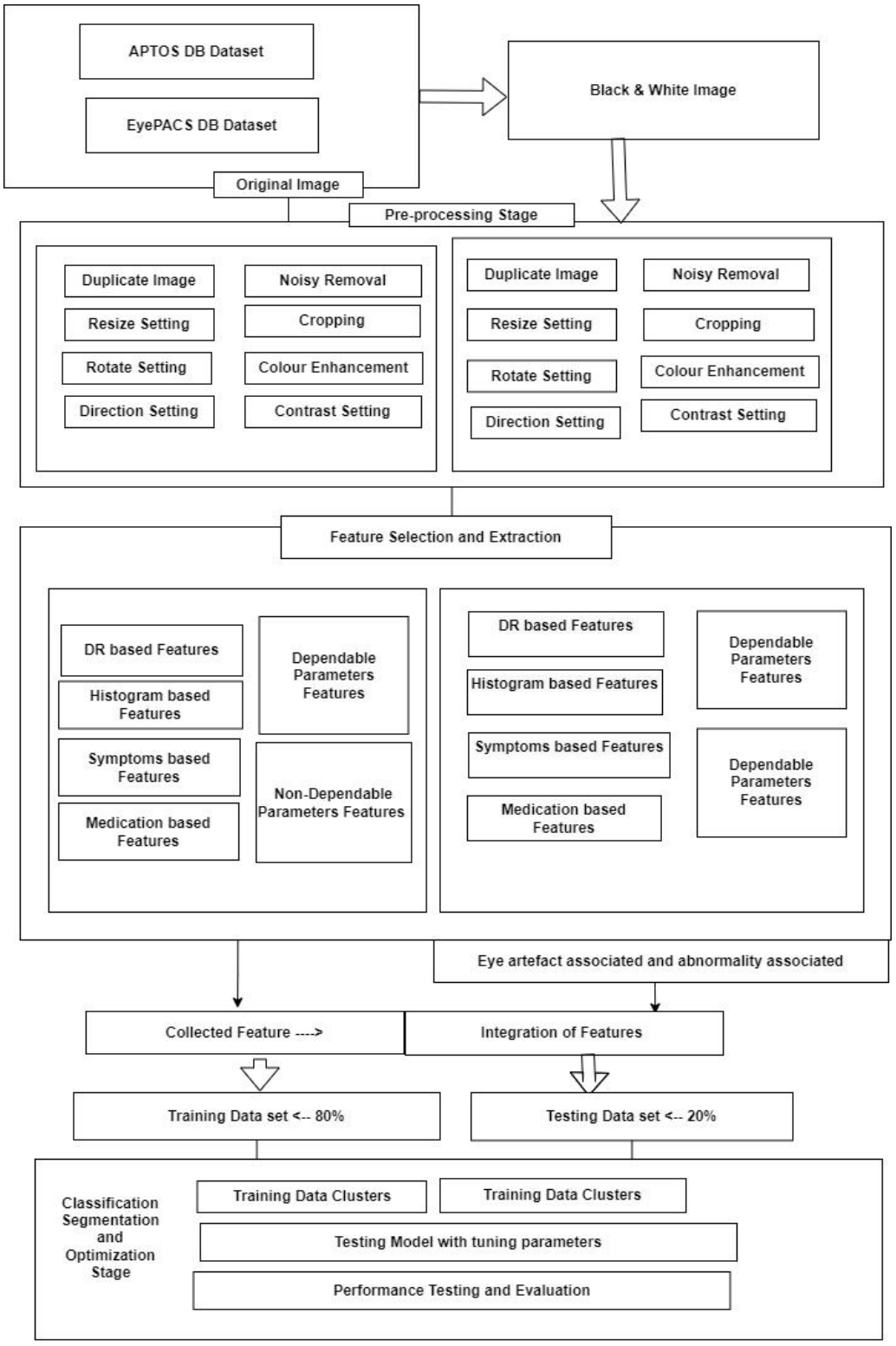

Figure 4.27. Dual-image multi-layer mapping methodology for identification of DR early stages [56]

The classification and detection of DR phases are integrated into the dual imaging approach, which mixes and aggregates color and black-and-white fundus images. Prior to combining the black-and-white and color fundus images with the missing pieces of each image sequence, both images are subjected to separate analyses. More than 10,000 images from a range of ages, including those between the ages of 3 and 10, 26 to 35, 46 to 55, and more than 56 —have been incorporated into this study. As a primary case of input images, all color fundus photographs from patients of different ages were initially gathered. All color fundus images gathered for data gathering are split into sequential and non-sequential groups. Sequential photos are those selected from the same subject and age group. The research employs a number of consecutive photographs with a minor difference in the color fundus, each of which has been used to obtain the best results and most accurate projections for the five stages of DR. The automated tuning mechanism appears to be complicated when tuning non-sequential images.

vi. D-CNN-based Dual Image ResNet Mapping Auto Fine-Tuning Algorithm

The data would be further analyzed using the suggested deep learning-based CNN-implicated dual-image multi-layer mapping technique. The suggested methodology must be modified for training and testing because its training proficiency ultimately rely on balanced error-free data. Both the color fundus and the black-and-white photos have the same amount of data for each DR stage, including Non-DR, MiDR, MoDR, SeDR, and PrDR. As a result, any inequality that may arise during the training and development of the recommended method is minimized by the model. In order to choose the combo photos for grading analysis and future forecasts, all of the input black-and-white and color fundus photographs are first analyzed. The classification work is mostly carried out using the deep learning inception-Resnet model. The classification work has also begun utilizing the cross-entropy loss function based on binary-class and multi-class classification in two separate forms.

Step 1: Data Collection and Analysis à Diabetic Symptoms (DSs)

DSs à {alopecia, age, sex, weakness class, genital thrush, polyuria, blurred vision, polyphagia, delayed healing, sudden weight loss, itching, and irritability. }

Step2: Pre-processing stage:

Step 2.1: Input Data: dataset integration

Original image size → color fundus image (CFI) = 256 X 256

Converted image size → black and white image (BWI) = 256 X 256

Axes path values = (X, Y) → (1800, 1800)

Rotation Feasibility in degree for CFI and BWI → {90, 180, 270, 360}

Step 2.2: First stage of an input image → color fundus image (CFI)

Set of original image class of CFI (O-CFI) = {O-CFI-X1, O-CFI-X3, O-CFI-5, O-CFI- X7, O-CFI-X9}

Set of augmented image class CFI (A-CFI) = {A-CFI-X2, A-CFI-X4, A-CFI-6, A-CFI- X8, A-CFI-X10}

Step 2.3: Second stage of an input image (converted image) → black and white image (BWI)

Set of original image class of BWI (O-BWI) = {O-BWI-X1, O-BWI-X3, O-BWI-X5, O- BWI-X7, O-BWI-X9}

Set of augmented image class BWI (A-BWI) = {A-BWI-X2, A-BWI-X4, A-BWI-X6, A- BWI-X8, A-BWI -X10}

Step 3: Insert the images in a sequential or non-sequential pattern.

Consider single Input Image ← II

for II = I_1 to I_n

Step 3.1:

Employed filters ← 3X3 kernel.

Extended brightness

Extended contrast

Removal of Image Blurriness ← height X width X outline

Reset the resolution, bottom, and top of an input image←x_1

resolution ← 1800 X 1800

bottom ← (h/2) - (y/2)

top ← (w/2) - (x/2)

zooming →z

trimming →t

Step 3.2:

Associated rescaling factor from x_1 to x_2

x_2 ← (x_1, 256, 256)

Eliminated murkiness from x_2

Associated labelling mechanism: labelling ~~not equal~~ 0

x_3 ← spin (x_2, 1^0)

x_4 ← spin (x_2, 45^0)

x_5 ← spin (x_2, 90^0)

x_6 ← spin (x_2, 120^0)

x_7 ← spin (x_2, 180^0)

x_8 ← spin (x_2, 270^0)

x_9 ← spin (x_2, 320^0)

Step 4:

Integrated labels ← (x_3, x_4, x_5, x_6, x_7, x_8, x_9)

Otherwise, employee mirroring

logic x_3 ← mirror (x_2, 1^0)

conserve the logic for further process ← x_3.

Step 5:

Insert the generated input image into the dataset file of CSV with the integration of (II- list, labelling, and rescaling)

CSV data ← (II-list, labelling, rescaling)

Array Vectors ← CSV data

Apply the same process for

{A-CFI-X2, A-CFI-X4, A-CFI-6, A-CFI-X8, A-CFI-X10}

And {A-BWI-X2, A-BWI-X4, A-BWI-X6, A-BWI-X8, A-BWI -X10}

Step 6: Decision-making labelling grades.

Step 6.1: Labelling grades:

fundus images $p \in P$; $P = \{p/\ p \in \{\text{A-CFI} \leftarrow 1, \text{A-BWI} \leftarrow 0\}\}$

positive ←1

true-positive (TrPo) ←11

true-negative (TrNe) ←10

false-positive (FaPo) ← 01

false-negative (FaNe) ← 00

Step 6.2:

Dual Labeling Mechanism $(P, Q) \leftarrow\rightarrow (\sim P, \sim Q)$

where $Q_1 = \{q_1 / q_1 \in \{000, 001, 010, 011, 100\}\}$ and $Q_2 = \{q_2 / q_2 \in \{00, 01, 10, 11\}\}$

Q1 represents primary case of labeling and Q2 representing secondary case of labeling based on positive (1), TrPo (11), TrNe (10), FaPo (01), FaNe (00)

Step 6.3: Binary data integration

Binary data integration for prediction

Normal ←000.00

Mild DR ← 001 Various levels → {001.01, 001.10, 001.11}

Moderate DR ← 010 Various levels → {010.01, 001.10, 001.11}

Severe DR ← 011 Various levels → {011.01, 001.10, 001.11}
Proliferate DR ← 100 Various levels → {100.01, 001.10, 001.11}

Decision making occurrence (DR-STAGE.OCCURENCE) = {(000.00), (001) => {001.01, 001.10, 001.11}, 010 => {010.01, 001.10, 001.11}, 011 => {011.01, 001.10, 001.11}, 100 => {100.01, 001.10, 001.11}}

Step 7: Input → Expected output.
Original input:
fundus images p∈; P = {p/ p∈{ A-CFI ←1, A-BWI ←0}}
Expected output:
The trained model forecasts the probability scores that correspond to ∀q for an input p based on p∈{ A-CFI ←1, A-BWI ←0}

Step 7.1:
Set of augmented images:
CFI = {A-CFI-X2, A-CFI-X4, A-CFI-6, A-CFI-X8, A-CFI-X10}
BWI = {A-BWI-X2, A-BWI-X4, A-BWI-X6, A-BWI-X8, A-BWI-X10}
imlr ← image learning
rate input shape ← IS.
patch size ← PS
patch color ←PC
kernel ←K
padding ← PADD
stride ← S
poling ← POLL

Step 7.2: Deep learning inception-ResNet based dual-Image Multi-Layer Mapping Image- based Classification Model (CM) and Regression Model (RM)

Dual-Image Multi-Layer Mapping Image-based Classification Model (CM)
Blended Hybrid Model (BHM) ←{{CM_1, CM_2}, RM}

Every ∀bhm∈BHM

imlr1 = 0.001, momentum1 = 0.4

imlr2 = 0.005, momentum2 = 0.8

Every imlr = 0.001 to 0.005 and momentum = 0.4 to 0.8

Every epoch=1 to 360, do

Every both tiny-cluster (Pmini, Qmini) ∈ (P, Q) do

Step 7.3:

Set Activation Function ← Act ← Rectified Linear Unit (Relu);

Initial plotting value (M) ← 0.5

Add Conv Layer (A-CFI-CNL1) ← (K, A-CFI, PADD, S, Act) at filter F ← 64

Add Conv Layer (A-BWI-CNL1) ← (K, A-BWI, PADD, S, Act) at filter F ← 64

Add Conv Layer (A-CFI-CNL2) ← (K, PADD, Act), L2=10-3, at filter F ← 32

Add Conv Layer (A-BWI-CNL2) ← (K, PADD, Act), L2=10-3, at filter F ← 32

Add Conv Layer (A-CFI-CNL3)← (K, PADD, Act), L2=10-3, at filter F ← 24

Add Conv Layer (A-BWI-CNL3) ← (K, PADD, Act), L2=10-3, at filter F ← 24

Add Conv Layer (A-CFI-CNL4)← (K, PADD, Act), L2=10-3, at filter F ← 12

Add Conv Layer (A-BWI-CNL4) ← (K, PADD, Act), L2=10-3, at filter F ← 12

Step 7.4:

Decision Making → dm

Test condition 1: initialized classification model → bhm

then Test condition 2: dm ← bhm then

Parameters turning and integration for classification-based decision making

Stochastic Gradient Decent optimization (SGD) ← Parameters turning and integration Test condition 1: epochs>70 then

imlr = 0.0001, momentum1 = 0.4

Test condition 2: epochs>140 then

imlr = 0.0002, momentum1 = 0.5

Test condition 3: epochs>210 then
imlr = 0.0003, momentum1 = 0.6

Test condition 4: epochs>280 then
imlr = 0.0004, momentum1 = 07
Test condition 5: epochs>350 then
imlr = 0.0005, momentum1 = 0.8

Step 7.5: Dual-Image Multi-Layer Mapping Image-based Regression Model (RM) Decision Making → dm
Test condition 1: initialized regression model → bhm then
Test condition 2: dm ← bhm then
Test condition 3: epochs<70 then
Parameters turning and integration for regression-based decision making
Adaptive Moment Estimation (Adam) ← Parameters depending on and integration

Step 8:
Employee Pooling Technique ← POLL
Employee Flatten ← Flat

Step 9:
Generated sequence value (N) ← (2048, Act, p, L1 = lin-8, L2 = lin-7)
Generated N ← cluster = 5, classifier = SoftMax, optimizer = AdamOpt, loss function = unqualified cross entropy)

Step 10: Deep learning inception-ResNet Model-based Dual-Image Multi-Layer Mapping Image features extraction

Step 10.1: A dual-image-based multi-layer mapping approach based on classification and regression →

Step 10.2: Every dual image based multi-layer mapping approach.
imlr1 = 0.001, momentum1 = 0.4
imlr2 = 0.005, momentum2 = 0.8

Step 10.3:
cim1 ← first moment of color image based exponential decomposition rate in AOpt
cim2 ← second moment of color image based exponential decomposition rate in AOpt bwim1 ← first moment of black-white image-based exponential decomposition rate in AOpt
bwim2 ← second moment of black-white image-based exponential decomposition rate in AOpt
cim1 =0.7, cim2=0.890
bwim1=0.7,
bwim2=0.890

Step 10.4:
Every epoch=1 to 70
for each tiny-cluster1 (Pmini, Qmini) ∈ (P, Q) do
Decision Making ← dm

Test condition 1: initialized Adaptive Moment Estimation ← bhm then
Adaptive Moment Estimation (Adam) ← Parameters turning and integration

Step 10.5:
Every epoch=71 to 90
for each tiny-cluster2 (Pmini, Qmini) ∈ (P, Q), do
Decision Making → dm

Test condition 2: initialized Adaptive Moment Estimation ← bhm then
Adaptive Moment Estimation (Adam) ← Parameters turning and integration

Step 10.6:

Adaptive Moment Estimation → Update the multitasking parameters.

If, after four epochs the validation error remains unchanged, then.

imlr1 = avg ((imlr1 * 0.01) + ((imlr2 * 0.01))

imlr2 = avg ((imlr1 * 0.01) + ((imlr2 * 0.01))

Step 11:

Evaluation dataset input ← N

Expected decision-based Output Grading ← N

4.2.1 Experimental Setup

To automatically detect DR stages, integration of dual-type sequential and non-sequential cluster pictures is required. This study suggested a dual image ResNet mapping strategy for an auto-tuning system to identify DR stages. Sequential and non-sequential images are processed simultaneously throughout the pre-processing and classification processes. To analyze and map the missing connections between the macula, cottonwool spots, retinal arterioles, microaneurysms, venules, and dot points of the fovea, mapping techniques were combined, amidst color and white photos of the back, together with hard exudates and hemorrhages. The sequence of the vectors includes missing computations, which facilitates the identification of DR phases. Test cases included the color fundus and the black-and-white retinal images in 5672 sequential and 7231 non-sequential forms. The 10-ford cross-validation technique was implicated by the 80/20 ratio of high- and low- quality photos in training and testing.

Because the suggested methodology's training capacity depends on sufficient error-free data, it is required to alter the data for training-testing purposes in order to manage it for advanced procedures in the predicted deep learning-based CNN (DL-CNN) using dual-image multi-layer mapping technique. Each DR stage, including Non-DR, MiDR, MoDR, SeDR, and PrDR, receives an equal distribution of data from the color fundus and black-and-white images, helping the model to eliminate any inequality as it advances through the training and testing of the suggested method. All of the input

black-and-white and color fundus images are of identical size, and after processing them all in a systematic order, the combination images are chosen for analysis and grading in order to make additional predictions.

Image Normalization Principal Component Analysis (PCA)

Features, the resulting standard deviation from the mean value for each feature indicated by x(i), and the features. Principal Component Analysis (PCA) was used for dimensionality reduction in the case of MNIST and Fashion-MNIST, which have chosen to represent features of image data, which is achieved using the sci-kit-learn based PCA, as well as the Standard Scaler (StdSca) based on sci-kit-learn (StdSca)[73].

$$z = \frac{X-\mu}{\alpha} \quad \text{—(4.20)}$$

A feed-forward neural network (FFNN) and CNN have been used, and they have jointly developed two separate classification functions, ReLU and SoftMax. For K classes, the SoftMax function shows a discrete probability distribution (DPD), is frequently used by DL solutions to classification problems, expressed as

$$\sum_{k=1}^{K} p_k \quad \text{—(4.21)}$$

$$o = \sum_{i}^{n-1} \theta_i x_i \quad \text{—(4.22)}$$

If it employs x as the activation at the penultimate layer of a neural network and as its weight parameters at the SoftMax layer, it has 'o' as the input to the SoftMax layer.

Subsequently, yˆ is expected class.

$$p_k = \frac{exp(o_k)}{\sum_{k=0}^{n-1} exp(o_k)} \quad \text{—(4.22)}$$

$$\hat{y} = argmax\, p_i\, where\, i\epsilon 1, \ldots\ldots, N \quad \text{—(4.23)}$$

The first instance of an activation function known as ReLU and its capacity to enhance deep neural network training was presented in 2011. To function, values must be thresholder at 0, and f (x)=max (0, x).

In this study, the ReLU was implicated as a classification function at the network's final layer in addition to its use as an activation function in each hidden layer. However, it produces 0 when x 0 and a linear function when x 0, respectively. As a result, the ReLU classifier would predict the class to be y.x

$$\hat{y} = argmax; i\epsilon 1, \ldots\ldots, N;\ max(0, o) \qquad \text{—(4.24)}$$

The SoftMax function is typically used as the classification function in neural networks, while the DL-based ReLU function is used as the activation function. These networks then use the softmax cross-entropy function to learn the weight parameters of the neural network. In this particular study, we did construct the loss function that was previously mentioned, but in contrast to earlier work, we used the ReLU for the prediction units, which is represented by equation 6. Then, using the ReLU classifier's gradients, a technique known as backpropagation is used to determine the parameters. Equation 7's explanation of the ReLU-based cross-entropy function's differentiation in order to accomplish this goal, the activation of the penultimate layer,

$$l(\theta) = -\sum y.log(max(0, \theta x + b)) \qquad \text{—(4.25)}$$

Let the penultimate activation output h replace the input x,

$$\frac{\partial l(\theta)}{\partial h} = -\frac{\theta.y}{max(0,\theta h+b).ln10} \qquad \text{—(4.26)}$$

The conventional SoftMax-based deep neural network uses the same backpropagation algorithm, as shown in Equation 8.

$$\frac{\partial l(\theta)}{\partial \theta} = \sum_i \left[\frac{\partial l(\theta)}{\partial p_i}\left(\sum_k \frac{\partial p_i}{\partial o_k}\frac{\partial o_k}{\partial \theta}\right)\right] \qquad \text{—(4.27)}$$

Multi-level ConvNets based Pooling and Feature Integrations

In this study, cross pooling (CxPool) and 1D pooling (1DPool) have been combined with the integration of the Xception net environment to extract multi-level features from the VGG32 through fc1 and fc2. The CxPool receives two distinct feature vectors (FV) of A and B as input, and creates a third FV C from which A, B, and C Rd. The output vector C's individual feature elements, ci, are each processed using equations 10 to 13.

$$c_i = max(a_i, b_i) \; \forall \; i\epsilon\{1,2,\ldots d\} \quad \text{—(4.28)}$$

$$c_i = min(a_i, b_i) \; \forall \; i\epsilon\{1,2,\ldots d\} \quad \text{—(4.29)}$$

$$c_i = mean(a_i, b_{i+1}) \; \forall \; i\epsilon\{1,2,\ldots d\} \quad \text{—(4.30)}$$

$$c_i = a_i + b_{i+1} \; \forall_i \; i\epsilon\{1,2,\ldots d\} \quad \text{—(4.31)}$$

The 1DPool is used to select the top regional features from each VGG32 region, and the CrPool allows for aggregating those features with a global interpretation of the Xception net environment. A first FV "K" is given as an input to the 1DPool-based synthesis, which creates a second FV of "K," where K belongs to Rd1 and K belongs to Rd2, with the executional condition of "d2d1." K is a shortened version of K, where K is "k1, k2... kd1" and K is "k1, k2... kd1". In this case, equations 14 to 17 are used to calculate each and every feature element ki of the output vector K

$$k^i = max(k_{i*2}, k_{i*2+1}) \; \forall \; i\epsilon\{1,2.\ldots d_2\} \quad \text{—(4.32)}$$

$$k^i = min(k_{i*2}, k_{i*2+1}) \; \forall \; i\epsilon\{1,2.\ldots d_2\} \quad \text{—(4.33)}$$

$$k^i = mean(k_{i*2}, k_{i*2+1}) \; \forall \; i\epsilon\{1,2.\ldots d_2\} \quad \text{—(4.34)}$$

$$k^i = k_{i*2} + k_{i*2+1} \; \forall \; i\epsilon\{1,2.\ldots d_2\} \quad \text{—(4.35)}$$

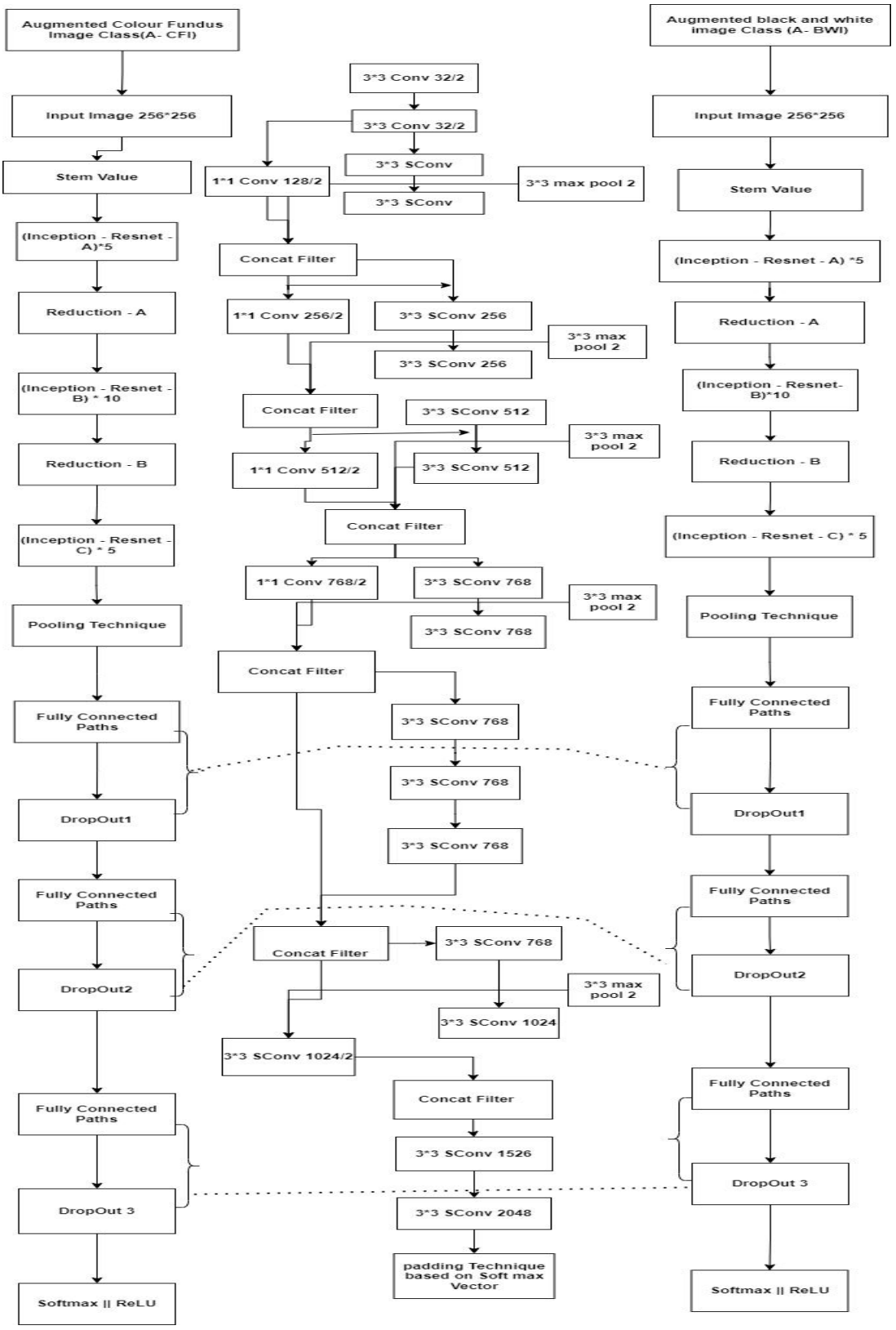

Figure 4.28. The Structural design of custom-built DL-CNN based network stem segment with extracted features. [57]

On retrieved VGG32-based fc1 and fc2 layer features, the 1DPool was used alone. Following that, the CxPool method used the pooled features shown in fig. 4 that were produced by employing CrPool, from the two separate sets of input picture classes, such as the Augmented Black and White picture Class and the Augmented Color Fundus Image Class sets. FV had united these features with the extracted features from the Xception. Because the final FV offers strong hyper characteristics, it is a united form of the global and local interpretations of the RIs.

4.7 Overall Methodology

Diabetic retinopathy is a leading cause of blindness among working-age individuals. To address this critical health issue, we propose an automated approach for diabetic retinopathy detection using retinal fundus images. Our methodology involves several key steps, including image preprocessing, image quality improvement, diabetic retinopathy detection, and diabetic retinopathy stage identification.

A comprehensive approach is also encompassed as part of this study, involving data preprocessing, feature extraction, and the training and evaluation of both traditional machine learning models and deep learning architectures. The primary goal is to effectively identify diabetic retinopathy severity based on a dataset of retinal images. Image processing techniques are employed to enhance image quality, followed by feature extraction to capture relevant characteristics from the images. The performance of various machine learning algorithms alongside a 2-dimensional (CNN) is explored to determine the most effective approach. The process also includes model evaluation, comparison, and the selection of the best-performing model for diabetic retinopathy prediction. By utilizing both traditional and deep learning techniques, valuable insights into the detection and classification of DR, a significant cause of blindness among working-age individuals, are aimed to be provided.

Algorithm for Diabetic Retinopathy Detection

Step 1 : Diabetic Retinopathy Detection

1.Input: Color fundus image (RGB format).

2.Preprocessing:

- Resize the input image to a standard size if needed.
- Perform any necessary color space conversion or normalization.

3.Image Quality Improvement:

- Apply Ben Graham's algorithm to enhance the image.
- Perform Gaussian blur to reduce noise.
- Use an auto-cropping algorithm to remove irrelevant parts.
- Convert the image to grayscale for further analysis.

4.Diabetic Retinopathy Detection:

- Divide the preprocessed image data into sequential (color fundus) and non-sequential (black-and-white retinal) data.
- Apply concurrent preprocessing and classification to both types of data.
- Use mapping techniques to identify features related to diabetic retinopathy on both color and white-back images.
- Sequence the vectors for improved identification of diabetic retinopathy stages.

5.Diabetic Retinopathy Stage Identification:

- Based on the processed data and identified features, classify the diabetic retinopathy stage.
- Output the identified stage of diabetic retinopathy.

Step 2 : Comparative Analysis

1.Data Preprocessing:

Load the diabetic retinopathy dataset.

Perform image processing techniques such as Tone Mapping and Unsharp Masking to reduce noise in the retinal images.

Normalize and standardize the image data.

Perform Principal Component Analysis (PCA) for dimensionality reduction on image features.

2.Feature Extraction:

Extract relevant features from the preprocessed images, such as histogram features and Gray-Level Co-occurrence Matrix (GLCM) features.

3.Machine Learning Model Training and Evaluation:

Split the dataset into training and testing sets (e.g., 80-20 split).

Train various machine learning algorithms (e.g., Logistic Regression, Decision Tree, Random Forest, SVM, etc.) on the training set using the extracted features.

Evaluate the trained models using metrics such as “accuracy, precision, recall, F1-score, and ROC curve”.

Select the best-performing machine learning model based on evaluation metrics.

4.Deep Learning Model Training and Evaluation:

Build a 2-dimensional Convolutional Neural Network (CNN) architecture using libraries like TensorFlow and Keras.

Split the dataset into training, validation, and testing sets.

Train the CNN model on the training set with backpropagation.

Evaluate the CNN model on the validation set to optimize hyperparameters.

Test the final CNN model on the testing set and evaluate using accuracy, precision, recall, F1-score, and weighted Kappa index.

5. Model Comparison:

Compare the performance of the best ML model and the CNN model in predicting diabetic retinopathy severity.

Analyze the F1-scores, accuracy, and other evaluation metrics to determine the most effective approach.

Architecture Diagram :

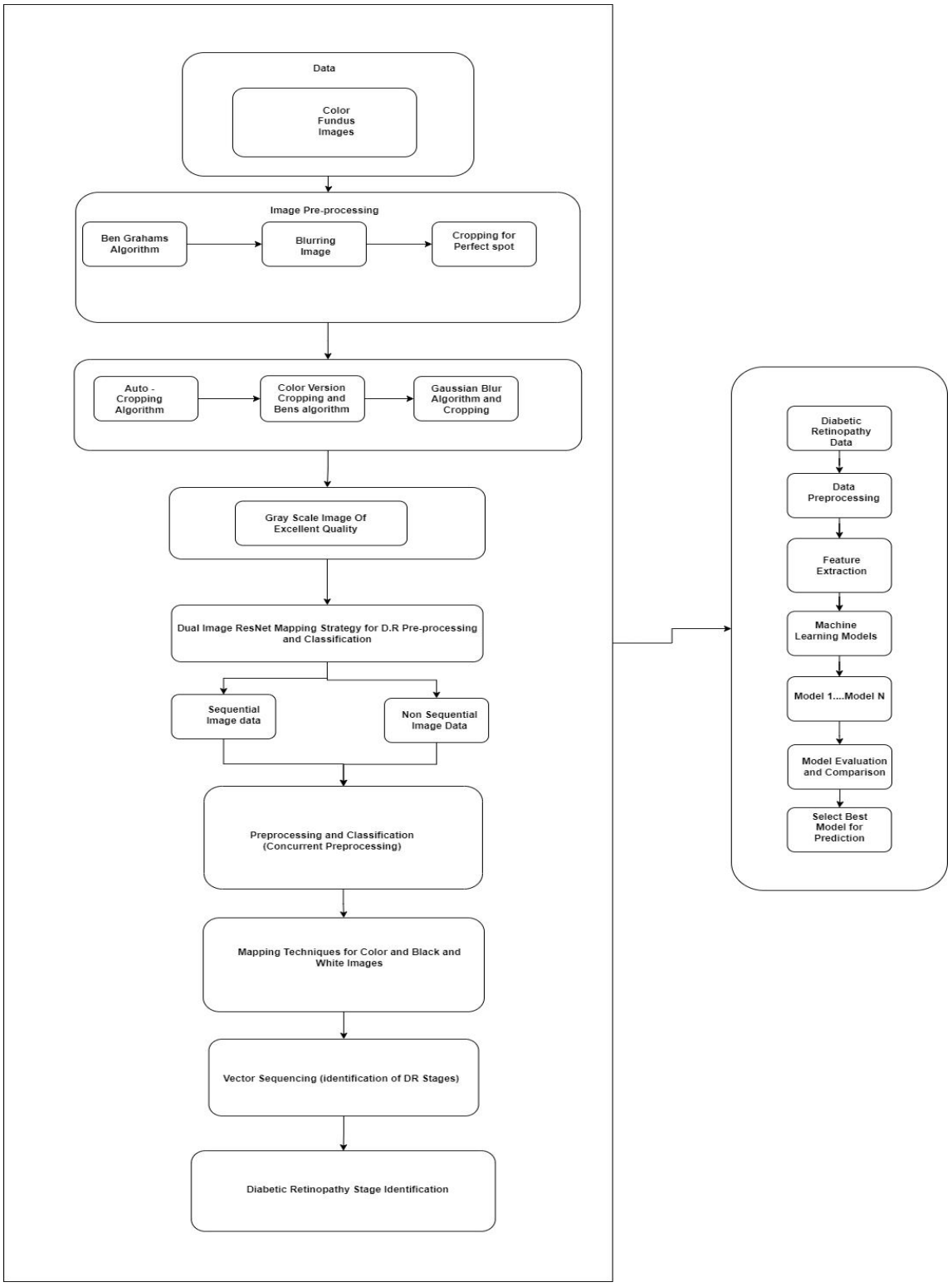

Figure 4.29: Architecture Diagram for Proposed Methodology for Diabetic Retinopathy Detection

4.8 Chapter Summary :

The chapter outlines a comprehensive methodology for automated diabetic retinopathy detection using retinal fundus images. The proposed approach involves image preprocessing, quality improvement, diabetic retinopathy detection, and stage identification. It employs both traditional machine learning models and deep learning architectures, aiming to effectively identify diabetic retinopathy severity based on a dataset of retinal images. The process includes image processing techniques, feature extraction, and model training and evaluation. The algorithm for diabetic retinopathy detection encompasses steps such as preprocessing, image quality improvement, and sequential and non-sequential data processing, integrating mapping techniques for stage identification. The comparative analysis involves data preprocessing, feature extraction, and training and evaluating both machine learning and deep learning models. The chapter emphasizes the importance of addressing diabetic retinopathy, a leading cause of blindness among working-age individuals, and seeks to provide valuable insights through the proposed methodology. The architecture diagram illustrates the proposed methodology's structure, combining various techniques to enhance the identification and classification of diabetic retinopathy stages.

CHAPTER 5
RESULTS AND ANALYSIS

5.1 Implementation System 1

Pre-processing Results:

The proposed pre-processing techniques improved image quality by focusing on informative areas, eliminating black borders, resizing images, converting to grayscale, applying Ben Graham's pre-processing algorithm, Gaussian Blur, and Circle Cropping Algorithm.

Model Performance:

In terms of “accuracy, precision, recall, and F1-score”, the enhanced image quality improved deep learning model performance. As compared to existing methods, the proposed method's pre-processing techniques enabled the model to concentrate on crucial features related to the severity of diabetic retinopathy.

5.2 Implementation System 2

The multi-layer, dual image-based parameters of the inception-ResNet blended hybrid model have been merged, processing both sequential and non-sequential pictures. The suggested model was trained using a multi-layered transfer learning process that was adjusted with 172 weighted multi-layers, plotted with 86 weighted layers linked to color fundus pictures and 86 additional weighted layers linked to the black-and-white image. The severity of the pictures is manually determined on a scale of 0 to 4 “(0, normal DR; 1, mild; 2, moderate; 3, severe; and 4, proliferative DR).” Additionally, binary bit form has been added to the grading process, such as **:**

Dual Labeling Mechanism (P, Q)←→ (~P, ~Q)

where $Q_1 = \{q_1 / q_1 \in \{000, 001, 010, 011, 100\}\}$ and $Q_2 = \{q_2 / q_2 \in \{00, 01, 10, 11\}\}$

Q1 representing primary case of labeling and Q2 representing secondary case of labeling based on positive (1), true-positive (11), true-negative (10), false-positive (01), false-negative (00)

Grade-0: Normal ←000.00

Grade-1: Mild DR ← 001 Various levels ➔ {001.01, 001.10, 001.11}

Grade-2: Moderate DR ← 010 Various levels ➔ {010.01, 001.10, 001.11}

Grade-3: Severe DR ← 011 Various levels ➔ {011.01, 001.10, 001.11}

Grade-4: Proliferate DR ← 100 Various levels ➔ {100.01, 001.10, 001.11}

Figure 5. 5 illustrates the Layered Integration using DL-CNN for DR stage identification in a training and testing scenario with grading procedure. As indicated in table 5.1, the data was clustered using binary bit formation and was gathered for training and testing purposes according to DR stage and DR symptoms.

Table 5.1. Integrated set of images and DR grading class

DR Stages / Grade	**Impact**	**Base binary class**	**Supporting sub-class**	**Sampling**	**Sequential and Non-sequential Images**	**Single / Dual Image Processing**
Grade-0	Normal	000	000.00	2150	Sequential	Dual Image
Grade-1	Mild DR	001	{001.01, 001.10, 001.11}	526	both	Dual Image
Grade-2	Moderate DR	010	{010.01, 001.10, 001.11}	1325	both	Dual Image
Grade-3	Severe DR	011	{011.01, 001.10, 001.11}	372	both	Dual Image
Grade-4	Proliferate DR	100	{100.01, 001.10, 001.11}	158	both	Dual Image

Table 5.2. Parameters turning and integration for classification-based decision making, and test- case conditions based on Stochastic Gradient Decent optimization (SGD) Parameters turning and integration.

Test conditions(TC)	Epochs Value	image learning rate (imlr)	momentum1
TC1	epochs>70 then	0.0001	0.4
TC2	epochs>140 then	0.0002	0.5
TC3	epochs>210 then	0.0003	0.6
TC4	epochs>280 then	0.0004	0.7
TC5	epochs>350 then	0.0005	0.8

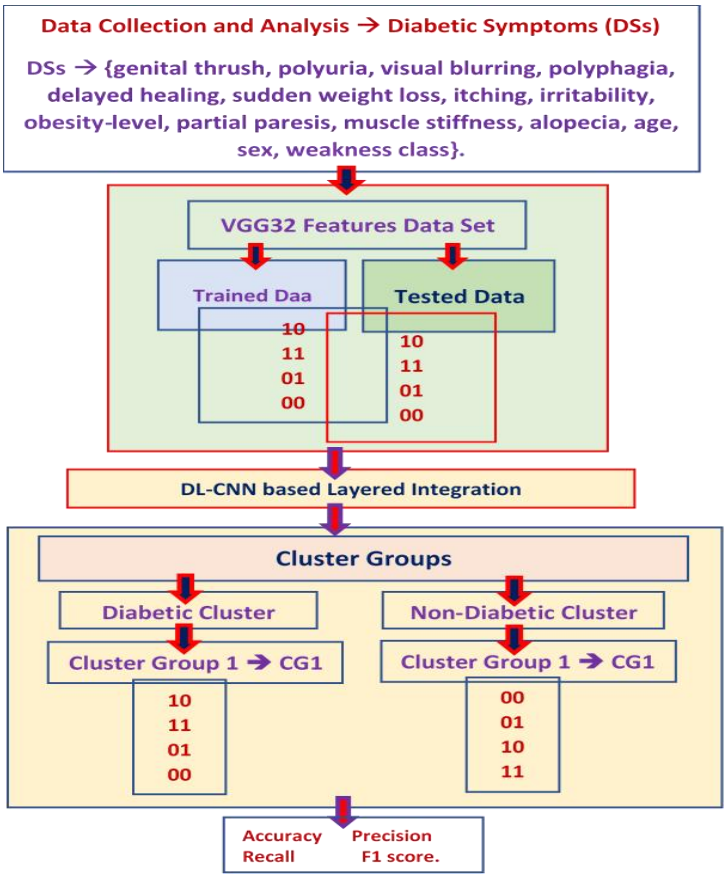

Figure 5.1 : DL-CNN based Layered Integration with training and testing scenario for detection of DR stages.

The dual-image-based multi-layer mapping strategy based on classification and regression is represented in the table. → Which stage consists of the following data.

Every dual image based multi-layer mapping approach.
imlr1 = 0.001, momentum1 = 0.4
imlr2 = 0.005, momentum2 = 0.8
cim1 ← first moment of color image based exponential decomposition rate in AOpt
cim2 ← second moment of color image based exponential decomposition rate in AOpt
bwim1 ←first moment of black-white image-based exponential decomposition rate in AOpt
bwim2 ← second moment of black-white image-based exponential decomposition rate in AOpt
cim1 =0.7, cim2=0.890
bwim1=0.7, bwim2=0.89

Table 5.3. A dual-image-based multi-layer mapping approach based on classification.

Test Condition stage1	Test Condition stage 2	Each epoch range	tiny cluster	cim1	cim 2	bwim1	bwim 2
initialized Adaptive Moment Estimation à bhm	Adaptive Moment Estimation (Adam) ß Parameters turning and integration.	1 to 70	for each tiny-cluster1 è (Pmini, Qmini) Î (P, Q)	0.7	0.89	0.7	0.89
initialized Adaptive Moment Estimation à bhm then.	Adaptive Moment Estimation (Adam) ß Parameters turning and integration.	71 to 90	for each tiny-cluster2 (Pmini, Qmini) Î (P, Q)	0.7	0.89	0.7	0.89
Adaptive Moment Estimation è	Update the multitasking parameters	above 90	After four epochs, if the validation error remains unchanged, imlr1 = avg ((imlr1 * 0.01) + ((imlr2 * 0.01)) imlr2 = avg ((imlr1 * 0.01) + ((imlr2 * 0.01))	0.7	0.89	0.7	0.89

In this study, dual pictures have been tested, which has aided in the in-depth analysis of the images for the detection of DR. stages, black-and-white photographs and color fundus pictures were used to identify and map the missing regions. Integrated D.R. symptoms have been used to compare the proposed methodology to current techniques, its affecting elements with data metrics, and the dual image processing techniques. The Kaggle APTOS dataset[186] is used to define the experimental scenarios. This dataset has demonstrated that the active approaches were more significantly outperformed by the trained modelized approach using blended features.

5.3 Machine learning-based attributes and data matrices for the prediction of diabetic effects in pregnant women:

The suggested columns comprise the five-health forecaster (self-determining) variable quantity, unity target (in need of), class variable conclusion, and that information. The proposed columns also include whether the patient has diabetes or not (encoded as a 0 or 1). One of the predictors is the patient's medical history. The associations between age, blood pressure, skin thickness, BMI, glucose, and pregnancy are shown in the Table 2.

A diabetes based on family history function assesses the likelihood that a person's connection to the patient is hereditary and provides broad details about the disease's historical prevalence in families. earlier than Currently, there are a total of eight medical analyst (self-determining) variable quantity columns in use, along with one objective (hooked-on) adjustable, class variable conclusion on whether a patient has diabetes (encoded as 0 or 1). The patient's history is one of the predictive variables. Table 1 lists the total number of pregnancies along with the women's ages, BMIs, and insulin levels. Glucagon: (mu U/ml) insulin 120-minute serum. After the oral glucose tolerance test, two hours later, the glucose plasma concentration was determined. Thickness of the Triceps Body Fold thickness in mm. Diastolic blood pressure is calculated using blood pressure (mm Hg). Body mass index (BMI) is calculated using the formula: (mass in m2/ height in kg).

Age is determined by years of experience. Pregnancy Rate: Total Number of Pregnancies. Diabetes Pedigree Function - Diabetes pedigree function The outcome is 1, and 0 if the patient does not have diabetes.

Table 5.4. The Existing Attributes of Gestational Diabetes.

Attributes	**Diabetic Women (1)**	**Healthy Women (0)**
Insulin	169.5	102.5
Glucose	140.0	107.0
Skin Thickness	32.0	27.0
Blood Pressure	74.5	70.0
Body mass index	33.8	30.1
Age	21-60(In years)	21-60(In years)
Pregnancies	1-8 (Number of times Pregnancies)	1-8 (Number of times Pregnancies)

Table 5.5. The proposed Attributes.

Attributes	Healthy Women (0)	Diabetic Women (1)
Glucose vs Age	Glucose <= 105, Age<=30	Glucose <= 105, Age<=30
Pregnancies vs Age	pregnancies<=6, Age<=30	pregnancies<=6, Age<=30
Blood pressure vs Glucose	Blood pressure<=80, glucose<=105	Blood pressure<=80, glucose<=105
Skin thickness vs BMI	Skin thickness<=20, BMI<=30	Skin thickness<=20, BMI<=30
Glucose vs BMI	Glucose<=105, BMI<=30	Glucose<=105, BMI<=30

5.4 Supporting attributes and data matrices:

Glucose vs Age: Age vs. Glucose Figure 5.2 depicts women with diabetes and women in good health. Age<= 30 and Glucose<=120.

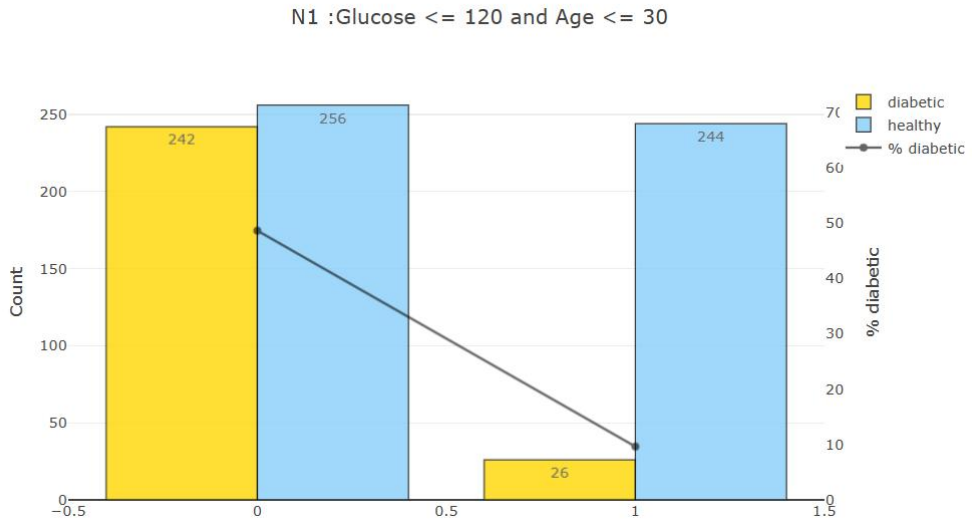

Figure 5. 2. Depicts the Glucose vs Age

Pregnancies vs Age: Age versus Pregnancies Figure 5.3 depicts the Healthy Living women, Diabetic women Pregnancies <= 6, Age <= 30

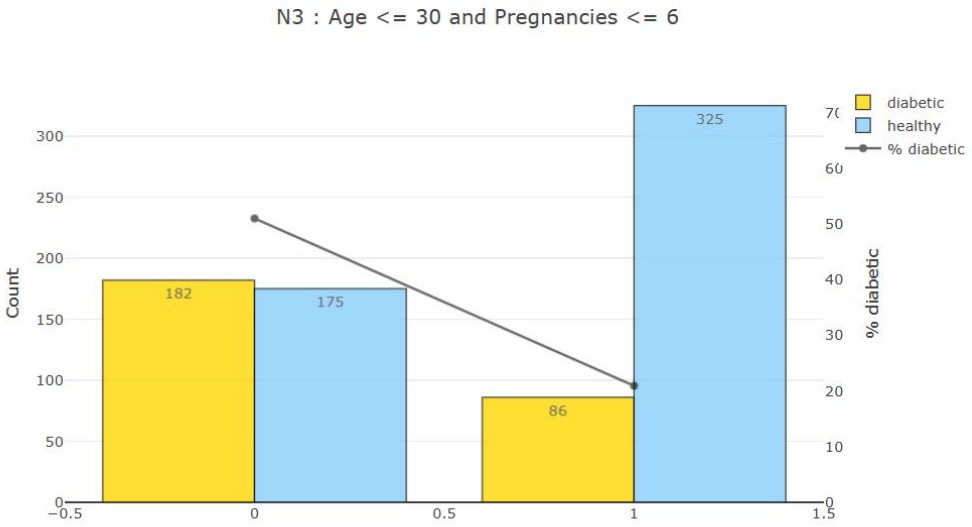

Figure 5. 3. Shows the Pregnancies vs Age

Glucose Vs Blood Pressure: Blood Pressure vs. Glucose Figure 5.4 displays the diabetic and healthy women. Blood pressure <= 80 and glucose <= 105.

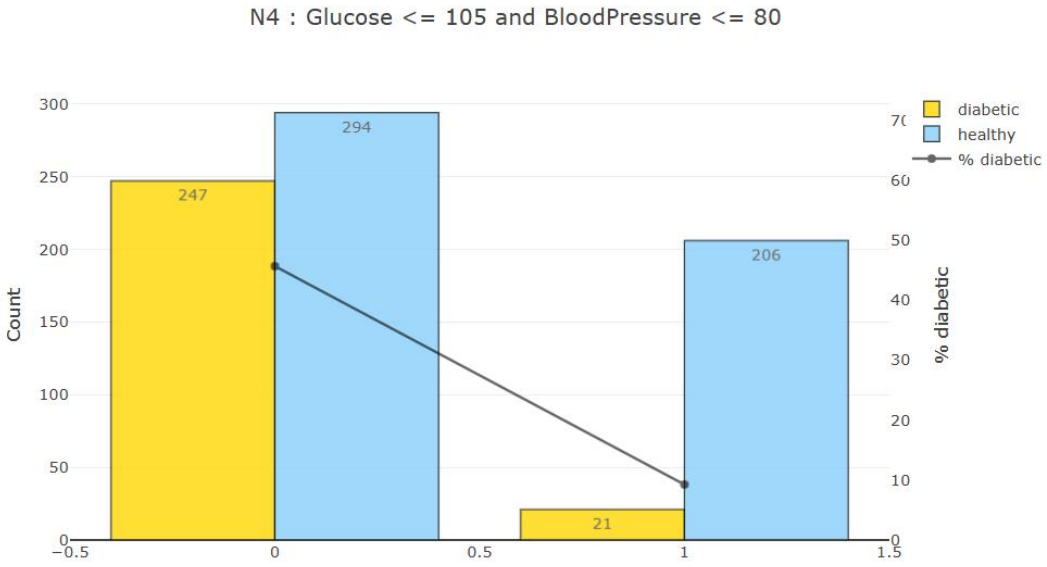

Figure 5. 4. Glucose Vs Blood Pressure

Skin Thickness Vs BMI: Skin Thickness vs BMI Figure 5.5 shows the good Health women, Diabetic women Skin thickness<=20, BMI<=30

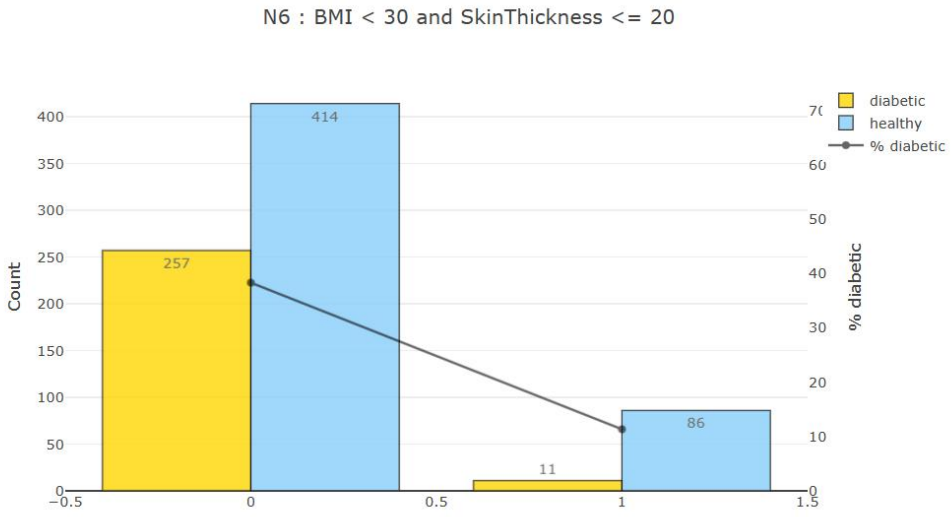

Figure 5. 5. Skin Thick ness Vs BMI

Glucose Vs BMI: Glucose vs BMI Figure 5.6 shows the good Health women, Diabetic women Glucose<=105, BMI<=30

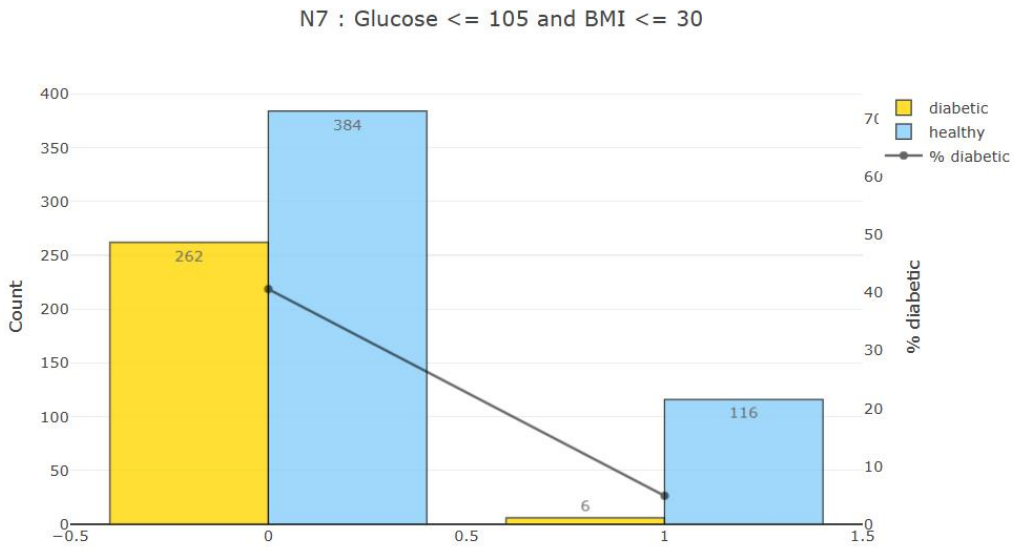

Figure 5. 6. Shows the Glucose Vs BMI

5.5 Comparative analysis of Diabetic Retinopathy prediction using Various Machine Learning Algorithms:

The dataset was previously kept up to date by the National Institute of Diabetes and Digestive and Kidney Diseases. The dataset aims to precisely predict a patient's presence or absence of diabetes. The dataset has 9 columns and 768 entries. There are numerous single objective and medical forecaster items in it. Because it enables more accurate calculation of trial correctness and more effective use of each observation during training and testing, cross validation is a crucial part of cross authentication.

Precision: A performance metric for machine learning models, precision measures how accurately a model predicts positively.

$$Precision = TP/(TP + FP) \quad \text{—(5.1)}$$

Recall: Recall, also known as sensitivity, probability of detection, and True Positive Rate, measures how well a machine learning model can identify the pertinent data.

$$Recall = TP/(TP + FN) \quad \text{—(5.2)}$$

Accuracy: Accuracy is defined as the proportion of accurate predictions to test data.

$$Accuracy = (TP + TN)/(TP + FP + TN + FN) \quad \text{—(5.3)}$$

F1 Score: The F score balances the use of precision and recall and is used to measure test accuracy.

$$F = 2 * precision * Recall/Precision + Recall \quad \text{—(5.4)}$$

Roc Curve: Performance of a classification prototypical is evaluated using a receiver operating characteristic arc.

Make use of various algorithms to improve the machine learning model's accuracy. Algorithms for machine learning are summarized in table figure 5.15.

Machine Learning Algorithms	**Cross Validation Fold 5 Accuracy**	**Precision & Recall**	**F1 Score**	**Roc curve**
Logistic Regression	0.81	0.731 & 0.717	0.724	0.884
Linear Discriminant Analysis	0.784	0.679 & 0.717	0.697	0.883
K. Neighbours Classifier	0.85	0.788 & 0.774	0.781	0.836
Decision Tree Classifier	0.882	0.821 & 0.849	0.86	0.87
Gaussian NB	0.516	0.413 & 0.943	0.575	0.826
SVM	0.824	0.76 & 0.717	0.738	0.893
Ada Boost Classifier	0.876	0.793 & 0.868	0.829	0.943
Gradient Boosting Classifier	0.908	0.882 & 0.849	0.865	0.958
Random Forest Classifier	0.882	0.857 & 0.83	0.824	0.951
Extra Trees Classifier	0.85	0.808 & 0.774	0.762	0.925
Light GBM	0.928	0.875 & 0.925	0.899	0.972
Light GBM & KNN	0.941	0.893 & 0.943	0.917	0.953

Figure 5. 15. The comparison of machine learning algorithms is shown in Table

5.6 Performance of machine learning algorithms in predicting diabetic retinopathy early-stage symptoms

The results and model evaluation show that the 2-dimensional convolutional neural network, with a dataset measured classification accuracy of 99%, achieves the highest classification accuracy possible. All machine learning models are currently running on the diabetic risk prediction dataset, and the results can be evaluated using the f-score in Table 1. The best models for predicting diabetes in the dataset, according to performance comparison with figure 4's chi squared test, are XGboost, Random Forest, and Decision Tree.

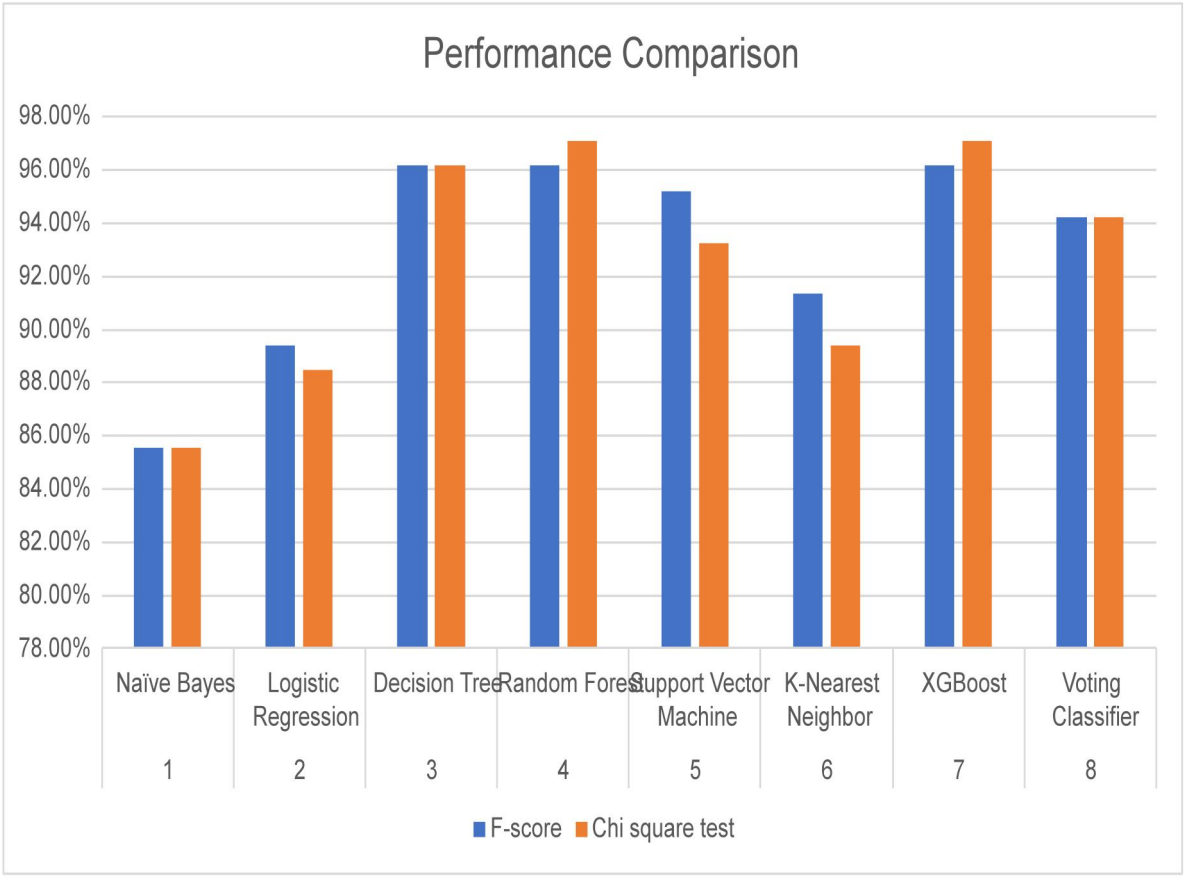

Figure:5.7 Shows the feature selection with chi squared test

5.6.1 Comparative Study

Table 5.6: Comparative study of machine learning algorithms, F score and Chi square test

S.No	Machine Learning Algorithms	F-score	Chi square test
1	Naïve Bayes	85.57%	85.57%
2	Logistic Regression	89.42%	88.46%
3	Decision Tree	96.15%	96.15%
4	Random Forest	96.15%	97.11%
5	Support Vector Machine	95.19%	93.26%
6	K-Nearest Neighbor	91.34%	89.42%
7	XGBoost	96.15%	97.11%
8	Voting Classifier	94.23%	94.23%

5.7 Experimental setup and Results of Classification of Diabetic Retinopathy Severity using Deep learning techniques on Retinal Images

Python performs data pre-processing and image processing. This process makes use of CV2 features. On a 2.6GHz Intel(R) Core i7 5-core CPU with 16GB of RAM, we train the model. The Python Kera Library and the CPU are backends for TensorFlow. Training data make up 80% of the dataset, followed by testing data and validation data. Every model is trained by repeatedly running up to 40 epochs with a regulating function that, if the model does not improve, automatically terminates the model. This keeps happening until the model is functioning properly.

When assessing a model on hypothetical or unproven data to determine its generalization Accuracy (Acc), performance measure parameters are crucial. These are just a few of them. as Precision (Pre), Recall (Rec), and F1-measure (F1).

$$Accuracy = \frac{TP+TN}{TP+FP+TN+FN} \quad \text{— (5.5)}$$

$$Pre = \frac{TP}{TP+FP} \quad \text{— (5.6)}$$

$$Rec = \frac{TP}{TP+FN} \quad \text{— (5.7)}$$

$$F1 = 2X\frac{PreXRec}{Pre+Rec} \quad \text{— (5.8)}$$

To optimize neural networks for deep learning, we'll use the Weighted Kappa index . When solving a multi-class classification problem with an a priori ordered category list, weighted kappa is used to measure rater agreement. High-level abstractions of the intrinsic data we want to extract are what will be categorized. This index is derived from the weight, observed, and predicted score matrices. Kappa with weights.

$$K = 1 - \frac{\sum_{i,j} \omega i,jOi,j}{\sum_{i,j} \omega i,jEi,j} \quad \text{— (5.9)}$$

C stands for the number of classes, which are 1, 2..., C. Observations that are classified are "Oi,j." Wi,j is the weight penalty for each pair, and Ei,j is the outer product of the classification histogram vectors. We contrast the observed classification of the prediction model with the actual assignments in the numerator of equation (20). The variances from the mean of all N items are calculated.

Results and analyses of classification on the complete feature Set

We used a “5-fold cross-validation” technique on the dataset to produce a more trustworthy categorization result. The “train-test split” of 80% to 20% was maintained in each fold. Figure 9 displays the classification results for the EfficientNet-B5 model on five different folds of the prepared dataset in terms of classification accuracy. We have shown the findings for the separate “feature sets and the combined set to show” how the model's performance increases when both sets of features are accessible. Using only the histogram and GLCM features, the average accuracy of the five classifications is 91.2% and 92.3%, respectively. When the features were combined, the score increased by over 2% from when only the histogram features were used, to an average of 93.2%.

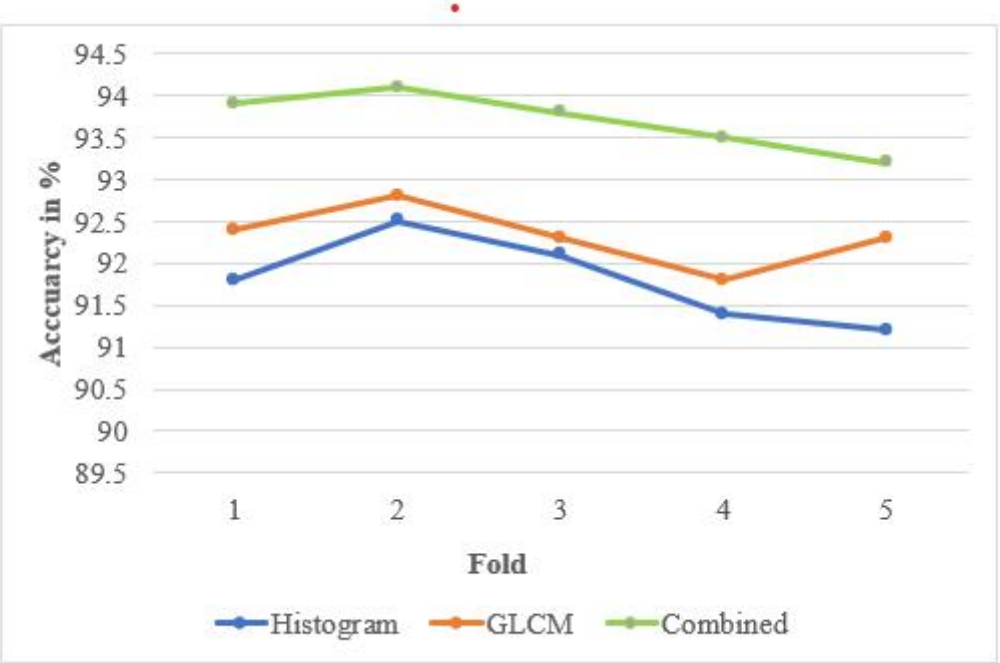

Figure 5.8: Comparison of the classification results at various accuracy folds

Figure displays the “F-measure scores” for each fold of the “5-fold cross-validation” process. The “precision and recall” scores for the classification are taken into account by the performance measurement score known as F-measure. More crucially, the F-measure is unaffected by the fact that the data in this case have different class sample sizes. The figure indicates that the “F-measure” bars attained heights comparable to the matching accuracy bars illustrated in Figure 10a. This shows that the model is not unduly biased despite the imbalance in the dataset. However, the accuracy scores are marginally better than the F- measure results. The average scores are 90.2%, 91.4%, and 92.3% based on the “histogram, GLCM, and integrated features”, respectively.

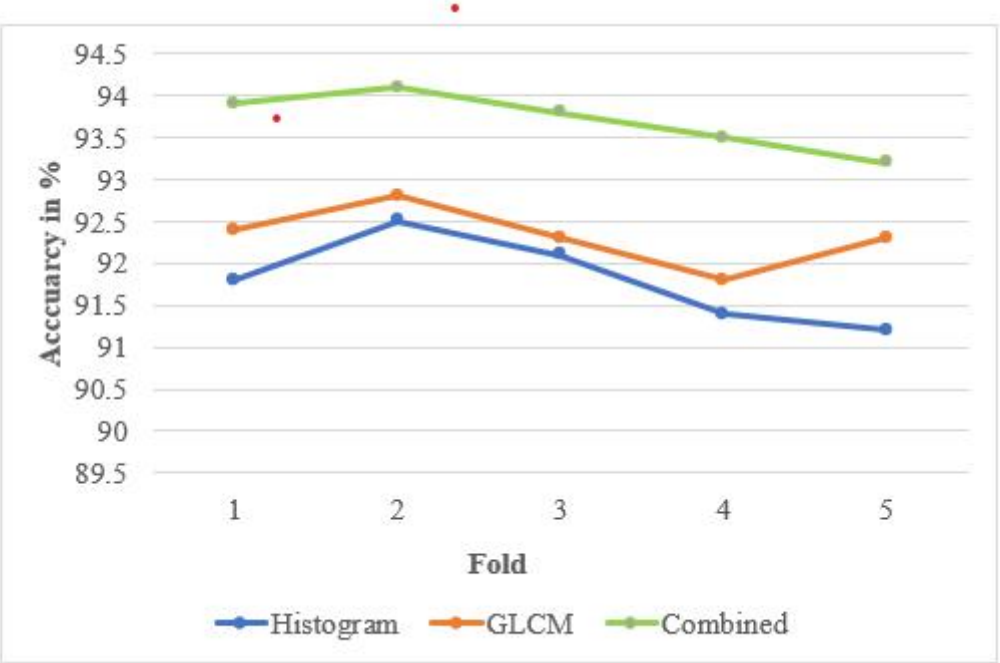

Figure 5.9: F-measure comparison of the classification results at various folds

The specificity, precision, recall, and F-measure scores for each class using the method are listed in Table 1 along with their individual scores. Apart from the MO class, which is shown in the table, we attained an "F-measure score of over 95% in each category. The MO class has a poor recall rate, which has also been shown in the previous results."

Table 5.7. Evaluation of the performance of classification by class

Class	**Accuracy (%)**	**Precision (%)**	**Recall (%)**	**F-Measure (%)**
NO	96.23	98.04	99.31	97.81
MI	92.40	99.10	99.12	96.12
MO	92.11	93.35	79.21	83.23
SE	91.80	96.97	99.35	95.22
PR	98.23	99.11	99.98	95.89
Average	**94.15**	**97.31**	**95.39**	**93.65**

Analysis on Diabetic Retinopathy comparison:

A number of Tone Mapping and Unsharp Masking stages are included in the suggested model. These steps were taken in order to reduce the amount of noise in the retinal pictures and increase the samples' capacity for learning. We show the categorization results in Table 2 without doing some of these actions.

Table 5.8: Performance of the classifier with and without particular phases of the proposed model

Fold	Without Tone Mapping		Without Unsharp Masking		Proposed work	
	Accuracy	**F-Measure**	**Accuracy**	**F-Measure**	**Accuracy**	**F-Measure**
1	0.916	0.917	0.924	0.917	0.934	0.925
2	0.919	0.919	0.926	0.919	0.936	0.938
3	0.914	0.912	0.919	0.915	0.931	0.922
4	0.912	0.911	0.918	0.912	0.928	0.918
5	0.911	0.909	0.914	0.910	0.927	0.916
Avg	**0.914**	**0.913**	**0.920**	**0.915**	**0.931**	**0.923**

The samples were re-shuffled during some of those classifications, as shown in the figure above, so it's possible that the samples in the training and testing subsets of the folds are different. Without tone mapping and unsharp masking, the accuracy of the average classification model decreases by 1.7% and 1.1%, respectively. The results of the F-measure can also be seen to have similar results. Based on these findings, it is possible to draw the conclusion that these pre-processing procedures improved the overall effectiveness of the proposed DR severity classification method.

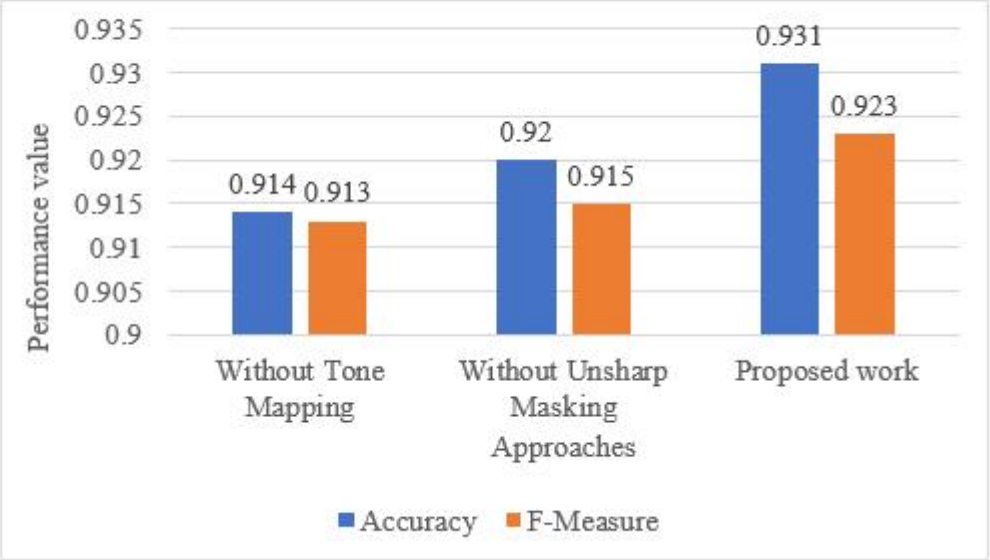

Figure 5.10: Comparison of the proposed work's various pre-processing operations on the APTOS 2019 BD dataset

Table 5.9: EfficientNet-B5 performance with a folds

Fold	**Train Kappa score**	**Validation Kappa score**	**Complete set Kappa score**
1	0.909	0.921	0.910
2	0.823	0.898	0.826
3	0.906	0.925	0.907
4	0.895	0.923	0.896
5	0.904	0.901	0.904

The performance comparison of various Weighted Kappa scores on the APTOS 2019 BD dataset is shown in Figure below. It is clear that after five folds, the training kappa score, validation kappa score, and complete set kappa score are each 0.904, 0.901, and 0.90 respectively.

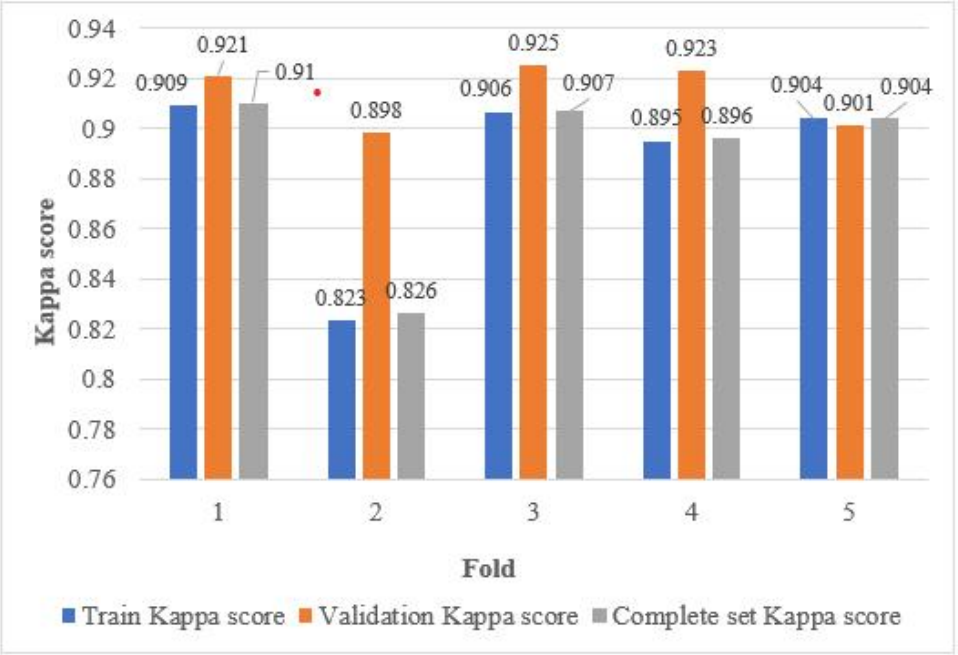

Figure 5.11: Comparison of different Weighted Kappa scores on APTOS 2019 BD dataset

5.8 Chapter Summary

Chapter 5, titled "Results and Analysis," provides an in-depth exploration of the implementation systems for detecting diabetic retinopathy. In Chapter 5, System 1 focuses on pre-processing techniques, enhancing image quality through various algorithms to improve deep learning model performance. The chapter emphasizes the significance of these techniques in concentrating on critical features related to diabetic retinopathy severity.

In System 2 of Chapter 5, a multi-layered, dual image-based parameters model is introduced, employing transfer learning and binary bit formation for DR grading. The chapter elaborates on parameters tuning using Stochastic Gradient Descent optimization, highlighting the intricacies of the model architecture.

The chapter proceeds to compare machine learning algorithms, presenting their performance metrics, including accuracy, precision, recall, F1 score, and Roc curve.

Notably, the 2-dimensional convolutional neural network achieves the highest classification accuracy of 99%. Chapter 5 includes a comparative study utilizing F-score and Chi-square test, showcasing the effectiveness of various machine learning algorithms, with XGBoost, Random Forest, and Decision Tree standing out.

Chapter 5 delves into the experimental setup and results of classifying diabetic retinopathy severity using deep learning techniques. The evaluation of performance metrics, such as specificity, precision, recall, and F-measure, underscores the effectiveness of the proposed model. The chapter concludes by analyzing diabetic retinopathy comparison, emphasizing the importance of specific pre-processing stages in enhancing the overall effectiveness of the proposed classification method.

CHAPTER 6

CONCLUSION AND FUTURE WORK

Conclusion

The application of machine learning and deep learning approaches in the identification of diabetic retinopathy has been examined in this thesis, demonstrating its enormous utility in this field. By automatically classifying retinal pictures, the created models and algorithms have shown amazing accuracy and efficiency, enabling the early detection and diagnosis of diabetic retinopathy.

Machine learning techniques have transformed the healthcare industry, and their use in the early identification of diabetic retinopathy shows great potential. Machine learning algorithms can effectively discover detailed patterns and features within retinal pictures by utilizing massive datasets and potent computer models, surpassing human skills in some respects. The accuracy, speed, and accessibility of diabetic retinopathy screening and diagnosis may be enhanced as a result.

Additionally, the scalability of machine learning approaches allows for generalization across a wide range of patient populations and imaging settings. This is made possible by their ability to be trained on enormous volumes of data. The capacity to deploy automated detection systems on a broad scale thanks to its scalability expands the scope of diabetic retinopathy screening programs and makes early intervention possible.

For the identification of DR, using ML and DL algorithms has many advantages, including increased efficiency, scalability, and accuracy. This study adds to the expanding body of information in the area by demonstrating the potential of these technologies to fundamentally alter how diabetic retinopathy is diagnosed and treated, ultimately improving patient outcomes and lowering the risk of vision loss in those who have the disease.

Future Scope:

Despite the progress made, there are several avenues for future exploration and improvement in the field of DR diagnosis:

1. Advanced Categorization Models: The proposed approach can be further enhanced by incorporating more advanced categorization models. Future research could involve exploring state-of-the-art DL architectures, such as (CNNs) or transformer models, to achieve even higher accuracy and robustness in DR classification. These models can leverage the rich spatial and temporal information present in fundus images for improved detection and staging of DR.
2. Integration of Multi-Modal Data: Currently, the focus primarily lies on utilizing fundus images for DR diagnosis. However, the integration of multi-modal data, such as optical coherence tomography (OCT) scans or patient health records, can provide complementary information and improve the accuracy of DR detection. The combination of different imaging modalities and data sources can offer a more comprehensive view of the disease and its progression.
3. Explainability and Interpretability: As the field moves towards automated diagnosis, it becomes crucial to develop methods that provide explainability and interpretability of the decision-making process. Developing techniques to visualize and explain the features and patterns learned by deep learning models can instill trust among clinicians and aid in understanding the underlying mechanisms of DR diagnosis.
4. Large-Scale Clinical Validation: While the proposed models show promising results, it is essential to conduct large-scale clinical validation studies to assess their performance and generalizability across diverse patient populations. Collaborations with medical institutions and access to extensive datasets can facilitate the evaluation and refinement of the proposed approaches in real-world clinical settings.

5. Real-Time Deployment and Integration: To make the proposed models and techniques practical for widespread adoption, efforts should be made to develop systems that can seamlessly integrate with existing healthcare infrastructure. Real-time deployment of automated DR diagnosis systems can enable timely interventions and improve patient outcomes.

By addressing these areas of future research, the field of DR diagnosis can continue to advance, leading to more accurate, accessible, and cost-effective methods for early detection and management of diabetic retinopathy.

BIBLIOGRAPHY

1. M.Salim, Nareen & Mohsin Abdulazeez, Adnan. (2021). Human Diseases Detection Based On Machine Learning Algorithms: A Review. 10.5281/zenodo.4462858.
2. Blashchuk, T. & Hushchuk, I. & Vivsiannyk, O.. (2023). The Health Care Code as a Legal Basis for the Reform of the National Health Care System. Medicne pravo. 16-29. 10.25040/medicallaw2023.01.016.
3. Saini, Ankita & Varshney, Adya & Saini, Ashok & Mani, Indra. (2023). Insight into epigenetics and human diseases. 10.1016/bs.pmbts.2023.01.007.
4. Keel, Stuart & Lingham, Gareth & Misra, Neha & Block, Sandra & Bourne, Rupert & Calonge, Margarita & Cheng, Ching-yu & Friedman, David & Furtado, Joao & Khanna, Rohit & Mariotti, Silvio & Mathenge, Wanjiku & Matoto, Elenoa & Müeller, Andreas & Rabiu, Mansur & Rasengane, Tuwani & Resnikoff, Serge & Wormald, Richard & Yasmin, Sumrana & Group, Package. (2022). Toward Universal Eye Health Coverage- Key Outcomes of the World Health Organization Package of Eye Care Interventions: A Systematic Review.
5. American Diabetes Association. (2021). Standards of Medical Care in Diabetes. Diabetes Care, 44(Supplement 1), S1-S232.
6. International Diabetes Federation. (2019). IDF Diabetes Atlas, 9th edn. Brussels, Belgium: International Diabetes Federation.
7. World Health Organization. (2021). Diabetes. Retrieved from https://www.who.int/health-topics/diabetes#tab=tab_1
8. Han, X., & Wang, J. (2020). Medical image synthesis with deep learning. IEEE Transactions on Medical Imaging, 39(7), 2304-2315.
9. Russell, Stuart & Norvig, Peter. (2023). Artificial Intelligence: A Modern Approach / S.J. Russell, P. Norvig.
10. Srividhya, E & S, Jayanthi & Cherukullapurath Mana, Suja & V.R, Niveditha & K, Amandeep. (2022). AN APPROACH TO DEEP LEARNING. 10.47716/MTS.B.978-93- 92090-12-7.

11. Grigorescu, A. A., & Petrescu, M. (2018). A review of non-invasive imaging modalities for early detection of hepatocellular carcinoma. World Journal of Hepatology, 10(9), 555- 566.
12. Kheradmand, A., & Tavakoli, N. (2018). Review on different imaging modalities in diagnosis, staging and treatment of prostate cancer. Journal of Biomedical Physics and Engineering, 8(4), 373-382.
13. Moccia, M., Capacchione, A., & Montella, M. (2018). The contribution of medical imaging to the diagnosis of lung cancer.
Journal of Radiology Case Reports, 12(6), 1-14.
14. Arora, S., Saxena, S., Kumar, A., & Jain, S. (2019). Diabetic retinopathy: An update. Journal of Endocrinological Investigation, 42(5), 491-504.
15. Das, R., Kerr, N. M., & Chinnery, H. R. (2020). Optical coherence tomography angiography in diabetic retinopathy and diabetic macular edema: A review. Eye, 34(7), 1181-1196.
16. Kowluru, R. A., Mishra, M., & Kowluru, A. (2019). Role of mitochondrial DNA damage in the development of diabetic retinopathy, and the metabolic memory phenomenon associated with its progression. Antioxidants & Redox Signaling, 30(14), 1854-1864.
17. Nentwich, M. M., & Ulbig, M. W. (2019). Diabetic retinopathy—ocular complications of diabetes mellitus. World Journal of Diabetes, 10(5), 270-282.
18. Querques, G., Bandello, F., & Souied, E. H. (2022). Diabetic retinopathy: Current and future strategies for treatment. Acta Diabetologica, 59(1), 1-10.
19. Wong, T. Y., Sun, J., Kawasaki, R., & Ruamviboonsuk, P. (2020). Guidelines on diabetic eye care: The International Council of Ophthalmology recommendations for screening, follow-up, referral, and treatment based on resource settings. Diabetes Research and Clinical Practice, 162, 108108.
20. Qummar, S.; Khan, F.G.; Shah, S.; Khan, A.; Shamshirband, S.; Rehman, Z.U.; Khan, I.A.; Jadoon,W. A deep learning ensemble approach for diabetic retinopathy detection. IEEE Access 2019, 7, 150530–150539.

21. AL-Saedi, K. H., and Jelinek, H. F. (2018). A data mining framework for the classification of retinopathy images based on a new multistage prediction algorithm. International Journal of Engineering and Technology, 7(4), 4201-4206.
22. Yabe, D., Kuwata, H., Fujiwara, Y., Sakaguchi, M., Moyama, S., Makabe, N., ...and Seino, Y. (2019). Dietary instructions focusing on meal-sequence and nutritional balance for prediabetes subjects: An exploratory, cluster-randomized, prospective, open-label, clinical trial. Journal of Diabetes and its Complications, 33(12), 107450.
23. Qiao, L., Zhu, Y.,and Zhou, H. (2020). Diabetic retinopathy detection using prognosis of microaneurysm and early diagnosis system for non-proliferative diabetic retinopathy based on deep learning algorithms. IEEE Access, 8, 104292-104302.
24. Zong, Y., Chen, J., Yang, L., Tao, S., Aoma, C., Zhao, J., and Wang, S. (2020). U- net Based Method for Automatic Hard Exudates Segmentation in Fundus Images Using Inception Module and Residual Connection. IEEE Access, 8, 167225-167235.
25. Shankar, K., Zhang, Y., Liu, Y., Wu, L. and Chen, C.H., 2020. Hyperparameter tuning deep learning for diabetic retinopathy fundus image classification. IEEE Access, 8, pp.118164-118173
26. Gulshan, V.; Peng, L.; Coram, M.; Stumpe, M.C.; Wu, D.; Narayanaswamy, A.; Venugopalan, S.; Widner, K.; Madams, T.; Cuadros, J. Development and validation of a deep learning algorithm for detection of diabetic retinopathy in retinal fundus photographs.JAMA 2016, 316, 2402–2410.
27. Gargeya, R.; Leng, T. Automated identification of diabetic retinopathy using deep learning. Ophthalmology 2017, 124, 962–969.
28. Sharmin Majumder and Nasser Kehtarnavaz, Multitasking Deep Learning Model for Detection of Five Stages of Diabetic Retinopathy,
DOI 10.1109/ACCESS.2021.3109240, IEEE Access
29. Hop, Patrick, Brandon Allgood, and Jessen Yu. "Geometric deep learning autonomously learns chemical features that outperform those engineered by domain experts." Molecular pharmaceutics 15.10 (2018): 4371-4377
30. Patel, Lauv, et al. "Machine learning methods in drug discovery." Molecules 25.22 (2020): 5277

31. Sarvamangala, D. R., and Raghavendra V. Kulkarni. "Convolutional neural networks in medical image understanding: a survey." Evolutionary intelligence (2021): 1-22., https://doi.org/10.1007/s12065-020-00540-3
32. Eftekhari, N.; Pourreza, H.-R.; Masoudi, M.; Ghiasi-Shirazi, K.; Saeedi, E. Microaneurysm detection in fundus images using a two-step convolutional neural network. Biomed. Eng. Online 2019, 18, 67.
33. García, G.; Gallardo, J.; Mauricio, A.; López, J.; Del Carpio, C. Detection of diabetic retinopathy based on a convolutional neural network using retinal fundus images. In Proceedings of the International Conference on Artificial Neural Networks, Alghero, Italy, 11–14 September 2017; pp. 635–642.
34. J. Wang, J. Luo, B. Liu, R. Feng, L. Lu, and H. Zou, "Automated diabetic retinopathy grading and lesion detection based on the modified R-FCN object-detection algorithm," IET Comput. Vis., vol.
35. S. Majumder and M. A. Ullah, "Feature extraction from dermoscopy images for melanoma diagnosis," SN Appl. Sci., vol. 1, no. 7, 2019, doi: 10.1007/s42452-019-0786- 8.
36. S. Majumder and M. A. Ullah, "A Computational Approach to Pertinent Feature Extraction for Diagnosis of Melanoma Skin Lesion," Pattern Recognit. Image Anal., vol. 29, no. 3, pp. 503–514, 2019, doi: 10.1134/S1054661819030131.
37. R. Pires, S. Avila, H. F. Jelinek, J. Wainer, E. Valle, and A. Rocha, "Beyond Lesion-Based Diabetic Retinopathy: A Direct Approach for Referral," IEEE J. Biomed. Heal. Informatics, 2017, doi: 10.1109/JBHI.2015.2498104.
38. Melissa delaPava, Hernán Ríos, Francisco J. Rodríguez, Oscar J. Perdomo, Fabio A. González, "A Deep Learning Model for Classification of Diabetic Retinopathy in Eye Fundus Images based on Retinal Lesion Detection", ,DOI: 10.1117/12.2606319, December 2021.
39. N. G. Ranamuka and R. G. N. Meegama, "Detection of hard exudates from diabetic retinopathy images using fuzzy logic," IET Image Process., 2013, doi: 10.1049/iet-ipr.2012.0134.
40. H. F. Jaafar, A. K. Nandi and W. Al-Nuaimy, "Automated detection and grading of hard exudates from retinal fundus images", 2011

41. S. S. Kar and S. P. Maity, “Gradation of diabetic retinopathy on reconstructed image using compressed sensing,” IET Image Process., vol. 12, no. 11, pp. 1956–1963, 2018, doi: 10.1049/iet-ipr.2017.1013.
42. J. Wang, Y. Bai, and B. Xia, “Feasibility of Diagnosing Both Severity and Features of Diabetic Retinopathy in Fundus Photography,” IEEE Access, 2019, doi: 10.1109/access.2019.2930941.
43. M. Leeza and H. Farooq, “Detection of severity level of diabetic retinopathy using Bag of features model,” IET Comput. Vis., 2019, doi: 10.1049/iet-cvi.2018.5263.
44. W. M. Gondal, J. M. Kohler, R. Grzeszick, G. A. Fink, and M. Hirsch, “Weakly-supervised localization of diabetic retinopathy lesions in retinal fundus images,” 2018, doi: 10.1109/ICIP.2017.8296646.
45. B. Richey, S. Majumder, M. V. Shirvaikar, and N. Kehtarnavaz, “Real-time detection of maize crop disease via a deep learning-based smartphone app,” 2020, doi: 10.1117/12.2557317.
46. S. Majumder and N. Kehtarnavaz, “Vision and Inertial Sensing Fusion for Human Action Recognition: A Review,” IEEE Sens. J., vol. 21, no. 3, pp. 2454–2467, 2021, doi: 10.1109/JSEN.2020.3022326.
47. Z. Wang, Y. Yin, J. Shi, W. Fang, H. Li, and X. Wang, “Zoom-in-net: Deep mining lesions for diabetic retinopathy detection,” Lect. Notes Comput. Sci. (including Subser. Lect. Notes Artif. Intell. Lect. Notes Bioinformatics), vol. 10435 LNCS, pp. 267– 275, 2017, doi: 10.1007/978-3-319-66179-7_31.
48. M. Pour, H. Seyedarabi, S. H. A. Jahromi, and A. Javadzadeh, “Automatic Detection and Monitoring of Diabetic Retinopathy using Efficient Convolutional Neural Networks and Contrast Limited Adaptive Histogram Equalization,” IEEE Access, 2020, doi: 10.1109/access.2020.3005044.
49. S. Dutta, B. C. S. Manideep, S. M. Basha, R. D. Caytiles, and N. C. S. N. Iyengar, “Classification of diabetic retinopathy images by using deep learning models,” Int. J. Grid Distrib. Comput., vol. 11, no.
50. S. Wan, Y. Liang, and Y. Zhang, “Deep convolutional neural networks for diabetic retinopathy detection by image classification,” Comput. Electr. Eng., 2018, doi: 10.1016/j.compeleceng.2018.07.042.

51. M. D. Abràmoff et al., “Improved automated detection of diabetic retinopathy on a publicly available dataset through integration of deep learning,” Investig. Ophthalmol. Vis. Sci., 2016, doi: 10.1167/iovs.16-19964.
52. D. Marín, A. Aquino, M. E. Gegúndez-Arias, and J. M. Bravo, “A new supervised method for blood vessel segmentation in retinal images by using gray-level and moment invariants-based features,” IEEE Trans. Med. Imaging, 2011, doi: 10.1109/TMI.2010.2064333.
53. W. Cao, N. Czarnek, J. Shan, and L. Li, “Microaneurysm detection using principal component analysis and machine learning methods,” IEEE Trans. Nanobioscience, 2018, doi: 10.1109/TNB.2018.2840084
54. Hardik Deshmukh, Medical X-ray Image Classification using Convolutional Neural Network, Construction of CNN model for detection of pneumonia in x-rays from scratch.
55. Li, Qing, et al. "Medical image classification with convolutional neural network." 2014 13th international conference on control automation robotics & vision (ICARCV). IEEE, 2014. https://doi.org/10.1109/ICARCV.2014.7064414
56. A Aruna kumari , Santosh Kumar Henge, A Hybrid Model on Deep Learning for the Diagnosis of Diabetic Retinopathy Using Image Cropping, Intelligent Sustainable Systems pp 515-525, DOI: https://doi.org/10.1007/978-981-16-6309-3_49, 01 January 2022.
57. Anumol Sajan, Anamika K, Simy Mary Kurian, Diabetic Retinopathy Detection using Deep Learning, International Journal of Engineering Research & Technology, Special Issue – 2022, Volume 10, Issue 04, pp. 154-159.
58. Wilkinson, C. et al. Proposed international clinical diabetic retinopathy and diabetic macular edema disease severity scales. Ophthalmology 110, 1677–1682 (2003).
59. Group ETDRSR. Treatment techniques and clinical guidelines for photocoagulation of diabetic macular edema: Early Treatment Diabetic Retinopathy Study report number 2. Ophthalmology 94, 761–774 (1987)
60. Fundus disease Group in Ophthalmology Branch of Chinese Medical Association. Guidelines of retinal image acquisition and reading for diabetic retinopathy screening in China. Chin. J. Ophthalmol. 53, 890–896 (2017).

61. S. R. Sadda et al., “Quantitative assessment of the severity of diabetic retinopathy,” Am.J. Ophthalmol., 2020, doi: 10.1016/j.ajo.2020.05.021.
62. Ying, G.-s. et al. Association between antiplatelet or anticoagulant drugs and retinal or subretinal hemorrhage in the comparison of age-related macular degeneration treatments trials. Ophthalmology 123, 352–360 (2016).
63. Hove, M. N., Kristensen, J. K., Lauritzen, T. & Bek, T. Quantitative analysis of retinopathy in type 2 diabetes: identification of prognostic parameters for developing visual loss secondary to diabetic maculopathy. Acta Ophthalmol. Scand. 82, 679–685 (2004).
64. Sadek, M. Elawady, and A. E. R. Shabayek, “Automatic Classification of Bright Retinal Lesions via Deep Network Features,” pp. 1–20, 2017.
65. M.D. Abràmoff, J.C. Folk , D.P. Han , et al. , Automated analysis of retinal images for detection of referable diabetic retinopathy, JAMA Ophthalmol. 131 (3) (2013) 351–357
66. E. Decencière , X. Zhang , G. Cazuguel , et al. , Feedback on a publicly distributed database: the messidor database, Image Anal. Stereol. 33 (3) (2014) 231–234 .
67. Ocular Disease Intelligent Recognition (ODIR-2019), 2013, (https://odir2019.grand-challenge.org/introduction/). Online; accessed accessed 5 January 2023.
68. DeepDR Diabetic Retinopathy Image Dataset (DeepDRiD), 2013, (https://isbi.deepdr.org/data.html). Online; accessed accessed 5 January 2023.
69. W. Abdulla, R.J. Chalakkal, University of Auckland Diabetic Retinopathy (UoA-DR) Database, 2018, 10.17608/k6.auckland.5985208.v5
70. T. Li , Y. Gao , K. Wang , S. Guo , H. Liu , H. Kang , Diagnostic assessment of deep learning algorithms for diabetic retinopathy screening, Inf. Sci. (Ny) 501 (2019) 511–522 .
71. Wejdan L. Alyoubi, Wafaa M. Shalash, Maysoon F. Abulkhair, Diabetic retinopathy detection through deep learning techniques: A review, Informatics in Medicine Unlocked, Volume 20, 2020, 100377, ISSN 2352-9148, https://doi.org/10.1016/j.imu.2020.100377.

72. Ayala, Angel, Tomás Ortiz Figueroa, Bruno Fernandes, and Francisco Cruz. 2021. "Diabetic Retinopathy Improved Detection Using Deep Learning" Applied Sciences 11, no. 24: 11970. https://doi.org/10.3390/app112411970.
73. AbdelMaksoud E, Barakat S, Elmogy M. A computer-aided diagnosis system for detecting various diabetic retinopathy grades based on a hybrid deep learning technique. Med Biol Eng Comput. 2022 Jul;60(7):2015-2038. doi: 10.1007/s11517-022-02564-6. Epub 2022 May 11. PMID: 35545738; PMCID: PMC9225981.
74. Nikos Tsiknakis, Dimitris Theodoropoulos, Georgios Manikis, Emmanouil Ktistakis, Ourania Boutsora, Alexa Berto, Fabio Scarpa, Alberto Scarpa, Dimitrios I. Fotiadis, Kostas Marias, Deep learning for diabetic retinopathy detection and classification based on fundus images: A review, Computers in Biology and Medicine, Volume 135, 2021, 104599, ISSN 0010-4825, https://doi.org/10.1016/j.compbiomed.2021.104599.
75. M. T. Al-Antary and Y. Arafa, "Multi-Scale Attention Network for Diabetic Retinopathy Classification," in IEEE Access, vol. 9, pp. 54190-54200, 2021, doi: 10.1109/ACCESS.2021.3070685.
76. Alfian, G.; Syafrudin, M.; Fitriyani, N.L.; Anshari, M.; Stasa, P.; Svub, J.; Rhee, J. Deep Neural Network for Predicting Diabetic Retinopathy from Risk Factors. Mathematics 2020, 8, 1620. https://doi.org/10.3390/math8091620
77. F. Pedregosa, G. Varoquaux, A. Gramfort, V. Michel, B. Thirion, O. Grisel, M. Blondel,
78. P. Prettenhofer, R. Weiss, V. Dubourg, J. Vanderplas, A. Passos, D. Cournapeau, M. Brucher, M. Perrot, and E. Duchesnay. 2011. Scikit-learn: Machine Learning in Python. Journal of Machine Learning Research 12 (2011), 825–2830.
79. Richard HR Hahnloser, Rahul Sarpeshkar, Misha A Mahowald, Rodney J Douglas, and H Sebastian Seung. 2000. Digital selection and analogue amplification coexist in a cortex- inspired silicon circuit. Nature 405, 6789 (2000), 947.
80. Rahul Kumar Jha, Santosh Kumar Henge, Sanjeev Kumar Mandal, Amit Sharma, Supriya Sharma, Ashok Sharma, Afework Aemro Berhanu, "Neural Fuzzy Hybrid Rule- Based Inference System with Test Cases for Prediction of Heart Attack Probability",

81. S. K. Henge and B. Rama, "Comprative study with analysis of OCR algorithms and invention analysis of character recognition approched methodologies," 2016 IEEE 1st International Conference on Power Electronics, Intelligent Control and Energy Systems (ICPEICES), 2016, pp. 1-6, doi: 10.1109/ICPEICES.2016.7853643
82. Henge, S.K., Rama, B. (2018). OCR-Assessment of Proposed Methodology Implications and Invention Outcomes with Graphical Representation Algorithmic Flow. In: Saeed, K., Chaki, N., Pati, B., Bakshi, S., Mohapatra, D. (eds) Progress in Advanced Computing and Intelligent Engineering. Advances in Intelligent Systems and Computing, vol 563. Springer, Singapore. https://doi.org/10.1007/978-981-10-6872-0_6
83. Asia, A.-O.; Zhu, C.-Z.; Althubiti, S.A.; Al-Alimi, D.; Xiao, Y.-L.; Ouyang, P.-B.; Al-Qaness, M.A.A. Detection of Diabetic Retinopathy in Retinal Fundus Images Using CNN Classification Models. Electronics 2022, 11, 2740.
84. Naz, H., Nijhawan, R., & Ahuja, N. J. (2022). An automated unsupervised deep learning–based approach for diabetic retinopathy detection. Medical & Biological Engineering & Computing, 60(12), 3635-3654. Chua, Jacqueline & Lim, Claire & Wong, T-Y & Sabanayagam, Charumathi. (2017). Diabetic Retinopathy in the Asia-Pacific. Asia-Pacific Journal of Ophthalmology. 7. 10.22608/APO.2017511.
85. Mustafa, Hamza & Ali, Syed & Bilal, Muhammad & Hanif, Muhammad Shehzad. (2022). Multi-Stream Deep Neural Network for Diabetic Retinopathy Severity Classification Under a Boosting Framework. IEEE Access. 10. 10.1109/ACCESS.2022.3217216.
86. R., Yasashvini & M., Vergin & Panjanathan, Rukmani & Jasmine, Graceline & Anbarasi, L.. (2022). Diabetic Retinopathy Classification Using CNN and Hybrid Deep Convolutional Neural Networks. Symmetry. 14. 1932. 10.3390/sym14091932.
87. Banterle, F.; Artusi, A.; Debattista, K.; Chalmers, A. Advanced High Dynamic Range Imaging; CRC Press: Boca Raton, FL, USA, 2017; ISBN 9781498706940.
88. R. Williams, M. Airey, H. Baxter, J. Forrester, T. Kennedy-Martin, and A. Girach, “Epidemiology of diabetic retinopathy and macular oedema: A systematic review,” Eye. 2004, doi: 10.1038/sj.eye.6701476.

89. M. Mateen, J. Wen, M. Hassan, N. Nasrullah, S. Sun, and S. Hayat, “Automatic Detection of Diabetic Retinopathy: A Review on Datasets, Methods and Evaluation Metrics,” IEEE Access, 2020, doi: 10.1109/ACCESS.2020.2980055.
90. Antal and A. Hajdu, “An ensemble-based system for microaneurysm detection and diabetic retinopathy grading,” IEEE Trans. Biomed. Eng., 2012, doi: 10.1109/TBME.2012.2193126.
91. R. Pires, H. F. Jelinek, J. Wainer, S. Goldenstein, E. Valle, and A. Rocha, “Assessing the need for referral in automatic diabetic retinopathy detection,” IEEE Trans. Biomed. Eng., 2013, doi: 10.1109/TBME.2013.2278845.
92. Sopharak, B. Uyyanonvara, S. Barman, and T. H. Williamson, “Automatic detection of diabetic retinopathy exudates from non-dilated retinal images using mathematical morphology methods” Comput. Med. Imaging Graph., 2008, doi: 10.1016/j.compmedimag.2008.08.009.
93. S. Majumder and N. Kehtarnavaz, “A review of real-time human action recognition involving vision sensing,” in Proc. SPIE 11736, 2021, pp. 11736–9.
94. Chandrakumar T and R Kathirvel, “Classifying Diabetic Retinopathy using Deep Learning Architecture,” Int. J. Eng. Res., vol. V5, no. 06, pp. 19–24, 2016, doi: 10.17577/ijertv5is060055.
95. W. Raja Memon, D. B. Lal, and D. A. Aziz Sahto, “DIABETIC RETINOPATHY; FREQUENCY AT LEVEL OF HbA1C GREATER THAN 6.5%,” Prof. Med. J., vol. 24, no. 02, pp. 234–238, 2017, doi: 10.17957/tpmj/17.3616.
96. X. Zeng, H. Chen, Y. Luo, and W. Ye, “Automated diabetic retinopathy detection based on binocular siamese-like convolutional neural network,” IEEE Access, 2019, doi: 10.1109/ACCESS.2019.2903171.
97. S. Majumder, Y. Elloumi, M. Akil, R. Kachouri, and N. Kehtarnavaz, “A deep learning- based smartphone app for real-time detection of five stages of diabetic retinopathy,” 2020, doi: 10.1117/12.2557554.
98. Z. Gao, J. Li, J. Guo, Y. Chen, Z. Yi, and J. Zhong, “Diagnosis of Diabetic Retinopathy Using Deep Neural Networks,” IEEE Access, 2019, doi: 10.1109/ACCESS.2018.2888639.

99. Playout, R. Duval, and F. Cheriet, “A Novel Weakly Supervised Multitask Architecture for Retinal Lesions Segmentation on Fundus Images,” IEEE Trans. Med. Imaging, 2019, doi: 10.1109/TMI.2019.2906319.
100. Playout, R. Duval, and F. Cheriet, “A multitask learning architecture for simultaneous segmentation of bright and red lesions in fundus images,” 2018, doi: 10.1007/978-3-030- 00934- 2_12.
101. D. Fleming, S. Philip, K. A. Goatman, J. A. Olson, and P. F. Sharp, “Automated microaneurysm detection using local contrast normalization and local vessel detection,” IEEE Trans. Med. Imaging, 2006, doi: 10.1109/TMI.2006.879953.
102. Mushtaq and Farheen Siddiqui 2021, Detection of diabetic retinopathy using deep learning methodology IOP Conf. Ser.: Mater. Sci. Eng. 1070 012049, pp. 1-13. DOI 10.1088/1757-899X/1070/1/012049.
103. S. K. Pandey and V. Sharma, “World diabetes day 2018: Battling the Emerging Epidemic of Diabetic Retinopathy,” Indian J Ophthalmol.
104. G. T. Zago, R. V. Andreão, B. Dorizzi, and E. O. Teatini Salles, “Diabetic retinopathy detection using red lesion localization and convolutional neural networks,” Comput. Biol. Med., vol. 116, p. 103537, 2020, doi: 10.1016/j.compbiomed.2019.103537.
105. Dai, L., Wu, L., Li, H. et al. A deep learning system for detecting diabetic retinopathy across the disease spectrum. Nat Commun 12, 3242 (2021). https://doi.org/10.1038/s41467-021-23458-5.
106. Shen, Y. et al. Domain-invariant interpretable fundus image quality assessment. Med. Image Anal. 61, 101654 (2020).
107. He, K., Zhang, X., Ren, S. & Sun, J. Deep residual learning for image recognition. In Proc. IEEE Conference on Computer Vision and Pattern Recognition 770–778 (IEEE, 2016).
108. Gülçehre, Ç. & Bengio, Y. Knowledge matters: importance of prior information for optimization. J. Mach. Learn. Res. 17, 226–257 (2016).
109. A.D. Hoover, V. Kouznetsova, M. Goldbaum, Locating blood vessels in retinal images by piece wise threshold probing of a matched filter response, IEEE Trans. Med. Imaging 19 (3) (2000) 203–210, doi: 10.1109/42.845178 .

110. J. Staal , M.D. Abramoff, M. Niemeijer , M.A. Viergever , B. van Ginneken , Ridge-based vessel segmentation in color images of the retina, IEEE Trans. Med. Imaging 23(4) (2004) 501–509 .

111. Budai, R. Bock, A. Maier, J. Hornegger, G. Michelson, Robust vessel segmentation in fundus images, Int. J. Biomed. Imaging 2013 (2013) 154860, doi: 10.1155/2013/154860 .

112. Sikder, N.; Masud, M.; Bairagi, A.K.; Arif, A.S.M.; Nahid, A.-A.; Alhumyani, H.A. Severity Classification of Diabetic Retinopathy Using an Ensemble Learning Algorithm through Analyzing Retinal Images. Symmetry 2021, 13, 670.https://doi.org/10.3390/sym13040670

113. Jha, R. K., Henge, S. K., & Sharma, A. (2021, August). Heart Disease Prediction and Hybrid GANN. In International Conference on Intelligent and Fuzzy Systems (pp. 438-445). Cham: Springer International Publishing.

114. Chetoui M, Akhloufi MA. Explainable end-to-end deep learning for diabetic retinopathy detection across multiple datasets. J Med Imaging (Bellingham). 2020 Jul;7(4):044503. doi: 10.1117/1.JMI.7.4.044503. Epub 2020 Aug 28. PMID: 32904519; PMCID: PMC7456641.

115. Shi, C., Lee, J., Wang, G. et al. Assessment of image quality on color fundus retinal images using the automatic retinal image analysis. Sci Rep 12, 10455 (2022). https://doi.org/10.1038/s41598-022-13919-2

116. Jha, R.K., Henge, S.K. and Sharma, A., 2020. Optimal machine learning classifiers for prediction of heart disease. Int. J. Control Autom, 13(1), pp.31-37. Available: http://sersc.org/journals/index.php/IJCA/article/view/6680.

117. Henge, S.K., Rama, B. (2017). Five-Layered Neural Fuzzy Closed-Loop Hybrid Control System with Compound Bayesian Decision-Making Process for Classification Cum Identification of Mixed Connective Conjunct Consonants and Numerals. In: Bhatia, S., Mishra, K., Tiwari, S., Singh, V. (eds) Advances in Computer and Computational Sciences. Advances in Intelligent Systems and Computing, vol 553. Springer, Singapore. https://doi.org/10.1007/978-981-10-3770-2_58

118. Nagaraja Gundluru, Dharmendra Singh Rajput, Kuruva Lakshmanna, Rajesh Kaluri, Mohammad Shorfuzzaman, Mueen Uddin, Mohammad Arifin Rahman Khan, "Enhancement of Detection of Diabetic Retinopathy Using Harris Hawks Optimization with Deep Learning Model", Computational Intelligence and Neuroscience, vol. 2022, Article ID 8512469, 13 pages, 2022. https://doi.org/10.1155/2022/8512469
119. https://www.health.harvard.edu/a_to_z/retinopathy-a-to-z
120. Mahmoud, Hanan. (2022). Diabetic Retinopathy Progression Prediction Using a Deep Learning Model. Axioms. 11. 614. 10.3390/axioms11110614.
121. Jain, A.K. Fundamentals of Digital Image Processing; Prentice Hall: Englewood Cliffs, NJ, USA, 1989; ISBN 978-0133361650.
122. Masud, M.; Bairagi, A.K.; Nahid, A.A.; Sikder, N.; Rubaiee, S.; Ahmed, A.; Anand, D. A Pneumonia Diagnosis Scheme Based on Hybrid Features Extracted from Chest Radiographs Using an Ensemble Learning Algorithm. J. Healthc. Eng. 2021, 2021, 8862089.
123. Kamil, R. A., Al-Saedi, K. H.,and Al-Azawi, R. J. (2017). A novel approach for optic disc detection in RGB retinal fundus images. International Journal of Science and Research, 6(8), 1263-1268.
124. Orlando, J.I.; Prokofyeva, E.; Del Fresno, M.; Blaschko, M.B. An ensemble deep learning based approach for red lesion detection in fundus images. Comput. Methods Programs Biomed. 2018, 153, 115–127.
125. Ting, D.S.W.; Cheung, C.Y.-L.; Lim, G.; Tan, G.S.W.; Quang, N.D.; Gan, A.; Hamzah, H.; Garcia-Franco, R.; San Yeo, I.Y.; Lee, S.Y. Development and validation of a deep learning system for diabetic retinopathy and related eye diseases using retinal images from multiethnic populations with diabetes. JAMA 2017, 318, 2211–2223.
126. S. Majumder and M. A. Ullah, “Feature extraction from dermoscopy images for an effective diagnosis of melanoma skin cancer,” in 2018 10th International Conference on Electrical and Computer Engineering (ICECE), Dec. 2018, pp. 185–188, doi: 10.1109/ICECE.2018.8636712.

127. S. Majumder, M. A. Ullah, and J. P. Dhar, “Melanoma Diagnosis from Dermoscopy Images Using Artificial Neural Network,” in 2019 5th International Conference on Advances in Electrical Engineering (ICAEE), 2019, pp. 855–859, doi: 10.1109/ICAEE48663.2019.8975434.
128. R. Casanova, S. Saldana, E. Y. Chew, R. P. Danis, C. M. Greven, and W. T. Ambrosius, “Application of random forests methods to diabetic retinopathy classification analyses,” PLoS One, 2014, doi: 10.1371/journal.pone.0098587.
129. H. Wei, A. Sehgal, and N. Kehtarnavaz, “A deep learning-based smartphone app for real- time detection of retinal abnormalities in fundus images,” vol. 1099602, no. May, p. 1, 2019, doi: 10.1117/12.2516665
130. H. Pratt, F. Coenen, D. M. Broadbent, S. P. Harding, and Y. Zheng, “Convolutional Neural Networks for Diabetic Retinopathy,” 2016, doi: 10.1016/j.procs.2016.07.014.
131. J. Amin, M. Sharif, and M. Yasmin, “A Review on Recent Developments for Detection of Diabetic Retinopathy,” Scientifica, vol. 2016. 2016, doi: 10.1155/2016/6838976.
132. Salz DA, Witkin AJ. Imaging in diabetic retinopathy. Middle East Afr J Ophthalmol. 2015 Apr-Jun;22(2):145-50. doi: 10.4103/0974-9233.151887. PMID: 25949070; PMCID: PMC4411609.
133. Lakshminarayanan, V., Kheradfallah, H., Sarkar, A. and Jothi Balaji, J., 2021. Automated Detection and Diagnosis of Diabetic Retinopathy: A Comprehensive Survey. Journal of Imaging, 7(9), p.165.
134. Su lot, D., Alonso-Caneiro, D., Ksieniewicz, P., Krzyzanowska-Berkowska, P. and Iskander, D.R., 2021. Glaucoma classification based on scanning laser ophthalmoscopic images using a deep learning ensemble method. Plos one, 16(6), p.e0252339.
135. Yasin, S.; Iqbal, N.; Ali, T.;Draz, U.; Alqahtani, A.; Irfan, M.;Rehman, A.; Glowacz, A.; Alqhtani,S.; Proniewska, K. Frantisek Brumercik, Lukasz Wzorek, Severity Grading and Early Retinopathy Lesion Detection through Hybrid Inception-ResNet Architecture, Sensors, 2021, 21, 6933. https://doi.org/10.3390/s21206933
136. Quellec, G.; Charrière, K.; Boudi, Y.; Cochener, B.; Lamard, M. Deep image mining for diabetic retinopathy screening. Med. Image Anal. 2017, 39, 178–193.

137. Sebti, R., Zroug, S., Kahloul, L., Benharzallah, S. (2022). A Deep Learning Approach for the Diabetic Retinopathy Detection. In: Ben Ahmed, M., Boudhir, A.A., Karaș, İ.R., Jain, V., Mellouli, S. (eds) Innovations in Smart Cities Applications Volume 5. SCA 2021. Lecture Notes in Networks and Systems, vol 393. Springer, Cham. https://doi.org/10.1007/978-3-030-94191-8_37.

138. Bhupinder Singh, Dr Santosh Kumar Henge, Neural Fuzzy Inference Hybrid System with SVM for Identification of False Singling in Stock Market Prediction for Profit Estimation, Intelligent Systems and Computing, https://doi.org/10.1007/978-3-030-51156-2_27, July 2020.

139. Taher, F., Kandil, H., Mahmoud, H., Mahmoud, A., Shalaby, A., Ghazal, M., Alhalabi, M.T., Sandhu, H.S. and El-Baz, A., 2021. A Comprehensive Review of Retinal Vascular and Optical Nerve Diseases Based on Optical Coherence Tomography Angiography. Applied Sciences, 11(9), p.4158.

140. Kipli, K., Hoque, M.E., Lim, L.T., Mahmood, M.H., Sahari, S.K., Sapawi, R., Rajaee, N. and Joseph, A., 2018. A review on the extraction of quantitative retinal microvascular image feature. Computational and mathematical methods in medicine, 2018.

141. Costa, P., Galdran, A., Smailagic, A. and Campilho, A., 2018. A weakly-supervised framework for interpretable diabetic retinopathy detection on retinal images. IEEE Access, 6, pp.18747-18758.

142. Playout, R. Duval, and F. Cheriet, "A Novel Weakly Supervised Multitask Architecture for Retinal Lesions Segmentation on Fundus Images," IEEE Trans. Med. Imaging, 2019, doi: 10.1109/TMI.2019.2906319.

143. Playout, R. Duval, and F. Cheriet, "A multitask learning architecture for simultaneous segmentation of bright and red lesions in fundus images," 2018, doi: 10.1007/978-3-030- 00934- 2_12.

144. Lay , C. Baudoin , J.-C. Klein , Automatic detection of microaneurysms in retinopathy fluoro-angiogram, in: Proceedings of SPIE - The International Society for Optical Engineering, vol. 432, 1983, pp. 165–173 .

145. Fatima, Muhammad Imran, Anayat Ullah, Muhammad Arif, Rida Noor, A unified technique for entropy enhancement based diabetic retinopathy detection using hybrid neural network, Computers in Biology and Medicine, Volume 145, 2022, 105424, ISSN 0010-4825, https://doi.org/10.1016/j.compbiomed.2022.105424.
146. Patil, V. B., Rai, M. V., and Barve, A. (2016). Blood vessel segmentation from color retinal images using unsupervised texture classification. International Journal of Science and Research (IJSR), 4(1), 2319-7064.
147. Gambhir, A. (2020). Advanced Practices on Detection and Classification of Diabetic Retinopathy from Fundus Images. International Journal of Innovative Re- search in Computer Science and Technology (IJIRCST) Volume-8, Issue-3.
148. Sarabi, M.S., Khansari, M.M., Zhang, J., Kushner-Lenhoff, S., Gahm, J.K., Qiao, Y., Kashani, A.H. and Shi, Y., 2020. 3D Retinal Vessel Density Mapping With OCT-Angiography. IEEE Journal of Biomedical and Health Informatics, 24(12), pp.3466-3479.
149. Shabbir, A., Rasheed, A., Shehraz, H., Saleem, A., Zafar, B., Sajid, M., Ali, N., Dar, S.H. and Shehryar, T., 2021. Detection of glaucoma using retinal fundus images: A comprehensive review. Mathematical Biosciences and Engineering, 18(3), pp.2033-2076.
150. Xiao, Z.; Zhang, X.; Geng, L.; Zhang, F.;Wu, J.; Tong, J.; Ogunbona, P.O.; Shan, C. Automatic non-proliferative diabetic retinopathy screening system based on color fundus image. Biomed. Eng. Online 2017, 16, 122.
151. Khojasteh, P.; Aliahmad, B.; Kumar, D.K. Fundus images analysis using deep features for detection of exudates, hemorrhages and microaneurysms. BMC Ophthalmol. 2018, 18, 288.
152. S. Majumder, Y. Elloumi, M. Akil, R. Kachouri, and N. Kehtarnavaz, “A deep learning- based smartphone app for real-time detection of five stages of diabetic retinopathy,” 2020, doi: 10.1117/12.2557554.
153. Veena Mayya, Sowmya Kamath S., Uma Kulkarni, Automated microaneurysms detection for early diagnosis of diabetic retinopathy: A Comprehensive review, Computer Methods and Programs in Biomedicine Update, Volume 1, 2021, 100013, https://doi.org/10.1016/j.cmpbup.2021.100013.

154. J. De Calleja, L. Tecuapetla, and M. A. Medina, “LBP and Machine Learning for Diabetic Retinopathy Detection,” pp. 110–117, 2014.

155. Butt, M.M.; Iskandar, D.N.F.A.; Abdelhamid, S.E.; Latif, G.; Alghazo, R. Diabetic Retinopathy Detection from Fundus Images of the Eye Using Hybrid Deep Learning Features. Diagnostics 2022, 12, 1607. https://doi.org/10.3390/diagnostics12071607

156. Tripathi, Alka & Kharya, Pradip & Agarwal, Richa. (2022). Awareness of diabetic retinopathy among diabetes mellitus patients visiting a hospital of North India. Journal of Family Medicine and Primary Care. 10.4103/jfmpc.jfmpc_977_21.

157. Carrera, Enrique & González, Andrés & Carrera, Ricardo. (2017). Automated detection of diabetic retinopathy using SVM. 10.1109/INTERCON.2017.8079692.

158. Kamil, R., Al-Saedi, K., and Al-Azawi, R. (2018). An accurate system to measure the diabetic retinopathy using svm classifier. Ciˆencia e T´ecnica Vitivin´ıcola, 33, 135- 139.

159. K. Wisaeng and W. Sa-Ngiamvibool, “Exudates Detection Using Morphology Mean Shift Algorithm in Retinal Images,” IEEE Access, 2019, doi: 10.1109/ACCESS.2018.2890426.

160. S. Gayathri, A. K. Krishna, V. P. Gopi, and P. Palanisamy, “Automated Binary and Multiclass Classification of Diabetic Retinopathy Using Haralick and Multiresolution Features,” IEEE Access, 2020, doi: 10.1109/ACCESS.2020.2979753.

161. Yang, T. Li, W. Li, H. Wu, W. Fan, and W. Zhang, “Lesion detection and grading of diabetic retinopathy via two-stages deep convolutional neural networks,” Lect. Notes Comput. Sci. (including Subser. Lect. Notes Artif. Intell. Lect. Notes Bioinformatics), vol. 10435 LNCS, pp. 533–540, 2017, doi: 10.1007/978-3-319-66179-7_61.

162. X. Wang, L. Ju, X. Zhao, and Z. Ge, “Retinal abnormalities recognition using regional multitask learning,” 2019, doi: 10.1007/978-3-030-32239-7_4.

163. Y. Kumaran and C. M. Patil, “A brief review of the detection of diabetic retinopathy in human eyes using pre-processing & segmentation techniques,” International Journal of Recent Technology and Engineering, vol. 7, no. 4. pp. 310–320, 2018.

164. K. A. Anant, T. Ghorpade, and V. Jethani, “Diabetic retinopathy detection through image mining for type 2 diabetes,” in 2017 International Conference on Computer Communication and Informatics, ICCCI 2017, 2017, doi: 10.1109/ICCCI.2017.8117738.

165. M. Gandhi and R. Dhanasekaran, “Diagnosis of diabetic retinopathy using morphological process and SVM classifier,” Int. Conf. Commun. Signal Process. ICCSP 2013 - Proc., pp. 873–877, 2013, doi: 10.1109/iccsp.2013.6577181.

166. U. R. Acharya, C. M. Lim, E. Y. K. Ng, C. Chee, and T. Tamura, “Computer-based detection of diabetes retinopathy stages using digital fundus images,” Proc. Inst. Mech. Eng. Part H J. Eng. Med., vol. 223, no. 5, pp. 545–553, 2009, doi: 10.1243/09544119JEIM486.

167. Decencière , X. Zhang , G. Cazuguel , et al. , Feedback on a publicly distributed database: the messidor database, Image Anal. Stereol. 33 (3) (2014) 231–234 .

168. Ocular Disease Intelligent Recognition (ODIR-2019), 2013, (https://odir2019.grand- challenge.org/introduction/). Online; accessed 5 January 2023.

169. DeepDR Diabetic Retinopathy Image Dataset (DeepDRiD), 2013, (https://isbi.deepdr.org/data.html). Online; accessed accessed 5 January 2023.

170. Yang, Y.; Li, T.; Li, W.; Wu, H.; Fan, W.; Zhang, W. Lesion detection and grading of diabetic retinopathy via two-stages deep convolutional neural networks. In Proceedings of the International Conference on Medical Image Computing and Computer-Assisted Intervention, Quebec City, QC, Canada, 11–13 September 2017; pp. 533–540.

171. Chudzik, P.; Majumdar, S.; Calivá, F.; Al-Diri, B.; Hunter, A. Microaneurysm detection using fully convolutional neural networks. Comput. Methods Programs Biomed. 2018, 158, 185–192.

172. H. Wei, A. Sehgal, and N. Kehtarnavaz, “A deep learning-based smartphone app for real- time detection of retinal abnormalities in fundus images,” vol. 1099602, no. May, p. 1, 2019, doi: 10.1117/12.2516665

173. S. Gayathri, A. K. Krishna, V. P. Gopi, and P. Palanisamy, “Automated Binary and Multiclass Classification of Diabetic Retinopathy Using Haralick and Multiresolution Features,” IEEE Access, 2020, doi: 10.1109/ACCESS.2020.2979753.

174. Yang, T. Li, W. Li, H. Wu, W. Fan, and W. Zhang, “Lesion detection and grading of diabetic retinopathy via two-stages deep convolutional neural networks,” Lect. Notes Comput. Sci. (including Subser. Lect. Notes Artif. Intell. Lect. Notes Bioinformatics), vol. 10435 LNCS, pp. 533–540, 2017, doi: 10.1007/978-3-319-66179-7_61.

175. X. Wang, L. Ju, X. Zhao, and Z. Ge, “Retinal abnormalities recognition using regional multitask learning,” 2019, doi: 10.1007/978-3-030-32239-7_4.

176. Y. Kumaran and C. M. Patil, “A brief review of the detection of diabetic retinopathy in human eyes using pre-processing & segmentation techniques,” International Journal of Recent Technology and Engineering, vol. 7, no. 4. pp. 310–320, 2018.

177. K. A. Anant, T. Ghorpade, and V. Jethani, “Diabetic retinopathy detection through image mining for type 2 diabetes,” in 2017 International Conference on Computer Communication and Informatics, ICCCI 2017, 2017, doi: 10.1109/ICCCI.2017.8117738.

178. Alfian, G.; Syafrudin, M.; Fitriyani, N.L.; Anshari, M.; Stasa, P.; Svub, J.; Rhee, J. Deep Neural Network for Predicting Diabetic Retinopathy from Risk Factors. Mathematics 2020, 8, 1620. https://doi.org/10.3390/math8091620

179. Mustafa, Hamza & Ali, Syed & Bilal, Muhammad & Hanif, Muhammad Shehzad. (2022). Multi-Stream Deep Neural Network for Diabetic Retinopathy Severity Classification Under a Boosting Framework. IEEE Access. 10. 10.1109/ACCESS.2022.3217216.

180. R., Yasashvini & M., Vergin & Panjanathan, Rukmani & Jasmine, Graceline & Anbarasi, L.. (2022). Diabetic Retinopathy Classification Using CNN and Hybrid Deep Convolutional Neural Networks. Symmetry. 14. 1932. 10.3390/sym14091932.

181. Rizal, Syamsul & Ibrahim, Nur & Pratiwi, Nor & Saidah, Sofia & FU’ADAH, RADEN. (2020). Deep Learning untuk Klasifikasi Diabetic Retinopathy menggunakan Model EfficientNet. ELKOMIKA: Jurnal Teknik Energi Elektrik, Teknik Telekomunikasi, & Teknik Elektronika. 8. 693. 10.26760/elkomika.v8i3.693.

182. Banterle, F.; Artusi, A.; Debattista, K.; Chalmers, A. Advanced High Dynamic Range Imaging; CRC Press: Boca Raton, FL, USA, 2017; ISBN 9781498706940.
183. Jain, A.K. Fundamentals of Digital Image Processing; Prentice Hall: Englewood Cliffs, NJ, USA, 1989; ISBN 978-0133361650.
184. Masud, M.; Bairagi, A.K.; Nahid, A.A.; Sikder, N.; Rubaiee, S.; Ahmed, A.; Anand, D. A Pneumonia Diagnosis Scheme Based on Hybrid Features Extracted from Chest Radiographs Using an Ensemble Learning Algorithm. J. Healthc. Eng. 2021, 2021, 8862089.
185. Perez-Cervera, J., Arce, J., Fattouh, M., Kuno, T., Schenone, A. L., Brahmanandam, V., ... & Slipczuk, L. (2023). Influence of BMI on virtual coronary artery calcium scoring. The International Journal of Cardiovascular Imaging, 39(4), 863-872.
186. APTOS 2019 Blindness Detection 2019, (https://www.kaggle.com/c/aptos2019-blindness-detection). Online; Sazli, Murat H. "A brief review of feed-forward neural networks." Communications Faculty of Sciences University of Ankara Series A2-A3 Physical Sciences and Engineering 50.01 (2006).
187. Alloghani, Mohamed, et al. "A systematic review on supervised and unsupervised machine learning algorithms for data science." Supervised and unsupervised learning for data science (2020): 3-21.
188. Chua, Leon O., and Tamas Roska. "The CNN paradigm." IEEE Transactions on Circuits and Systems I: Fundamental Theory and Applications 40.3 (1993): 147-156.
189. Li, Shuai, et al. "Independently recurrent neural network (indrnn): Building a longer and deeper rnn." Proceedings of the IEEE conference on computer vision and pattern recognition. 2018.
190. Yu, Yong, et al. "A review of recurrent neural networks: LSTM cells and network architectures." Neural computation 31.7 (2019): 1235-1270.
191. Dey, Rahul, and Fathi M. Salem. "Gate-variants of gated recurrent unit (GRU) neural networks." 2017 IEEE 60th international midwest symposium on circuits and systems (MWSCAS). IEEE, 2017.
192. Salz, David A., and Andre J. Witkin. "Imaging in diabetic retinopathy." Middle East African journal of ophthalmology 22.2 (2015): 145.

193. Abràmoff, Michael D., et al. "Automated analysis of retinal images for detection of referable diabetic retinopathy." JAMA ophthalmology 131.3 (2013): 351-357.
194. Abràmoff, Michael D., et al. "Automated analysis of retinal images for detection of referable diabetic retinopathy." JAMA ophthalmology 131.3 (2013): 351-357.
195. Klein, Ronald, Barbara EK Klein, and Scot E. Moss. "Epidemiology of proliferative diabetic retinopathy." Diabetes care 15.12 (1992): 1875-1891.
196. Kauppi, Tomi, et al. "The diaretdb1 diabetic retinopathy database and evaluation protocol." BMVC. Vol. 1. No. 1. 2007.
197. LaValley, Michael P. "Logistic regression." Circulation 117.18 (2008): 2395-2399.
198. Yu, Hua, and Jie Yang. "A direct LDA algorithm for high-dimensional data—with application to face recognition." Pattern recognition 34.10 (2001): 2067-2070.
199. Zhang, Min-Ling, and Zhi-Hua Zhou. "ML-KNN: A lazy learning approach to multi- label learning." Pattern recognition 40.7 (2007): 2038-2048.
200. Zhang, Shichao, et al. "Learning k for knn classification." ACM Transactions on Intelligent Systems and Technology (TIST) 8.3 (2017): 1-19.
201. Myles, Anthony J., et al. "An introduction to decision tree modeling." Journal of Chemometrics: A Journal of the Chemometrics Society 18.6 (2004): 275-285.
202. Vishwanathan, S. V. M., and M. Narasimha Murty. "SSVM: a simple SVM algorithm." Proceedings of the 2002 International Joint Conference on Neural Networks. IJCNN'02 (Cat. No. 02CH37290). Vol. 3. IEEE, 2002.
203. ÇINAR, TUNAHAN, et al. "Detection of Heterobasidion Root Rot on Pinus Brutia Ten. Using Different Vegetation Indices Generated from Sentinel-2a Satellite Imagery." Using Different Vegetation Indices Generated from Sentinel-2a Satellite Imagery.
204. Palaniswamy, T., & Vellingiri, M. (2023). Internet of Things and Deep Learning Enabled Diabetic Retinopathy Diagnosis Using Retinal Fundus Images. *IEEE Access*, *11*, 27590-27601.
205. Akhter, A., Fatema, K., Ahmed, S. F., Afroz, A., Ali, L., & Hussain, A. (2013). Prevalence and associated risk indicators of retinopathy in a rural Bangladeshi population with and without diabetes. *Ophthalmic epidemiology*, *20*(4), 220-227

IMAGES

1. https://subscription.packtpub.com/book/big-data-and-business-intelligence/9781788474399/2/ch02lvl1sec13/building-a-machine-learning-application.
2. https://www.researchgate.net/figure/Comparison-of-deep-learning-and-traditional-machine- learning-methods_fig1_336238415
3. https://s7280.pcdn.co/wp-content/uploads/2020/07/Two-or-more-hidden-layers-comprise-a- Deep-Neural-Network.png
4. Wankmüller, S. (2021). Introduction to Neural Transfer Learning with Transformers for Social Science Text Analysis. *ArXiv*. /abs/2102.02111
5. Lamsal, R., & of Rabindra Lamsal's posts., V. A. (2021, April 24). *Derivative of Sigmoid Function*. The Neural Blog. https://theneuralblog.com/derivative-sigmoid-function/
6. *OpenCV 3 Image Edge Detection : Sobel and Laplacian - 2020*. (n.d.). OpenCV 3 Image Edge Detection : Sobel and Laplacian - 2020. https://www.bogotobogo.com/python/OpenCV_Python/python_opencv3_Image_Gradient_ Sobel_Laplacian_Derivatives_Edge_Detection.php
7. *Zhang, M., Yu, Z., Wang, H., Qin, H., Zhao, W., & Liu, Y. (2019, May 27). Automatic Digital Modulation Classification Based on Curriculum Learning. MDPI. https://doi.org/10.3390/app9102171*
8. *The Simple Recurrent Network: A Simple Model that Captures the Structure inSequences*. (n.d.). 7 the Simple Recurrent Network: A Simple Model That Captures the Structure inSequences. https://web.stanford.edu/group/pdplab/pdphandbook/handbookch8.html
9. https://www.researchgate.net/figure/Simple-Recurrent-Neural-Networks-26-In-a-simple- RNN-each-cell-represents-a-unique_fig11_343320122
10. https://www.researchgate.net/figure/Long-Short-term-Memory-Neural-Network_fig3_324600237
11. https://paperswithcode.com/method/gru
12. https://www.pinterest.fr/pin/90775748713616828/
13. https://www.kcretina.com/blog/retinal-vascular-disease-symptoms

14. https://in.pinterest.com/pin/236790892891326752/

15. https://www.researchgate.net/figure/Fundus-retina-images_fig1_356016103

16. https://zerotofinals.com/medicine/ophthalmology/hypertensiveretinopathy/

17. https://provider-dr.vision-relief.com/introduction/pathophysiology/

18. *Retina Care Research Institue*. (n.d.). Retina Care Research Institue. http://retinacareresearchinstitute.com/diabetic-retinopathy.php

19. https://www.geeksforgeeks.org/introduction-to-recurrent-neural-network/

20. Karthikeyan, M., A., E., & T. (2022, January 1). *IM-EDRD from Retinal Fundus Images Using Multi-Level Classification Techniques*. Tech Science Press. https://doi.org/10.32604/iasc.2023.026243

21. Journals, I. (n.d.). *Detection Of Cotton Wool Spots In Retinopathy Images: A Review*. (PDF) Detection of Cotton Wool Spots in Retinopathy Images: A Review | IOSR Journals - Academia.edu. https://www.academia.edu/37246071/Detection_Of_Cotton_Wool_Spots_In_Retinopathy_ Images_A_Review

22. https://ushersyndroom.nl/kennisportaal/wat-is-ushersyndroom/zicht/retinitis-pigmentosa/

23. https://www.coburntechnologies.com/2021/06/24/retinal-imaging-diseases/

24. https://discover.hubpages.com/education/The-Human-Eye-Color-Chart

25. https://entokey.com/neoplastic-diseases-of-the-retina/

26. *Deep Learning for Retinal Image Quality Assessment of Optic . . . : The Asia-Pacific Journal of Ophthalmology*. (n.d.). LWW. https://doi.org/10.1097/APO.0000000000000404

27. Liu, Y., & Moore, A. T. (2020). Congenital focal abnormalities of the retina and retinal pigment epithelium. *Eye*, *34*(11), 1973-1988. https://doi.org/10.1038/s41433-020-0902-4

28. Ralph, R. A. (2017, February 12). *Retinal Images Enhancement Methods for Fundus and OCT Imaging*. RSIP Vision. https://www.rsipvision.com/retinal-images-enhancement/

29. *Retinal vessel segmentation using color image morphology and local binary patterns*. (n.d.). Retinal Vessel Segmentation Using Color Image Morphology and Local Binary Patterns | IEEE Conference Publication | IEEE Xplore. https://ieeexplore.ieee.org/document/5941129
30. *Pharmacologic Therapy for Diabetic Retinopathy*. https://www.tandfonline.com/doi/full/10.3109/08820538.2013.859280.
31. *Pharmacologic Therapy for Diabetic Retinopathy*. https://www.tandfonline.com/doi/full/10.3109/08820538.2013.859280.
32. Image Bank, T. R. (n.d.). *Severe NPDR - Retina Image Bank*. Severe NPDR - Retina Image Bank. https://imagebank.asrs.org/file/5343/severe-npdr
33. https://www.profile-anz.com/wp-content/uploads/2018/10/Diabetic-retinopathy_Charlie- Wang.png
34. Achu, S. (2022, April 10). *A Guide to Activation functions in Artificial Neural Networks*. EJable. https://www.ejable.com/tech-corner/ai-machine-learning-and-deep-learning/a- guide-to-activation-functions-in-artificial-neural-networks/
35. Tyagi, N., & A. (2019, November 28). *Introduction to Linear Discriminant Analysis in Supervised Learning | Analytics Steps*. Introduction to Linear Discriminant Analysis in Supervised Learning | Analytics Steps. https://www.analyticssteps.com/blogs/introduction-linear-discriminant-analysis-supervised-learning
36. *K-Nearest Neighbors*. (n.d.). K-Nearest Neighbors | Kaggle. https://www.kaggle.com/code/stieranka/k-nearest-neighbors
37. *https://www.shiksha.com/online-courses/articles/decision-tree-algorithm-for-classification/*
38. https://miro.medium.com/v2/resize:fit:921/1*06GSco3ItM3gwW2scY6Tmg.png
39. Random forest - Wikipedia. (2016, June 5). Random Forest - Wikipedia. https://en.wikipedia.org/wiki/Random_forest
40. Saini, A. (2021, September 15). Master the AdaBoost Algorithm: Guide to Implementing & Understanding AdaBoost. Analytics Vidhya. https://www.analyticsvidhya.com/blog/2021/09/adaboost-algorithm-a-complete-guide-for- beginners/

41. Niakan Kalhori, S. R., Zeng, X. J., & Publishing, S. R. (2013, July 31). *Evaluation and Comparison of Different Machine Learning Methods to Predict Outcome of Tuberculosis Treatment Course*. Evaluation and Comparison of Different Machine Learning Methods to Predict Outcome of Tuberculosis Treatment Course. https://doi.org/10.4236/jilsa.2013.53020
42. Schoonjans, F. (n.d.). *ROC curve analysis*. MedCalc. https://www.medcalc.org/manual/roc- curves.php
43. Z., & posts by Zach, V. A. (2021, September 9). *How to Create a Precision-Recall Curve in Python - Statology*. Statology. https://www.statology.org/precision-recall-curve-python/
44. Fundamentals of Deep Learning (n.d.) Analytics Vidhya https://www.analyticsvidhya.com/blog/2020/01/fundamentals-deep-learning-activation-functions-when-to-use-them/
45. Uma. B(2021, November 3) Overfitting and underfitting. Medium. https://miro.medium.com/max/411/1*Y74aFrvEfs5AR79t8N7AUw.png
46. Mungloo-Dilmohamudet al.(2022) Balancing Data through Data Augmentation Improves the Generality of Transfer Learning for Diabetic Retinopathy Classification https://www.researchgate.net/profile/Maleika-Heenaye-Mamode-Khan/publication/360845455/figure/fig1/AS:1159633779597313@1653489646556/Augmented-APTOS-dataset.ppm
47. Yadav, H. (2022, July 5). *Computer Vision: Convolution Basics*. Medium. https://towardsdatascience.com/computer-vision-convolution-basics-2d0ae3b79346
48. *Activation Function - AI Wiki*. (n.d.). Activation Function - AI Wiki. https://machine-learning.paperspace.com/wiki/activation-function
49. Ganguly, M. (2020, April 29). *A simple guide to Bias-Variance Trade-off— Part 1*. Medium. https://medium.com/analytics-vidhya/a-simple-guide-to-bias-variance-trade-off-part-1- 2418229c78e0
50. Kumari, A. A., & Henge, S. K. (2022, January 3). *A Hybrid Model onDeep Learning fortheDiagnosis ofDiabetic Retinopathy Using Image Cropping*. A Hybrid Model on Deep Learning for the Diagnosis of Diabetic Retinopathy Using Image Cropping | SpringerLink. https://doi.org/10.1007/978-981-16-6309-3_49

51. Kumari, A. A., & Henge, S. K. (2022, January 3). *A Hybrid Model onDeep Learning fortheDiagnosis ofDiabetic Retinopathy Using Image Cropping*. A Hybrid Model on Deep Learning for the Diagnosis of Diabetic Retinopathy Using Image Cropping | SpringerLink. https://doi.org/10.1007/978-981-16-6309-3_49
52. Kumari, A. A., & Henge, S. K. (2022, January 3). *A Hybrid Model onDeep Learning fortheDiagnosis ofDiabetic Retinopathy Using Image Cropping*. A Hybrid Model on Deep Learning for the Diagnosis of Diabetic Retinopathy Using Image Cropping | SpringerLink. https://doi.org/10.1007/978-981-16-6309-3_49
53. Kumari, A. A., & Henge, S. K. (2022, January 3). *A Hybrid Model onDeep Learning fortheDiagnosis ofDiabetic Retinopathy Using Image Cropping*. A Hybrid Model on Deep Learning for the Diagnosis of Diabetic Retinopathy Using Image Cropping | SpringerLink. https://doi.org/10.1007/978-981-16-6309-3_49
54. Kumari, A. A., & Henge, S. K. (2022, January 3). *A Hybrid Model onDeep Learning fortheDiagnosis ofDiabetic Retinopathy Using Image Cropping*. A Hybrid Model on Deep Learning for the Diagnosis of Diabetic Retinopathy Using Image Cropping | SpringerLink. https://doi.org/10.1007/978-981-16-6309-3_49
55. Kumari, A. A., & Henge, S. K. (2022, January 3). *A Hybrid Model onDeep Learning fortheDiagnosis ofDiabetic Retinopathy Using Image Cropping*. A Hybrid Model on Deep Learning for the Diagnosis of Diabetic Retinopathy Using Image Cropping | SpringerLink. https://doi.org/10.1007/978-981-16-6309-3_49
56. Kumari, A. A., & Henge, S. K. (2022, January 3). *A Hybrid Model onDeep Learning fortheDiagnosis ofDiabetic Retinopathy Using Image Cropping*. A Hybrid Model on Deep Learning for the Diagnosis of Diabetic Retinopathy Using Image Cropping | SpringerLink. https://doi.org/10.1007/978-981-16-6309-3_49
57. Kumari, A. A., & Henge, S. K. (2022, January 3). *A Hybrid Model onDeep Learning fortheDiagnosis ofDiabetic Retinopathy Using Image Cropping*. A Hybrid Model on Deep Learning for the Diagnosis of Diabetic Retinopathy Using Image Cropping | SpringerLink. https://doi.org/10.1007/978-981-16-6309-3_49

58. Kumari, A. A., & Henge, S. K. (2022, January 3). *A Hybrid Model onDeep Learning fortheDiagnosis ofDiabetic Retinopathy Using Image Cropping*. A Hybrid Model on Deep Learning for the Diagnosis of Diabetic Retinopathy Using Image Cropping | SpringerLink. https://doi.org/10.1007/978-981-16-6309-3_49
59. Kumari, A. A., & Henge, S. K. (2022, January 3). *A Hybrid Model onDeep Learning fortheDiagnosis ofDiabetic Retinopathy Using Image Cropping*. A Hybrid Model on Deep Learning for the Diagnosis of Diabetic Retinopathy Using Image Cropping | SpringerLink. https://doi.org/10.1007/978-981-16-6309-3_49
60. Kumari, A. A., Bhagat, A., Henge, S. K., & Mandal, S. K. (2003, March 2). Automated Decision Making ResNet Feed-Forward Neural Network based Methodology for Diabetic Retinopathy Detection. Automated Decision Making ResNet Feed-Forward Neural Network Based Methodology for Diabetic Retinopathy Detection. https://doi.org/10.14569/IJACSA.2023.0140532
61. Kumari, A. A., Bhagat, A., Henge, S. K., & Mandal, S. K. (2003, March 2). Automated Decision Making ResNet Feed-Forward Neural Network based Methodology for Diabetic Retinopathy Detection. Automated Decision Making ResNet Feed-Forward Neural Network Based Methodology for Diabetic Retinopathy Detection. https://doi.org/10.14569/IJACSA.2023.0140532

LIST OF ABBREVIATIONS

CT - Computed Tomography

MRI - Magnetic Resonance Imaging ID - Identification

AI - Artificial Intelligence ML - Machine Learning

IDC - Invasive Ductal Carcinoma CNN - Convolutional Neural Network

VGGN - Very Deep Convolutional Networks for Large-Scale Visual Recognition

RNN - Recurrent Neural Network

LSTM - Long Short-Term Memory GRU - Gated Recurrent Unit

DR - Diabetic Retinopathy

PDR - Proliferative Diabetic Retinopathy NPDR - Non-Proliferative Diabetic Retinopathy DRG - Digital Retinography Grading

AL - Active Learning RGB - Red Green Blue

SVM - Support Vector Machine IDR - Inverse Document Retrieval ANN - Artificial Neural Network DNN - Deep Neural Network

PCA - Principal Component Analysis FPN - Feature Pyramid Network

AMD - Age-Related Macular Degeneration

CSME - Clinically Significant Macular Edema LBP - Local Binary Pattern

OCR - Optical Character Recognition GANN - Genetic Algorithm Neural Network HDR - High Dynamic Range

HMM - Hidden Markov Model BMI - Body Mass Index

HE - Hematoxylin and Eosin

IRMA - Intraretinal Microvascular Abnormalities FOV - Field of View

JPEG - Joint Photographic Experts Group RI - Retinal Image

AD - Adaptive Boosting CFI - Capillary Flow Index BWI - Basal Width Index II - Inferior Inward

CSV - Comma-Separated Values DR - Diabetic Retinopathy

IS - Image Segmentation PS - Pixel Shift

PC - Pixel Classification

PADD - Peripheral Anterior Drift Detection POLL - Peripheral Occlusive Limb Lesions CM - Confusion Matrix

RM - Relevance Matrix AO - Area of Operations

MNIST - Modified National Institute of Standards and Technology DL - Deep Learning

FV - Feature Vector RI - Retinal Image

APTOS - Automatic Photographic Testing of Ocular Systems BD - Brightness Distribution

IA - Independent Component Analysis NO - Normal

MI - Macular Infarction SE - Sensitivity

PR - Precision DO - Depth Order RL - Red Light GL - Green Light BL - Blue Light

RH - Red Hue GH - Green Hue BH - Blue Hue

GLCM - Gray Level Co-occurrence Matrix XGB - Extreme Gradient Boosting

DT - Decision Tree

WMV - Weighted Majority Voting DL - Deep Learning

AO - Area of Operations

CPU - Central Processing Unit RAM - Random Access Memory

MO - Morbidity

GBM - Gradient Boosting Machine

IEEE - Institute of Electrical and Electronics Engineers DNA - Deoxyribonucleic Acid

KH - Knowledge Hub

OCT - Optical Coherence Tomography SCA - Single Cell Analysis

DA - Data Analysis HR - Heart Rate TP - True Positive FP - False Positive TN - True Negative

FN - False Negative

LIST OF PUBLICATIONS

1. The paper entitled “Automated Decision Making ResNet Feed-Forward Neural Network based Methodology for Diabetic Retinopathy Detection " is Published in (IJACSA) International Journal of Advanced Computer Science and Applications, Vol. 14, No. 5, 2023
2. The paper entitled “Classification of Diabetic Retinopathy Severity using Deep learning techniques on Retinal Images” is under Communication stage
3. The paper entitled “Scrutiny of Diabetic Retinopathy Severity Levels using Deep Learning Mapping Sequences “is under Communication stage

Papers published in SCOPUS indexed Conference Proceedings:

1. Aruna Kumari, A., and Santosh Kumar Henge. "A Hybrid Model on Deep Learning for the Diagnosis of Diabetic Retinopathy Using Image Cropping." Intelligent Sustainable Systems: Selected Papers of WorldS4 2021, Volume 1. Singapore: Springer Nature Singapore, 2022. 515-525.
2. Aruna Kumari, A., and Henge Santosh Kumar. "Comparative Analysis of Machine Learning Approaches of Prediction of Diabetes Consequences in Pregnancy with Implications of Data Matrices." Soft Computing for Security Applications: Proceedings of ICSCS 2022. Singapore: Springer Nature Singapore, 2022. 613-626.
3. The paper entitled “Detection of early-stage symptoms of diabetic retinopathy prediction performance in machine learning algorithms
   DOI: 10.1201/9781003405573